

Justus-Liebig-Universität Gießen

Fachbereich Medizin

Zentrum für Innere Medizin

Abteilung für Kardiologie

des Universitätsklinikums Gießen und Marburg GmbH, Standort Gießen

Direktor: Prof. Dr. Christian Hamm

**Bioresorbierbare Scaffolds zur Behandlung der
koronaren Herzerkrankung**

Habilitationsschrift

zur Erlangung der Lehrbefähigung für das Fach Innere Medizin
im Fachbereich Medizin der Justus-Liebig-Universität Gießen

vorgelegt von

Dr. med. Niklas Frederik Boeder

Gießen 2021

Dicebat Bernardus Carnotensis nos esse quasi nanos gigantum umeris insidentes, ut possimus plura eis et remotiora videre, non utique proprii visus acumine, aut eminentia corporis, sed quia in altum subvehimur et extollimur magnitudine gigantea

Johannes von Salisbury, Metalogicon

Für Bettina, Linus und Philip

Bibliographische Beschreibung

Dieser kumulativen Habilitationsschrift liegen folgende Arbeiten zu Grunde:

Boeder, N.F.; Dörr, O.; Bauer, T.; Mattesini, A.; Elsässer, A.; Liebetrau, C.; Achenbach, S.; Hamm, C.W.; Nef, H.M. Impact of strut thickness on acute mechanical performance: A comparison study using optical coherence tomography between DESolve 150 and DESolve 100. *Int J Cardiol* **2017**, 246, 74-79.

Boeder, N.F.; Koepp, T.; Dörr, O.; Bauer, T.; Mattesini, A.; Elsässer, A.; Möllmann, H.; Blachutzik, F.; Achenbach, S.; Ghanem, A., et al. A new novolimus-eluting bioresorbable scaffold for large coronary arteries: an OCT study of acute mechanical performance. *Int J Cardiol* **2016**, 220, 706-710.

Boeder, N.F.; Dörr, O.; Bauer, T.; Elsässer, A.; Möllmann, H.; Achenbach, S.; Hamm, C.W.; Nef, H.M. Effect of Plaque Composition, Morphology, and Burden on DESolve Novolimus-Eluting Bioresorbable Vascular Scaffold Expansion and Eccentricity - An Optical Coherence Tomography Analysis. *Cardiovasc Revasc Med* **2019**, 20(6), 480-484.

Blachutzik, F.; **Boeder, N.⁺**; Wiebe, J.; Mattesini, A.; Dörr, O.; Most, A.; Bauer, T.; Röther, J.; Tröbs, M.; Schlundt, C., et al. Post-dilatation after implantation of bioresorbable everolimus- and novolimus-eluting scaffolds: an observational optical coherence tomography study of acute mechanical effects. *Clin Res Cardiol* **2017**, 106(4), 271-279.

Blachutzik, F.; **Boeder, N.⁺**; Wiebe, J.; Mattesini, A.; Dörr, O.; Most, A.; Bauer, T.; Tröbs, M.; Röther, J.; Schlundt, C., et al. Overlapping implantation of bioresorbable novolimus-eluting scaffolds: an observational optical coherence tomography study. *Heart Vessels* **2017**, 32(7), 781-789.

Boeder, N.F.; Johnson, V.; Dörr, O.; Wiebe, J.; Elsässer, A.; Möllmann, H.; Hamm, C.W.; Nef, H.M.; Bauer, T. Bioresorbable scaffold implantation in patients with indication for oral anticoagulation: A propensity matched analysis. *Int J Cardiol* **2017**, 231, 73-77.

Boeder, N.F.; Weissner, M.; Blachutzik, F.; Ullrich, H.; Anadol, R.; Tröbs, M.; Münzel, T.; Hamm, C.W.; Dijkstra, J.; Achenbach, S., et al. Incidental Finding of Strut Malapposition Is a Predictor of Late and Very Late Thrombosis in Coronary Bioresorbable Scaffolds. *J Clin Med* **2019**, 8(5), 580.

⁺ geteilte Erstautorenschaft

Inhaltsverzeichnis

Inhaltsverzeichnis	5
Abbildungsverzeichnis	7
Tabellenverzeichnis	8
Abkürzungsverzeichnis	9
1 Einleitung	12
1.1 Epidemiologie und Relevanz der koronaren Herzerkrankung	12
1.2 Pathophysiologie der koronaren Herzerkrankung	14
1.3 Diagnostik der koronaren Herzerkrankung	16
1.3.1 Chronisches Koronarsyndrom	16
1.3.2 Akutes Koronarsyndrom	17
1.4 Therapieoptionen der koronaren Herzerkrankung	19
1.4.1 Konservative Behandlungsstrategie	19
1.4.2 Myokardiale Revaskularisation	20
1.5 Bioresorbierbare Scaffolds: Eine neue Stenttechnologie	26
1.6 Intravaskuläre Bildgebung: optische Kohärenztomographie	30
2 Zielsetzung der kumulativen Habilitationsschrift	35
3 Eigene Arbeiten	36
3.1 Akutes mechanisches Ergebnis	36
3.1.1 Einfluss der Strutdicke auf das akute mechanische Ergebnis	37
3.1.2 Akutes mechanisches Ergebnis bei Implantation von Scaffolds in Gefäßen mit großem Durchmesser	38
3.1.3 Einfluss der Plaque auf das akute mechanische Ergebnis	39
3.2 Prozedurale Aspekte im Rahmen der PCI	41
3.2.1 Einfluss der Nachdilatation auf das Implantationsergebnis	41
3.2.2 Effekt der überlappenden Implantation von bioresorbierbaren Scaffolds	42
3.3 Antithrombotische Behandlung nach Implantation von bioresorbierbaren Scaffolds	44
3.4 Späte und sehr späte Scaffoldthrombosen	46
4 Diskussion	48
5 Zusammenfassung	58
6 Literaturverzeichnis	61

7	Eidesstattliche Erklärung	82
8	Danksagung.....	83
9	Zugrundeliegende Publikationen.....	84

Abbildungsverzeichnis

ABBILDUNG 1: TODESURSACHEN IN DEUTSCHLAND NACH KRANKHEITSARTEN 2019	12
ABBILDUNG 2: HÄUFIGSTE TODESURSACHEN IN DEUTSCHLAND 2019.....	13
ABBILDUNG 3: ATHEROSKLEROSE ALS VORANSCHREITENDER PROGRESS.....	14
ABBILDUNG 4: ZEITLEISTE DER WESENTLICHEN MEILENSTEINE DES HERZKATHETERS	23
ABBILDUNG 5: ABBAU DER BIORESORBIERBAREN STRUTS (OBEN) IM SCHWEINEMODELL IM VERGLEICH ZU EINEM DE-STENT (XIENCE).....	26
ABBILDUNG 6: ABSORB BVS (A) UND DESOLVE-SCAFFOLD (B)	28
ABBILDUNG 7: SCHEMATISCHE DARSTELLUNG DIVERGENTER LATERALER AUFLÖSUNGEN: DIE BEIDEN BLAUEN HERZEN IM LINKEN TEIL KÖNNEN IM GEGENSATZ ZUM RECHTEN BEISPIEL AUFGRUND DER NIEDRIGEREN AUFLÖSUNG NICHT ALS ZWEI SEPARATE OBJEKTE DARGESTELLT WERDEN.	31
ABBILDUNG 8: LONGITUDINALER „PULLBACK“ UND EXEMPLARISCHE QUERSCHNITTE ZUR BERECHNUNG DER KENNPARAMETER	34

Tabellenverzeichnis

TABELLE 1: ÜBERSICHT ÜBER PLLA-BASIERTE SCAFFOLDS	27
TABELLE 2: GEGENÜBERSTELLUNG VON OPTISCHER KOHÄRENZTOMOGRAPHIE (OCT) UND INTRAVASKULÄREM ULTRASCHALL (IVUS).....	32

Abkürzungsverzeichnis

ACC	American College of Cardiology
ACE	Angiotensin-Converting-Enzym
ACS	Akutes Koronarsyndrom
AHA	American Heart Association
AP	Angina pectoris
ASCVD	Atherosclerotic cardiovascular disease
ASS	Acetylsalicylsäure
BARC	Bleeding Academic Research Consortium
BMS	Bare-metal Stent (Metallstent)
BRS	Bioresorbierbarer Scaffold
CCS	Chronisches Koronarsyndrom
CE	Conformité Européenne
DAPT	Duale Thrombozytenaggregationshemmung
DES	Drug-eluting Stent (medikamentenfreisetzender Stent)
EES	Everolimus-freisetzender Stent
EKG	Elektrokardiogram
ESC	Europäische Gesellschaft für Kardiologie
FD-OCT	Frequency-Domain-OCT
HbA _{1c}	Hämoglobin A _{1c}
ISA	Inkomplette Strutapposition
ISR	In-Stent-Restenose
IVUS	Intravaskulärer Ultraschall
KHK	Koronare Herzerkrankung
LAD	Left anterior descending
LDL	Low-density Lipoprotein
LVEF	Linksventrikuläre Ejektionsfraktion

MACE	Major Adverse Cardiac Event (kombinierter Endpunkt aus Schlaganfall, Myokardinfarkt und kardiovaskulärem Tod)
MIT	Massachusetts Institute of Technology
MLA	Minimale Lumenfläche („minimal lumen area“)
NOAK	Nicht-Vitamin-K basierte orale Antikoagulation
NSTEMI	Nicht-ST-Streckenhebungsinfarkt
OAK	Orale Antikoagulation
OCT	Optische Kohärenztomographie
PCI	Perkutane Koronarintervention
PES	Paclitaxel-freisetzender Stent
PLLA	Poly-L-Laktid
POBA	Plain old balloon angioplasty
PTP	Vortestwahrscheinlichkeit
RAS	Residuale Flächenstenose
ScT	Scaffoldthrombose
SEC	Scaffold Excentricity Index
SEI	Scaffold Expansion Index
SES	Sirolimus-freisetzender Stent
ST	Stentthrombose
STEMI	ST-Streckenhebungsinfarkt
TAT	Dreifache antithrombotische Therapie (ASS+(N)OAK+ P2Y12-Inhibitor)
TD-OCT	Time-Domain-OCT
TIMI	Thrombolysis in Myocardial Infarction
TLF	Target lesion failure (Zielläsion-Versagen)
TLR	Target lesion revascularization (Zielläsion-Revaskularisation)

TVR	Target vessel revascularization (Zielgefäß-Revaskularisation)
US	Vereinigte Staaten von Amerika
WHO	Weltgesundheitsorganisation
ZES	Zotarolimus-freisetzender Stent

1 Einleitung

1.1 Epidemiologie und Relevanz der koronaren Herzerkrankung

Herz-Kreislauf-Erkrankungen gehören zu den häufigsten Todesursachen in Deutschland (1). Sie haben einen Anteil von 35 % (siehe Abbildung 1). Die geschätzte Lebenserwartung steigt weiter an, sodass unter rein epidemiologischer Betrachtung zukünftig mit einer Zunahme der Patienten mit Herz-Kreislauf-Erkrankungen zu erwarten ist (1,2).

Sterbefälle in Deutschland 2019

nach Todesursachen in Prozent

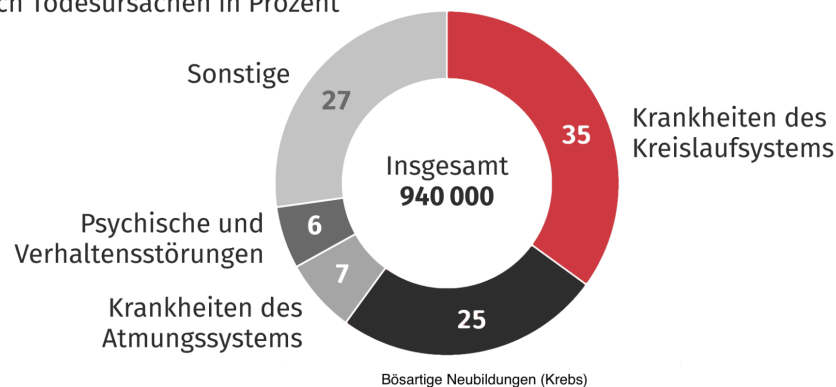


Abbildung 1: Todesursachen in Deutschland nach Krankheitsarten 2019

Quelle: Statistisches Bundesamt (Destatis), 2021

Der Großteil der Todesfälle, die sich durch Herz-Kreislauf-Erkrankungen begründen, ereignete sich im Rahmen einer chronisch ischämischen Herzerkrankung oder eines akuten Myokardinfarktes (siehe Abbildung 2). Im Jahr 2019 entsprach dies in Deutschland 7,9 % für die chronische und 4,7 % für die akute Form der koronaren Herzerkrankung (KHK) (1). Die Lebenszeitprävalenz – auf der anderen Seite – für einen akuten Myokardinfarkt bei 40- bis 79-Jährigen liegt bei 4,7 % und die der KHK (ohne Myokardinfarkt) bei 9,3 % (3).

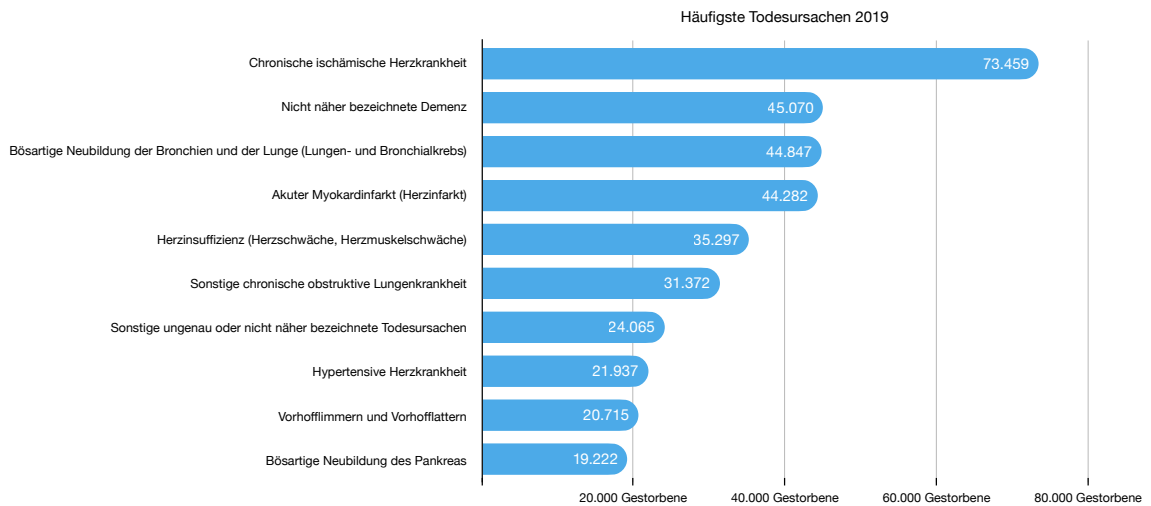


Abbildung 2: Häufigste Todesursachen in Deutschland 2019

Quelle: eigene Abbildung nach (1)

Epidemiologische Untersuchungen konnten Risikofaktoren für die Entwicklung einer koronaren Herzerkrankung identifizieren (4). Hierzu zählen unter anderem die arterielle Hypertonie, die Hypercholesterinämie, der Diabetes mellitus und das Rauchen (Nikotinabusus). Diese Risikofaktoren lassen sich positiv beeinflussen, sodass die KHK nach Möglichkeit nicht auftritt (Primärprävention) oder in ihrem Voranschreiten (Sekundärprävention) verlangsamt werden kann (siehe Abbildung 3) (5). Die Fortschritte in der Risikomodifikation durch Prävention und Akutbehandlung tragen wesentlich zu einer Reduktion der Sterblichkeit durch Herz-Kreislauf-Erkrankungen bei. Dennoch bleiben sie weiterhin die häufigste Todesursache (6). Hieraus ergibt sich die gesellschafts- und gesundheitspolitische Relevanz der Herz-Kreislauf-Erkrankungen, auch vor dem Hintergrund des demographischen Wandels.

1.2 Pathophysiologie der koronaren Herzerkrankung

Die koronare Herzerkrankung stellt eine klinische Manifestation der Atherosklerose in den epikardialen Gefäßen des Herzens dar. Hierbei kommt es zur Reduktion des Gefäßlumens und im Verlauf gegebenenfalls zu einer sich konsekutiv entwickelnden Minderperfusion. Die Erkrankung verläuft in aller Regel chronisch und häufig mit klinischem Progress durch Zunahme der Atherosklerose. Der stabile Verlauf kann jederzeit durch ein Akutereignis wie eine Plaqueruptur oder -erosion unterbrochen werden („ASCVD event“, siehe Abbildung 3). Die Erkrankung kann damit eine ausgeprägte Dynamik aufweisen, sodass die Europäische Gesellschaft für Kardiologie (ESC) die beiden Hauptmanifestationen der koronaren Herzerkrankung inzwischen als chronisches (CCS) oder akutes Koronarsyndrom (ACS) betitelt. Mit dieser Formulierung versucht die ESC insbesondere den Stellenwert der Chronizität hervorzuheben (7).

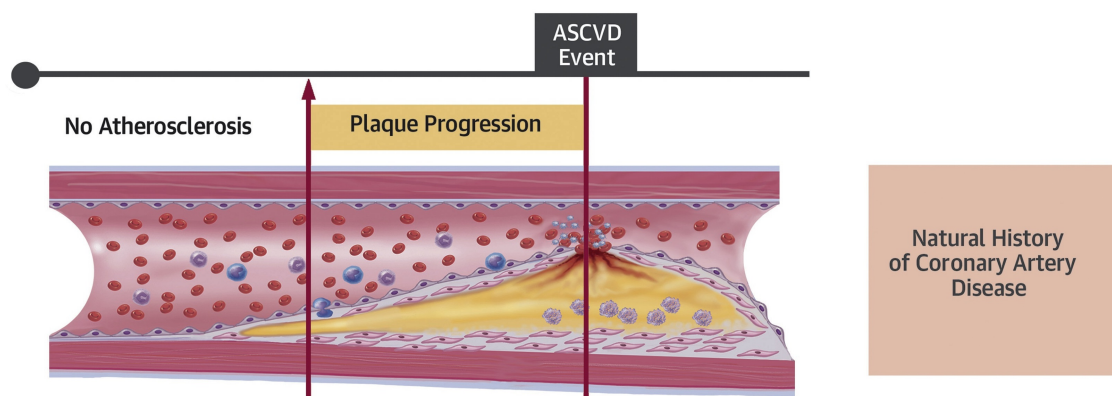


Abbildung 3: Atherosklerose als voranschreitender Progress

ASCVD: Atherosclerotic cardiovascular disease

Quelle: Ahmadi et al. (8)

Die Entwicklung der Atherosklerose ist multifaktoriell. Die Weltgesundheitsorganisation (WHO) definiert den Begriff als variable Kombination aus Intimaveränderungen mit fokaler Anreicherung von Lipiden, Kohlenhydraten, Blut/-produkten, fibrösem Gewebe und Kalziumablagerungen (9). Sie ist das Ergebnis veränderter Gefäßwandabnormitäten und einer komplexen Interaktion der Blutbestandteile.

Es lassen sich sechs Stufen beschreiben (10,11). In der ersten Entwicklungsstufe (Typ-I-Läsion) zeigen sich anfängliche Lipideinlagerungen, die Low-density-Lipoproteine (LDL), in der Intima. Sie finden sich insbesondere im jungen Alter und im Bereich von Gefäßabgängen und -bifurkationen (12). Die histologischen Veränderungen sind zunächst gering. Oxidiertes LDL vermittelt die Expression von Adhäsionsmolekülen und Ausschüttung von Chemokinen. Hierdurch kommt es zu einer Einwanderung von

Leukozyten. Makrophagen formieren sich unter Einschluss der Lipide vor allem in Bereichen verdickter Intima zu kleinen Zellverbänden (Schaumzellen) (13). Dies wird dann als Typ-II-Läsion beschrieben und lässt sich auch durch eine gelbliche Streifung („fatty streaks“) mikroskopisch erkennen. Es wurde beobachtet, dass sich die gelblichen Streifungen in den Koronararterien bereits ab etwa dem 15. Lebensjahr entwickeln können (14). Bei einem Voranschreiten zeigen sich extrazelluläre Lipidablagerungen als Kennzeichen der Typ-III-Läsion, dem Präatherom. Sie differenziert sich im Weiteren mit zunehmender Einwanderung von glatten Muskelzellen und durch das Konfluieren der Lipidpools zu einem Atherom mit lipidreichem Kern (Typ-IV-Läsion) (11,12). Im folgenden Stadium (Typ-V-Läsion) kommt es zur Ausbildung einer fibrösen Kappe. In Verbindung mit dem Lipidkern (Typ-IV-Läsion) wird dann von einem Fibroatherom gesprochen. Es kann zu einer zunehmenden Einengung des Gefäßlumens kommen. Die Typ-V-Läsion ist die häufigste Ausgangsläsion für Komplikationen (12), die in der Regel durch einen Einriss der fibrösen Kappe entstehen. Auch die Typ-IV-Läsion gilt als kompliziert und wird durch eine dominierende Kalzifikation im Atheromkern gelegener nekrotischer Areale charakterisiert.

Läsionen mit vergleichbarer Größe können morphologisch unterschiedlich zusammengesetzt sein. Ihre Zusammensetzung definiert das Risiko für Gefäßkomplikationen. Während hartes, kollagenreiches Bindegewebe den größten Anteil darstellt und als stabilisierend gilt, geht von einem weichen, lipidreichen (sog. atheromatösen) Kern ein destabilisierender Effekt aus. Hieraus ergibt sich, dass die Instabilität einer Läsion oder Plaque maßgeblich von dem Vorhandensein und der Größe des Atheromkerns definiert wird und ausgeht (15,16). In einem Gefäß, das einen thrombotischen Verschluss aufzeigt, lässt sich demnach häufiger ein Nekrosekern finden (17).

1.3 Diagnostik der koronaren Herzerkrankung

1.3.1 Chronisches Koronarsyndrom

Das klinische Beschwerdebild des chronischen Koronarsyndroms (CCS) ist variabel. Man fasst hierunter zunächst folgende typische Szenarien zusammen: i) Patienten mit vermuteter koronarer Herzerkrankung und stabiler pektanginöser Beschwerden oder Luftnot; ii) Patienten mit neu aufgetretener Herzinsuffizienz oder Dysfunktion des linken Ventrikels und vermuteter koronarer Herzerkrankung; iii) asymptomatisch oder symptomatische Patienten mit stabiler Beschwerdesymptomatik < 1 Jahr nach einem akuten Koronarsyndrom oder kurz zurückliegender Revaskularisation; iv) asymptomatisch oder symptomatische Patienten > 1 Jahr nach initialer Diagnose oder Revaskularisation; v) Patienten mit pektanginösen Beschwerden, vermuteter vasospastischer oder mikrovaskulärer Erkrankung; vi) asymptomatische Patienten, bei denen eine koronare Herzerkrankung im Rahmen einer Screeninguntersuchung aufgefallen ist (7). Die Diagnostik baut auf einer inkrementellen Evaluation auf (7):

Schritt 1: Zunächst muss eine gewissenhafte Erhebung der Patientenanamnese erfolgen. Sie sollte auch das Erfragen extrakardialer atherosklerotischer Erkrankungen und bekannter Risikofaktoren (z. B. familiäre Prädisposition hinsichtlich einer Herz-Kreislauf-Erkrankung, Hypercholesterinämie, Diabetes mellitus, arterielle Hypertonie, Rauchen) einschließen. Insbesondere das Kardinalssymptom der Angina pectoris (AP) muss kritisch hinterfragt werden, allerdings kann sich ein chronisches Koronarsyndrom auch durch Dyspnoe äußern. Von typischen pektanginösen Beschwerden spricht man beim Auftreten eines retrosternalen Drucks (ggf. mit Ausstrahlung in den Arm, die Schulter oder den Hals) unter Belastung, der durch körperliche Ruhe oder Nitrateinnahme innerhalb von fünf Minuten vergeht. Nicht immer werden die Beschwerden klassisch als belastungsabhängiger Druck beschrieben, auch ein Schweregefühl, eine thorakale Einengung, ein retrosternales (Sod-)Brennen oder Luftnot werden angegeben. Von atypischen pektanginösen Beschwerden spricht man daher, wenn zwei der drei Kriterien, die zur typischen AP zählen, vorhanden sind. Ein nicht anginöser Brustschmerz liegt bei einem oder keinem der Kriterien vor. Gemeinhin halten die Beschwerden durch Beenden der körperlichen Anstrengung insgesamt nicht länger als zehn Minuten an. Auf der anderen Seite sind nur sehr kurze Beschwerden ebenfalls untypisch für AP. Ein wichtiger Aspekt ist der Zusammenhang zwischen Auftreten der Beschwerden und körperlicher Belastung; dies sollte in der Anamnese herausgearbeitet werden. Die Mehrheit der Patienten stellt sich mit atypischen oder nicht anginösen Beschwerden vor (ca. 85–90 %) (18-20).

Schritt 2: Vor Anschluss eines klinischen Tests werden die Begleiterkrankungen und Komorbiditäten evaluiert. Dies schließt auch die kritische Prüfung der Indikation zur weiterführenden kardiologischen Diagnostik bei Verdacht auf das Vorliegen einer nicht kardialen Ursache ein. Darüber hinaus sollte in Abhängigkeit des Gesamtzustandes des Patienten auch geprüft werden, ob eine Revaskularisation überhaupt in Frage kommt.

Schritt 3: Die Basisdiagnostik umfasst im Weiteren eine Blutentnahme. Sie dient zum Ausschluss internistischer Differentialdiagnosen (z. B. Anämie), aber auch zur Prüfung etwaiger Risikofaktoren (z. B. HbA1c, LDL). Nur bei klinischer Instabilität, Unsicherheit oder begründetem Verdacht sollte die Blutentnahme myokardialen Nekrosemarker wie Troponin beinhalten. In Ergänzung erfolgt das Schreiben eines Ruhe-Elektrokardiograms (EKG) mit zwölf Ableitungen. Im EKG können beim beschwerdefreien Patienten womöglich Hinweise für einen abgelaufenen Herzinfarkt gefunden werden (Pardée-Q, R-Verlust). ST-Streckenveränderungen unter supraventrikulärer Tachykardie haben keinen prädiktiven Wert für die KHK (21). Es schließt sich eine transthorakale Echokardiographie mit der Frage nach der linksventrikulären Ejektionsfraktion und dem Vorliegen regionaler Wandbewegungsstörungen an. Auch ein Vitium cordis sollte ausgeschlossen werden.

Schritt 4: Unter Berücksichtigung der klinischen Beschwerden, dem Alter, dem Geschlecht und der Komorbiditäten erfolgt die Abschätzung der Vortestwahrscheinlichkeit (PTP) für das Vorliegen einer KHK. Bei einer PTP unter 15 % gilt die Prognose gemeinhin als gut, eine weiterführende Diagnostik ist üblicherweise nicht notwendig.

Schritt 5: Bei hoher Vortestwahrscheinlichkeit und hohem kardiovaskulärem Risiko, refraktärer Beschwerden unter optimierter medikamentöser Therapie oder typischen Beschwerden bereits bei geringer körperlicher Belastung kann eine invasive Koronardiagnostik mit der Möglichkeit einer Funktionsmessung erfolgen (7). Anderenfalls eignen sich insbesondere funktionelle Tests in der weiteren Abklärung (22,23). Hierzu zählt die Stress-Echokardiographie (ggf. mit Perfusionsanalyse), Stress-Magnetresonanztomographie oder Myokardszintigraphie.

1.3.2 Akutes Koronarsyndrom

Bei Patienten mit anhaltenden, akuten Beschwerden spricht man von einem akuten Koronarsyndrom (24). Zeigen sich im Ruhe-EKG signifikante ST-Streckenhebungen, erfolgt eine unmittelbare Zuweisung in ein Herzkatheterlabor zur invasiven Koronarangiographie unter dem Verdacht eines akuten Myokardinfarktes mit ST-Streckenhebungen (STEMI). Im anderen Fall entscheidet das Ergebnis der sequenziellen Bestimmung des

myokardialen Nekrosemarkers Troponin über das weitere Vorgehen (Nicht-ST-Streckenhebungsinfarkt, NSTEMI).

1.4 Therapieoptionen der koronaren Herzerkrankung

Hinsichtlich der möglichen Therapieoptionen bei der Behandlung der koronaren Herzerkrankung können zwei Ansätze unterschieden werden, die jedoch im Sinne eines personalisierten und individualisierten Ansatzes auch komplementär Anwendung finden können.

Man unterscheidet die *konservative und medikamentöse Strategie* von der Möglichkeit einer *interventionellen oder chirurgischen Revaskularisation*. Hierbei verfolgt man in beiden Fällen auf der einen Seite das Ziel einer größtmöglichen Reduktion der Symptomlast zur Verbesserung der krankheitsbezogenen Lebensqualität. Dies umfasst die Verminderung der Angina-pectoris-Häufigkeit und ihre Intensität. Auf der anderen Seite soll mittel- und langfristig eine Reduktion der Sterblichkeit und Verbesserung der Prognose erzielt werden (7,25).

1.4.1 Konservative Behandlungsstrategie

Die konservative Therapie der koronaren Herzerkrankung umfasst zunächst die Veränderung des Lebensstils. Hierunter versteht man den Verzicht auf Rauchen, die Aufnahme einer regelmäßigen körperlichen sportlichen Aktivität, eine gesunde Ernährung und Kontrolle eines Normalgewichts (26,27). Eine Verbesserung der Prognose kann nach circa sechs Monaten gemessen werden (28).

Die konservative Strategie schließt auch die medikamentöse Therapie mit ein. Diese umfasst als wesentlichen Baustein Medikamente mit anti-anginöser Wirkung. Als optimal wird in diesem Zusammenhang das Verhältnis aus bester Therapieadhärenz, größtmöglicher körperlicher Belastbarkeit und geringster Nebenwirkungen bezeichnet. Hierfür ist stets eine Individualisierung notwendig. Medikamente der ersten Wahl sind *Betablocker* oder *Kalziumkanalblocker* (29,30). Der Betablocker reduziert den myokardialen Sauerstoffverbrauch und ökonomisiert den Herzzyklus durch Verlängerung der Diastole. Für Patienten mit vorausgegangenem Herzinfarkt oder Vorliegen einer Herzinsuffizienz konnte für den Beta-Blocker eine signifikante Reduktion der Mortalität und Rate kardiovaskulärer Ereignisse nachgewiesen werden (31). Patienten mit chronischem Koronarsyndrom ohne Myokardinfarkt oder Herzinsuffizienz scheinen nicht in gleichem Umfang von der Einnahme des Beta-Blockers zu profitieren (32). Bei unzureichendem Ansprechen kann eine Kombination der beiden Wirkstoffe erwogen werden (33). Zu den anti-anginösen Medikamenten gehören auch *Nitrate*. Als weitere Substanzgruppen stehen *Ivabradin* (34) oder auch *Ranolazin* (35) zur Verfügung. Zur Vermeidung von kardiovaskulären Ereignissen, welche die Prognose beeinträchtigen, erfolgt die Empfehlung zur Einnahme

eines *Thrombozytenaggregationshemmers*. In aller Regel erfolgt dies mit Acetylsalicylsäure (ASS), was eine irreversible Hemmung der Cyclooxygenase-1 und hierdurch Thromboxan-Produktion bedingt (36). ASS kann hierdurch Ereignisse bei Patienten mit und ohne vorausgegangenem Myokardinfarkt verhindern (37). Eine intensivere Thrombozytenaggregation mittels P2Y₁₂-Inhibitoren (Prasugrel, Ticagrelor, Clopidogrel) über das ASS hinaus erfolgt zeitlich begrenzt üblicherweise nur nach Implantation eines Stents oder ACS (38-40). Als weitere Substanzgruppe kommen *Statine* zum Einsatz. Patienten mit koronarer Herzerkrankung gelten als Hochrisikokollektiv für kardiovaskuläre Ereignisse, sodass ein LDL-Cholesterin von < 55 mg/dl, aber mindestens eine Reduktion um 50 % vom Basiswert angestrebt werden sollte (41). Kann das durch Statine allein nicht erreicht werden, können Ezetimib, PCSK9-Hemmer (Proproteinkonvertase Subtilisin/Kexin Typ 9) oder Bempedoinsäure ergänzt werden. Außerdem findet sich die Gruppe der ACE (Angiotensin-Converting-Enzym)-Hemmer. Sie können die Mortalität reduzieren, beeinflussen die Myokardinfarkt- und Schlaganfallrate und haben einen positiven Effekt auf den Verlauf der Herzinsuffizienz. Sie sollten bei Patienten mit chronischem Koronarsyndrom und begleitender arterieller Hypertonie, eingeschränkter systolischer Funktion (LVEF unter 40 %), nach Myokardinfarkt und hohem kardiovaskulären Risikoprofil (z. B. Diabetes mellitus) eingesetzt werden (42,43).

1.4.2 Myokardiale Revaskularisation

Eine myokardiale Revaskularisation kann chirurgisch oder interventionell erfolgen. Sie hat – in Ergänzung zur medikamentösen Therapie – die Reduktion der klinischen Beschwerden und vor allem Verbesserung der Prognose zum Ziel (25).

Die kardiovaskuläre Mortalität konnte erheblich reduziert werden. Während 1950 noch mehr als 400 Todesfälle auf 100 000 Menschen durch kardiovaskuläre Erkrankungen fielen, liegt diese Zahl zwanzig Jahre später bei nur noch einem Viertel (44). Diese dramatische Verbesserung liegt unter anderem in den Entwicklungssprüngen der koronaren Bypass-Chirurgie durch die Herz- und Gefäßchirurgen und perkutanen Interventionen durch die Kardiologen begründet.

Beide Methoden können die Angina pectoris effektiv reduzieren. Hierdurch kommt es zu einer Verbesserung der Lebensqualität und körperlichen Belastbarkeit. Dies konnte beispielsweise in den fünf Jahresdaten der FAME-2 (Fractional Flow Reserve versus Angiography for Multivessel Evaluation 2)-Studie gezeigt werden. Während im Rahmen eines akuten Koronarsyndroms eine frühe Revaskularisation indiziert ist (25), zeigten Meta-Analysen für Patienten mit CCS bisher nicht, dass die PCI im Vergleich zur optimalen medikamentösen Therapie das Überleben oder die Herzinfarktrate grundsätzlich positiv

beeinflusst (45-49). Es findet sich in den Leitlinien eine Indikation zur Revaskularisation – nach Ischämietestung – bei Vorliegen einer mindestens 50%igen Hauptstammstenose, einer mindestens 50%igen Stenose der proximalen Vorderwandarterie (LAD), einer Mehrgefäßerkrankung mit mindestens 50%iger Stenosierung und reduzierter systolischer LV-Funktion, Ischämiearealen von größer 10% (25). Im Folgenden wird vor dem Hintergrund des Schwerpunkts der Arbeit der Fokus auf die PCI gelegt.

1.4.2.1 Perkutane koronare Revaskularisation

Die perkutane koronare Intervention (PCI) ist im Laufe ihrer Entwicklung zu einer der häufigsten Prozeduren weltweit geworden (siehe Abbildung 4). Die Anzahl von Linksherzkatheter-Untersuchungen im Rahmen einer stationären Behandlung in Deutschland im Jahr 2018 lag bei 867 137. Zu einer Intervention kam es bei 366 840 Patienten (1).

Die erstmalige Katheterisierung des Herzens wurde 1929 von Forssmann vorgenommen. Hierbei diente er selbst als Proband (50). Der Versuch wurde aufgrund zu großer Bedenken seiner Kollegen nach 35 cm abgebrochen. Forssmann erhielt später im Jahr 1956 zusammen mit Cournand und Richards für die Standardisierung der Herzkatheterisierung zur Ableitung der intrakardialen Drücke den Nobelpreis. Im Jahr 1953 beschrieb Seldinger die später nach ihm benannte perkutane Technik zur Katheterisierung (51). Eine selektive Darstellung der Koronargefäße gelang Sones fünf Jahre später (52). Die ersten Schritte der Gefäßbehandlung, also der Aufdehnung im Sinne einer Angioplastie, wurden im Bereich peripherer Gefäße von Dotter und Judkins unter Verwendung unterschiedlich großer Katheter zunehmender Größe unternommen (53). Die Kardiologie wurde 1978 von Grüntzig durch eine Ballonangioplastie einer Koronararterie revolutioniert (54). Es fand ein – aus heutiger Sicht einfacher – Ballon Anwendung. Doch diese Ballonangioplastie – heute als *plain old balloon angioplasty* (POBA) bezeichnet – war der wegweisende Schritt auf dem Weg zur modernen interventionellen Kardiologie.

Die POBA wurde mit viel Enthusiasmus und gesellschaftlichem Interesse verfolgt und von Kritik begleitet. So wurden etwa zeitgleich die ersten Over-the-wire-Techniken und Monorail-Systeme entwickelt (55,56). Allerdings wurde die erste Begeisterung für die neue Technik schnell getrübt, denn Limitationen wurden offensichtlich. Dazu gehörten die akuten Komplikationen, wie ein kompletter Gefäßverschluss als Folge einer direkten Verletzung durch Dissektionen, Bildung von Thrombus in immerhin 3–8 % der Fälle (57,58) und ein frühes Recoil durch elastisches Gewebe in 5–10 % innerhalb von wenigen Stunden (59). Es waren häufig eine erneute Angioplastie oder gar eine notfallmäßige Bypassoperation notwendig. Im mittel- bis langfristigen Verlauf zeigten sich mit

immerhin 33 % der Fälle hohe Raten von Restenosierungen, die auf eine neointimale Proliferation als inflammatorische Antwort auf die Dilatation zurückzuführen sind (60,61).

Die Limitationen der POBA haben die technologische Entwicklung zur Stabilisierung des primären Lumengewinns und die Behandlung der auftretenden Akut- oder Spätkomplikationen vorangetrieben. Bei der Entwicklung der ersten Koronarstents handelte es sich um eine gemeinsame Weiterentwicklung und Forschungsarbeit von Palmaz und Schatz, die 1985 einen ersten aus Metall bestehenden Koronarstent (*bare metal stent*, BMS) in das Herzkranzgefäßsystem eines Hundes implantierten (62). Ihr ging eine erfolgreiche Stentbehandlung im Bereich eines peripheren Gefäßes voraus (63). Die Implantation bei einem Menschen erfolgte 1986 durch Jaques Puel in Frankreich und kurz hierauf durch die Kollegen um Ulrich Sigwart in der Schweiz (64). Der Stainless-steel-self-expanding-mesh-Stent (Medinvent SA, Lausanne, Schweiz) wurde aufgrund einer Akutkomplikation mit drohendem Gefäßkomplettverschluss nach POBA notfallmäßig angewendet. Das Konzept der Stentimplantation rückte hieraufhin in den Fokus des Interesses und sorgte erfreulicherweise für einen Rückgang der notfallmäßigen Bypass-Chirurgie. Schatz und seine Kollegen konnten im Verlauf die Beobachtung machen, dass es unter der Hinzunahme von Thrombozytenaggregationshemmern zu einer deutlichen Abnahme der subakuten Thrombosen kam (65). Hieraus begründeten sich zwei abgeleitete Studien zu BMS: der European Belgium-Netherlands Stent Trial (BENESTENT) (66) und die American Stent Restenosis Study (STRESS) (67). In den Untersuchungen konnte bei über 900 eingeschlossenen Patienten die Rate von Zweiteingriffen nach einer Stentimplantation reduziert werden. Ebenfalls zeigte sich eine signifikante Reduktion der Restenoserraten (22 % vs. 32 %; $p = 0,02$ bzw. 31,6 % vs. 42,1 %; $p = 0,046$). In Bezug auf den kombinierten Endpunkt aus Tod, Myokardinfarkt, Bypassoperation, Gefäßverschluss und Stentthrombose zeigte sich zwischen der Stent- und POBA-Gruppe kein signifikanter Unterschied (80,5 % vs. 76,25 %; $p = 0,16$). Dies drückt sich auch in der Abnahme einer neuerlichen Intervention im Bereich der Zielläsion (*target lesion*) durch Myokardinfarkt aus (10,2 % vs. 15,4 %; $p = 0,06$). Die Ergebnisse dieser beiden Landmarkenstudien sorgten 1994 für die Zulassung durch die US-Behörde für Lebens- und Arzneimittel. Nur fünf Jahre später erfolgte bei ungefähr 84 % der Koronareingriffe die Implantation eines Metallstents (68).

Wenngleich durch die Metallstents eine deutliche Verbesserung der Patientenversorgung erreicht werden konnte, trat beispielsweise weiterhin eine übermäßige Hyperplasie der Neointima mit Ausbildung einer In-Stent-Restenose (ISR) in bis zu 30 % der Fälle oder eine akute Stentthrombose (ST) auf. Die wiederholten Eingriffe waren insbesondere bei Patienten mit erhöhtem kardiovaskulärem Risiko, wie Diabetes mellitus oder Bifurkationsläsionen, notwendig (69-71). Es wurden daher Versuche unternommen, das

Therapiekonzept weiter zu verbessern. In erster Linie betrifft dies das mechanistische Design des Stents. Nach Versuchen mit verschiedener Konfiguration („tubular“, „coil“, „ring“, „multi-design“) zeigte sich ein gekerbter oder geschlitzter („slotted“) Aufbau überlegen, da hierdurch zum einen die Intimahyperplasie positiv beeinflusst werden konnte und zum anderen der Stent eine höhere Radialkraft zur Vermeidung des Recoils aufwies (72,73). Es wurden ferner erste Versuche zur Beschichtung der Stentstreben mit Gold, Karbon oder Phosphorylcholine als auch zum Aufbau aus Tantal oder Nitinol unternommen. Hinsichtlich des Implantationsprozesses stellten sich Stents, die auf einem Ballon montiert implantiert wurden, denen gegenüber überlegen, die selbstexpandierend konzipiert waren. Hier spielte vor allem die bessere Handhabbarkeit eine entscheidende Rolle. Ein Problem, dass beispielsweise in schwer verkalkten oder torquierten Gefäßverläufen die Platzierung und den Einsatz der verfügbaren Stents maßgeblich einschränkte. Über die Weiterentwicklung des Stents selbst hinaus zeigte sich in Anschluss an die Beobachtung des besseren klinischen Verlaufs unter Thrombozytenaggregation von Schatz eine wachsende Evidenz für eine Reduktion der ST unter dualer Thrombozytenaggregation (DAPT) (74). Da sich hierdurch allerdings die ISR nicht signifikant reduzieren ließ, erfolgte die Entwicklung von Stents, die eine antiproliferative Beschichtung aufwiesen. Konzeptionell sollte die Beschichtung den Wirkstoff unmittelbar in das Gefäßendothel abgeben.

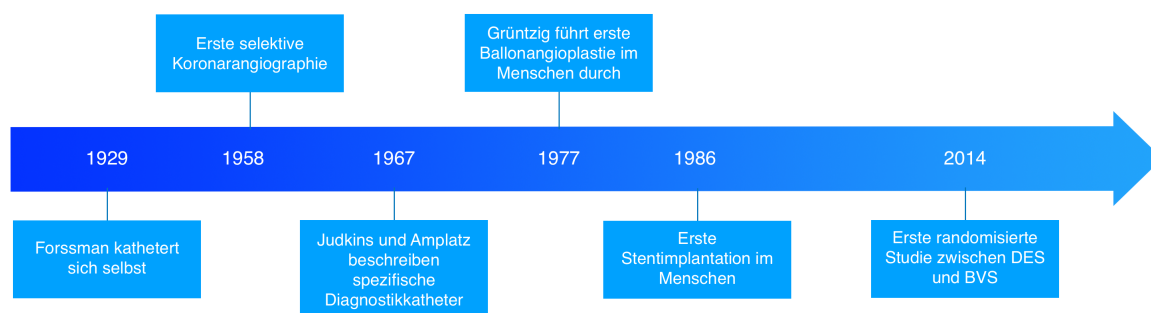


Abbildung 4: Zeitleiste der wesentlichen Meilensteine des Herzkatheters

Quelle: eigene Abbildung

Die medikamentenfreisetzenden Stents (DES) bestanden in ihrer *ersten Generation* aus drei Komponenten: dem Metallgerüst (*metal stent scaffold*), dem Medikament und einem Polymer, das auf dem Stent aufgetragen für die langsame Abgabe im Sinne eines Wirkstoffreservoirs verantwortlich war. Die beiden 2003 durch die US-Behörde für Lebens- und Arzneimittel zugelassenen DES waren Taxus (Boston Scientific Corporation, USA) und Cypher (Cordis Corporation, USA). Der jeweilige Stent basierte auf dem Grund-BMS-Modell und war im Falle von Taxus mit Paclitaxel beschichtet. Diese antimittotisch

wirkende Substanz inhibiert die Proliferation und Migration von glatten Muskel- und Endothelzellen (75). Cypher auf der anderen Seite nutzte Sirolimus, ein mTOR-Inhibitor (76,77). Beiden Stents war gemein, dass für sie eine Überlegenheit hinsichtlich des Auftretens von ISR und einer wiederholten Revaskularisierung des Zielgefäßes (TVR) nachgewiesen werden konnte (61,75,78-81). Im direkten Vergleich zwischen Paclitaxel-freisetzenden Stents (PES) und Sirolimus-freisetzenden Stents (SES) konnte kein signifikanter Vorteil für eine der beiden Plattformen gezeigt werden (78). Trotz der beschriebenen Überlegenheit gelang im klinischen Verlauf kein Nachweis einer Mortalitätsreduktion (79,82). Der Grund hierfür liegt unter anderem in der Rate später ST (83,84). In histopathologischen Untersuchungen ließ sich zeigen, dass eine chronische Inflammation, die sich durch Lymphozyten, Makrophagen und Infiltration eosinophiler Zellen in die Intima und Media charakterisiert, beteiligt sein muss. Die Genese der späten ST ist insgesamt aber sicher multifaktoriell, komplex und nicht vollständig verstanden (85,86).

Hieraus entwickelte sich im Verlauf die *zweite Generation* der medikamentenfreisetzenden Stents. Eine der Grundlagen hierfür war die Beobachtung, dass die Medikamente ihre Wirkung in der Gefäßwand besser entfalten können, wenn sie lipophiler sind (87). Dieses Kriterium wird von Everolimus (z. B. Xience von Abbott Vascular) oder Zotarolimus (z. B. Resolute von Medtronic) erfüllt. Im Weiteren wechselte man Edelstahl (stainless steel) gegen eine chrombasierende Plattform aus. Die Legierung ermöglichte eine erleichterte Platzierung im Gefäß durch verbesserte Beweglichkeit (88). Platinum-Chrom kombinierte die elastische Eigenschaft von Edelstahl mit erhöhter Stabilität, Sichtbarkeit (89) und geringerer Materialdicke (80–90 µm vs. 130–140 µm) (90). In einem dritten Punkt unterscheidet sich die zweite DES-Generation auch in der Zusammensetzung des Polymers, das durch eine bessere Biokompatibilität die Hypersensitivitätsreaktion positiv beeinflusst und so die Rate an späten ST reduzieren sollte (91). In einer Meta-Analyse von Dangas et al. wurden 4989 Patienten nachverfolgt, die prospektiv randomisiert entweder mit einem Everolimus(EES)- oder Paclitaxel(PES)-Stent behandelt wurden. Es konnte unter anderem gezeigt werden, dass es bei EES zu einer geringeren Rate von Zielläsionsversagen (target lesion failure, TLF), ST und dem kombinierten kardialen Endpunkt MACE (Schlaganfall, Myokardinfarkt und kardiovaskulärer Tod) kommt (92). Ähnliche Ergebnisse wurden von Wijns et al. beschrieben, die Zotarolimus-freisetzende Stents (ZES) untersuchten. Im Zeitraum der klinischen Nachverfolgung von vier Jahren zeigte sich durch ZES eine Risikoreduktion für eine ST und dem kombinierten Endpunkt aus Tod und Myokardinfarkt (93). ZES und EES scheinen sich in Hinblick auf ihre Sicherheit in Studien und Meta-Analysen nicht signifikant zu unterscheiden (94,95). Die Zweitgeneration der verfügbaren DES zeigte sich demnach in der Zusammenfassung der

Erstgeneration überlegen (96). Diese Überlegenheit der neu entwickelten Plattformen drückt sich allerdings nicht nur über die genannten Komplikationen aus, sondern betraf auch und im Besonderen die Möglichkeit einer verkürzten DAPT (97). Während die Empfehlung zur DAPT anfänglich noch bei 12 Monaten lag, wird mittlerweile empfohlen dies im chronischen Koronarsyndrom nach Implantation der neueren Generation von DES üblicherweise auf 3 Monate zu beschränken (98). Hierdurch konnten auch die Blutungskomplikationen signifikant reduziert werden (99,100).

Bereits bei der Zweitgeneration der DES war der beobachtete chronische Inflammationsprozess, der bei der Entstehung später ST beteiligt ist, Antrieb zur Weiterentwicklung der Plattform. In einem weiteren, sich anschließenden Schritt wurde versucht, auf das Polymer zu verzichten. Die so entstandene Plattform ähnelt im langfristigen Verlauf den BMS. Bei sogenannten *polymerfreien Stents* ist das freizusetzende Medikament in der Legierung eingelagert und reduziert so den Inflammationsprozess auf lange Sicht. Hierdurch konnte insbesondere die Dauer der DAPT und das damit einhergehende Blutungsrisiko minimiert werden. Die sogenannte LEADERS-FREE-Studie (101) untersuchte bei 2466 Patienten mit erhöhtem Blutungsrisiko die Sicherheit (BioFreedom) im Vergleich zu BMS. In der polymerfreien Stentgruppe wurde nach 390 Tagen der primäre Endpunkt (kombinierter Endpunkt aus kardialen Tod, Myokardinfarkt oder ST) von 9,4 % der Patienten erreicht und von 12,9 % in der BMS-Gruppe ($p < 0,001$ für nicht unterlegen bzw. $p = 0,005$ für überlegen). Im selben Zeitraum fand sich eine TLR von 5,1 % bzw. 9,8 % ($p < 0,001$).

Im Unterschied zu den polymerfreien Stents wird das Polymer bei *bioabsorbierbaren Polymer-DES* in einem Zeitraum von 6 bis 12 Monaten absorbiert. Auch hierdurch soll die Gefahr einer späten ST reduziert werden, da das Polymer den chronischen Inflammationsprozess nicht dauerhaft unterhalten soll. In der LEADERS-Studie (102) konnten Seruys et al. mit der Unterstützung von zehn Zentren insgesamt 1707 Patienten einschließen. In dieser „all-comers“-Studie sollte die Nichtunterlegenheit im Vergleich zu konventionellen Polymer-Stents gezeigt werden. Hierfür wurden die Patienten in eine der beiden Gruppen randomisiert. Nach fünf Jahren konnte gezeigt werden, dass es zu einer signifikanten Reduktion der späten ST ($n = 5$ [0,7 %] vs. $n = 19$ [2,5 %]; RR: 0,26 [95 % CI: 0,10–0,68]; $p = 0,003$) und Abnahme des primären Endpunktes, der als kardialer Tod, Myokardinfarkt und klinisch motivierte TVR innerhalb von neun Monaten definiert wurde, kommt ($n = 3$ aus 749 vs. $n = 14$ aus 738; RR: 0,20 [95 % CI: 0,06–0,71]; $p = 0,005$). In einer Meta-Analyse, die 16 randomisierte Studien und insgesamt 19886 Patienten umfasste, zeigte sich keine signifikante Verbesserung in Hinblick auf TVR, kardialen Tod, Myokardinfarkt oder Stentthrombose (103).

1.5 Bioresorbierbare Scaffolds: Eine neue Stenttechnologie

Die existierenden Stentplattformen vereint das Persistieren eines Metallgeflechts. Dieses bleibt nach endgültiger Freisetzung des Medikamentes und ggf. der Resorption des Polymer im Gefäß dauerhaft liegen. Im Idealfall ist es vollständig endothelialisiert. Der Verbleib birgt über die Akutphase und den Heilungsprozess des erkrankten Abschnittes hinaus allerdings die Gefahr für Interaktionen und Komplikationen. Hinweise hierfür leiten sich beispielsweise aus Autopsiestudien ab, welche die Entstehung von Neoatherosklerose im Stent beschreiben (104). Das Metallgeflecht behindert ferner die vasomotorische Funktion und kann auch im langfristigen Verlauf zu mechanischen Problemen durch beispielsweise Frakturen führen (105). Die treibende konzeptionelle Idee hinter der Entwicklung einer neuen Generation von Stents beruht also auf dem Wunsch einer transienten – ergo zeitlich begrenzten – Stabilisierung des Gefäßes, aber rechtzeitigen Resorption (siehe Abbildung 5). So sollen anfänglich ein Recoil vermieden und die Gefäßintegrität unterstützt werden, und auf der anderen Seite die Ausbildung von Neoatherosklerose, ein negatives Remodelling und dauerhafter Verbleib von Fremdmaterial mit Chronifizierung eines Inflammationsprozesses sinnvoll abgewogen werden. Man spricht von bioresorbierbaren Scaffolds (BRS), um den temporären Ansatz der sich im Verlauf auflösenden Stents hervorzuheben.

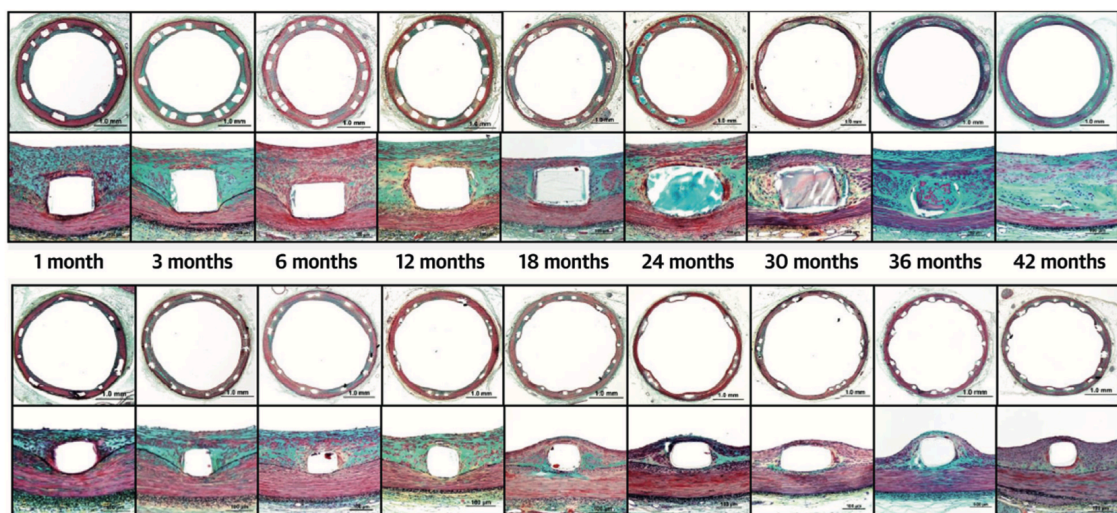


Abbildung 5: Abbau der bioresorbierbaren Struts (oben) im Schweinemodell im Vergleich zu einem DE-Stent (Xience)

Quelle: Wiebe et al. (106)

Es gibt verschiedene Materialien, die bei der Entwicklung der BRS Anwendung finden (siehe Tabelle 1). Das häufigste genutzte Material ist Poly-L-Laktid (PLLA). Das PLLA-Polymer hat gegenüber Polycaprolacton und Polycarbonate zum einen eine bessere

longitudinale Kraft und weist zum anderen durch eine zusätzliche Methylgruppe eine langsamere Absorptionsgeschwindigkeit auf, sodass es insgesamt hydrophober und weniger anfällig für die Hydrolyse ist (107,108). Die longitudinale Kraft erklärt sich unter anderem durch das teilkristalline Polymer mit hoher Glasübergangstemperatur (*glass transition temperature*, T_g) (109). Die Radialkraft auf der anderen Seite ist im Vergleich zu den aktuellen DES geringer, sodass ein höherer Materialeinsatz und Dicke der Struts gewählt werden muss, um dies zu kompensieren (110). Die Strutdicke beträgt üblicherweise 150 μm .

Die Bioresorption durch Degradation durchläuft drei Schritte. In einem ersten Schritt kommt es zur Hydrolyse des amorphen Anteils des Polymers. Dieser ist weniger kompakt und wegen der endständigen Carbonsäure-Gruppe anfälliger. Die Molekularmasse reduziert sich, die mechanischen Eigenschaften zunächst jedoch nicht (111). Im zweiten Schritt kommt es durch Aufspaltung der amorphen Verbindungen zu einem Verlust der Polymerstruktur und damit zu struktureller Diskontinuität (111). Hieran schließt sich eine Transformation von L-Lactat in Pyruvat an, was dann in den Citratzyklus eingespeist und schließlich in diesem zu Wasser und Kohlenstoffdioxid umgewandelt wird. Das Endprodukt wird über Niere und Lunge ausgeschieden (112).

	Absorb BVS	DESolve	DESolve CX
Strebendicke	150 μm	150 μm	120 μm
Design	PLLA	PLLA	PLLA
Medikament	Everolimus	Myolimus	Novolimus
Konzentration	10 $\mu\text{g}/\text{cm}^2$	5 $\mu\text{g}/\text{mm}^2$	k. A.
Degradierung	ca. 3 Jahre	1 Jahr	6 Monate
Resorption	ca. 3 Jahre	ca. 1–2 Jahre	ca. 2 Jahre
Hersteller	Abbott Vascular, USA	Elixir Medical Corp., USA	

Tabelle 1: Übersicht über PLLA-basierte Scaffolds

Folgende PLLA-basierte BRS konnten eine CE (Conformité Européenne)-Zertifizierung erlangen: der *Absorb BVS* von *Abbott Vascular* (Abbott Vascular Inc, Santa Clara, CA, USA) und der *DESolve-Scaffold* von *Elixir* (Elixir Medical Corporation, Milpitas, USA). Für den Absorb BVS (siehe Abbildung 6) liegen die meisten klinischen Daten vor (113). Der Absorb-Scaffold ist mit Everolimus beschichtet und wurde in den ABSORB-Studien untersucht. In der „first-in human“-ABSORB-Cohort-A-Studie, angelegt mit einem open-label Design, wurden insgesamt 30 Patienten mit einer singulären De-novo-Stenose behandelt. Der prozedurale Erfolg lag bei 100 % (114). Im Nachbeobachtungszeitraum

von fünf Jahren berechnete sich die MACE-Rate auf 3,4 % (115). Man fand zwar einen Hinweis für die Erholung der vasomotorischen Funktion (116), jedoch zeigte sich eine Abnahme der *minimalen Lumenfläche* (MLA) innerhalb von zwei Jahren und – mittels intravaskulärem Ultraschall (IVUS) – ein Verlust der Radialkraft durch Recoil (117,118). Hieraufhin wurde der Absorb BVS 1.1 entwickelt, der eine erhöhte und verlängerte Radialkraft bei unveränderter Strutdicke aufweist. In der ABSORB-II-Studie wurde der BVS mit EES verglichen und zeigte vergleichbare 1-Jahresdaten, wenngleich sich für den BVS in der quantitativen Auswertung ein etwas geringerer akuter Lumengewinn darstellte (119). Hierauf folgte die ABSORB-III-Studie, eine randomisierte Studie bei 1322 Patienten zwischen BVS und EES, die nach einem Jahr eine Nichtunterlegenheit mit TLF-Raten von 7,8 % in der BVS-Gruppe und 6,1 % in der EES-Gruppe zeigen konnte ($p = 0,007$) (120). Auch die Rate an kardialen Tod, Myokardinfarkt oder ischämiegetriggelter TLR waren vergleichbar. Es fanden sich jedoch erste Hinweise auf eine erhöhte Rate an ST (1,5 % BVS vs. 0,7 % EES; $p = 0,13$). Über die ABSORB-Studien hinaus hat auch die Amsterdam Investigator-initiated Absorb (AIDA)-Studie BVS gegenüber DES untersucht (121). Ihr Stellenwert ergibt sich unter anderem aus den weniger streng definierten Einschlusskriterien für die Patienten, die im Durchschnitt zwei Jahre lang nachverfolgt werden sollten. Die Studie wurde jedoch aufgrund von Sicherheitsbedenken vorzeitig veröffentlicht, da sich bereits vor Abschluss der Nachverfolgung eine signifikant erhöhte Rate an ST abzeichnete. Diese Beobachtung wurde in den Meta-Analysen um Cassese et al. (122) und Lipinski et al. (123) bestätigt. Sie zeigten eine Verdoppelung der ST- (OR 2,06; 95 % CI: 1,07–3,98) und MI-Raten (OR 2,06; 95 % CI: 1,31–3,22). Als mögliche Ursachen wurden die dickeren Struts im Vergleich zum DES und die Implantationstechnik genannt. Letztere kann durch Postdilatation beispielsweise zu Frakturen oder Malapposition führen, sodass der Implantationsprozess sich an das Device adaptieren musste (124).

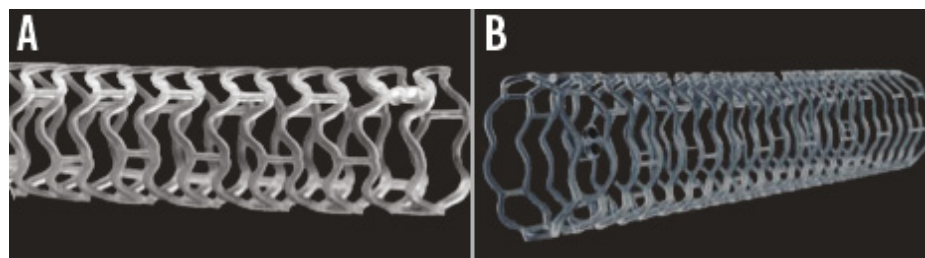


Abbildung 6: Absorb BVS (A) und DESolve-Scaffold (B)

Quelle: Mattesini et al. (125)

Der DESolve-BRS (siehe Abbildung 6) baut ebenfalls auf einer PLLA-Plattform auf. Er setzt Novolimus frei und seine Struts sind in der ersten Generation ebenfalls 150 μm dick. Der sogenannte DESolve CX in der zweiten Generation zeigt eine Strutdicke von 120 μm . Schätzungsweise 95 % des Devices sind nach ungefähr einem Jahr resorbiert (126). Eine Überexpansion bei der Implantation wird nicht empfohlen, auch wenn der DESolve größere Sicherheitsmargen für die Expansion zur Vermeidung von Frakturen im Vergleich zum Absorb ausweist (127). Als weiteres Alleinstellungsmerkmal kann der DESolve geringe Malappositionen durch Selbstkorrektur kompensieren (126,128). In einer Beobachtungsstudie wurden 102 Patienten eingeschlossen. Nach zwölf Monaten wurde bei 1,0 % eine Scaffoldthrombose (ScT) beobachtet und es kam in 3,0 % zu einem Myokardinfarkt mit TLR (129).

1.6 Intravaskuläre Bildgebung: optische Kohärenztomographie

Die optische Kohärenztomographie (OCT) geht auf die ursprünglichen Untersuchungen um 1990 von David Huang zurück, der im Rahmen seiner Teilnahme am Postgraduierten-Programm am Massachusetts Institute of Technology (MIT) die Kohärenztomographie (Optische Frequenzbereichsreflektometrie) und ihren Einsatz als bildgebende Modalität im Bereich des Auges erforschte. Die ersten Aufnahmen erfolgten in Wellenform und waren für das menschliche Auge und Gehirn schwer zu interpretieren, sodass ergänzende transversale Aufnahmen in Kombination mit einer intelligenten Software notwendig waren, um – in Analogie zu der Ultraschalltechnik – eine räumliche Auflösung und damit Berücksichtigung der Gewebetiefe möglich zu machen (130). Die Arbeitsgruppe am MIT fokussierte ihr Interesse zunächst auf die Anwendung im augenärztlichen Bereich, da sie großes Potential im Einsatz als In-vivo-Mikroskop sahen, ohne dass eine Gewebeprobe entnommen werden musste. Bereits 1996 wurde von Brezinski jedoch der In-vitro-Einsatz im Koronargefäßsystem als erfolgsversprechende Erweiterung in der Diagnostik der koronaren Herzerkrankung berichtet (131), sodass diese ihren Weg in die klinische Routine gefunden hat (132-134).

OCT kann mit dem gepulsten Ultraschallverfahren der Echokardiographie verglichen werden, verwendet allerdings im Gegensatz hierzu keine Schallwellen, sondern beruht auf einer Licht-basierenden Technologie. Ultraschall nutzt die reflektierten Schallwellen, um hieraus ein Bild zu generieren. OCT dahingegen verwendet Infrarotlichtwellen, die von den Mikrostrukturen innerhalb des Gewebes reflektiert werden. Die Wellenlänge des verwendeten Lichts liegt um $1,3\ \mu\text{m}$. Im Gegensatz dazu liegt die Wellenlänge beim intravaskulären Ultraschall (IVUS) im Megahertz-Bereich (siehe Tabelle 2). Damit erreicht die OCT eine zehnfach höhere Auflösung im Vergleich zu intravaskulärem Ultraschall (IVUS).

Die Auflösungskapazität der OCT wird durch die Lichtwellengeschwindigkeit definiert. Damit wird der minimale Abstand zweier Punkte beschrieben, die als solche individuell abgebildet werden können. Die *axiale Auflösung* beschreibt die Diskriminierung zweier Punkte parallel zum Lichtstrahl und liegt um $10\text{--}20\ \mu\text{m}$. Das Licht wird durch eine Linse am Katheter-Ende fokussiert und in Richtung der Gefäßwand gerichtet. Dieser Fokus („minimum diameter spot“) liegt üblicherweise $1\text{--}3\ \text{mm}$ hinter dem Katheter-Ende und definiert sich unter Berücksichtigung der Rayleigh-Streuung als axialer Abstand vom Fokus, wo sich der Diameter des Spots um den Faktor $\sqrt{2}$ vergrößert. Die *laterale Auflösung* wiederum diskriminiert zwei Punkte perpendicular zum Lichtstrahl und liegt um $25\text{--}30\ \mu\text{m}$ (siehe Abbildung 7). Sie ist im Bereich des Fokus am höchsten. Je weiter der Punkt

von der Linse entfernt ist, desto ungenauer kann seine Abbildung sein. Die hohe Ortsauflösung geht aus technischen Aspekten zu Lasten der *Eindringtiefe* („penetration depth“). Die maximale Eindringtiefe liegt bei etwa 1,5–2 mm und wird durch die Schallschwächung des Lichts beeinflusst. Der vordergründige Aspekt bei der Dämpfung stellt die Zerstreuung des Lichts im Gewebe dar. So zeigt lipidreiches Gewebe beispielsweise ein vergleichsweise hohes Maß an Dämpfung, sodass die Eindringtiefe in betroffenen Abschnitten geringer ausfällt. Gewebe mit hohem Anteil an Kollagen und Calcium wiederum schränken die Ausbreitung durch Dämpfung in geringerem Umfang ein, sodass die Eindringtiefe hier größer ausfällt. Hinsichtlich der Eindringtiefe muss im Rahmen der Akquisition – dem sogenannten „Pullback“ – auch der Aspekt berücksichtigt werden, dass das Gefäß durch Kontrastmittelinjektion blutleer gemacht werden muss, da es andernfalls insbesondere durch Erythrozyten zu Signalartefakten kommt.

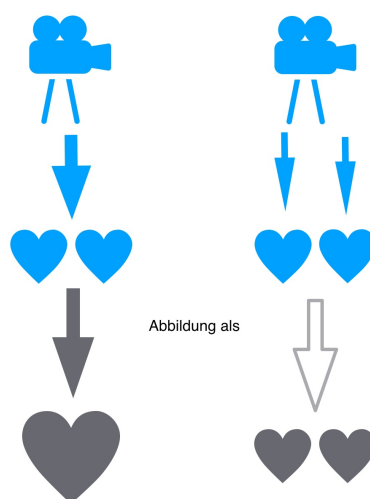


Abbildung 7: Schematische Darstellung divergenter lateraler Auflösungen: die beiden blauen Herzen im linken Teil können im Gegensatz zum rechten Beispiel aufgrund der niedrigeren Auflösung nicht als zwei separate Objekte dargestellt werden.

Quelle: eigene Abbildung

Das der OCT zugrunde liegende Licht hat eine höhere Geschwindigkeit als Ultraschallwellen, sodass ein Interferometer benutzt wird (135). Das Interferometer spaltet das (Anregungs)Licht in zwei Anteile („Arme“) – ein sogenanntes Referenzlicht („reference arm“) und ein Probenlicht („sample arm“). Letzterer Anteil wird in das zu untersuchende Gewebe gesendet, ersterer legt eine vordefinierte Strecke zurück. Beide Arme werden im Detektor registriert und zum Interferogramm zusammengefasst (136,137). Hierdurch entsteht ein Interferenzmuster mit hoher und niedriger Intensität, das durch das OCT-System analysiert wird, um eine Funktion aus Verzögerungszeit bzw. Eindringtiefe aus dem

zurückgestreuten Licht zu erstellen (A-Linie). Der Brechungsindex oder Wellenwiderstand („optical impedance“) zwischen zwei Schichten oder Geweben beeinflusst den Anteil des zurückgestreuten Lichts und definiert hierüber die Intensität des OCT-Bildes. Für eine planare Struktur mit Dimensionen oberhalb der Lichtwellenlänge, beispielsweise den Struts von Stents, ist das reflektierte Licht demnach bei möglichst perpendikularem Auftreffen am höchsten. Die einzelnen Querschnittsbilder („cross-sectional image“) werden durch eine Rotation der Linse beim Rückzug („Pullback“) erstellt.

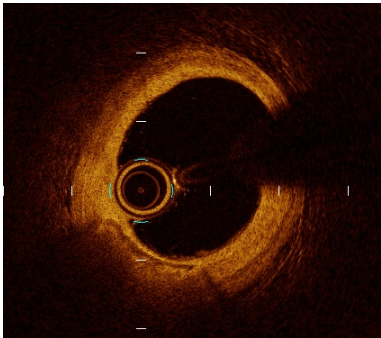
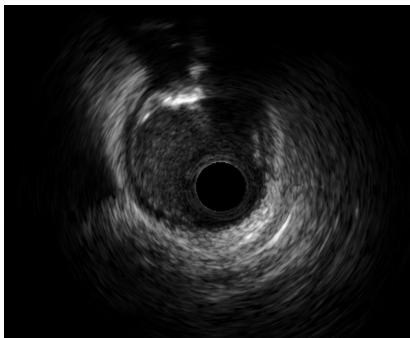
		
	OCT	IVUS
Wellenlänge	1,3 μm	20–45 MHz
Axiale Auflösung	10–20 μm	100–150 μm
Laterale Auflösung	25–30 μm	150–300 μm
Bildfrequenz	100 Bilder/Sekunde	30 Bilder/Sekunde
Eindringtiefe	1,5–2 mm	4–8 mm
Größe	2,7 Fr	2,9–3,2 Fr
Blutleere	Ja	Nein
Gefäßokklusion	Nein	Nein

Tabelle 2: Gegenüberstellung von optischer Kohärenztomographie (OCT) und Intravaskulärem Ultraschall (IVUS)

Es existieren grundsätzliche zwei OCT-Systeme. Bei dem früheren *Time-Domain-OCT* (*TD-OCT*) findet kurzkohärentes, breitbandiges Licht Anwendung. Es entsteht nur dann ein Interferenzsignal, wenn die Längen des Referenz- und Probenlichts im Interferometer vergleichbar sind. Hierfür muss eine mechanische Spiegelbewegung erfolgen, um die Rückstreuamplitude in den korrespondierenden Tiefenpositionen der Probe zu bestimmen. Benachbarte Lichtstrahlen ergeben durch die Rotation des Systems schließlich ein Querschnittsbild. Dies hat zur Folge, dass sich die TD-OCT nicht für schnelle Bildgebung eignet (138,139). Im klinischen Alltag finden sich daher überwiegend OCT-Systeme, die

auf dem Prinzip der *Frequency-Domain-OCT* (FD-OCT) basieren. Das interferierte Licht wird spektral zerlegt und ermöglicht so die Detektion des Interferenzspektrums, das mit den zu den Wegdifferenzen zwischen Proben- und Referenzlicht proportionalen Frequenzen moduliert ist. Durch Aufnahme der gesamten Tiefeninformation wird eine wesentliche Verbesserung des Signal-zu-Rausch-Verhältnisses erreicht. Mit Hilfe der Fourier-Transformation berechnet sich die Tiefeninformation, ohne dass eine Spiegelbewegung notwendig ist. Aufgrund der fehlenden Mechanik erreicht das auf FD-OCT basierende System damit eine deutlich erhöhte Auslesegeschwindigkeit. Dies geht einher mit einer erhöhten Sensitivität, mit größerer Abtastrate und Scantiefe (140-142). Es können so etwa 10^5 A-Linien pro Sekunde generiert werden. Die Eindringtiefe mit akzeptabler Qualität erhöht sich etwa um den Faktor 3 (139).

In der klinischen Routine wird die OCT sowohl zur Darstellung von Strukturen als auch für die Beurteilung des Schweregrads der Koronarerkrankung in großem Detailreichtum genutzt. Die beispiellose Auflösung erlaubt dabei die Charakterisierung des Gewebes und Darstellung der Zusammensetzung von Plaques. So können diese aus kalzifizierenden, fibrösen oder lipidreichen Anteilen zusammengesetzt sein. Gleichermäßen erlaubt die OCT die Beurteilung der Stentimplantation bzw. unterstützt den Implantationsprozess. Unter methodischen Aspekten wird der angefertigte „OCT-Pullback“ in einzelne Querschnittsbilder „geschnitten“ (siehe Abbildung 8). Diese werden für die Berechnung folgender beispielhafter Kennparameter herangezogen:

- Anteil inkomplett appositionierter Struts (ISA): prozentualer Anteil der Struts mit Malapposition im 1-mm-Intervall/Gesamtanzahl Struts
- ISA Fläche (in mm^2)
- prolabierende Gewebefläche (in mm^2): Differenz zwischen der abluminalen Scaffoldfläche und der Querschnittsfläche des Gefäßes
- verbliebende residuale Flächenstenose (RAS, in %): $(1 - [\text{minimale Lumenfläche} / \text{Referenz Gefäßfläche}]) \times 100$
- Referenzgefäßfläche (in mm^2): Summe aus proximaler und distaler Referenzfläche durch 2
- Exzentrizitätsindex: Verhältnis aus minimalem und maximalem Diameter. Für jeden Scaffold wurde der Index querschnittsweise (Intervall 1 mm) berechnet und so hieraus der mittlere und minimale Exzentrizitätsindex berechnet.
- Symmetrieindex: Verhältnis aus der Differenz aus maximalem und minimalem Scaffold-Diameter und dem maximalen Scaffold-Diameter.

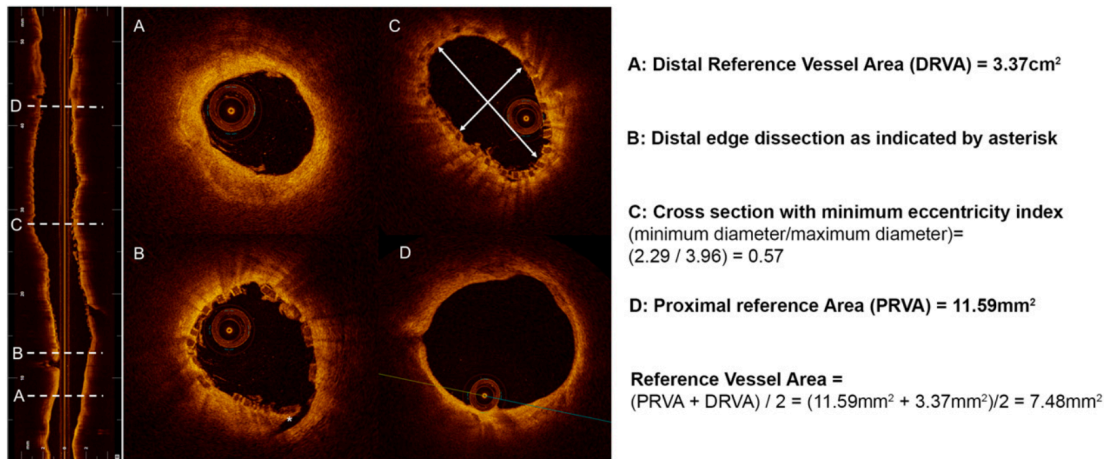


Abbildung 8: Longitudinaler „Pullback“ und exemplarische Querschnitte zur Berechnung der Kennparameter

DRVA: distale Referenzfläche; PRVA: proximale Referenzfläche

Quelle: Boeder et al. (143)

Insbesondere bei unklaren Situationen oder Läsionen hilft die OCT aber auch in der Beurteilung, um hieraus therapeutische Schritte abzuleiten.

2 Zielsetzung der kumulativen Habilitationsschrift

Der vorliegenden Habilitationsschrift liegt die Fragestellung zu Grunde, wie das akute mechanische Implantationsergebnis in einem unselektierten Patientenkollektiv ist, das mit bioresorbierbaren Gefäßstützen (BRS) behandelt wurde – unter Berücksichtigung und Verwendung der optischen Kohärenztomographie als intravaskuläre Bildgebungsmodalität. Im Weiteren sollen Aspekte der prozeduralen Implantationsstrategie auf das Primärergebnis und die Abhängigkeit von der vorliegenden Plaquelast, -Morphologie und -Zusammensetzung untersucht werden. In Hinblick auf klinische Endpunkte und Sicherheit soll insbesondere der Stellenwert der oralen Antikoagulation im Kontext der anti-thrombotischen Therapie unter Berücksichtigung der bisher gemachten klinischen Erkenntnisse bewertet werden. Ferner soll das zentrale Problem des Scaffold-Versagens adressiert und die Frage nach dem prospektiven Stellenwert der Malapposition für das zukünftige Auftreten von Scaffoldthrombosen untersucht werden.

3 Eigene Arbeiten

3.1 Akutes mechanisches Ergebnis

Der technologische Fortschritt der BRS soll im Besonderen in der zeitlich beschränkten Stabilisierung des behandelten Gefäßabschnittes liegen, denn langfristig löst sich die Scaffoldstruktur über verschiedene Abbauwege auf. In Verbindung mit ihrem klinischen Einsatz entstanden Bedenken hinsichtlich der Sicherheit, u. a. bedingt durch eine erhöhte Thrombogenität. So untersuchte das GHOST-EU-Register knapp 1200 Patienten, die mit einem Absorb BVS behandelt worden sind. Die Rate der Scaffoldthrombosen (ScT) lag nach 30 Tagen bei 1,5 % und nach sechs Monaten bei 2,1 % (144). Diese Rate wurde in großen Registerstudien sogar bereits nach 30 Tagen erreicht (145). Die Rate an Thrombosen bei Patienten, die mit DES behandelt wurden, liegt demgegenüber auch nach zwölf Monaten noch unter 1 % (146). Der Mechanismus der Thrombosierung ist multifaktoriell. Bekannte Aspekte sind die Stentlänge, die reduzierte systolische Ejektionsfraktion und ein kleiner Stentdiameter (147,148). Da die ScT-Rate bereits früh erhöht ist, leitet sich hieraus die Hypothese ab, dass auch deviceassoziierte Faktoren eine Rolle spielen. Stentstruts modulieren hierbei in Abhängigkeit ihrer Größe und Position in relativem Verhältnis zur Gefäßwand die Thrombogenität (149). Aufgrund der Strutdicke kann es zu einer verstärkten Aktivierung des Gerinnungssystems u. a. durch Flussturbulenzen kommen. Dies kann das Auftreten einer ScT begünstigen oder aber die Reendothelialisierung verlangsamen (150). Die im Folgenden aufgeführten Publikationen untersuchen vor dem beschriebenen Hintergrund das akute Implantationsergebnis nach Implantation eines DESolve-BRS mit entweder 100 µm bzw. 150 µm Strutdicke mit Hilfe der OCT (151). Ferner untersuchen sie das akute mechanische Ergebnis nach Implantation der BRS in Gefäßen mit großem Diameter und die Abhängigkeit von der zugrundeliegenden Plaque.

Publikation #1:

Boeder, N.F.; Dörr, O.; Bauer, T.; Mattesini, A.; Elsässer, A.; Liebetrau, C.; Achenbach, S.; Hamm, C.W.; Nef, H.M. Impact of strut thickness on acute mechanical performance: A comparison study using optical coherence tomography between DESolve 150 and DESolve 100. *Int J Cardiol* **2017**, 246, 74-79.

Publikation #2:

Boeder, N.F.; Koepp, T.; Dörr, O.; Bauer, T.; Mattesini, A.; Elsässer, A.; Möllmann, H.; Blachutzik, F.; Achenbach, S.; Ghanem, A., et al. A new novolimus-eluting

bioresorbable scaffold for large coronary arteries: an OCT study of acute mechanical performance. *Int J Cardiol* **2016**, *220*, 706-710.

Publikation #3:

Boeder, N.F.; Dörr, O.; Bauer, T.; Elsässer, A.; Möllmann, H.; Achenbach, S.; Hamm, C.W.; Nef, H.M. Effect of Plaque Composition, Morphology, and Burden on DESolve Novolimus-Eluting Bioresorbable Vascular Scaffold Expansion and Eccentricity - An Optical Coherence Tomography Analysis. *Cardiovasc Revasc Med* **2019**, *20*(6), 480-484.

3.1.1 Einfluss der Strutdicke auf das akute mechanische Ergebnis

Es wurden 57 Patienten mit vergleichbaren Basischarakteristika zwischen Januar 2014 und Oktober 2015 untersucht. Jeder Querschnitt in einem Intervall von 1 mm des abschließenden „OCT-Pullbacks“ wurde manuell und offline analysiert. Circa die Hälfte der Patienten wurde im Rahmen eines chronischen Koronarsyndroms behandelt. Ein Großteil wies eine Mehrgefäßerkrankung auf und wurde im Bereich des Ramus interventricularis anterior behandelt. Der dominierende Läsionstyp war „*de-novo*“ und die Läsionen wurden überwiegend nach AHA/ACC als Typ A oder B1 eingestuft (152). Es fand sich kein signifikanter Unterschied bzgl. der QCA („quantitative coronary angiography“)-Analyse zwischen den beiden Gruppen. Die Läsionspräparation unterschied sich insofern, als die gewählte Länge des Ballons zur Vordilatation in der DESolve-100-Gruppe etwas länger ausfiel ($15,0 \pm 3,5$ mm vs. $17,4 \pm 3,3$ mm; $p = 0,02$). Dafür war der gewählte Scaffold in der DESolve-150-Gruppe etwas größer ($3,2 \pm 0,3$ mm vs. $2,9 \pm 0,4$ mm; $p = 0,01$). Die übrigen Aspekte und Parameter der Implantation waren zwischen beiden Gruppen vergleichbar. Die OCT-Analyse zeigt hinsichtlich des mittleren und maximalen Scaffold-Diameters keinen statistisch signifikanten Unterschied ($3,0 \pm 0,4$ mm vs. $2,9 \pm 0,4$ mm; $p = 0,09$). Dahingegen zeigt sich bezüglich der finalen Lumenfläche ein Trend hin zu einer kleineren Fläche bei der DESolve-100-Gruppe ($7,7 \pm 2,2$ mm² vs. $6,7 \pm 1,8$ mm²; $p = 0,06$). Bei vergleichbarem Implantationsdruck ($13,1 \pm 2,7$ atm vs. $13,8 \pm 1,7$ atm; $p = 0,44$) zeigt sich in der DESolve-100-Gruppe ebenfalls ein Trend hin zu einer höheren Rate an verbliebener Stenose über 20 % ($45,2$ % vs. $52,9$ %; $p = 0,22$). Bezüglich der geometrischen Entfaltung wurden mit Hilfe eines Symmetrie- und Exzentrizitätsindex ein vergleichbares Ergebnis zwischen den beiden Gruppen dokumentiert. Die OCT zeigte darüber hinaus fünf Kantendissektionen, die ausschließlich in der DESolve-150-Gruppe auftraten (8 % vs. 0 %; $p = 0,28$). Dahingegen fanden sich gehäuft Frakturen der Struts in der DESolve-100-Gruppe ($12,9$ % vs. $23,5$ %; $p = 0,30$). Malapposition der Struts fanden sich bei $2,5$ % bzw. $1,7$ % der Patienten ($p = 0,70$). Die Patienten wurden im Median 356

Tage nachverfolgt. In diesem Nachverfolgungszeitraum trat kein Ereignis – und insbesondere keine ScT – ein.

In dieser Untersuchung konnte erstmalig das akute mechanische Ergebnis nach Implantation zweier BRS mit unterschiedlichen Strutdicken in einer unselektionierten Patientenkohorte verglichen werden. In der OCT-Analyse finden sich ähnliche Scaffold-Geometrien und -Kennparameter, sodass ein vergleichbares und zufriedenstellendes Akutergebnis angenommen werden kann. So könnte die Reduktion der Strut-Dicke also in der Folge zu einer Reduktion des Thrombosisrisikos beitragen. Auf der anderen Seite zeigte sich ein Trend hin zu erhöhten Frakturen und geringerer MLA als Hinweise für eine unzureichende Radialkraft, was diesen Vorteil in größeren Studien womöglich aufhebt. Eine wesentliche Limitation ergibt sich durch die kleine Studienpopulation, sodass zum einen klinisch seltene Ereignisse sicherlich unterschätzt werden.

3.1.2 Akutes mechanisches Ergebnis bei Implantation von Scaffolds in Gefäßen mit großem Diameter

BRS sollten langfristige Limitationen der bestehenden Stentplattformen, wie z. B. die Wiederherstellung der vasomotorischen Funktion als auch ein positives Remodelling, überwinden (153,154). Der Everolimus-freisetzende BRS Absorb wird hinsichtlich der Implantation in Gefäße mit einem Referenzdiameter größer als 4,0 mm insofern eingeschränkt, als das eine Expansionsbegrenzung auf 0,5 mm vorgegeben ist. Eine Überexpansion hierüber hinaus kann zu Diskontinuität der Struts oder gar ihrer Fraktur führen. Es ist dann mit einem Verlust der mechanischen (Radial-)Kräfte und Zunahme von Malappositionen zu rechnen. Dies schränkt BRS in bestimmten Szenarien ein, z. B. im Hauptstamm oder in hauptstammnahen Abschnitten (127,155). Hieraus ableitend wurde ein Everolimus-freisetzender BRS, der DESolve XL, mit einem nominalen Diameter von 4,0 mm zugelassen. Sein primäres mechanisches Ergebnis nach Implantation wurde mit Hilfe der OCT untersucht (143).

Es wurden insgesamt zehn Patienten eingeschlossen. Die Patienten wiesen ein typisches kardiovaskuläres Risikoprofil auf, befanden sich aber allesamt zuvor wegen eines akuten Koronarsyndroms noch nicht in Behandlung. Dennoch fanden sich bei 44,4 % der Patienten Mehrgefäßerkrankungen. Insgesamt waren alle drei Gefäße gleichermaßen bei der Behandlung betroffen. Hinsichtlich der ACC/AHA-Klassifikation lagen überwiegend Typ B1- oder B2-Läsionen vor (152). In Hinblick auf den Implantationsprozess fand in allen Fällen eine Vor- und Nachdilatation statt. Erstere unter Verwendung eines Ballons mit einem Diameter von $3,75 \pm 0,29$ mm, der mit $14,7 \pm 5,0$ atm inflatiert wurde. Die Nachdilatation erfolgte durch Inflation eines durchschnittlich $4,8 \pm 0,3$ mm großen NC-

Ballons mit $14,7 \pm 4,2$ atm. Der Längsschnitt des „OCT-Pullbacks“ wurde hierfür in Abständen von nur einem Millimeter unterteilt. Die jeweiligen Querschnitte wurden manuell und offline ausgewertet. Es zeigte sich ein maximaler BRS-Diameter von $4,2 \pm 0,39$ mm, der minimale Diameter lag bei $3,4 \pm 0,24$ mm. Die MLA betrug $8,7 \pm 2,0$ mm². Der Exzentrizitätsindex im Kollektiv lag bei $0,81 \pm 0,05$, der Symmetrieindex bei $0,39 \pm 0,25$. Der Anteil malappositionierter Struts lag bei $0,09 \pm 0,26$ %. Hieraus errechnete sich eine Fläche durch inkomplette Apposition von durchschnittlich $0,1 \pm 0,2$ mm². Die Integrität der Stents war erhalten, sodass sich weder Frakturen der Struts noch Kantendissektionen finden ließen. Im kurzfristigen Nachbeobachtungszeitraum von 30 Tagen fand sich kein kardiales Ereignis.

In der Untersuchung wurde erstmalig das akute mechanische Ergebnis nach Implantation von Novolimus-freisetzenden BRS in Gefäßen mit großem Diameter untersucht. Die Analyse der Querschnitte zeigt ein gutes Primärergebnis inklusive der geometrischen Implantationsaspekte und unter Berücksichtigung niedriger Raten von Frakturen und Dissektionen.

3.1.3 Einfluss der Plaque auf das akute mechanische Ergebnis

Die Expansion eines Metallstents beeinflusst signifikant das Auftreten klinischer Endpunkte. Hierzu zählen beispielsweise der Exzentrizitäts- und Symmetrieindex. Die optische Kohärenztomographie hat in der klinischen Routine unter anderem wegen der auflösungsstarken Beurteilbarkeit eben dieser Expansionsparameter an Relevanz gewinnen können. Für den Everolimus-freisetzenden Absorb BVS (Absorb, Abbott Vascular, Santa Clara, CA, USA) konnte durch Shaw et al. mit Hilfe der intravaskulären Bildgebung gezeigt werden, dass das Expansionsergebnis von der Plaquelast, ihrer -Morphologie und -Zusammensetzung abhängt (156). Über den Absorb BVS hinaus wurde ein Novolimus-freisetzender BRS, der DESolve (DESolve, Elixir Medical Corporation, Sunnyvale, CA, USA), zugelassen. Er weist als Alleinstellungsmerkmal über den Aufbau hinaus eine Selbstkorrekturfunktion auf (157). In diesem Zusammenhang wurde untersucht, ob und inwiefern das akute Implantationsergebnis des DESolve-BRS von Plaquelast, Plaque-Morphologie und -Zusammensetzung abhängt (158).

Es wurden insgesamt 15 Patienten zwischen April 2014 und März 2015 in die Untersuchung eingeschlossen. Der longitudinale „Pullback“ der OCT-Untersuchung wurde in Intervalle von 200 µm unterteilt. Die hieraus resultierten Querschnitte wurden von zwei unabhängigen Untersuchern manuell ausgewertet. Es zeigte sich, dass eine größere Plaquelast – ausgedrückt in Form der gemessenen Fläche, Dicke, Winkel des die Plaque einschließenden Kreisbogens und Tiefe als Ausdruck der Entfernung vom äußeren Rand

der Gefäßwand – nicht zu einer statistisch signifikanten Veränderung des *Scaffold Expansion Index* (SEI) führt. Der *Scaffold Excentricity Index* (SEC) als Maß für die Exzentrizität zeigte eine weniger runde Form in Abhängigkeit einer größeren Plaquelast an, wenn eine fibrös-dominierte Plaque mit größerer Fläche, Dicke oder Winkel des die Plaque einschließenden Kreisbogens vorlag. Diese Beobachtung konnte bei dominierend kalzifizierter Plaque in der Kohorte nicht gemacht werden.

In der Untersuchung wurde erstmalig das akute mechanische Ergebnis nach Implantation von Novolimus-freisetzenden BRS in Abhängigkeit der Plaquelast untersucht. Es konnte gezeigt werden, dass im untersuchten Kollektiv das Primärergebnis im Gegensatz zu den vorangegangenen Ergebnissen mit dem Absorb BVS ausschließlich von der Last einer Plaque mit dominierend fibröser Zusammensetzung abhing.

3.2 Prozedurale Aspekte im Rahmen der PCI

Experten empfehlen nach Implantation eines BRS eine Nachdilatation, um klinische Ereignisraten positiv zu beeinflussen (159,160). Der Einfluss der Nachdilatation auf das Implantationsergebnis wurde bisher nicht mit intravaskulärer Bildgebung untersucht. Hinsichtlich prozeduraler Aspekte wurde im Weiteren ein Zusammenhang zwischen der überlappenden Implantation von DES der ersten Generation und erhöhter Mortalität und Myokardinfarkttrisiko beobachtet. Für die zweite Generation der DES wurde gezeigt, dass eine überlappende Implantation nicht mit einer erhöhten Rate an Gefäßrevaskularisation (TVR) verbunden ist. Randomisierte Studien schlossen die Implantation überlappender BRS jedoch aus, sodass hier wissenschaftliche Erkenntnisse fehlen.

Folgende der Habilitationsschrift zugrunde liegende Studien beschäftigen sich mit dem akuten mechanischen Ergebnis nach Implantation und Nachdilatation PLLA-basierter BRS bzw. dem Ergebnis nach überlappender BRS-Implantation (161,162):

Publikation #4 (geteilte Erstautorenschaft):

Blachutzik, F.; **Boeder, N.**⁺; Wiebe, J.; Mattesini, A.; Dörr, O.; Most, A.; Bauer, T.; Röther, J.; Tröbs, M.; Schlundt, C., et al. Post-dilatation after implantation of bioresorbable everolimus- and novolimus-eluting scaffolds: an observational optical coherence tomography study of acute mechanical effects. *Clin Res Cardiol* **2017**, *106*(4), 271-279.

Publikation #5 (geteilte Erstautorenschaft):

Blachutzik, F.; **Boeder, N.**; Wiebe, J.; Mattesini, A.; Dörr, O.; Most, A.; Bauer, T.; Tröbs, M.; Röther, J.; Schlundt, C., et al. Overlapping implantation of bioresorbable novolimus-eluting scaffolds: an observational optical coherence tomography study. *Heart Vessels* **2017**, *32*(7), 781-789.

3.2.1 Einfluss der Nachdilatation auf das Implantationsergebnis

Klinische Ereignisse nach Implantation eines BRS können durch eine Nachdilatation positiv beeinflusst werden (159,160). Studien unter Verwendung von intravaskulärer Bildgebung lagen hierzu bisher nicht vor. In der folgenden Arbeit wurde daher der Einfluss der Nachdilatation auf das mechanische Implantationsergebnis mit Hilfe der OCT untersucht (161).

Es wurden insgesamt 47 Patienten eingeschlossen, die mit 51 BRS behandelt worden sind. Die Patienten wurden in Abhängigkeit der Durchführung einer Nachdilatation in zwei Gruppen unterteilt, die sich in ihren Basischarakteristika nicht signifikant

voneinander unterschieden. Eine Vordilatation wurde bei allen Patienten vorgenommen. Der mittlere Druck für die Vordilatation lag in der Gruppe ohne Nachdilatation bei 16 ± 5 bar, respektive in der Gruppe mit Nachdilatation bei 14 ± 5 atm ($p = 0,25$). Auch die übrigen Aspekte, wie Ballonlänge und -diameter, waren ohne signifikanten Unterschied. Der implantierte BRS hatte in beiden Gruppen vergleichbare Parameter. In beiden Gruppen fand sich jeweils ein Patient, bei dem zwei Läsionen behandelt bzw. aufgrund der Läsionslänge zwei BRS implantiert wurden. In der Patientengruppe, bei der die Nachdilatation durchgeführt wurde, war der Ballon im Mittel $3,3 \pm 1,8$ mm groß und ein Druck von $16,0 \pm 9,0$ bar wurde angewendet. Der gewählte Ballon für die Nachdilatation war also im adäquaten Verhältnis zum BRS und Gefäß gewählt. Im finalen „OCT-Pullback“ wurden die Querschnitte in Abständen von einem Millimeter analysiert. Insgesamt wurden 1654 Querschnitte manuell ausgewertet. Die Fläche, die sich durch eine inadäquate Apposition der Struts ergibt, war in der Gruppe mit abschließender Nachdilatation signifikant kleiner ($0,16 \pm 0,49$ mm² vs. $2,65 \pm 2,78$ mm²; $p < 0,001$). Entsprechend fand sich eine deutlich kleinere Anzahl malappositionierter Struts. Bei Vorliegen einer Malapposition konnte der mittlere orthogonale Abstand zur Gefäßinnenwand durch die Nachdilatation reduziert werden. Der erreichte Scaffold-Diameter in Bezug zu ihrem Minimum und Maximum unterschied sich nicht signifikant zwischen den beiden Gruppen, ebenso wie der erreichte Exzentrizitäts- und Symmetrieindex. Die Nachdilatation führte zu keinem höheren Auftreten von Strut-Frakturen oder Kantendissektionen in der untersuchten Kohorte. Im untersuchten Patientenkollektiv ging die zusätzliche Nachdilatation ferner nicht mit einer statistisch erhöhten Durchleuchtungszeit (15 ± 9 min vs. 16 ± 8 min; $p = 0,74$) oder Kontrastmittelmenge (169 ± 77 ml vs. 175 ± 80 ml; $p = 0,58$) einher.

In dieser Untersuchung konnte erstmalig der Einfluss der Nachdilatation auf das primäre Implantationsergebnis mit Hilfe der optischen Kohärenztomographie untersucht und ihr wesentlicher Beitrag zur adäquaten Entfaltung und Apposition, ohne dass es zu einer messbaren Zunahme der mechanischen Komplikationen gekommen ist, gezeigt werden.

3.2.2 Effekt der überlappenden Implantation von bioresorbierbaren Scaffolds

Wegen erhöhter klinischer Ereignisraten wurde von einer überlappenden Implantation der ersten nicht beschichteten Metallstents (BMS) abgeraten (163). Auch für die erste Generation der medikamentenfreisetzenden Stents blieb ein Zusammenhang zu erhöhter Mortalität und Myokardinfarkt erkennbar (164,165). Für die zweite Generation der DES konnte gezeigt werden, dass eine überlappende Implantation nicht mit einer erhöhten Rate an Gefäßrevaskularisation (TVR) verbunden ist (165,166). Randomisierte Studien schlossen

die Implantation überlappender BRS aus. In der folgenden Studie wurde das akute mechanische Ergebnis nach überlappender Implantation von BRS untersucht (162).

Insgesamt konnten 46 Patienten in die Untersuchung eingeschlossen werden. Sie wurden mit Novolimus-freisetzenden BRS behandelt. Die Kohorte wurde in Abhängigkeit von der Implantation mindestens zweier BRS unterteilt. Die Kontrollgruppe bestand aus 23 Patienten. Die „OCT-Pullbacks“ wurden manuell ausgewertet und für die Analyse in Querschnitte im Abstand von einem Millimeter unterteilt. Die Patientengruppen unterschieden sich in ihren Basischarakteristika nicht, wenn man von der Läsionslänge absieht (Überlappungsgruppe $16,8 \pm 5,9$ mm vs. $10,8 \pm 5,2$ mm; $p < 0,001$). In der Überlappungsgruppe bemisst sich die Strecke der Überlappung im Mittel mit $3,8 \pm 2,9$ mm. Die Doppelage der Struts im Bereich der Überlappung zweier BRS führte zu einer messbaren Dickenzunahme der Strutschicht – also der Messgröße zwischen innerer Strutkante und Gefäßinnenwand (349 ± 27 μm vs. 182 ± 21 μm ; $p < 0,001$). Es ließ sich jedoch hieraus keine statistisch signifikante Reduktion der minimalen Gefäßfläche (MLA) oder OCT-Scaffold-Fläche im Vergleich zu den proximal oder distal angrenzenden Abschnitten mit nur einer Strutschicht messen ($6,83 \pm 2,71$ mm^2 vs. $6,62 \pm 2,44$ mm^2 ; $p = 0,54$). Hiermit einhergehend fand sich keine Zunahme der verbliebenen Stenose. Ferner zeigte sich durch die überlappende Implantation und nachfolgende Nachdilatation in diesem Bereich keine statistisch signifikante Häufung von Strut-Frakturen. In dem medianen Nachverfolgungszeitraum von neun Monaten trat kein klinisches, unerwünschtes Ereignis ein.

In dieser Untersuchung konnte erstmalig der Einfluss der überlappenden Implantation von BRS wegen langer Läsionen auf das primäre Implantationsergebnis untersucht und dabei gezeigt werden, dass es zu keiner relevanten Reduktion der MLA oder Scaffold-Fläche sowie zu keiner mechanischen Diskontinuität kommt, sodass eine sichere Implantation hintereinander liegender BRS angenommen werden kann.

3.3 Antithrombotische Behandlung nach Implantation von bioresorbierbaren Scaffolds

Nach Implantation eines Stents wird eine duale Thrombozytenaggregation (DAPT) empfohlen, die neben Aspirin aus einem P2Y₁₂-Inhibitor besteht (167). In Ergänzung haben schätzungsweise 5–10 % der behandelten Patienten hierüber hinaus eine Indikation zur dauerhaften oralen Antikoagulation (OAK) (168). Patienten mit Indikation zur dauerhaften OAK sind in Hinblick auf die Behandlung mit BRS unzureichend untersucht, unter anderem durch ihren Ausschluss in den randomisierten Studien (169,170). In der folgenden Studie wurde daher diese Patientenpopulation in Hinblick auf unerwünschte, klinische Ereignisse („Outcome“) untersucht und mit einer Gruppe von Patienten verglichen, die aufgrund fehlender Indikation lediglich mit DAPT behandelt werden mussten (171).

Publikation #6:

Boeder, N.F.; Johnson, V.; Dörr, O.; Wiebe, J.; Elsässer, A.; Möllmann, H.; Hamm, C.W.; Nef, H.M.; Bauer, T. Bioresorbable scaffold implantation in patients with indication for oral anticoagulation: A propensity matched analysis. *Int J Cardiol* **2017**, *231*, 73-77.

Patienten, die mit einem BRS behandelt worden sind und eine begleitende Indikation zur OAK hatten, wurden Patienten ohne OAK in einem Verhältnis von 1:3 zugeordnet. Die für die Propensity-Score-Matching-Analyse herangezogenen Parameter waren das Alter, Vorliegen einer Mehrgefäßerkrankung, Einschränkung in der systolischen Ejektionsfraktion, Scaffold-Länge und die klinische Präsentation. Die beiden Kohorten wiesen sowohl rechnerisch ein vergleichbares Blutungsrisiko (HAS-BLED-Score $1,78 \pm 0,53$ vs. $1,78 \pm 0,52$; $p = 0,89$) als auch Thrombembolierisiko (CHA₂DS₂-VASc-Score $3,45 \pm 1,12$ vs. $3,47 \pm 1,22$; $p = 0,91$) auf. Im Median wurden die Patienten 361,5 Tage nachverfolgt. Beide Gruppen zeigten keinen Unterschied in Hinblick auf die Sterblichkeit („all-cause mortality“). Die Häufigkeit der erneuten Revaskularisierung im Bereich der behandelten Läsion (TLF) erreichte keinen signifikanten Unterschied (TAT 7,3 % vs. DAPT 2,5 %; $p = 0,11$). Auch der kombinierte Endpunkt MACE unterschied sich zwischen den beiden Gruppen nicht relevant ($\chi^2(1) = 1,567$; $p = 0,21$). Es wurden, unter Verwendung der BARC-Klassifikation, keine schwerwiegenden Blutungskomplikationen dokumentiert. Der Großteil der Patienten wurde mit einem NOAK behandelt, sofern eine Indikation zur OAK bestand. Die Dauer der TAT wurde überwiegend auf einen Monat beschränkt.

In dieser Untersuchung konnte erstmalig gezeigt werden, dass es durch die begleitende Indikation zur dauerhaften oralen Antikoagulation zu keiner Zunahme der schwerwiegenden Blutungskomplikationen kommt. In dem untersuchten Patientenkollektiv konnte

ebenso gezeigt werden, dass es zu keiner relevanten Zunahme der ischämischen Ereignisse kommt. Dennoch bleibt die hohe Rate an ScT und MACE auffällig. Eine Limitierung ergibt sich durch die Größe der untersuchten Patientenpopulation.

3.4 Späte und sehr späte Scaffoldthrombosen

In Registerstudien fiel nach Implantation eines Absorb BVS eine erhöhte Rate an Scaffoldthrombosen (ScT) auf, die sowohl früh als auch spät nach der Implantation auftraten (172,173). Aus Beobachtungsstudien ergab sich die Hypothese, dass Malappositionen und die hierdurch bedingte Zunahme der Blutflussturbulenzen diese begünstigen (174), da sie ein häufig beobachtetes Phänomen zum Zeitpunkt des Ereignisses darstellten. Die folgende Studie untersucht daher den prospektiven Stellenwert von Malappositionen als Prädiktor für späte oder sehr späte ScT (175).

Publikation #7:

Boeder, N.F.; Weissner, M.; Blachutzik, F.; Ullrich, H.; Anadol, R.; Tröbs, M.; Münzel, T.; Hamm, C.W.; Dijkstra, J.; Achenbach, S., et al. Incidental Finding of Strut Malapposition Is a Predictor of Late and Very Late Thrombosis in Coronary Bioresorbable Scaffolds. *J Clin Med* **2019**, 8(5), 580.

Es wurden 197 Patienten in die Untersuchung eingeschlossen. Es lag ein elektives Kontroll-OCT nach PCI im Median nach 353 Tagen vor. Die beobachteten Malappositionen wurden zum Zeitpunkt der Aufnahme von zwei erfahrenen, interventionell tätigen Kardiologen als nicht akut behandlungsbedürftig eingestuft. Eine vollständige Nachbeobachtung („Follow-Up“) lag im Median bis 1059 Tage nach der Prozedur vor. Innerhalb dieses Nachverfolgungszeitraums erlitten sieben Patienten eine späte oder sehr späte ScT. Sie trat 579 (341–623) Tage nach der PCI bzw. 293 (38–579) Tage nach der OCT auf. Obwohl die elektive OCT zu keinem vordefinierten Zeitpunkt nach der PCI durchgeführt wurde, zeigte sich in Hinblick auf die Diagnose der Malapposition und der folgenden ScT kein signifikanter Unterschied in Abhängigkeit des Zeitpunktes der OCT ($p = 0,871$). Die Basischarakteristika zwischen den beiden Gruppen waren ähnlich und zeigten mit Ausnahme früherer Revaskularisationen (ScT 71,4 % vs. No ScT 34,7 %; $p = 0,04$) keine wesentlichen Unterschiede. Mit Hilfe einer Kaplan-Meier-Kurve wurde der zeitliche Zusammenhang zwischen dem Auftreten einer späten oder sehr späten ScT in Abhängigkeit der Beobachtung von einer Malapposition im Rahmen der elektiven OCT dargestellt. Bei Patienten mit vorbeschriebener Malapposition trat die ScT statistisch signifikant häufiger auf (Log-Rank-Test $p < 0,001$). In einer multivariablen Cox-Regression konnte unabhängig vom Zeitpunkt (frühe oder späte Diagnose) die Malapposition als unabhängiger Prädiktor für die ScT bestätigt werden.

In einem separaten Register wurden 16 Patienten geführt, für die ein OCT zum Zeitpunkt der ScT vorlag. Fünf dieser Patienten wurden in der prospektiven Nachverfolgung eingeschlossen. In neun der 16 Fälle handelt es sich um eine späte oder sehr späte ScT. Da bei

allen Patienten ein OCT vorlag, wurde die ScT als definitiv eingestuft. Es konnte beobachtet werden, dass späte und sehr späte ScT häufiger Frauen und solche Patienten betrafen, die zuvor bereits behandelt worden sind. Es fand sich im überwiegenden Anteil der untersuchten OCT-Querschnitte Thrombus ($78 \pm 37\%$ vs. $55 \pm 12,4\%$; $p = 0,18$). Während eine inkomplette Expansion in den Fällen der frühen ScT häufiger zu sehen war, findet sich eine Malapposition oder Strut-Diskontinuität eher bei den Patienten mit später oder sehr später ScT. Die Parameter, welche die Scaffold-Geometrie beurteilen, unterschieden sich in den beiden untersuchten Gruppen nicht.

In dieser Untersuchung konnte erstmalig gezeigt werden, dass die Beobachtung von Malappositionen bei Patienten, die mit einem BRS behandelt worden sind, ein Prädiktor für das zukünftige Auftreten von späten und sehr späten ScT ist. Ferner fand sich in der retrospektiven Auswertung ein Zusammenhang zwischen Thrombus und dem Auftreten von ScT insbesondere bei größeren Gefäßen bzw. Scaffolds.

4 Diskussion

Seit der ersten Eigenkatheterisierung im Jahr 1929 und der darauf aufbauenden Idee zur perkutanen Behandlung von Patienten mit stenosierenden Gefäßerkrankungen des Herzens bis zur Entwicklung und zum klinischen Einsatz bioresorbierbarer Gefäßstützen (BRS) sind acht Jahrzehnte vergangen. Die Entwicklung dieser neuen Stentplattform begründet sich in Limitationen der bestehenden Plattformen. So ist mit dem Einsatz von Stentplattformen mit Metallgeflecht dessen dauerhaftes Verbleiben nach Abschluss der Freisetzung der Medikamente und ggf. der Resorption des Polymers verbunden. Das Metallgeflecht stellt damit beispielsweise Grundlage für chronische Inflammationsprozesse dar. Die konzeptionelle Idee der Entwicklung einer neuen Stentgeneration beruhte also auf der Vorstellung einer transienten Stabilisierung und dessen langfristiger Resorption. BRS wurden daher in Analogie zu medikamentenfreisetzenden Metallstents (DES) als neuer Entwicklungssprung beschrieben.

In Verbindung mit dem klinischen Einsatz der BRS entstanden unter anderem durch Ergebnisse des GHOST-EU-Registers hinsichtlich ihrer Sicherheit Bedenken. Hier fand sich bei den 1200 untersuchten Patienten nach sechs Monaten eine Scaffoldthromboserate von 2,1 % (144). In einer von Brugaletta et al. untersuchten Patientenkohorte, bei denen der BRS im Rahmen eines ST-Streckenhebungsinfarktes implantiert wurde, wird diese sogar bereits nach 30 Tagen erreicht (145). Der Mechanismus einer Scaffoldthrombose ist sicher multifaktoriell und neben bekannten Risikofaktoren wie etwa der Stentlänge (147) entstand aus den bereits früh auftretenden ScT die Hypothese, dass es auch device- oder prozedurassoziierte Faktoren geben muss, die zum Auftreten des klinischen Ereignisses prädisponieren. So kann die Strutdicke, die zum Erhalt der Radialkraft größer ausfällt, Flussturbulenzen hervorrufen und damit einhergehend eine übermäßige Aktivierung des Gerinnungssystems begünstigen.

In der vorliegenden Arbeit wurde daher das akute mechanische Implantationsergebnis nach Behandlung mit einem BRS mit verringerter Strutdicke (151) und eines solchen, der für Gefäße mit größerem Diameter (143) entwickelt worden ist, untersucht. Im Grundsatz ergibt sich in beiden Fällen aus der Auswertung der „OCT-Pullbacks“ der Hinweis auf ein positives Primärergebnis. Die Aspekte, die für ein gutes mechanisches Ergebnis sprechen, stammen aus früheren Bildgebungsstudien. Hierbei wurden vor allem BMS und DES der ersten Generation mit Hilfe von IVUS untersucht (176-178). Es zeigte sich, dass eine abschließende minimale Querschnittsfläche (MLA) von kleiner als 5,5 cm² bzw. 6 cm² oder aber eine verbliebene residuale Stenose im Bereich des Scaffolds von größer als 20 % mit einem erhöhten Risiko für Stentthrombosen verbunden war. Die Kriterien

wurden anhand von Patienten entwickelt, die eine simple Läsionskomplexität aufwiesen. Hier findet sich eine weite Übereinstimmung mit unseren Patientencharakteristika, sodass ein Vergleich möglich erscheint, wenngleich gezeigt werden konnte, dass Messungen im OCT sowohl in vivo als auch in vitro verglichen mit IVUS geringer ausfallen können (179). In den eigenen Studien zeigten sich die Messwerte im vorbeschriebenen Bereich, wiesen aber aufgrund der erreichten MLA auf eine verringerte Expansionskapazität und Radialkraft für den BRS mit dünneren Struts hin. Der MLA-Referenzwert aus der Literatur wird bei Patienten, die mit einem DESolve XL behandelt worden sind, deutlich überschritten. Es zeigt sich jedoch ein heterogenes Bild, denn die verbliebene Stenose ist im Durchschnitt knapp oberhalb der 20 %. Als integrativer Ansatz zur Beurteilung eines positiven Primärergebnisses können auch geometrische Parameter, die sich durch die Stentplattform definieren, herangezogen werden (180,181). So konnte gezeigt werden, dass der DESolve-BRS aufgrund eines geringeren Exzentrizitätsindex anfälliger für eine asymmetrische Expansion sein könnte (125). Unter klinisch-angiographischen Gesichtspunkten findet sich mit der MUSIC-Studie verbunden ein Hinweis für ein gutes Primärergebnis bei einem Exzentrizitätsindex von 0,70 (182). Dies wird ergänzt von Symmetrieindizes nahe null, um eine gleichmäßige und symmetrische Expansion entlang des Scaffolds zu beschreiben. Dieser Teilaspekt findet sich in den erreichten geometrischen Parametern in den beiden vorliegenden Untersuchungen deutlich abgebildet, die so das positive Primärergebnis unterstützen.

In den durchgeführten Studien wurde hierüber hinaus der Umfang des prolabierenden Gewebes beurteilt. Hierbei handelt es sich um das Gewebe, das durch die Streben in das Gefäß ragt. Die Fläche zeigte sich in den Untersuchungen statistisch unabhängig von der verwendeten Strutdicke und besonders klein in der Kohorte, in denen der BRS für große Gefäßdiameter untersucht wurde. Letzteres kann an der Läsionspräparation gelegen haben oder aber an dem Verhältnis aus Strutmaterial zur Scaffoldzelle, die bei größeren Scaffolds, wie dem DESolve XL, kleiner ausfallen und so die Gefäßwand besser abdecken. Sugiyama et al. (183) haben gezeigt, dass es abhängig von der Prolapsfläche zu einem Anstieg der postprozeduralen CK-MB als Hinweis für ein eine Post-PCI-Myokardverletzung („myocardial injury“) kommt. Im kurzfristigen Verlauf von neun Monaten resultierte dies jedoch nicht in einem Anstieg der kardialen Ereignisse. Der Trend zu einer größeren Prolapsfläche bei Patienten, die mit dem Scaffold mit geringerer Strutdicke behandelt worden sind, könnte in diesem Zusammenhang nicht nur durch das Device, sondern auch mit dem zumindest numerisch größeren Anteil an akuten Koronarsyndromen erklärbar sein.

Einen weiteren Aspekt in der Beurteilung des mechanischen Akutergebnisses sind Frakturen und Dissektionen. In der Beobachtung des DESolve XL für große Gefäßdiameter

zeigten sich keine solche mechanischen Komplikationen. In der Untersuchung, die Scaffolds mit einer Strutdicke von 150 μm und 100 μm vergleicht, findet sich ein Trend zu einer höheren Anzahl von Frakturen in letzterer Gruppe (12,9 % vs. 23,5 %; $p = 0,30$). Dies scheint in direktem örtlichem Zusammenhang mit einer erhöhten Anzahl von Fibroatheromen in den korrespondierenden Gefäßquerschnitten zu sein (10 % vs. 50 %, $p = 0,50$). Wenngleich diese Beobachtung aufgrund der kleinen Fallzahl mit Einschränkungen beurteilt werden muss, so kann der Trend zu höheren Frakturraten auch durch die mechanischen Eigenschaften des DESolve 100 μm erklärt werden, was wiederum gut zu dem Eindruck der geringeren Expansions- und Radialkraft passt. Auch die Dissektionen zeigten einen örtlichen Bezug zu Plaquestrukturen. Dies ist gut vereinbar mit den Ergebnissen von Chamiê et al., die verbunden mit Plaque und Thin-cap Fibroatheromen (TCFA) im Bereich der Platzierungszone einen signifikanten Anstieg des Risikos für Stentkantendissektion beschrieben (184). In unserer Kohorte ließ sich diesbezüglich ergänzen, dass die Dissektionen zumeist nicht in Zusammenhang mit der Vordilatation stehen, da das hiernach angefertigte OCT im Rahmen der Implantationsplanung diese noch nicht zeigte. Es muss also die Implantation des Scaffolds selbst oder aber die nachgeschaltete Nachdilatation ursächlich gewesen sein. Für die Nachdilatation spricht, dass hierbei üblicherweise der höchste Inflationsdruck Anwendung fand. Die vorliegenden Ergebnisse müssen auch vor dem Hintergrund des kleinen Patientenkollektivs bewertet werden.

In einer weiteren Studie wurde aufgrund der gezeigten Abhängigkeit der Scaffoldexpansion des Absorb BVS von Plaquelast, -Morphologie und -Zusammensetzung (156) untersucht, ob der Novolimus-freisetzende DESolve diese Abhängigkeit ebenfalls aufweist (158). Dieser Aspekt hat für die Frage des optimalen Implantationsergebnisses einen hohen Stellenwert. Im Ergebnis zeigt sich in der untersuchten Kohorte unter Berücksichtigung der zuvor beschriebenen IVUS-Kriterien ein gutes mechanisches Ergebnis. Sowohl die residuale Reststenose (RAS) als auch die erreichte Lumenfläche (MLA) sind innerhalb der beschriebenen Grenzwerte. Es konnte damit gezeigt werden, dass diese Parameter nicht in gleichem Maße von der Plaquelast negativ beeinflusst werden, und damit anders als in der Untersuchung von Shaw et al. (156) beobachtet. Dies könnte durch die Läsionspräparation bzw. das prozedurale Management der Scaffoldimplantation begünstigt worden sein, denn es konnte gezeigt werden, dass eine 1:1-Vordilatation zu einer besseren MLA führen kann (185). In der durchgeführten Studie fand diese immerhin in 87 % der Fälle statt. Die Nachdilatation scheint keine Verbesserung der Expansion zu bewirken (185), allerdings liegen dafür keine bekannten randomisierten Studien vor. In der Studie von Shaw et al. zur Expansion des Absorb BVS werden keine genauen

Angaben zum periprozeduralen Vorgehen berichtet. Insofern bleibt offen, ob eine sorgfältige Läsionsvor- und Nachbearbeitung die in der Studie beschriebene Expansionseinschränkung durch die Plaquelast hätte günstig beeinflussen können. Einschränkend muss man in diesem Zusammenhang hierbei sicher berücksichtigen, dass sich beim direkten Vergleich der beiden Studien eine Limitation dadurch ergibt, dass die kalzifizierte Plaquelast in unserer Kohorte etwas geringer ausfiel. Ein weiterer Aspekt, der die bessere Expansion womöglich mit beeinflusst hat, ist die Selbstkorrekturfunktion der DESolve-Plattform. Über die Expansion hinaus lässt sich das geometrische Ergebnis untersuchen und vergleichen. Legt man die Referenzwerte aus der MUSIC-Studie zugrunde, zeigte sich ein positives Ergebnis. Allerdings haben fibrös dominierte Plaques – ausgedrückt als Fläche, Dicke, Winkel des die Plaque einschließenden Kreisbogens – einen negativen Einfluss auf die Exzentrizität. Dies konnte für kalzifiziert dominierte Plaque nicht gezeigt werden. Die fibrös dominierten Plaques in unserer Kohorte sind, anders als bei Shaw et al., typischerweise zirkumferentiell aufgetreten. Lipidreichere Plaques gelten als empfindlicher für die Dilatation, aber womöglich hat gerade der hohe zirkumferentielle Anteil einen besseren Exzentrizitätsindex behindert. Es muss berücksichtigt werden, dass die Beurteilung der Plaquezusammensetzung im direkten In-vivo-Vergleich anhand der OCT Limitationen aufweist und die Gewebecharakterisierung gegenwärtig an ihre technischen Grenzen stößt. Die Plaque ist typischerweise nie uniform von einem Typ, sodass es bei der Beurteilung des vorherrschenden Typs bleibt.

Bisher durchgeführte Studien zeigten regelmäßig das Vorhandensein von Malappositionen in den finalen „OCT-Pullbacks“ (143,151,158). In randomisierten Studien wurde die Nachdilatation anfänglich nicht ausdrücklich empfohlen, da eine Beschädigung der Integrität und Diskontinuität der Struts befürchtet wurde. Brown et al. zeigten zunächst keinen Effekt der Nachdilatation mit einem NC-Ballon mit Diameter + 0,25 mm und Nominaldruck auf die Apposition (185). Aufgrund der anfänglich zurückhaltenden Durchführung der Nachdilatation und dem Ausschluss in randomisierten Studien wurde erstmalig das akute Implantationsergebnis in Abhängigkeit der prozeduralen Strategie mit der Hilfe der OCT beurteilt. Die Behandlung fand entweder mit einem Novolimus- oder Everolimus-freisetzenden BRS statt. Hierbei wurde eine Reduktion der durch die Malapposition entstandenen Fläche (ISA) und Malappositionshäufigkeit durch die Nachdilatation festgestellt. Der NC-Ballon für die Nachdilatation war mit $3,3 \pm 1,8$ mm etwas größer als der Scaffold ($3,1 \pm 0,3$ mm). Der maximale Inflationsdruck lag bei $16 \pm 9,0$ atm im Bereich der Hochdruckdilatation. Die mechanische Integrität des Scaffolds wurde hierdurch – anders als befürchtet – nicht relevant beeinflusst, da im Vergleich zur ausbleibenden Nachdilatation keine Anzahl erhöhter Kantendissectionen oder Strut-Frakturen

beobachtet werden konnte. Die Nachdilatation mit Hochdruckballons erscheint im untersuchten Kollektiv demnach als sicher. Hierdurch könnte die Rate unerwünschter klinischer Ereignisse („Outcome“) perspektivisch positiv beeinflusst werden, denn eine höhere Anzahl von Struts erreicht die Gefäßwand und entzieht sich somit nicht einer fehlenden neointimalen Endothelialisierung (186), wenngleich die Malapposition durch den Verbleib im Gefäß plattformbedingt nur transient sein sollte. Eine Transformation des verbesserten mechanischen Ergebnisses, der im untersuchten Kollektiv gezeigt werden konnte, in eine Verbesserung harter klinischer Endpunkte muss Aufgabe zukünftiger Untersuchungen sein. De Ribamar Costa et al. berichten, dass das Überleben nach einem Jahr bei mit Absorb BVS behandelten Patienten nicht beeinflusst wird (187). Weitere randomisierte Untersuchungen sind zur Beantwortung dieser Frage folglich notwendig.

Über den Effekt der Nachdilatation bei Patienten, die mit einem BRS behandelt worden sind, hinaus, stellt sich die Frage, ob in Bezug auf das periprozedurale Management auch längere Stenosen durch Überlappung zweier Devices mit BRS behandelt werden können. Nicht zuletzt bestand die Sorge, dass die Überlappung zu der in der Literatur beschriebenen Erhöhung der Scaffoldthrombosen durch späten Lumenverlust und Aktivierung von Flussturbulenzen durch Doppellagen beiträgt. Hierzu wurde eine vergleichende Beobachtungsstudie durchgeführt. Im Grundsatz konnte dabei festgestellt werden, dass die überlappende Implantation zweier BRS sowohl hinsichtlich des akuten Implantationsergebnisses als auch im mittelfristigen Follow-Up von im Median neun Monaten ein zufriedenstellendes Ergebnis zeigt. Dies könnte durch eine fehlende substantielle Reduktion der MLA beeinflusst worden sein. Die Überlagerung zweier Scaffolds führt in dem betroffenen Abschnitt zu einer Duplikatur der Scaffoldstreben. Hiermit einher geht theoretisch eine Reduktion der Gefäßfläche, wenn auch nur zeitlich begrenzt. In der Untersuchung konnte gezeigt werden, dass in unserem Kollektiv die Stentexpansion und Lumenfläche in den Abschnitten der Überlagerung keine signifikante Reduktion im Vergleich zu den unmittelbar proximal und distal dazu liegenden Abschnitten aufweist. Damit werden tierexperimentelle Beobachtung von Farooq et al. unterstützt (188). Es zeigte sich ferner keine Zunahme der mechanischen Komplikationen wie Frakturen im Bereich der Überlappung. Dies könnte durch die größere Überexpansionskapazität erklärbar sein. Im zur Verfügung stehenden Nachverfolgungszeitraum kommt es nicht zu einem signifikanten Anstieg der klinischen Ereignisse und damit unterstützen unsere Daten die Ergebnisse, die Ortega-Paz et al. (189) oder Costa Jr et al. (190) für den Absorb BVS demonstrieren konnten. Weitere multizentrische, randomisierte Untersuchungen sind für die langfristige Beurteilung der Sicherheit notwendig. Ferner ergibt sich auch durch die geringe

Komplexität der behandelten Läsionen eine Einschränkung, sodass die Erkenntnisse sich nicht verallgemeinern lassen.

Nach Implantation eines Stents besteht die Indikation zur dualen Thrombozytenaggregation mit Aspirin und einem P2Y₁₂-Inhibitor. Die Auswahl aus einem der drei oral verfügbaren P2Y₁₂-Inhibitoren hängt unter anderem davon ab, ob es sich um ein akutes Koronarsyndrom handelt, und ist zeitlich beschränkt (25). Schätzungsweise 5–10 % der Patienten, die mit einem Stent behandelt werden, haben allerdings eine ergänzende Indikation zur oralen Antikoagulation (OAK) (168). Während die Thrombozytenaggregation das Ziel verfolgt Ischämieereignisse zu reduzieren, soll die OAK das thrombembolische Risiko bei z. B. Patienten mit Vorhofflimmern reduzieren. Hierbei zeigt sich konkret die OAK der DAPT bei Vorhofflimmerpatienten hinsichtlich der Vermeidung der Schlaganfälle überlegen, jedoch bezüglich einer relevanten Reduktion der Stentthromboseraten im Vergleich zur DAPT unterlegen (25,191). Nach PCI in dieser Patientengruppe muss jedoch beides adressiert werden, denn eine frühzeitige Beendigung der Thrombozytenaggregation kann das Risiko für eine Stentthrombose erhöhen und ein Pausieren der Antikoagulation birgt die Gefahr des thrombembolischen Ereignisses, sodass zumeist eine dreifache antithrombotische Therapiekombination (TAT) angewendet wird. Durch die Verfügbarkeit von drei P2Y₁₂-Inhibitoren und vier NOAKs ergibt sich eine Vielzahl von Kombinationsmöglichkeiten. Patienten mit Indikation zur dauerhaften OAK sind allerdings in Hinblick auf die Behandlung mit BRS unzureichend untersucht, unter anderem durch den Ausschluss in den randomisierten Studien (169,170). Es wurde daher diese Patientenpopulation in Hinblick auf das Auftreten unerwünschter klinischer Ereignisse („Outcome“) untersucht (171). Als Vergleichsgruppe wurden Patienten ausgewählt, die lediglich mit einer DAPT behandelt werden mussten. Im Grundsatz zeigte sich, dass es in dem zur Verfügung stehenden Nachverfolgungszeitraum keine signifikante Zunahme von schwerwiegenden Blutungskomplikationen (BARC \geq 3 (192)) kam.

Grundsätzlich ist anzunehmen, dass eine Dreifachtherapie das Risiko für schwerwiegende Blutungen erhöht. Blutungen stellen einen unabhängigen Risikofaktor für die Langzeitprognose von Patienten mit koronarer Herzerkrankung dar. Das damit verbundene Mortalitätsrisiko steigt mit Schwere der auftretenden Blutung an (193). In dem untersuchten Kollektiv mit TAT fanden sich lediglich Blutungen mit niedriger klinischer Relevanz. Die zum Zeitpunkt der Untersuchung gültigen Empfehlungen der Europäischen Gesellschaft für Kardiologie empfahlen eine Dreifachtherapie mit angepasstem INR bei Marcumartherapie oder ein NOAK in Verbindung mit Aspirin und Clopidogrel einzusetzen (167). Das bezüglich der Ereignisrate schwerer Blutungen positiv ausfallende Studienergebnis könnte durch die Limitierung der dreifachen antithrombotischen Therapie für

einen Monat begünstigt worden sein,. Allerdings wurde in etwa 10 % die TAT auf zwölf Monate ausgeweitet. In der ISAR-Triple-Studie, einer randomisierten Open-Label-Studie, wurde beobachtet, dass eine sechswöchige Dreifachtherapie mit Clopidogrel einer sechsmonatigen nicht überlegen ist. Die Reduzierung der TAT auf lediglich sechs Wochen war weder mit einer Reduzierung der Ischämie- noch der Blutungskomplikationen verbunden (194). Neben Clopidogrel finden die weiteren oralen P2Y₁₂-Inhibitoren Ticagrelor und Prasugrel wegen statistisch signifikanter Überlegenheit bei Patienten mit akutem Koronarsyndrom standardmäßige Anwendung (25,167). Sarafoff et al. untersuchte Prasugrel anstelle von Clopidogrel als Kombinationspartner im TAT-Regime nach DES-Implantation (195). Durch Kombination mit Prasugrel kam es zu einem Anstieg der TIMI-major- und -minor-Blutungen etwa um den Faktor vier, ohne dass dabei gleichzeitig eine Reduktion der Ischämieereignisse einherging. Eine weitere Arbeitsgruppe nutzte Ticagrelor als Kombinationspartner mit einem Vitamin-K-Antagonisten und konnte ebenfalls keine Abnahme der Ischämieereignisse im Vergleich zur TAT mit Clopidogrel, ASS und Vitamin-K-Antagonisten bei gleichbleibenden Blutungskomplikationen zeigen (196). Auch im untersuchten Kollektiv der durchgeführten Studien fanden sich TAT-Kombinationen mit Prasugrel oder Ticagrelor. Zum Zeitpunkt der Untersuchung war die Empfehlung bezüglich des Kombinationspartners noch weicher bzw. unklarer. Die Blutungsrate insgesamt zeigte keinen signifikanten Unterschied zur DAPT-Gruppe. Dies kann an dem günstigen Blutungsrisiko der Kohorte, abgeschätzt mit HAS-BLAD-Score, gelegen haben. Auf der anderen Seite erfolgte die Antikoagulation bei der Mehrheit der Patienten mit Hilfe eines NOAKs, die im Vergleich zu den Vitamin-K-Antagonisten ein günstigeres Risikoprofil aufweisen (197-200). Die verfügbaren Studien berücksichtigten jedoch Patienten mit gleichzeitiger Indikation zur DAPT nicht; solche Patienten waren von den Studien ausgeschlossen. Zuletzt konnte mit der PIONEER-AF-PCI-Studie für Rivaroxaban(201), der AUGUSTUS-Studie für Apixaban (202) und der REDUAL-PCI-Studie für Dabigatran (203) gezeigt werden, dass diese NOAKs hinsichtlich der Endpunkte gegenüber dem konventionellen Vitamin-K-Antagonisten als Kombinationspartner vorteilhaft sind.

Nach PCI gilt es neben dem individuellen Blutungsrisiko auch das Risiko für ischämie-mediierte klinische Ereignisse abzuschätzen und durch die Auswahl der antithrombotischen Therapie zu reduzieren. Zwischen den beiden Gruppen konnte kein signifikanter Unterschied hinsichtlich der MACE-Rate festgestellt werden, jedoch fällt die Rate im Vergleich zu Literaturangaben überraschend hoch aus. In der Kaplan-Meier-Kurve zur zeitlichen Abbildung der MACE-Ereignisse in Abhängigkeit der postprozeduralen Medikationsempfehlung zeigt sich ein frühes Auftreten der Ereignisse nach BRS-Implantation, insbesondere in der TAT-Gruppe. Diese Ereignisse unterstützen die Hypothese, dass

prozedurale Aspekte die Ereignisse begünstigen. Die Rate bleibt trotz des deutlich höheren Einsatzes von optischer Kohärenztomographie im Vergleich mit den Ergebnissen des GHOST-EU-Registers (144) als auffällig hoch einzustufen. Die fehlende statistische Signifikanz könnte am Studiendesign, der kleinen Studienpopulation und der Höhe der tendenziell kränkeren Patienten und höheren Läsionskomplexität liegen, sodass abschließend vor dem Hintergrund der erhöhten Gesamtsterblichkeit („all-cause mortality“) im Vergleich zu anderen BRS-Studien (144) – wenngleich sie einen kürzeren Nachverfolgungszeitraum überblicken – weiterführende randomisierte Studien notwendig sind, um diesen komplexen Aspekt weiter zu untersuchen. Hierbei sollte der Aspekt der chronischen Niereninsuffizienz und ihr Stellenwert berücksichtigt werden. Eine größere Studienpopulation könnte Überlegenheit- oder Nachteil der gewählten antithrombotischen Therapie besser abbilden.

Der Everolimus-freisetzende BRS, Abbott Absorb BVS, zeigte eine unerwartet hohe Anzahl an Scaffoldthrombosen. Es finden sich in der Literatur mono- und multizentrische Beobachtungsstudien, die von ihrem Auftreten sowohl früh als auch spät nach der initialen Implantation berichten (121,173). Der Absorb ist in der Folge der Sicherheitsbedenken vom Markt genommen worden. Studien, die auf quantitativen Aspekten der Koronarangiographie beruhen, sehen zwischen einem „Undersizing“ – gemeint ist ein zu kleiner BRS in Relation zum Referenzgefäßdiameter – und dem Auftreten später klinischer Ereignisse einen starken Zusammenhang (204,205). Der zugrundeliegende Mechanismus hierfür ist nicht geklärt, aber angenommen werden kann, dass Malapposition durch die Aktivierung der Gerinnung und ihr Auslösen von Flussturbulenzen hierbei eine Rolle spielt. Der mechanistische Hintergrund hierfür erscheint solide (206,207), allerdings fußt der Zusammenhang darüber hinaus auf Beobachtungsstudien, die Malappositionen zum Zeitpunkt der ScT häufig beschreiben (174,208). Es wurde daher der Stellenwert der Malapposition – diagnostiziert im Rahmen einer elektiven OCT-Untersuchung – mit Hinblick auf das Auftreten von späten und sehr späten ScT hin untersucht. Im Grundsatz konnte der prädiktive Wert der Malapposition gezeigt werden. Darüber hinaus fand sich in der OCT-Analyse zum Zeitpunkt der ScT häufiger Thrombus im Bereich einer Malapposition, als dies bei frühen ScT beobachtet werden konnte. Frühere Studien konnten zeigen, dass die früh auftretenden ScT in vielen Fällen mit der Implantation assoziiert sind und sich durch eine angepasste Implantationsstrategie vermeiden lassen (209). Die späten und sehr späten ScT überraschten, denn zu diesem Zeitpunkt sollte die neue Stentplattform durch Resorption ihren größten Vorteil gegenüber den konventionellen Metallstents ausspielen. OCT-Fallserien beschrieben daraufhin Malapposition und die damit verbundenen Phänomene der nicht endothelialisierten Struts oder ihre Diskontinuität zum Zeitpunkt

der ScT. Die Ätiologie und der genaue Mechanismus des hiermit verbundenen Verlustes der Scaffoldgeometrie ist ungeklärt. Sowohl das Verbleiben von Malapposition nach der Implantation als auch ihre Ausbildung im Rahmen von beobachteter Evagination führten zu einem Verlust der Integrität und adäquaten Apposition an der Gefäßinnenwand. Zu ähnlichen Beobachtungen kamen die Autoren des Bern- und PESTO-Registers bei Metallstents (210). Im PRESTIGE-Register fand sich Malapposition unter den ersten drei Hauptgründen, die mit einem ST-Ereignis verbunden waren (211). Die beobachtete Nichtendothelialisierung der Scaffoldstruts ist in hohem Maße vereinbar mit Flussturbulenzen, die sich durch die inadäquate Apposition ergeben. So finden sich an der adluminalen und abluminalen Seite der Struts unterschiedlich hohe Scherspannungen, welche die lokale Blutviskosität beeinflussen und somit über die Aktivierung von Thrombozyten und Anregung zur Bildung von Neointima die Thrombogenität der Scaffolds begünstigen (212). Trotz dieser mechanistisch-rationalen und retrospektiven Beschreibung des Zusammenhangs zwischen erhöhtem Risiko für die späte und sehr späte ScT und Malappositionen finden sich in der Literatur prospektive Daten lediglich für die erste Generation DES. Hassan et al. errechneten in ihrer Meta-Analyse für das Auftreten von Stentthrombosen nach spät entwickelter Malapposition eine Odds-Ratio von 6,51 (1,34–34,91) (213). Die eingeschlossenen Studien sind in ihrem Ergebnis heterogen und ihre Berücksichtigung ist insofern eingeschränkt, als BRS mit der Resorption ihrer Struts die Thrombogenität mit zeitlichem Abstand zur Implantation eigentlich verkleinern sollten. Die vorliegende Arbeit konnte erstmalig den Zusammenhang zwischen Malapposition und dem Auftreten von späten und sehr späten ScT im Rahmen der klinischen Nachbeobachtung gezeigt werden. Der Zusammenhang bestand unabhängig vom Zeitpunkt, zu dem die Malapposition im Rahmen einer elektiven OCT-Untersuchung beobachtet wurde. Aus diesem Ergebnis kann beispielsweise die Hypothese aufgestellt werden, dass die Patienten von einer verlängerten DAPT profitieren. Die Studie weist jedoch zahlreiche Limitationen auf. So ist die ScT kein uniformes Ereignis. Ferner handelt es sich um eine kleine Patientenkohorte, in der der Zeitpunkt der Durchführung der OCTs nicht vorgegeben worden war. Weitere Studien sind demnach notwendig, auch um beispielsweise zu untersuchen, ob womöglich Plattformen mit dünneren Struts einen positiven Effekt auf die Ereignisraten haben.

Die hohe Rate unerwünschter klinischer Ereignisse im Vergleich zu DES führte schließlich im Verlauf dazu, dass der PLLA-basierte Absorb BVS und DESolve-BRS nicht mehr in der klinischen Routine verwendet wird. Das Konzept der transienten Gefäßstütze wird jedoch weiterverfolgt. Neue, bioresorbierbare Plattformen, wie der Magmaris-

(BIOTRONIK SE & Co. KG, Berlin, Deutschland) und Fantom-BRS (REVA Medical GmbH, Frankfurt am Main, Deutschland) sind derzeit Gegenstand klinischer Studien (214,215).

5 Zusammenfassung

Die perkutane Behandlung von Stenosen der Koronargefäße durch Implantation von Gefäßstützen („Stents“) ist durch ihre voranschreitende Entwicklung eine wesentliche Therapiemöglichkeit der koronaren Herzerkrankung. Bioresorbierbare Scaffolds (BRS) werden als eine neue Stentgeneration – in Analogie zum Entwicklungssprung, der mit der Einführung der medikamentenfreisetzenden Metallstents einherging – beschrieben. Die BRS der vorliegenden Habilitationsschrift sind Poly-L-Laktid (PLLA) basierend. Die intravaskuläre Bildgebung erlaubt die Darstellung und Charakterisierung untersuchter und behandelter Gefäßabschnitte. Die optische Kohärenztomographie hat aufgrund ihrer hohen Auflösung – insbesondere im Zusammenhang mit BRS – einen besonderen Stellenwert.

Registerstudien beobachten im Vergleich zu DES eine frühe und hohe Rate an Scaffold-Thrombosen (ScT). Stentstruts modulieren in Abhängigkeit ihrer Größe und Position die Thrombogenität. Es kann aufgrund der Strutdicke daher zu einer verstärkten Aktivierung des Gerinnungssystems kommen und dies kann ScT begünstigen. Vor diesem Hintergrund wurde der Novolimus-freisetzende DESolve-BRS mit reduzierter Strutdicke von 100 µm zugelassen. Mit Hilfe der optischen Kohärenztomographie konnte gezeigt werden, dass dieser BRS im Vergleich zu einem BRS mit 150 µm nach Implantation eine ähnliche Scaffold-Geometrie und Kennparameter aufweist. Es kann ein vergleichbares und zufriedenstellendes mechanisches Akutergebnis angenommen werden. Allerdings zeigte sich für den BRS mit geringerer Strutdicke ein Trend hin zu erhöhten Stentfrakturen und einer geringeren MLA als Hinweis auf eine unzureichende Radialkraft. Es muss Gegenstand langfristiger klinischer Verlaufsuntersuchungen sein, ob diese Beobachtung zugunsten der verringerten Thrombogenität akzeptiert werden kann.

Aus Beobachtungsstudien leitete sich die Hypothese ab, dass Malappositionen und die hierdurch bedingte Zunahme der Blutflussturbulenzen die Rate an Scaffold-Thrombosen begünstigen. Es wurde daher der prospektive Stellenwert von Malappositionen für das Auftreten von ScT untersucht. Die durchgeführte Studie konnte erstmalig zeigen, dass die Beobachtung von Malappositionen bei Patienten ein Prädiktor für das zukünftige Auftreten von späten und sehr späten ScT ist. Ferner fand sich ein Zusammenhang zwischen Thrombus und dem Auftreten von ScT insbesondere bei größeren Gefäßen bzw. Scaffolds. Es konnte im Weiteren beobachtet werden, dass späte und sehr späte ScT häufiger Frauen betrafen und solche Patienten, die zuvor bereits behandelt worden sind.

Der Everolimus-freisetzende, PLLA-basierte BRS Absorb BVS ist hinsichtlich der Implantation in Gefäße mit einem Referenzdiameter größer als 4,0 mm insofern

eingeschränkt, als das eine Expansionsbegrenzung auf 0,5 mm vorgegeben ist. Die Überexpansion kann zu Diskontinuität der Struts oder Frakturen führen. Der Einsatz der BRS wird somit in bestimmten Szenarien, wie z. B. im Hauptstamm oder in hauptstammnahen Abschnitten, limitiert. Hieraus ableitend wurde der Everolimus-freisetzender BRS DESolve XL zugelassen. Durch Analyse des abschließenden „OCT-Pullbacks“ konnte erstmalig das akute mechanische Ergebnis nach Implantation von Novolimus-freisetzenden BRS in Gefäßen mit großem Diameter dokumentiert werden. Die Analyse der OCT-Querschnitte zeigte ein positives Primärergebnis inklusive der geometrischen Implantationsaspekte und unter Berücksichtigung niedriger Raten von Frakturen und Dissektionen. Hieraus kann abgeleitet werden, dass die PLLA-basierte BRS-Plattform grundsätzlich für die Verwendung in Gefäßen mit großem Diameter geeignet scheint.

Für den Everolimus-freisetzenden Absorb BVS konnte mit Hilfe der intravaskulären Bildgebung gezeigt werden, dass das Expansionsergebnis von der Plaquelast, ihrer -Morphologie und -Zusammensetzung abhängt. Über den Absorb BVS hinaus wurde ein Novolimus-freisetzender, PLLA-basierter BRS zugelassen. Der DESolve weist als Alleinstellungsmerkmal über den Aufbau hinaus eine Selbstkorrekturfunktion auf. Es konnte erstmalig gezeigt werden, dass das mechanische Ergebnis unmittelbar nach Implantation von Novolimus-freisetzenden DESolve-BRS im Gegensatz zu den vorangegangenen Ergebnissen mit dem Absorb BVS nicht in gleichem Maße von der zu Grunde liegenden Läsion abhängig ist. Das Primärergebnis zeigte sich ausschließlich von der Last einer Plaque mit dominierend fibröser Zusammensetzung signifikant abhängig. Der DESolve-BRS könnte demnach dem Absorb BVS in Abhängigkeit der Plaque hinsichtlich des primären Implantationsergebnisses überlegen sein.

In weiteren Studien wurden prozedurale Aspekte im Rahmen der Implantation der BRS untersucht. Es konnte erstmalig der Einfluss der Nachdilatation auf das primäre Implantationsergebnis mit Hilfe der OCT untersucht und ihr wesentlicher Beitrag zur adäquaten Entfaltung und Apposition gezeigt werden. Durch die Nachdilatation kam es zu keiner messbaren Zunahme der mechanischen Komplikationen. Im Weiteren wurde der Einfluss der überlappenden Implantation von BRS wegen langer Läsionen auf das primäre Implantationsergebnis untersucht. Mit Hilfe der OCT zeigte sich keine relevante Reduktion der MLA und Scaffold-Fläche oder Zunahme der mechanischen Diskontinuität. Es kann daher mit Hinblick auf das Akutergebnis eine sichere Implantation hintereinander liegender BRS angenommen werden.

Nach Implantation eines Stents wird eine duale Thrombozytenaggregation empfohlen. Circa 5–10 % der behandelten Patienten haben jedoch auch eine Indikation zur dauerhaften oralen Antikoagulation (OAK). Sie sind mit Hinblick auf die Behandlung mit BRS

unzureichend untersucht. Es wurde daher eine Studie durchgeführt, in der diese Population mit Patienten verglichen wurde, die keine begleitende Indikation zur OAK haben. Es konnte gezeigt werden, dass der Großteil der Patienten mit Indikation zur OAK mit einem NOAK behandelt wurde. Die Dauer der begleitenden Thrombozytenaggregation wurde überwiegend auf einen Monat beschränkt. Es kam zu keiner Zunahme schwerwiegender Blutungskomplikationen in der Gruppe mit Indikation zur OAK. In dem untersuchten Patientenkollektiv konnte ebenso gezeigt werden, dass es zu keiner relevanten Zunahme der ischämischen Ereignisse kommt. Dennoch blieb die hohe Rate an ScT und MACE auffällig.

Die hohe Rate unerwünschter klinischer Ereignisse im Vergleich zu DES führte schließlich im Verlauf dazu, dass PLLA-basierte Absorb BVS und DESolve-BRS nicht mehr in der klinischen Routine verwendet werden. Neue bioresorbierbare Plattformen, wie der Magmaris- und Fantom-BRS, sind derzeit Gegenstand klinischer Studien.

6 Literaturverzeichnis

1. Deutsche Herzstiftung e.V. *Deutscher Herzbericht 2020*; Georg Thieme Verlag KG: 2021.
2. Statistisches Bundesamt (Destatis), 2021. In: Genesis-Online. Verfügbar online: <https://www-genesis.destatis.de/genesis/online?sequenz=tabelleErgebnis&selectionname=12621-0002&zeitscheiben=16&sachmerkmal=ALT577&sachschlüssel=ALTVOLL000,ALTVOLL020,ALTVOLL040,ALTVOLL060,ALTVOLL065,ALTVOLL080> (Abgerufen 04.08.2021); Datenlizenz by-2-0.
3. Gosswald, A.; Schienkiewitz, A.; Nowossadeck, E.; Busch, M.A. Prevalence of myocardial infarction and coronary heart disease in adults aged 40-79 years in Germany: results of the German Health Interview and Examination Survey for Adults (DEGS1). *Bundesgesundheitsblatt Gesundheitsforschung Gesundheitsschutz* **2013**, 56(5-6), 650-655.
4. Dawber, T.R.; Moore, F.E.; Mann, G.V. Coronary heart disease in the Framingham study. *Am J Public Health Nations Health* **1957**, 47(4 Pt 2), 4-24.
5. Piepoli, M.F.; Hoes, A.W.; Agewall, S.; Albus, C.; Brotons, C.; Catapano, A.L.; Cooney, M.T.; Corra, U.; Cosyns, B.; Deaton, C.; Graham, I.; Hall, M.S.; Hobbs, F.D.R.; Lochen, M.L.; Lollgen, H.; Marques-Vidal, P.; Perk, J.; Prescott, E.; Redon, J.; Richter, D.J.; Sattar, N.; Smulders, Y.; Tiberi, M.; van der Worp, H.B.; van Dis, I.; Verschuren, W.M.M.; Binno, S.; Group, E.S.C.S.D. 2016 European Guidelines on cardiovascular disease prevention in clinical practice: The Sixth Joint Task Force of the European Society of Cardiology and Other Societies on Cardiovascular Disease Prevention in Clinical Practice (constituted by representatives of 10 societies and by invited experts) Developed with the special contribution of the European Association for Cardiovascular Prevention & Rehabilitation (EACPR). *Eur Heart J* **2016**, 37(29), 2315-2381.
6. Robert Koch-Institut (Hrsg). *Gesundheit in Deutschland. Gesundheitsberichterstattung des Bundes. Gemeinsam getragen von RKI und Destatis. RKI, Berlin* **2015**, 10.17886/rkipubl-2015-003.
7. Knuuti, J.; Wijns, W.; Saraste, A.; Capodanno, D.; Barbato, E.; Funck-Brentano, C.; Prescott, E.; Storey, R.F.; Deaton, C.; Cuisset, T.; Agewall, S.; Dickstein, K.; Edvardsen, T.; Escaned, J.; Gersh, B.J.; Svitil, P.; Gilard, M.; Hasdai, D.; Hatala, R.; Mahfoud, F.; Masip, J.; Muneretto, C.; Valgimigli, M.; Achenbach, S.; Bax, J.J.; Group, E.S.C.S.D. 2019 ESC Guidelines for the diagnosis and management of chronic coronary syndromes. *Eur Heart J* **2019**, 41, 407-477.
8. Ahmadi, A.; Argulian, E.; Leipsic, J.; Newby, D.E.; Narula, J. From Subclinical Atherosclerosis to Plaque Progression and Acute Coronary Events. *JACC Cardiovasc Imaging* **2019**, 74(12), 1608-1617.
9. World Health Organization. CLASSIFICATION of atherosclerotic lesions; report of a study group. *World Health Organ Tech Rep Ser* **1958**, 57(143), 1-20.
10. Stryer, H.C.; Chandler, A.B.; Glagov, S.; Guyton, J.R.; Insull, W., Jr.; Rosenfeld, M.E.; Schaffer, S.A.; Schwartz, C.J.; Wagner, W.D.; Wissler, R.W. A definition of initial, fatty streak, and intermediate lesions of atherosclerosis. A report from

- the Committee on Vascular Lesions of the Council on Arteriosclerosis, American Heart Association. *Circulation* **1994**, *89*(5), 2462-2478.
11. Stary, H.C.; Chandler, A.B.; Dinsmore, R.E.; Fuster, V.; Glagov, S.; Insull, W., Jr.; Rosenfeld, M.E.; Schwartz, C.J.; Wagner, W.D.; Wissler, R.W. A definition of advanced types of atherosclerotic lesions and a histological classification of atherosclerosis. A report from the Committee on Vascular Lesions of the Council on Arteriosclerosis, American Heart Association. *Circulation* **1995**, *92*(5), 1355-1374.
 12. Brasen, J.H.; Niendorf, A. Atherosclerosis. Formal pathogenesis, classification and functional significance. *Pathologie* **1997**, *18*(3), 218-227.
 13. Chistiakov, D.A.; Melnichenko, A.A.; Myasoedova, V.A.; Grechko, A.V.; Orekhov, A.N. Mechanisms of foam cell formation in atherosclerosis. *J Mol Med (Berl)* **2017**, *95*(11), 1153-1165.
 14. Eggen, D.A.; Solberg, L.A. Variation of atherosclerosis with age. *Lab Invest* **1968**, *18*(5), 571-579.
 15. Falk, E. Morphologic features of unstable atherothrombotic plaques underlying acute coronary syndromes. *Am J Cardiol* **1989**, *63*(10), 114E-120E.
 16. Richardson, P.D.; Davies, M.J.; Born, G.V. Influence of plaque configuration and stress distribution on fissuring of coronary atherosclerotic plaques. *Lancet* **1989**, *2*(8669), 941-944.
 17. Gertz, S.D.; Roberts, W.C. Hemodynamic shear force in rupture of coronary arterial atherosclerotic plaques. *Am J Cardiol* **1990**, *66*(19), 1368-1372.
 18. Douglas, P.S.; Hoffmann, U.; Patel, M.R.; Mark, D.B.; Al-Khalidi, H.R.; Cavanaugh, B.; Cole, J.; Dolor, R.J.; Fordyce, C.B.; Huang, M.; Khan, M.A.; Kosinski, A.S.; Krucoff, M.W.; Malhotra, V.; Picard, M.H.; Udelson, J.E.; Velazquez, E.J.; Yow, E.; Cooper, L.S.; Lee, K.L.; Investigators, P. Outcomes of anatomical versus functional testing for coronary artery disease. *N Engl J Med* **2015**, *372*(14), 1291-1300.
 19. Scot-Heart investigators. CT coronary angiography in patients with suspected angina due to coronary heart disease (SCOT-HEART): an open-label, parallel-group, multicentre trial. *Lancet* **2015**, *385*(9985), 2383-2391.
 20. Scot-Heart investigators; Newby, D.E.; Adamson, P.D.; Berry, C.; Boon, N.A.; Dweck, M.R.; Flather, M.; Forbes, J.; Hunter, A.; Lewis, S.; MacLean, S.; Mills, N.L.; Norrie, J.; Roditi, G.; Shah, A.S.V.; Timmis, A.D.; van Beek, E.J.R.; Williams, M.C. Coronary CT Angiography and 5-Year Risk of Myocardial Infarction. *N Engl J Med* **2018**, *379*(10), 924-933.
 21. Androulakis, A.; Aznaouridis, K.A.; Aggeli, C.J.; Roussakis, G.N.; Michaelides, A.P.; Kartalis, A.N.; Stougiannos, P.N.; Dilaveris, P.E.; Misovoulos, P.I.; Stefanadis, C.I.; Kallikazaros, I.E. Transient ST-segment depression during paroxysms of atrial fibrillation in otherwise normal individuals: relation with underlying coronary artery disease. *J Am Coll Cardiol* **2007**, *50*(19), 1909-1911.
 22. Greenwood, J.P.; Ripley, D.P.; Berry, C.; McCann, G.P.; Plein, S.; Bucciarelli-Ducci, C.; Dall'Armellina, E.; Prasad, A.; Bijsterveld, P.; Foley, J.R.; Mangion, K.; Sculpher, M.; Walker, S.; Everett, C.C.; Cairns, D.A.; Sharples, L.D.; Brown, J.M.; Investigators, C.-M. Effect of Care Guided by Cardiovascular Magnetic Resonance, Myocardial Perfusion Scintigraphy, or NICE Guidelines on

- Subsequent Unnecessary Angiography Rates: The CE-MARC 2 Randomized Clinical Trial. *JAMA* **2016**, *316*(10), 1051-1060.
23. Knuuti, J.; Ballo, H.; Juarez-Orozco, L.E.; Saraste, A.; Kolh, P.; Rutjes, A.W.S.; Juni, P.; Windecker, S.; Bax, J.J.; Wijns, W. The performance of non-invasive tests to rule-in and rule-out significant coronary artery stenosis in patients with stable angina: a meta-analysis focused on post-test disease probability. *Eur Heart J* **2018**, *39*(35), 3322-3330.
24. Thygesen, K.; Alpert, J.S.; Jaffe, A.S.; Chaitman, B.R.; Bax, J.J.; Morrow, D.A.; White, H.D.; Executive Group on behalf of the Joint European Society of Cardiology /American College of Cardiology /American Heart Association /World Heart Federation Task Force for the Universal Definition of Myocardial, I. Fourth Universal Definition of Myocardial Infarction (2018). *Circulation* **2018**, *138*(20), e618-e651.
25. Neumann, F.J.; Sousa-Uva, M.; Ahlsson, A.; Alfonso, F.; Banning, A.P.; Benedetto, U.; Byrne, R.A.; Collet, J.P.; Falk, V.; Head, S.J.; Juni, P.; Kastrati, A.; Koller, A.; Kristensen, S.D.; Niebauer, J.; Richter, D.J.; Seferovic, P.M.; Sibbing, D.; Stefanini, G.G.; Windecker, S.; Yadav, R.; Zembala, M.O. 2018 ESC/EACTS Guidelines on myocardial revascularization. *Eur Heart J* **2019**, *40*(2), 87-165.
26. Booth, J.N., 3rd; Levitan, E.B.; Brown, T.M.; Farkouh, M.E.; Safford, M.M.; Muntner, P. Effect of sustaining lifestyle modifications (nonsmoking, weight reduction, physical activity, and mediterranean diet) after healing of myocardial infarction, percutaneous intervention, or coronary bypass (from the REasons for Geographic and Racial Differences in Stroke Study). *Am J Cardiol* **2014**, *113*(12), 1933-1940.
27. Giannuzzi, P.; Temporelli, P.L.; Marchioli, R.; Maggioni, A.P.; Balestroni, G.; Ceci, V.; Chieffo, C.; Gattone, M.; Griffo, R.; Schweiger, C.; Tavazzi, L.; Urbinati, S.; Valagussa, F.; Vanuzzo, D.; Investigators, G. Global secondary prevention strategies to limit event recurrence after myocardial infarction: results of the GOSPEL study, a multicenter, randomized controlled trial from the Italian Cardiac Rehabilitation Network. *Arch Intern Med* **2008**, *168*(20), 2194-2204.
28. Chow, C.K.; Jolly, S.; Rao-Melacini, P.; Fox, K.A.; Anand, S.S.; Yusuf, S. Association of diet, exercise, and smoking modification with risk of early cardiovascular events after acute coronary syndromes. *Circulation* **2010**, *121*(6), 750-758.
29. Rousan, T.A.; Mathew, S.T.; Thadani, U. Drug Therapy for Stable Angina Pectoris. *Drugs* **2017**, *77*(3), 265-284.
30. Thadani, U. Management of Stable Angina - Current Guidelines: A Critical Appraisal. *Cardiovasc Drugs Ther* **2016**, *30*(4), 419-426.
31. Dahl Aarvik, M.; Sandven, I.; Dondo, T.B.; Gale, C.P.; Ruddox, V.; Munkhaugen, J.; Atar, D.; Otterstad, J.E. Effect of oral beta-blocker treatment on mortality in contemporary post-myocardial infarction patients: a systematic review and meta-analysis. *Eur Heart J Cardiovasc Pharmacother* **2019**, *5*(1), 12-20.
32. Bangalore, S.; Steg, G.; Deedwania, P.; Crowley, K.; Eagle, K.A.; Goto, S.; Ohman, E.M.; Cannon, C.P.; Smith, S.C.; Zeymer, U.; Hoffman, E.B.; Messerli, F.H.; Bhatt, D.L.; Investigators, R.R. beta-Blocker use and clinical outcomes in

- stable outpatients with and without coronary artery disease. *JAMA* **2012**, *308*(13), 1340-1349.
33. Klein, W.W.; Jackson, G.; Tavazzi, L. Efficacy of monotherapy compared with combined antianginal drugs in the treatment of chronic stable angina pectoris: a meta-analysis. *Coron Artery Dis* **2002**, *13*(8), 427-436.
 34. Borer, J.S.; Tardif, J.C. Efficacy of ivabradine, a selective I(f) inhibitor, in patients with chronic stable angina pectoris and diabetes mellitus. *Am J Cardiol* **2010**, *105*(1), 29-35.
 35. Wilson, S.R.; Scirica, B.M.; Braunwald, E.; Murphy, S.A.; Karwatowska-Prokopczuk, E.; Buros, J.L.; Chaitman, B.R.; Morrow, D.A. Efficacy of ranolazine in patients with chronic angina observations from the randomized, double-blind, placebo-controlled MERLIN-TIMI (Metabolic Efficiency With Ranolazine for Less Ischemia in Non-ST-Segment Elevation Acute Coronary Syndromes) 36 Trial. *J Am Coll Cardiol* **2009**, *53*(17), 1510-1516.
 36. Szummer, K.; Jernberg, T.; Wallentin, L. From Early Pharmacology to Recent Pharmacology Interventions in Acute Coronary Syndromes: JACC State-of-the-Art Review. *J Am Coll Cardiol* **2019**, *74*(12), 1618-1636.
 37. Antithrombotic Trialists Collaboration; Baigent, C.; Blackwell, L.; Collins, R.; Emberson, J.; Godwin, J.; Peto, R.; Buring, J.; Hennekens, C.; Kearney, P.; Meade, T.; Patrono, C.; Roncaglioni, M.C.; Zanchetti, A. Aspirin in the primary and secondary prevention of vascular disease: collaborative meta-analysis of individual participant data from randomised trials. *Lancet* **2009**, *373*(9678), 1849-1860.
 38. Wiviott, S.D.; Braunwald, E.; McCabe, C.H.; Montalescot, G.; Ruzyllo, W.; Gottlieb, S.; Neumann, F.J.; Ardissino, D.; De Servi, S.; Murphy, S.A.; Riesmeyer, J.; Weerakkody, G.; Gibson, C.M.; Antman, E.M.; Investigators, T.-T. Prasugrel versus clopidogrel in patients with acute coronary syndromes. *N Engl J Med* **2007**, *357*(20), 2001-2015.
 39. Wallentin, L.; Becker, R.C.; Budaj, A.; Cannon, C.P.; Emanuelsson, H.; Held, C.; Horrow, J.; Husted, S.; James, S.; Katus, H.; Mahaffey, K.W.; Scirica, B.M.; Skene, A.; Steg, P.G.; Storey, R.F.; Harrington, R.A.; Investigators, P.; Freij, A.; Thorsen, M. Ticagrelor versus clopidogrel in patients with acute coronary syndromes. *N Engl J Med* **2009**, *361*(11), 1045-1057.
 40. Committee, C.S. A randomised, blinded, trial of clopidogrel versus aspirin in patients at risk of ischaemic events (CAPRIE). CAPRIE Steering Committee. *Lancet* **1996**, *348*(9038), 1329-1339.
 41. Arbel, R.; Hammerman, A.; Triki, N.; Greenberg, D. PCSK9 inhibitors may improve cardiovascular outcomes-Can we afford them? *Int J Cardiol* **2016**, *220*, 242-245.
 42. Braunwald, E.; Domanski, M.J.; Fowler, S.E.; Geller, N.L.; Gersh, B.J.; Hsia, J.; Pfeffer, M.A.; Rice, M.M.; Rosenberg, Y.D.; Rouleau, J.L.; Investigators, P.T. Angiotensin-converting-enzyme inhibition in stable coronary artery disease. *N Engl J Med* **2004**, *351*(20), 2058-2068.
 43. Heart Outcomes Prevention Evaluation Study Investigators; Yusuf, S.; Sleight, P.; Pogue, J.; Bosch, J.; Davies, R.; Dagenais, G. Effects of an angiotensin-

- converting-enzyme inhibitor, ramipril, on cardiovascular events in high-risk patients. *N Engl J Med* **2000**, *342*(3), 145-153.
44. Nabel, E.G.; Braunwald, E. A tale of coronary artery disease and myocardial infarction. *N Engl J Med* **2012**, *366*(1), 54-63.
45. Bangalore, S.; Pursnani, S.; Kumar, S.; Bagos, P.G. Percutaneous coronary intervention versus optimal medical therapy for prevention of spontaneous myocardial infarction in subjects with stable ischemic heart disease. *Circulation* **2013**, *127*(7), 769-781.
46. Johnson, N.P.; Toth, G.G.; Lai, D.; Zhu, H.; Acar, G.; Agostoni, P.; Appelman, Y.; Arslan, F.; Barbato, E.; Chen, S.L.; Di Serafino, L.; Dominguez-Franco, A.J.; Dupouy, P.; Esen, A.M.; Esen, O.B.; Hamilos, M.; Iwasaki, K.; Jensen, L.O.; Jimenez-Navarro, M.F.; Katritsis, D.G.; Kocaman, S.A.; Koo, B.K.; Lopez-Palop, R.; Lorin, J.D.; Miller, L.H.; Muller, O.; Nam, C.W.; Oud, N.; Puymirat, E.; Rieber, J.; Rioufol, G.; Rodes-Cabau, J.; Sedlis, S.P.; Takeishi, Y.; Tonino, P.A.; Van Belle, E.; Verna, E.; Werner, G.S.; Fearon, W.F.; Pijls, N.H.; De Bruyne, B.; Gould, K.L. Prognostic value of fractional flow reserve: linking physiologic severity to clinical outcomes. *J Am Coll Cardiol* **2014**, *64*(16), 1641-1654.
47. Stergiopoulos, K.; Brown, D.L. Initial coronary stent implantation with medical therapy vs medical therapy alone for stable coronary artery disease: meta-analysis of randomized controlled trials. *Arch Intern Med* **2012**, *172*(4), 312-319.
48. Trikalinos, T.A.; Alsheikh-Ali, A.A.; Tatsioni, A.; Nallamothu, B.K.; Kent, D.M. Percutaneous coronary interventions for non-acute coronary artery disease: a quantitative 20-year synopsis and a network meta-analysis. *Lancet* **2009**, *373*(9667), 911-918.
49. Windecker, S.; Stortecky, S.; Stefanini, G.G.; da Costa, B.R.; Rutjes, A.W.; Di Nisio, M.; Silleto, M.G.; Maione, A.; Alfonso, F.; Clemmensen, P.M.; Collet, J.P.; Cremer, J.; Falk, V.; Filippatos, G.; Hamm, C.; Head, S.; Kappetein, A.P.; Kastrati, A.; Knuuti, J.; Landmesser, U.; Laufer, G.; Neumann, F.J.; Richter, D.; Schauerte, P.; Sousa Uva, M.; Taggart, D.P.; Torracca, L.; Valgimigli, M.; Wijns, W.; Witkowski, A.; Kolh, P.; Juni, P. Revascularisation versus medical treatment in patients with stable coronary artery disease: network meta-analysis. *BMJ* **2014**, *348*, g3859.
50. Forssmann, W. Die Sondierung des rechten Herzens. *Klinische Wochenschrift* **1929**, *8*(45), 2085-2087.
51. Seldinger, S.I. Catheter replacement of the needle in percutaneous arteriography; a new technique. *Acta radiol* **1953**, *39*(5), 368-376.
52. Sones, F.M., Jr. Cine-cardio-angiography. *Pediatr Clin North Am* **1958**, *5*(4), 945-979.
53. Dotter, C.T.; Judkins, M.P. Transluminal treatment of arteriosclerotic obstruction. Description of a new technic and a preliminary report of its application. *Circulation* **1964**, *30*, 654-670.
54. Gruntzig, A. Transluminal dilatation of coronary-artery stenosis. *Lancet* **1978**, *1*(8058), 263.
55. Simpson, J.B.; Baim, D.S.; Robert, E.W.; Harrison, D.C. A new catheter system for coronary angioplasty. *Am J Cardiol* **1982**, *49*(5), 1216-1222.

56. Bonzel, T.; Wollschlager, H.; Just, H. A new catheter system for the mechanical dilatation of coronary stenoses with exchangeable intracoronary catheters, fast flow of the contrast agent and improved control. *Biomed Tech (Berl)* **1986**, *31*(9), 195-200.
57. Huber, M.S.; Mooney, J.F.; Madison, J.; Mooney, M.R. Use of a morphologic classification to predict clinical outcome after dissection from coronary angioplasty. *Am J Cardiol* **1991**, *68*(5), 467-471.
58. Lincoff, A.M.; Popma, J.J.; Ellis, S.G.; Hacker, J.A.; Topol, E.J. Abrupt vessel closure complicating coronary angioplasty: clinical, angiographic and therapeutic profile. *J Am Coll Cardiol* **1992**, *19*(5), 926-935.
59. Iqbal, J.; Gunn, J.; Serruys, P.W. Coronary stents: historical development, current status and future directions. *Br Med Bull* **2013**, *106*, 193-211.
60. Pendyala, L.; Jabara, R.; Robinson, K.; Chronos, N. Passive and active polymer coatings for intracoronary stents: novel devices to promote arterial healing. *J Interv Cardiol* **2009**, *22*(1), 37-48.
61. Serruys, P.W.; Rutherford, J.D. The Birth, and Evolution, of Percutaneous Coronary Interventions: A Conversation With Patrick Serruys, MD, PhD. *Circulation* **2016**, *134*(2), 97-100.
62. Schatz, R.A.; Palmaz, J.C.; Tio, F.O.; Garcia, F.; Garcia, O.; Reuter, S.R. Balloon-expandable intracoronary stents in the adult dog. *Circulation* **1987**, *76*(2), 450-457.
63. Palmaz, J.C.; Sibbitt, R.R.; Reuter, S.R.; Tio, F.O.; Rice, W.J. Expandable intraluminal graft: a preliminary study. Work in progress. *Radiology* **1985**, *156*(1), 73-77.
64. Sigwart, U.; Puel, J.; Mirkovitch, V.; Joffre, F.; Kappenberger, L. Intravascular stents to prevent occlusion and restenosis after transluminal angioplasty. *N Engl J Med* **1987**, *316*(12), 701-706.
65. Schatz, R.A. A view of vascular stents. *Circulation* **1989**, *79*(2), 445-457.
66. Serruys, P.W.; de Jaegere, P.; Kiemeneij, F.; Macaya, C.; Rutsch, W.; Heyndrickx, G.; Emanuelsson, H.; Marco, J.; Legrand, V.; Materne, P.; et al. A comparison of balloon-expandable-stent implantation with balloon angioplasty in patients with coronary artery disease. Benestent Study Group. *N Engl J Med* **1994**, *331*(8), 489-495.
67. Savage, M.P.; Fischman, D.L.; Rake, R.; Leon, M.B.; Schatz, R.A.; Penn, I.; Nobuyoshi, M.; Moses, J.; Hirshfeld, J.; Heuser, R.; Baim, D.; Cleman, M.; Brinker, J.; Gebhardt, S.; Goldberg, S. Efficacy of coronary stenting versus balloon angioplasty in small coronary arteries. Stent Restenosis Study (STRESS) Investigators. *J Am Coll Cardiol* **1998**, *31*(2), 307-311.
68. Holmes, D.R., Jr.; Savage, M.; LaBlanche, J.M.; Grip, L.; Serruys, P.W.; Fitzgerald, P.; Fischman, D.; Goldberg, S.; Brinker, J.A.; Zeiher, A.M.; Shapiro, L.M.; Willerson, J.; Davis, B.R.; Ferguson, J.J.; Popma, J.; King, S.B., 3rd; Lincoff, A.M.; Tchong, J.E.; Chan, R.; Granett, J.R.; Poland, M. Results of Prevention of REStenosis with Tranilast and its Outcomes (PRESTO) trial. *Circulation* **2002**, *106*(10), 1243-1250.

69. Kimura, T.; Tamura, T.; Yokoi, H.; Nobuyoshi, M. Long-term clinical and angiographic follow-up after placement of Palmaz-Schatz coronary stent: a single center experience. *J Interv Cardiol* **1994**, *7*(2), 129-139.
70. Moliterno, D.J. Healing Achilles--sirolimus versus paclitaxel. *N Engl J Med* **2005**, *353*(7), 724-727.
71. Savage, M.P.; Fischman, D.L.; Schatz, R.A.; Teirstein, P.S.; Leon, M.B.; Baim, D.; Ellis, S.G.; Topol, E.J.; Hirshfeld, J.W.; Cleman, M.W.; et al. Long-term angiographic and clinical outcome after implantation of a balloon-expandable stent in the native coronary circulation. Palmaz-Schatz Stent Study Group. *J Am Coll Cardiol* **1994**, *24*(5), 1207-1212.
72. Hoffmann, R.; Jansen, C.; König, A.; Haager, P.K.; Kerckhoff, G.; vom Dahl, J.; Klauss, V.; Hanrath, P.; Mudra, H. Stent design related neointimal tissue proliferation in human coronary arteries; an intravascular ultrasound study. *Eur Heart J* **2001**, *22*(21), 2007-2014.
73. Ormiston, J.A.; Dixon, S.R.; Webster, M.W.; Ruygrok, P.N.; Stewart, J.T.; Minchington, I.; West, T. Stent longitudinal flexibility: a comparison of 13 stent designs before and after balloon expansion. *Catheter Cardiovasc Interv* **2000**, *50*(1), 120-124.
74. Rossini, R.; Musumeci, G.; Aprile, A.; Valsecchi, O. Long-term outcomes in patients undergoing percutaneous coronary intervention with drug-eluting stents. *Expert Rev Pharmacoecon Outcomes Res* **2010**, *10*(1), 49-61.
75. Abal, M.; Andreu, J.M.; Barasoain, I. Taxanes: microtubule and centrosome targets, and cell cycle dependent mechanisms of action. *Curr Cancer Drug Targets* **2003**, *3*(3), 193-203.
76. Gallo, R.; Padurean, A.; Jayaraman, T.; Marx, S.; Roque, M.; Adelman, S.; Chesebro, J.; Fallon, J.; Fuster, V.; Marks, A.; Badimon, J.J. Inhibition of intimal thickening after balloon angioplasty in porcine coronary arteries by targeting regulators of the cell cycle. *Circulation* **1999**, *99*(16), 2164-2170.
77. Marx, S.O.; Marks, A.R. Bench to bedside: the development of rapamycin and its application to stent restenosis. *Circulation* **2001**, *104*(8), 852-855.
78. Goy, J.J.; Stauffer, J.C.; Siegenthaler, M.; Benoît, A.; Seydoux, C. A prospective randomized comparison between paclitaxel and sirolimus stents in the real world of interventional cardiology: the TAXi trial. *J Am Coll Cardiol* **2005**, *45*(2), 308-311.
79. Laarman, G.J.; Suttorp, M.J.; Dirksen, M.T.; van Heerebeek, L.; Kiemeneij, F.; Slagboom, T.; van der Wieken, L.R.; Tijssen, J.G.; Rensing, B.J.; Patterson, M. Paclitaxel-eluting versus uncoated stents in primary percutaneous coronary intervention. *N Engl J Med* **2006**, *355*(11), 1105-1113.
80. Morice, M.C.; Colombo, A.; Meier, B.; Serruys, P.; Tamburino, C.; Guagliumi, G.; Sousa, E.; Stoll, H.P. Sirolimus- vs paclitaxel-eluting stents in de novo coronary artery lesions: the REALITY trial: a randomized controlled trial. *Jama* **2006**, *295*(8), 895-904.
81. Stone, G.W.; Ellis, S.G.; Cox, D.A.; Hermiller, J.; O'Shaughnessy, C.; Mann, J.T.; Turco, M.; Caputo, R.; Bergin, P.; Greenberg, J.; Popma, J.J.; Russell, M.E. One-year clinical results with the slow-release, polymer-based, paclitaxel-eluting TAXUS stent: the TAXUS-IV trial. *Circulation* **2004**, *109*(16), 1942-1947.

82. Stone, G.W.; Moses, J.W.; Ellis, S.G.; Schofer, J.; Dawkins, K.D.; Morice, M.C.; Colombo, A.; Schampaert, E.; Grube, E.; Kirtane, A.J.; Cutlip, D.E.; Fahy, M.; Pocock, S.J.; Mehran, R.; Leon, M.B. Safety and efficacy of sirolimus- and paclitaxel-eluting coronary stents. *N Engl J Med* **2007**, *356*(10), 998-1008.
83. Iakovou, I.; Schmidt, T.; Bonizzoni, E.; Ge, L.; Sangiorgi, G.M.; Stankovic, G.; Airolidi, F.; Chieffo, A.; Montorfano, M.; Carlino, M.; Michev, I.; Corvaja, N.; Briguori, C.; Gerckens, U.; Grube, E.; Colombo, A. Incidence, predictors, and outcome of thrombosis after successful implantation of drug-eluting stents. *Jama* **2005**, *293*(17), 2126-2130.
84. McFadden, E.P.; Stabile, E.; Regar, E.; Cheneau, E.; Ong, A.T.; Kinnaird, T.; Suddath, W.O.; Weissman, N.J.; Torguson, R.; Kent, K.M.; Pichard, A.D.; Satler, L.F.; Waksman, R.; Serruys, P.W. Late thrombosis in drug-eluting coronary stents after discontinuation of antiplatelet therapy. *Lancet* **2004**, *364*(9444), 1519-1521.
85. Joner, M.; Finn, A.V.; Farb, A.; Mont, E.K.; Kolodgie, F.D.; Ladich, E.; Kutys, R.; Skorija, K.; Gold, H.K.; Virmani, R. Pathology of drug-eluting stents in humans: delayed healing and late thrombotic risk. *J Am Coll Cardiol* **2006**, *48*(1), 193-202.
86. Nakazawa, G.; Finn, A.V.; Joner, M.; Ladich, E.; Kutys, R.; Mont, E.K.; Gold, H.K.; Burke, A.P.; Kolodgie, F.D.; Virmani, R. Delayed arterial healing and increased late stent thrombosis at culprit sites after drug-eluting stent placement for acute myocardial infarction patients: an autopsy study. *Circulation* **2008**, *118*(11), 1138-1145.
87. Heldman, A.W.; Cheng, L.; Jenkins, G.M.; Heller, P.F.; Kim, D.W.; Ware, M., Jr.; Nater, C.; Hruban, R.H.; Rezaei, B.; Abella, B.S.; Bunge, K.E.; Kinsella, J.L.; Sollott, S.J.; Lakatta, E.G.; Brinker, J.A.; Hunter, W.L.; Froehlich, J.P. Paclitaxel stent coating inhibits neointimal hyperplasia at 4 weeks in a porcine model of coronary restenosis. *Circulation* **2001**, *103*(18), 2289-2295.
88. Menown, I.B.; Noad, R.; Garcia, E.J.; Meredith, I. The platinum chromium element stent platform: from alloy, to design, to clinical practice. *Adv Ther* **2010**, *27*(3), 129-141.
89. O'Brien, B.J.; Stinson, J.S.; Larsen, S.R.; Eppihimer, M.J.; Carroll, W.M. A platinum-chromium steel for cardiovascular stents. *Biomaterials* **2010**, *31*(14), 3755-3761.
90. Joner, M.; Nakazawa, G.; Finn, A.V.; Quee, S.C.; Coleman, L.; Acampado, E.; Wilson, P.S.; Skorija, K.; Cheng, Q.; Xu, X.; Gold, H.K.; Kolodgie, F.D.; Virmani, R. Endothelial cell recovery between comparator polymer-based drug-eluting stents. *J Am Coll Cardiol* **2008**, *52*(5), 333-342.
91. Nebeker, J.R.; Virmani, R.; Bennett, C.L.; Hoffman, J.M.; Samore, M.H.; Alvarez, J.; Davidson, C.J.; McKoy, J.M.; Raisch, D.W.; Whisenant, B.K.; Yarnold, P.R.; Belknap, S.M.; West, D.P.; Gage, J.E.; Morse, R.E.; Gligoric, G.; Davidson, L.; Feldman, M.D. Hypersensitivity cases associated with drug-eluting coronary stents: a review of available cases from the Research on Adverse Drug Events and Reports (RADAR) project. *J Am Coll Cardiol* **2006**, *47*(1), 175-181.
92. Dangas, G.D.; Serruys, P.W.; Kereiakes, D.J.; Hermiller, J.; Rizvi, A.; Newman, W.; Sudhir, K.; Smith, R.S., Jr.; Cao, S.; Theodoropoulos, K.; Cutlip, D.E.; Lansky, A.J.; Stone, G.W. Meta-analysis of everolimus-eluting versus paclitaxel-eluting stents in coronary artery disease: final 3-year results of the SPIRIT clinical

- trials program (Clinical Evaluation of the Xience V Everolimus Eluting Coronary Stent System in the Treatment of Patients With De Novo Native Coronary Artery Lesions). *JACC Cardiovasc Interv* **2013**, *6*(9), 914-922.
93. Wijns, W.; Steg, P.G.; Mauri, L.; Kurowski, V.; Parikh, K.; Gao, R.; Bode, C.; Greenwood, J.P.; Lipsic, E.; Alamgir, F.; Rademaker-Havinga, T.; Boersma, E.; Radke, P.; van Leeuwen, F.; Camenzind, E. Endeavour zotarolimus-eluting stent reduces stent thrombosis and improves clinical outcomes compared with cypher sirolimus-eluting stent: 4-year results of the PROTECT randomized trial. *Eur Heart J* **2014**, *35*(40), 2812-2820.
94. Piccolo, R.; Stefanini, G.G.; Franzone, A.; Spitzer, E.; Blöchliger, S.; Heg, D.; Jüni, P.; Windecker, S. Safety and efficacy of resolute zotarolimus-eluting stents compared with everolimus-eluting stents: a meta-analysis. *Circ Cardiovasc Interv* **2015**, *8*(4).
95. Serruys, P.W.; Silber, S.; Garg, S.; van Geuns, R.J.; Richardt, G.; Buszman, P.E.; Kelbaek, H.; van Boven, A.J.; Hofma, S.H.; Linke, A.; Klauss, V.; Wijns, W.; Macaya, C.; Garot, P.; DiMario, C.; Manoharan, G.; Kornowski, R.; Ischinger, T.; Bartorelli, A.; Ronden, J.; Bressers, M.; Gobbens, P.; Negoita, M.; van Leeuwen, F.; Windecker, S. Comparison of zotarolimus-eluting and everolimus-eluting coronary stents. *N Engl J Med* **2010**, *363*(2), 136-146.
96. Bangalore, S.; Kumar, S.; Fusaro, M.; Amoroso, N.; Attubato, M.J.; Feit, F.; Bhatt, D.L.; Slater, J. Short- and long-term outcomes with drug-eluting and bare-metal coronary stents: a mixed-treatment comparison analysis of 117 762 patient-years of follow-up from randomized trials. *Circulation* **2012**, *125*(23), 2873-2891.
97. Collet, J.P.; Silvain, J.; Kerneis, M.; Cuisset, T.; Meneveau, N.; Boueri, Z.; Barthélémy, O.; Rangé, G.; Cayla, G.; Belle, E.V.; Elhadad, S.; Carrié, D.; Caussin, C.; Rousseau, H.; Aubry, P.; Monségu, J.; Sabouret, P.; O'Connor, S.A.; Abtan, J.; Saint-Etienne, C.; Beygui, F.; Vicaut, E.; Montalescot, G. Clinical Outcome of First- vs Second-Generation DES According to DAPT Duration: Results of ARCTIC-Generation. *Clin Cardiol* **2016**, *39*(4), 192-200.
98. Sousa-Uva, M.; Neumann, F.J.; Ahlsson, A.; Alfonso, F.; Banning, A.P.; Benedetto, U.; Byrne, R.A.; Collet, J.P.; Falk, V.; Head, S.J.; Jüni, P.; Kastrati, A.; Koller, A.; Kristensen, S.D.; Niebauer, J.; Richter, D.J.; Seferovic, P.M.; Sibbing, D.; Stefanini, G.G.; Windecker, S.; Yadav, R.; Zembala, M.O. 2018 ESC/EACTS Guidelines on myocardial revascularization. *Eur J Cardiothorac Surg* **2019**, *55*(1), 4-90.
99. Palmerini, T.; Benedetto, U.; Biondi-Zoccai, G.; Della Riva, D.; Bacchi-Reggiani, L.; Smits, P.C.; Vlachojannis, G.J.; Jensen, L.O.; Christiansen, E.H.; Berencsi, K.; Valgimigli, M.; Orlandi, C.; Petrou, M.; Rapezzi, C.; Stone, G.W. Long-Term Safety of Drug-Eluting and Bare-Metal Stents: Evidence From a Comprehensive Network Meta-Analysis. *J Am Coll Cardiol* **2015**, *65*(23), 2496-2507.
100. Stefanini, G.G.; Siontis, G.C.; Cao, D.; Heg, D.; Jüni, P.; Windecker, S. Short versus long duration of DAPT after DES implantation: a meta-analysis. *J Am Coll Cardiol* **2014**, *64*(9), 953-954.
101. Urban, P.; Abizaid, A.; Chevalier, B.; Greene, S.; Meredith, I.; Morice, M.C.; Pocock, S. Rationale and design of the LEADERS FREE trial: A randomized double-blind comparison of the BioFreedom drug-coated stent vs the Gazelle bare

- metal stent in patients at high bleeding risk using a short (1 month) course of dual antiplatelet therapy. *Am Heart J* **2013**, *165*(5), 704-709.
102. Serruys, P.W.; Farooq, V.; Kalesan, B.; de Vries, T.; Buszman, P.; Linke, A.; Ischinger, T.; Klauss, V.; Eberli, F.; Wijns, W.; Morice, M.C.; Di Mario, C.; Corti, R.; Antoni, D.; Sohn, H.Y.; Eerdmans, P.; Rademaker-Havinga, T.; van Es, G.A.; Meier, B.; Jüni, P.; Windecker, S. Improved safety and reduction in stent thrombosis associated with biodegradable polymer-based biolimus-eluting stents versus durable polymer-based sirolimus-eluting stents in patients with coronary artery disease: final 5-year report of the LEADERS (Limus Eluted From A Durable Versus ERodable Stent Coating) randomized, noninferiority trial. *JACC Cardiovasc Interv* **2013**, *6*(8), 777-789.
103. El-Hayek, G.; Bangalore, S.; Casso Dominguez, A.; Devireddy, C.; Jaber, W.; Kumar, G.; Mavromatis, K.; Tamis-Holland, J.; Samady, H. Meta-Analysis of Randomized Clinical Trials Comparing Biodegradable Polymer Drug-Eluting Stent to Second-Generation Durable Polymer Drug-Eluting Stents. *JACC Cardiovasc Interv* **2017**, *10*(5), 462-473.
104. Otsuka, F.; Byrne, R.A.; Yahagi, K.; Mori, H.; Ladich, E.; Fowler, D.R.; Kutys, R.; Xhepa, E.; Kastrati, A.; Virmani, R.; Joner, M. Neoatherosclerosis: overview of histopathologic findings and implications for intravascular imaging assessment. *Eur Heart J* **2015**, *36*(32), 2147-2159.
105. Yamaji, K.; Kimura, T.; Morimoto, T.; Nakagawa, Y.; Inoue, K.; Soga, Y.; Arita, T.; Shirai, S.; Ando, K.; Kondo, K.; Sakai, K.; Goya, M.; Iwabuchi, M.; Yokoi, H.; Nosaka, H.; Nobuyoshi, M. Very long-term (15 to 20 years) clinical and angiographic outcome after coronary bare metal stent implantation. *Circ Cardiovasc Interv* **2010**, *3*(5), 468-475.
106. Wiebe, J.; Nef, H.M.; Hamm, C.W. Current status of bioresorbable scaffolds in the treatment of coronary artery disease. *J Am Coll Cardiol* **2014**, *64*(23), 2541-2551.
107. Makadia, H.K.; Siegel, S.J. Poly Lactic-co-Glycolic Acid (PLGA) as Biodegradable Controlled Drug Delivery Carrier. *Polymers (Basel)* **2011**, *3*(3), 1377-1397.
108. Vroman, I.; Tighzert, L. Biodegradable Polymers. *Materials* **2009**, *2*, 307-344.
109. Kwon, D.Y.; Kim, J.I.; Kim, D.Y.; Kang, H.J.; Lee, B.; Lee, K.W.; Kim, M.S. Biodegradable stent. *J Biomed Sci Eng* **2012**, *5*, 208-216.
110. Berglund, J.; Guo, Y.; Wilcox, J.N. Challenges related to development of bioabsorbable vascular stents. *EuroIntervention* **2009**, *5 Suppl F*, F72-79.
111. Oberhauser, J.P.; Hossainy, S.; Rapoza, R.J. Design principles and performance of bioresorbable polymeric vascular scaffolds. *EuroIntervention* **2009**, *5 Suppl F*, F15-22.
112. Gajjar, R.; King, W. Degradation Process. In *Resorbable Fiber-Forming Polymers for Biotextile Applications*, Springer International Publishing: 2014; pp. 7-10.
113. Caiazzo, G.; Kilic, I.D.; Fabris, E.; Serdoz, R.; Mattesini, A.; Foin, N.; De Rosa, S.; Indolfi, C.; Di Mario, C. Absorb bioresorbable vascular scaffold: What have we learned after 5 years of clinical experience? *Int J Cardiol* **2015**, *201*, 129-136.

114. Ormiston, J.A.; Serruys, P.W.; Regar, E.; Dudek, D.; Thuesen, L.; Webster, M.W.I.; Onuma, Y.; Garcia-Garcia, H.M.; McGreevy, R.; Veldhof, S. A bioabsorbable everolimus-eluting coronary stent system for patients with single de-novo coronary artery lesions (ABSORB): a prospective open-label trial. *Lancet* **2008**, *371*(9616), 899-907.
115. Onuma, Y.; Dudek, D.; Thuesen, L.; Webster, M.; Nieman, K.; Garcia-Garcia, H.M.; Ormiston, J.A.; Serruys, P.W. Five-Year Clinical and Functional Multislice Computed Tomography Angiographic Results After Coronary Implantation of the Fully Resorbable Polymeric Everolimus-Eluting Scaffold in Patients With De Novo Coronary Artery Disease: The ABSORB Cohort A Trial. *JACC Cardiovasc Interv* **2013**, *6*(10), 999-1009.
116. Serruys, P.W.; Ormiston, J.A.; Onuma, Y.; Regar, E.; Gonzalo, N.; Garcia-Garcia, H.M.; Nieman, K.; Bruining, N.; Dorange, C.; Miquel-Hébert, K.; Veldhof, S.; Webster, M.; Thuesen, L.; Dudek, D. A bioabsorbable everolimus-eluting coronary stent system (ABSORB): 2-year outcomes and results from multiple imaging methods. *Lancet* **2009**, *373*(9667), 897-910.
117. Tanimoto, S.; Bruining, N.; van Domburg, R.T.; Rotger, D.; Radeva, P.; Ligthart, J.M.; Serruys, P.W. Late Stent Recoil of the Bioabsorbable Everolimus-Eluting Coronary Stent and its Relationship With Plaque Morphology. *J Am Coll Cardiol* **2008**, *52*(20), 1616-1620.
118. Tanimoto, S.; Serruys, P.W.; Thuesen, L.; Dudek, D.; de Bruyne, B.; Chevalier, B.; Ormiston, J.A. Comparison of in vivo acute stent recoil between the bioabsorbable everolimus-eluting coronary stent and the everolimus-eluting cobalt chromium coronary stent: insights from the ABSORB and SPIRIT trials. *Catheter Cardiovasc Interv* **2007**, *70*(4), 515-523.
119. Serruys, P.W.; Chevalier, B.; Dudek, D.; Cequier, A.; Carrié, D.; Iniguez, A.; Dominici, M.; van der Schaaf, R.J.; Haude, M.; Wasungu, L.; Veldhof, S.; Peng, L.; Staehr, P.; Grundeken, M.J.; Ishibashi, Y.; Garcia-Garcia, H.M.; Onuma, Y. A bioresorbable everolimus-eluting scaffold versus a metallic everolimus-eluting stent for ischaemic heart disease caused by de-novo native coronary artery lesions (ABSORB II): an interim 1-year analysis of clinical and procedural secondary outcomes from a randomised controlled trial. *Lancet* **2015**, *385*(9962), 43-54.
120. Ellis, S.G.; Kereiakes, D.J.; Metzger, D.C.; Caputo, R.P.; Rizik, D.G.; Teirstein, P.S.; Litt, M.R.; Kini, A.; Kabour, A.; Marx, S.O.; Popma, J.J.; McGreevy, R.; Zhang, Z.; Simonton, C.; Stone, G.W. Everolimus-Eluting Bioresorbable Scaffolds for Coronary Artery Disease. *N Engl J Med* **2015**, *373*(20), 1905-1915.
121. Wykrzykowska, J.J.; Kraak, R.P.; Hofma, S.H.; van der Schaaf, R.J.; Arkenbout, E.K.; AJ, I.J.; Elias, J.; van Dongen, I.M.; Tijssen, R.Y.G.; Koch, K.T.; Baan, J., Jr.; Vis, M.M.; de Winter, R.J.; Piek, J.J.; Tijssen, J.G.P.; Henriques, J.P.S. Bioresorbable Scaffolds versus Metallic Stents in Routine PCI. *N Engl J Med* **2017**, *376*(24), 2319-2328.
122. Cassese, S.; Byrne, R.A.; Ndrepepa, G.; Kufner, S.; Wiebe, J.; Repp, J.; Schunkert, H.; Fusaro, M.; Kimura, T.; Kastrati, A. Everolimus-eluting bioresorbable vascular scaffolds versus everolimus-eluting metallic stents: a meta-analysis of randomised controlled trials. *Lancet* **2016**, *387*(10018), 537-544.
123. Lipinski, M.J.; Escarcega, R.O.; Baker, N.C.; Benn, H.A.; Gaglia, M.A., Jr.; Torguson, R.; Waksman, R. Scaffold Thrombosis After Percutaneous Coronary

- Intervention With ABSORB Bioresorbable Vascular Scaffold: A Systematic Review and Meta-Analysis. *JACC Cardiovasc Interv* **2016**, 9(1), 12-24.
124. Stone, G.W.; Abizaid, A.; Onuma, Y.; Seth, A.; Gao, R.; Ormiston, J.; Kimura, T.; Chevalier, B.; Ben-Yehuda, O.; Dressler, O.; McAndrew, T.; Ellis, S.G.; Kereiakes, D.J.; Serruys, P.W. Effect of Technique on Outcomes Following Bioresorbable Vascular Scaffold Implantation: Analysis From the ABSORB Trials. *J Am Coll Cardiol* **2017**, 70(23), 2863-2874.
125. Mattesini, A.; Boeder, N.; Valente, S.; Löblich, K.; Dörr, O.; Secco, G.G.; Foin, N.; Caiazzo, G.; Ghione, M.; Gensini, G.F.; Porto, I.; Di Mario, C.; Nef, H. Absorb vs. DESolve: an optical coherence tomography comparison of acute mechanical performances. *EuroIntervention* **2016**, 12(5), e566-573.
126. Ormiston, J.A.; Webber, B.; Ubod, B.; Darremont, O.; Webster, M.W. An independent bench comparison of two bioresorbable drug-eluting coronary scaffolds (Absorb and DESolve) with a durable metallic drug-eluting stent (ML8/Xpedition). *EuroIntervention* **2015**, 11(1), 60-67.
127. Foin, N.; Lee, R.; Mattesini, A.; Caiazzo, G.; Fabris, E.; Kilic, I.D.; Chan, J.N.; Huang, Y.; Venkatraman, S.S.; Di Mario, C.; Wong, P.; Nef, H. Bioabsorbable vascular scaffold overexpansion: insights from in vitro post-expansion experiments. *EuroIntervention* **2016**, 11(12), 1389-1399.
128. Nef, H.M.; Wiebe, J.; Foin, N.; Blachutzik, F.; Dörr, O.; Toyloy, S.; Hamm, C.W. A new novolimus-eluting bioresorbable coronary scaffold: Present status and future clinical perspectives. *Int J Cardiol* **2017**, 227, 127-133.
129. Nef, H.; Wiebe, J.; Boeder, N.; Dörr, O.; Bauer, T.; Hauptmann, K.E.; Latib, A.; Colombo, A.; Fischer, D.; Rudolph, T.; Foin, N.; Richardt, G.; Hamm, C. A multicenter post-marketing evaluation of the Elixir DESolve® Novolimus-eluting bioresorbable coronary scaffold system: First results from the DESolve PMCF study. *Catheter Cardiovasc Interv* **2018**, 92(6), 1021-1027.
130. Huang, D.; Swanson, E.A.; Lin, C.P.; Schuman, J.S.; Stinson, W.G.; Chang, W.; Hee, M.R.; Flotte, T.; Gregory, K.; Puliafito, C.A.; et al. Optical coherence tomography. *Science* **1991**, 254(5035), 1178-1181.
131. Brezinski, M.E.; Tearney, G.J.; Bouma, B.E.; Boppart, S.A.; Hee, M.R.; Swanson, E.A.; Southern, J.F.; Fujimoto, J.G. Imaging of coronary artery microstructure (in vitro) with optical coherence tomography. *Am J Cardiol* **1996**, 77(1), 92-93.
132. Regar, E.; van Leeuwen, A.; Serruys, P. *Optical Coherence Tomography in Cardiovascular Research*; CRC Press: London, 2007.
133. Johnson, T.W.; Räber, L.; di Mario, C.; Bourantas, C.; Jia, H.; Mattesini, A.; Gonzalo, N.; de la Torre Hernandez, J.M.; Prati, F.; Koskinas, K.; Joner, M.; Radu, M.D.; Erlinge, D.; Regar, E.; Kunadian, V.; Maehara, A.; Byrne, R.A.; Capodanno, D.; Akasaka, T.; Wijns, W.; Mintz, G.S.; Guagliumi, G. Clinical use of intracoronary imaging. Part 2: acute coronary syndromes, ambiguous coronary angiography findings, and guiding interventional decision-making: an expert consensus document of the European Association of Percutaneous Cardiovascular Interventions. *Eur Heart J* **2019**, 40(31), 2566-2584.
134. Räber, L.; Mintz, G.S.; Koskinas, K.C.; Johnson, T.W.; Holm, N.R.; Onuma, Y.; Radu, M.D.; Joner, M.; Yu, B.; Jia, H.; Meneveau, N.; de la Torre Hernandez, J.M.; Escaned, J.; Hill, J.; Prati, F.; Colombo, A.; Di Mario, C.; Regar, E.;

- Capodanno, D.; Wijns, W.; Byrne, R.A.; Guagliumi, G. Clinical use of intracoronary imaging. Part 1: guidance and optimization of coronary interventions. An expert consensus document of the European Association of Percutaneous Cardiovascular Interventions. *EuroIntervention* **2018**, *14*(6), 656-677.
135. Michelson, A.; Morley, E. On the relative motion of the Earth and the luminiferous ether. *Am Jour Sci* **1887**, *s3-34*(203), 333-345.
136. Schmitt, J.M. Optical coherence tomography (OCT): a review. *IEEE J Sel Top Quantum Electron* **1999**, *5*(4), 1205-1215.
137. Schmitt, J.M.; Knüttel, A.; Yadlowsky, M.; Eckhaus, M.A. Optical-coherence tomography of a dense tissue: statistics of attenuation and backscattering. *Phys Med Biol* **1994**, *39*(10), 1705-1720.
138. Tearney, G.J.; Regar, E.; Akasaka, T.; Adriaenssens, T.; Barlis, P.; Bezerra, H.G.; Bouma, B.; Bruining, N.; Cho, J.M.; Chowdhary, S.; Costa, M.A.; de Silva, R.; Dijkstra, J.; Di Mario, C.; Dudek, D.; Falk, E.; Feldman, M.D.; Fitzgerald, P.; Garcia-Garcia, H.M.; Gonzalo, N.; Granada, J.F.; Guagliumi, G.; Holm, N.R.; Honda, Y.; Ikeno, F.; Kawasaki, M.; Kochman, J.; Koltowski, L.; Kubo, T.; Kume, T.; Kyono, H.; Lam, C.C.; Lamouche, G.; Lee, D.P.; Leon, M.B.; Maehara, A.; Manfrini, O.; Mintz, G.S.; Mizuno, K.; Morel, M.A.; Nadkarni, S.; Okura, H.; Otake, H.; Pietrasik, A.; Prati, F.; Räber, L.; Radu, M.D.; Rieber, J.; Riga, M.; Rollins, A.; Rosenberg, M.; Sirbu, V.; Serruys, P.W.; Shimada, K.; Shinke, T.; Shite, J.; Siegel, E.; Sonoda, S.; Suter, M.; Takarada, S.; Tanaka, A.; Terashima, M.; Thim, T.; Uemura, S.; Ughi, G.J.; van Beusekom, H.M.; van der Steen, A.F.; van Es, G.A.; van Soest, G.; Virmani, R.; Waxman, S.; Weissman, N.J.; Weisz, G. Consensus standards for acquisition, measurement, and reporting of intravascular optical coherence tomography studies: a report from the International Working Group for Intravascular Optical Coherence Tomography Standardization and Validation. *J Am Coll Cardiol* **2012**, *59*(12), 1058-1072.
139. Eeckhout, R.d.P.E.; Serruys, P.W.; Wijns, W.; Vahanian, A.; Sambeek, M.v. *The PCR-EAPCI Textbook - Percutaneous Interventional Cardiovascular*; Europa Edition: 2012.
140. Choma, M.; Sarunic, M.; Yang, C.; Izatt, J. Sensitivity advantage of swept source and Fourier domain optical coherence tomography. *Opt Express* **2003**, *11*(18), 2183-2189.
141. de Boer, J.F.; Cense, B.; Park, B.H.; Pierce, M.C.; Tearney, G.J.; Bouma, B.E. Improved signal-to-noise ratio in spectral-domain compared with time-domain optical coherence tomography. *Opt Lett* **2003**, *28*(21), 2067-2069.
142. Leitgeb, R.; Hitzenberger, C.; Fercher, A. Performance of fourier domain vs. time domain optical coherence tomography. *Opt Express* **2003**, *11*(8), 889-894.
143. Boeder, N.F.; Koepp, T.; Dörr, O.; Bauer, T.; Mattesini, A.; Elsässer, A.; Möllmann, H.; Blachutzik, F.; Achenbach, S.; Ghanem, A.; Hamm, C.W.; Nef, H.M. A new novolimus-eluting bioresorbable scaffold for large coronary arteries: an OCT study of acute mechanical performance. *Int J Cardiol* **2016**, *220*, 706-710.
144. Capodanno, D.; Gori, T.; Nef, H.; Latib, A.; Mehilli, J.; Lesiak, M.; Caramanno, G.; Naber, C.; Di Mario, C.; Colombo, A.; Capranzano, P.; Wiebe, J.; Araszkiwicz, A.; Geraci, S.; Pyxaras, S.; Mattesini, A.; Naganuma, T.; Münzel,

- T.; Tamburino, C. Percutaneous coronary intervention with everolimus-eluting bioresorbable vascular scaffolds in routine clinical practice: early and midterm outcomes from the European multicentre GHOST-EU registry. *EuroIntervention* **2015**, *10*(10), 1144-1153.
145. Brugaletta, S.; Gori, T.; Low, A.F.; Tousek, P.; Pinar, E.; Gomez-Lara, J.; Scalone, G.; Schulz, E.; Chan, M.Y.; Kocka, V.; Hurtado, J.; Gomez-Hospital, J.A.; Münzel, T.; Lee, C.-H.; Cequier, A.; Valdés, M.; Widimsky, P.; Serruys, P.W.; Sabaté, M. Absorb Bioresorbable Vascular Scaffold Versus Everolimus-Eluting Metallic Stent in ST-Segment Elevation Myocardial Infarction: 1-Year Results of a Propensity Score Matching Comparison: The BVS-EXAMINATION Study (Bioresorbable Vascular Scaffold-A Clinical Evaluation of Everolimus Eluting Coronary Stents in the Treatment of Patients With ST-segment Elevation Myocardial Infarction). *JACC Cardiovasc Interv* **2015**, *8*(1, Part B), 189-197.
146. von Birgelen, C.; Sen, H.; Lam, M.K.; Danse, P.W.; Jessurun, G.A.J.; Hautvast, R.W.M.; van Houwelingen, G.K.; Schramm, A.R.; Gin, R.M.T.J.; Louwerenburg, J.W.; de Man, F.H.A.F.; Stoel, M.G.; Löwik, M.M.; Linssen, G.C.M.; Saïd, S.A.M.; Nienhuis, M.B.; Verhorst, P.M.J.; Basalus, M.W.Z.; Doggen, C.J.M.; Tandjung, K. Third-generation zotarolimus-eluting and everolimus-eluting stents in all-comer patients requiring a percutaneous coronary intervention (DUTCH PEERS): a randomised, single-blind, multicentre, non-inferiority trial. *Lancet* **2014**, *383*(9915), 413-423.
147. Brodie, B.; Pokharel, Y.; Garg, A.; Kissling, G.; Hansen, C.; Milks, S.; Cooper, M.; McAlhany, C.; Stuckey, T. Predictors of Early, Late, and Very Late Stent Thrombosis After Primary Percutaneous Coronary Intervention With Bare-Metal and Drug-Eluting Stents for ST-Segment Elevation Myocardial Infarction. *JACC Cardiovasc Interv* **2012**, *5*(10), 1043-1051.
148. Lim, S.; Koh, Y.-S.; Kim, P.-J.; Kim, H.-Y.; Park, C.S.; Lee, J.M.; Kim, D.-B.; Yoo, K.-D.; Jeon, D.S.; Her, S.-H.; Yim, H.-W.; Chang, K.; Ahn, Y.; Jeong, M.H.; Seung, K.-B. Incidence, Implications, and Predictors of Stent Thrombosis in Acute Myocardial Infarction. *Am J Cardiol* **2016**, *117*(10), 1562-1568.
149. Kolandaivelu, K.; Swaminathan, R.; Gibson, W.J.; Kolachalama, V.B.; Nguyen-Ehrenreich, K.L.; Giddings, V.L.; Coleman, L.; Wong, G.K.; Edelman, E.R. Stent thrombogenicity early in high-risk interventional settings is driven by stent design and deployment and protected by polymer-drug coatings. *Circulation* **2011**, *123*(13), 1400-1409.
150. Pache, J.; Kastrati, A.; Mehilli, J.; Schühlen, H.; Dotzer, F.; Hausleiter, J.; Fleckenstein, M.; Neumann, F.-J.; Sattelberger, U.; Schmitt, C.; Müller, M.; Dirschinger, J.; Schömig, A. Intracoronary stenting and angiographic results: strut thickness effect on restenosis outcome (ISAR-STEREO-2) trial. *J Am Coll Cardiol* **2003**, *41*(8), 1283-1288.
151. Boeder, N.F.; Dörr, O.; Bauer, T.; Mattesini, A.; Elsässer, A.; Liebetau, C.; Achenbach, S.; Hamm, C.W.; Nef, H.M. Impact of strut thickness on acute mechanical performance: A comparison study using optical coherence tomography between DESolve 150 and DESolve 100. *Int J Cardiol* **2017**, *246*, 74-79.
152. Ellis, S.G.; Vandormael, M.G.; Cowley, M.J.; DiSciascio, G.; Deligonul, U.; Topol, E.J.; Bulle, T.M. Coronary morphologic and clinical determinants of procedural outcome with angioplasty for multivessel coronary disease.

- Implications for patient selection. Multivessel Angioplasty Prognosis Study Group. *Circulation* **1990**, 82(4), 1193-1202.
153. Gogas, B.D.; Benham, J.J.; Hsu, S.; Sheehy, A.; Lefer, D.J.; Goodchild, T.T.; Polhemus, D.J.; Bouchi, Y.H.; Hung, O.Y.; Yoo, S.Y.; Joshi, U.; Giddens, D.P.; Veneziani, A.; Quyyumi, A.; Rapoza, R.; King, S.B., 3rd; Samady, H. Vasomotor Function Comparative Assessment at 1 and 2 Years Following Implantation of the Absorb Everolimus-Eluting Bioresorbable Vascular Scaffold and the Xience V Everolimus-Eluting Metallic Stent in Porcine Coronary Arteries: Insights From In Vivo Angiography, Ex Vivo Assessment, and Gene Analysis at the Stented/Scaffolded Segments and the Proximal and Distal Edges. *JACC Cardiovasc Interv* **2016**, 9(7), 728-741.
154. Costopoulos, C.; Naganuma, T.; Latib, A.; Colombo, A. Looking into the future with bioresorbable vascular scaffolds. *Expert Rev Cardiovasc Ther* **2013**, 11(10), 1407-1416.
155. Shand, J.A.; Sharma, D.; Hanratty, C.; McClelland, A.; Menown, I.B.; Spence, M.S.; Richardson, G.; Herity, N.A.; Walsh, S.J. A prospective intravascular ultrasound investigation of the necessity for and efficacy of postdilatation beyond nominal diameter of 3 current generation DES platforms for the percutaneous treatment of the left main coronary artery. *Catheter Cardiovasc Interv* **2014**, 84(3), 351-358.
156. Shaw, E.; Allahwala, U.K.; Cockburn, J.A.; Hansen, T.C.E.; Mazhar, J.; Figtree, G.A.; Hansen, P.S.; Bhindi, R. The effect of coronary artery plaque composition, morphology and burden on Absorb bioresorbable vascular scaffold expansion and eccentricity — A detailed analysis with optical coherence tomography. *Int J Cardiol* **2015**, 184, 230-236.
157. Wiebe, J.; Bauer, T.; Dörr, O.; Möllmann, H.; Hamm, C.; Nef, H.M. Implantation of a novolimus-eluting bioresorbable scaffold with a strut thickness of 100 µm showing evidence of self-correction. *EuroIntervention* **2015**, 11(2), 204.
158. Boeder, N.F.; Dörr, O.; Bauer, T.; Elsässer, A.; Möllmann, H.; Achenbach, S.; Hamm, C.W.; Nef, H.M. Effect of Plaque Composition, Morphology, and Burden on DESolve Novolimus-Eluting Bioresorbable Vascular Scaffold Expansion and Eccentricity - An Optical Coherence Tomography Analysis. *Cardiovasc Revasc Med* **2019**, 20(6), 480-484.
159. Everaert, B.; Wykrzykowska, J.J.; Koolen, J.; van der Harst, P.; den Heijer, P.; Henriques, J.P.; van der Schaaf, R.; de Smet, B.; Hofma, S.H.; Diletti, R.; Weevers, A.; Hoorntje, J.; Smits, P.; van Geuns, R.J. Recommendations for the use of bioresorbable vascular scaffolds in percutaneous coronary interventions : 2017 revision. *Neth Heart J* **2017**, 25(7-8), 419-428.
160. Tamburino, C.; Latib, A.; van Geuns, R.J.; Sabate, M.; Mehilli, J.; Gori, T.; Achenbach, S.; Alvarez, M.P.; Nef, H.; Lesiak, M.; Di Mario, C.; Colombo, A.; Naber, C.K.; Caramanno, G.; Capranzano, P.; Brugaletta, S.; Geraci, S.; Araszkiwicz, A.; Mattesini, A.; Pyxaras, S.A.; Rzeszutko, L.; Depukat, R.; Diletti, R.; Boone, E.; Capodanno, D.; Dudek, D. Contemporary practice and technical aspects in coronary intervention with bioresorbable scaffolds: a European perspective. *EuroIntervention* **2015**, 11(1), 45-52.
161. Blachutzik, F.; Boeder, N.; Wiebe, J.; Mattesini, A.; Dörr, O.; Most, A.; Bauer, T.; Röther, J.; Tröbs, M.; Schlundt, C.; Achenbach, S.; Hamm, C.W.; Nef, H.M.

- Post-dilatation after implantation of bioresorbable everolimus- and novolimus-eluting scaffolds: an observational optical coherence tomography study of acute mechanical effects. *Clin Res Cardiol* **2017**, *106*(4), 271-279.
162. Blachutzik, F.; Boeder, N.; Wiebe, J.; Mattesini, A.; Dörr, O.; Most, A.; Bauer, T.; Tröbs, M.; Röther, J.; Schlundt, C.; Achenbach, S.; Hamm, C.; Nef, H. Overlapping implantation of bioresorbable novolimus-eluting scaffolds: an observational optical coherence tomography study. *Heart Vessels* **2017**, *32*(7), 781-789.
163. Kereiakes, D.J.; Wang, H.; Popma, J.J.; Kuntz, R.E.; Donohoe, D.J.; Schofer, J.; Schampaert, E.; Meier, B.; Leon, M.B.; Moses, J.W. Periprocedural and late consequences of overlapping Cypher sirolimus-eluting stents: pooled analysis of five clinical trials. *J Am Coll Cardiol* **2006**, *48*(1), 21-31.
164. Räber, L.; Jüni, P.; Löffel, L.; Wandel, S.; Cook, S.; Wenaweser, P.; Togni, M.; Vogel, R.; Seiler, C.; Eberli, F.; Lüscher, T.; Meier, B.; Windecker, S. Impact of stent overlap on angiographic and long-term clinical outcome in patients undergoing drug-eluting stent implantation. *J Am Coll Cardiol* **2010**, *55*(12), 1178-1188.
165. O'Sullivan, C.J.; Stefanini, G.G.; Räber, L.; Heg, D.; Taniwaki, M.; Kalesan, B.; Pilgrim, T.; Zanchin, T.; Moschovitis, A.; Büllsfeld, L.; Khattab, A.A.; Meier, B.; Wenaweser, P.; Jüni, P.; Windecker, S. Impact of stent overlap on long-term clinical outcomes in patients treated with newer-generation drug-eluting stents. *EuroIntervention* **2014**, *9*(9), 1076-1084.
166. Farooq, V.; Vranckx, P.; Mauri, L.; Cutlip, D.E.; Belardi, J.; Silber, S.; Widimsky, P.; Leon, M.; Windecker, S.; Meredith, I.; Negoita, M.; van Leeuwen, F.; Neumann, F.J.; Yeung, A.C.; Garcia-Garcia, H.M.; Serruys, P.W. Impact of overlapping newer generation drug-eluting stents on clinical and angiographic outcomes: pooled analysis of five trials from the international Global RESOLUTE Program. *Heart* **2013**, *99*(9), 626-633.
167. Windecker, S.; Kolh, P.; Alfonso, F.; Collet, J.P.; Cremer, J.; Falk, V.; Filippatos, G.; Hamm, C.; Head, S.J.; Jüni, P.; Kappetein, A.P.; Kastrati, A.; Knuuti, J.; Landmesser, U.; Laufer, G.; Neumann, F.J.; Richter, D.J.; Schauerte, P.; Sousa Uva, M.; Stefanini, G.G.; Taggart, D.P.; Torracca, L.; Valgimigli, M.; Wijns, W.; Witkowski, A. 2014 ESC/EACTS Guidelines on myocardial revascularization: The Task Force on Myocardial Revascularization of the European Society of Cardiology (ESC) and the European Association for Cardio-Thoracic Surgery (EACTS) Developed with the special contribution of the European Association of Percutaneous Cardiovascular Interventions (EAPCI). *Eur Heart J* **2014**, *35*(37), 2541-2619.
168. Schömig, A.; Sarafoff, N.; Seyfarth, M. Triple antithrombotic management after stent implantation: when and how? *Heart* **2009**, *95*(15), 1280-1285.
169. Stone, G.W.; Gao, R.; Kimura, T.; Kereiakes, D.J.; Ellis, S.G.; Onuma, Y.; Cheong, W.F.; Jones-McMeans, J.; Su, X.; Zhang, Z.; Serruys, P.W. 1-year outcomes with the Absorb bioresorbable scaffold in patients with coronary artery disease: a patient-level, pooled meta-analysis. *Lancet* **2016**, *387*(10025), 1277-1289.
170. Kereiakes, D.J.; Ellis, S.G.; Popma, J.J.; Fitzgerald, P.J.; Samady, H.; Jones-McMeans, J.; Zhang, Z.; Cheong, W.F.; Su, X.; Ben-Yehuda, O.; Stone, G.W.

- Evaluation of a fully bioresorbable vascular scaffold in patients with coronary artery disease: design of and rationale for the ABSORB III randomized trial. *Am Heart J* **2015**, *170*(4), 641-651.e643.
171. Boeder, N.F.; Johnson, V.; Dörr, O.; Wiebe, J.; Elsässer, A.; Möllmann, H.; Hamm, C.W.; Nef, H.M.; Bauer, T. Bioresorbable scaffold implantation in patients with indication for oral anticoagulation: A propensity matched analysis. *Int J Cardiol* **2017**, *231*, 73-77.
172. Arroyo, D.; Gendre, G.; Schukraft, S.; Kallinikou, Z.; Müller, O.; Baeriswyl, G.; Stauffer, J.C.; Goy, J.J.; Togni, M.; Cook, S.; Puricel, S. Comparison of everolimus- and biolimus-eluting coronary stents with everolimus-eluting bioresorbable vascular scaffolds: Two-year clinical outcomes of the EVERBIO II trial. *Int J Cardiol* **2017**, *243*, 121-125.
173. Ali, Z.A.; Gao, R.; Kimura, T.; Onuma, Y.; Kereiakes, D.J.; Ellis, S.G.; Chevalier, B.; Vu, M.T.; Zhang, Z.; Simonton, C.A.; Serruys, P.W.; Stone, G.W. Three-Year Outcomes With the Absorb Bioresorbable Scaffold: Individual-Patient-Data Meta-Analysis From the ABSORB Randomized Trials. *Circulation* **2018**, *137*(5), 464-479.
174. Cuculi, F.; Puricel, S.; Jamshidi, P.; Valentin, J.; Kallinikou, Z.; Toggweiler, S.; Weissner, M.; Münzel, T.; Cook, S.; Gori, T. Optical Coherence Tomography Findings in Bioresorbable Vascular Scaffolds Thrombosis. *Circ Cardiovasc Interv* **2015**, *8*(10), e002518.
175. Boeder, N.F.; Weissner, M.; Blachutzik, F.; Ullrich, H.; Anadol, R.; Tröbs, M.; Münzel, T.; Hamm, C.W.; Dijkstra, J.; Achenbach, S.; Nef, H.M.; Gori, T. Incidental Finding of Strut Malapposition Is a Predictor of Late and Very Late Thrombosis in Coronary Bioresorbable Scaffolds. *J Clin Med* **2019**, *8*(5), 580.
176. Sonoda, S.; Morino, Y.; Ako, J.; Terashima, M.; Hassan, A.H.; Bonneau, H.N.; Leon, M.B.; Moses, J.W.; Yock, P.G.; Honda, Y.; Kuntz, R.E.; Fitzgerald, P.J. Impact of final stent dimensions on long-term results following sirolimus-eluting stent implantation: serial intravascular ultrasound analysis from the sirius trial. *J Am Coll Cardiol* **2004**, *43*(11), 1959-1963.
177. Doi, H.; Maehara, A.; Mintz, G.S.; Yu, A.; Wang, H.; Mandinov, L.; Popma, J.J.; Ellis, S.G.; Grube, E.; Dawkins, K.D.; Weissman, N.J.; Turco, M.A.; Ormiston, J.A.; Stone, G.W. Impact of post-intervention minimal stent area on 9-month follow-up patency of paclitaxel-eluting stents: an integrated intravascular ultrasound analysis from the TAXUS IV, V, and VI and TAXUS ATLAS Workhorse, Long Lesion, and Direct Stent Trials. *JACC Cardiovasc Interv* **2009**, *2*(12), 1269-1275.
178. Fujii, K.; Carlier, S.G.; Mintz, G.S.; Yang, Y.M.; Moussa, I.; Weisz, G.; Dangas, G.; Mehran, R.; Lansky, A.J.; Kreps, E.M.; Collins, M.; Stone, G.W.; Moses, J.W.; Leon, M.B. Stent underexpansion and residual reference segment stenosis are related to stent thrombosis after sirolimus-eluting stent implantation: an intravascular ultrasound study. *J Am Coll Cardiol* **2005**, *45*(7), 995-998.
179. Gonzalo, N.; Serruys, P.W.; García-García, H.M.; van Soest, G.; Okamura, T.; Ligthart, J.; Knaapen, M.; Verheye, S.; Bruining, N.; Regar, E. Quantitative ex vivo and in vivo comparison of lumen dimensions measured by optical coherence tomography and intravascular ultrasound in human coronary arteries. *Rev Esp Cardiol* **2009**, *62*(6), 615-624.

180. Rieu, R.; Barragan, P.; Garitey, V.; Roquebert, P.O.; Fuseri, J.; Commeau, P.; Sainsous, J. Assessment of the trackability, flexibility, and conformability of coronary stents: a comparative analysis. *Catheter Cardiovasc Interv* **2003**, *59*(4), 496-503.
181. Sangiorgi, G.; Melzi, G.; Agostoni, P.; Cola, C.; Clementi, F.; Romitelli, P.; Virmani, R.; Colombo, A. Engineering aspects of stents design and their translation into clinical practice. *Ann Ist Super Sanita* **2007**, *43*(1), 89-100.
182. de Jaegere, P.; Mudra, H.; Figulla, H.; Almagor, Y.; Doucet, S.; Penn, I.; Colombo, A.; Hamm, C.; Bartorelli, A.; Rothman, M.; Nobuyoshi, M.; Yamaguchi, T.; Voudris, V.; DiMario, C.; Makovski, S.; Hausmann, D.; Rowe, S.; Rabinovich, S.; Sunamura, M.; van Es, G.A. Intravascular ultrasound-guided optimized stent deployment. Immediate and 6 months clinical and angiographic results from the Multicenter Ultrasound Stenting in Coronaries Study (MUSIC Study). *Eur Heart J* **1998**, *19*(8), 1214-1223.
183. Sugiyama, T.; Kimura, S.; Akiyama, D.; Hishikari, K.; Kawaguchi, N.; Kamiishi, T.; Hikita, H.; Takahashi, A.; Isobe, M. Quantitative assessment of tissue prolapse on optical coherence tomography and its relation to underlying plaque morphologies and clinical outcome in patients with elective stent implantation. *Int J Cardiol* **2014**, *176*(1), 182-190.
184. Chamié, D.; Bezerra, H.G.; Attizzani, G.F.; Yamamoto, H.; Kanaya, T.; Stefano, G.T.; Fujino, Y.; Mehanna, E.; Wang, W.; Abdul-Aziz, A.; Dias, M.; Simon, D.I.; Costa, M.A. Incidence, predictors, morphological characteristics, and clinical outcomes of stent edge dissections detected by optical coherence tomography. *JACC Cardiovasc Interv* **2013**, *6*(8), 800-813.
185. Brown, A.J.; McCormick, L.M.; Braganza, D.M.; Bennett, M.R.; Hoole, S.P.; West, N.E. Expansion and malapposition characteristics after bioresorbable vascular scaffold implantation. *Catheter Cardiovasc Interv* **2014**, *84*(1), 37-45.
186. Gutiérrez-Chico, J.L.; Gijzen, F.; Regar, E.; Wentzel, J.; de Bruyne, B.; Thuesen, L.; Ormiston, J.; McClean, D.R.; Windecker, S.; Chevalier, B.; Dudek, D.; Whitbourn, R.; Brugaletta, S.; Onuma, Y.; Serruys, P.W. Differences in neointimal thickness between the adluminal and the abluminal sides of malapposed and side-branch struts in a polylactide bioresorbable scaffold: evidence in vivo about the abluminal healing process. *JACC Cardiovasc Interv* **2012**, *5*(4), 428-435.
187. De Ribamar Costa, J., Jr.; Abizaid, A.; Bartorelli, A.L.; Whitbourn, R.; van Geuns, R.J.; Chevalier, B.; Perin, M.; Seth, A.; Botelho, R.; Serruys, P.W. Impact of post-dilation on the acute and one-year clinical outcomes of a large cohort of patients treated solely with the Absorb Bioresorbable Vascular Scaffold. *EuroIntervention* **2015**, *11*(2), 141-148.
188. Farooq, V.; Serruys, P.W.; Heo, J.H.; Gogas, B.D.; Onuma, Y.; Perkins, L.E.; Diletti, R.; Radu, M.D.; Räber, L.; Bourantas, C.V.; Zhang, Y.; van Remortel, E.; Pawar, R.; Rapoza, R.J.; Powers, J.C.; van Beusekom, H.M.; García-García, H.M.; Virmani, R. Intracoronary optical coherence tomography and histology of overlapping everolimus-eluting bioresorbable vascular scaffolds in a porcine coronary artery model: the potential implications for clinical practice. *JACC Cardiovasc Interv* **2013**, *6*(5), 523-532.

189. Ortega-Paz, L.; Capodanno, D.; Giacchi, G.; Gori, T.; Nef, H.; Latib, A.; Caramanno, G.; Di Mario, C.; Naber, C.; Lesiak, M.; Capranzano, P.; Wiebe, J.; Mehilli, J.; Araszkiwicz, A.; Pyxaras, S.; Mattesini, A.; Geraci, S.; Naganuma, T.; Colombo, A.; Münzel, T.; Sabaté, M.; Tamburino, C.; Brugaletta, S. Impact of overlapping on 1-year clinical outcomes in patients undergoing everolimus-eluting bioresorbable scaffolds implantation in routine clinical practice: Insights from the European multicenter GHOST-EU registry. *Catheter Cardiovasc Interv* **2017**, *89*(5), 812-818.
190. Costa, J.R., Jr.; Abizaid, A.; Bartorelli, A.L.; Whitbourn, R.; Serruys, P.W.; Smits, P.C. Two-year clinical outcomes of patients treated with overlapping absorb scaffolds: An analysis of the ABSORB EXTEND single-arm study. *Catheter Cardiovasc Interv* **2018**, *91*(7), 1202-1209.
191. Connolly, S.; Pogue, J.; Hart, R.; Pfeffer, M.; Hohnloser, S.; Chrolavicius, S.; Pfeffer, M.; Hohnloser, S.; Yusuf, S. Clopidogrel plus aspirin versus oral anticoagulation for atrial fibrillation in the Atrial fibrillation Clopidogrel Trial with Irbesartan for prevention of Vascular Events (ACTIVE W): a randomised controlled trial. *Lancet* **2006**, *367*(9526), 1903-1912.
192. Mehran, R.; Rao, S.V.; Bhatt, D.L.; Gibson, C.M.; Caixeta, A.; Eikelboom, J.; Kaul, S.; Wiviott, S.D.; Menon, V.; Nikolsky, E.; Serebruany, V.; Valgimigli, M.; Vranckx, P.; Taggart, D.; Sabik, J.F.; Cutlip, D.E.; Krucoff, M.W.; Ohman, E.M.; Steg, P.G.; White, H. Standardized bleeding definitions for cardiovascular clinical trials: a consensus report from the Bleeding Academic Research Consortium. *Circulation* **2011**, *123*(23), 2736-2747.
193. Ndrepepa, G.; Schuster, T.; Hadamitzky, M.; Byrne, R.A.; Mehilli, J.; Neumann, F.J.; Richardt, G.; Schulz, S.; Laugwitz, K.L.; Massberg, S.; Schömig, A.; Kastrati, A. Validation of the Bleeding Academic Research Consortium definition of bleeding in patients with coronary artery disease undergoing percutaneous coronary intervention. *Circulation* **2012**, *125*(11), 1424-1431.
194. Fiedler, K.A.; Maeng, M.; Mehilli, J.; Schulz-Schüpke, S.; Byrne, R.A.; Sibbing, D.; Hoppmann, P.; Schneider, S.; Fusaro, M.; Ott, I.; Kristensen, S.D.; Ibrahim, T.; Massberg, S.; Schunkert, H.; Laugwitz, K.L.; Kastrati, A.; Sarafoff, N. Duration of Triple Therapy in Patients Requiring Oral Anticoagulation After Drug-Eluting Stent Implantation: The ISAR-TRIPLE Trial. *J Am Coll Cardiol* **2015**, *65*(16), 1619-1629.
195. Sarafoff, N.; Martischnig, A.; Wealer, J.; Mayer, K.; Mehilli, J.; Sibbing, D.; Kastrati, A. Triple therapy with aspirin, prasugrel, and vitamin K antagonists in patients with drug-eluting stent implantation and an indication for oral anticoagulation. *J Am Coll Cardiol* **2013**, *61*(20), 2060-2066.
196. Braun, O.; Bico, B.; Chaudhry, U.; Wagner, H.; Koul, S.; Tydén, P.; Scherstén, F.; Jovinge, S.; Svensson, P.J.; Gustav Smith, J.; van der Pals, J. Concomitant use of warfarin and ticagrelor as an alternative to triple antithrombotic therapy after an acute coronary syndrome. *Thromb Res* **2015**, *135*(1), 26-30.
197. Brambatti, M.; Darius, H.; Oldgren, J.; Clemens, A.; Noack, H.H.; Brueckmann, M.; Yusuf, S.; Wallentin, L.; Ezekowitz, M.D.; Connolly, S.J.; Healey, J.S. Comparison of dabigatran versus warfarin in diabetic patients with atrial fibrillation: Results from the RE-LY trial. *Int J Cardiol* **2015**, *196*, 127-131.

198. Connolly, S.J.; Eikelboom, J.; Joyner, C.; Diener, H.C.; Hart, R.; Golitsyn, S.; Flaker, G.; Avezum, A.; Hohnloser, S.H.; Diaz, R.; Talajic, M.; Zhu, J.; Pais, P.; Budaj, A.; Parkhomenko, A.; Jansky, P.; Commerford, P.; Tan, R.S.; Sim, K.H.; Lewis, B.S.; Van Mieghem, W.; Lip, G.Y.; Kim, J.H.; Lanus-Zanetti, F.; Gonzalez-Hermosillo, A.; Dans, A.L.; Munawar, M.; O'Donnell, M.; Lawrence, J.; Lewis, G.; Afzal, R.; Yusuf, S. Apixaban in patients with atrial fibrillation. *N Engl J Med* **2011**, *364*(9), 806-817.
199. O'Donoghue, M.L.; Ruff, C.T.; Giugliano, R.P.; Murphy, S.A.; Grip, L.T.; Mercuri, M.F.; Rutman, H.; Shi, M.; Kania, G.; Cermak, O.; Braunwald, E.; Antman, E.M. Edoxaban vs. warfarin in vitamin K antagonist experienced and naive patients with atrial fibrillation. *Eur Heart J* **2015**, *36*(23), 1470-1477.
200. Sardar, P.; Chatterjee, S.; Lavie, C.J.; Giri, J.S.; Ghosh, J.; Mukherjee, D.; Lip, G.Y. Risk of major bleeding in different indications for new oral anticoagulants: insights from a meta-analysis of approved dosages from 50 randomized trials. *Int J Cardiol* **2015**, *179*, 279-287.
201. Berkman, S.A. Prevention of Bleeding in Patients With Atrial Fibrillation Undergoing PCI (PIONEER): Three May End Up Being a Crowd. *Clin Appl Thromb Hemost* **2018**, *24*(3), 393-395.
202. Lopes, R.D.; Heizer, G.; Aronson, R.; Vora, A.N.; Massaro, T.; Mehran, R.; Goodman, S.G.; Windecker, S.; Darius, H.; Li, J.; Averkov, O.; Bahit, M.C.; Berwanger, O.; Budaj, A.; Hijazi, Z.; Parkhomenko, A.; Sinnaeve, P.; Storey, R.F.; Thiele, H.; Vinereanu, D.; Granger, C.B.; Alexander, J.H. Antithrombotic Therapy after Acute Coronary Syndrome or PCI in Atrial Fibrillation. *N Engl J Med* **2019**, *380*(16), 1509-1524.
203. Cannon, C.P.; Bhatt, D.L.; Oldgren, J.; Lip, G.Y.H.; Ellis, S.G.; Kimura, T.; Maeng, M.; Merkely, B.; Zeymer, U.; Gropper, S.; Nordaby, M.; Kleine, E.; Harper, R.; Manassie, J.; Januzzi, J.L.; Ten Berg, J.M.; Steg, P.G.; Hohnloser, S.H. Dual Antithrombotic Therapy with Dabigatran after PCI in Atrial Fibrillation. *N Engl J Med* **2017**, *377*(16), 1513-1524.
204. Ellis, S.G.; Gori, T.; Serruys, P.W.; Nef, H.; Steffenino, G.; Brugaletta, S.; Munzel, T.; Feliz, C.; Schmidt, G.; Sabaté, M.; Onuma, Y.; van Geuns, R.J.; Gao, R.L.; Menichelli, M.; Kereiakes, D.J.; Stone, G.W.; Testa, L.; Kimura, T.; Abizaid, A. Clinical, Angiographic, and Procedural Correlates of Very Late Absorb Scaffold Thrombosis: Multistudy Registry Results. *JACC Cardiovasc Interv* **2018**, *11*(7), 638-644.
205. Gori, T.; Weissner, M.; Gönner, S.; Wendling, F.; Ullrich, H.; Ellis, S.; Anadol, R.; Polimeni, A.; Münzel, T. Characteristics, Predictors, and Mechanisms of Thrombosis in Coronary Bioresorbable Scaffolds: Differences Between Early and Late Events. *JACC Cardiovasc Interv* **2017**, *10*(23), 2363-2371.
206. Foin, N.; Lu, S.; Ng, J.; Bulluck, H.; Hausenloy, D.J.; Wong, P.E.; Virmani, R.; Joner, M. Stent malapposition and the risk of stent thrombosis: mechanistic insights from an in vitro model. *EuroIntervention* **2017**, *13*(9), e1096-e1098.
207. Foin, N.; Gutiérrez-Chico, J.L.; Nakatani, S.; Torii, R.; Bourantas, C.V.; Sen, S.; Nijjer, S.; Petraco, R.; Kouser, C.; Ghione, M.; Onuma, Y.; Garcia-Garcia, H.M.; Francis, D.P.; Wong, P.; Di Mario, C.; Davies, J.E.; Serruys, P.W. Incomplete stent apposition causes high shear flow disturbances and delay in neointimal coverage as a function of strut to wall detachment distance: implications for the

- management of incomplete stent apposition. *Circ Cardiovasc Interv* **2014**, 7(2), 180-189.
208. Anadol, R.; Gori, T. The mechanisms of late scaffold thrombosis. *Clin Hemorheol Microcirc* **2017**, 67(3-4), 343-346.
209. Ortega-Paz, L.; Brugaletta, S.; Sabaté, M. Impact of PSP Technique on Clinical Outcomes Following Bioresorbable Scaffolds Implantation. *J Clin Med* **2018**, 7(2).
210. Souteyrand, G.; Amabile, N.; Mangin, L.; Chabin, X.; Meneveau, N.; Cayla, G.; Vanzetto, G.; Barnay, P.; Trouillet, C.; Rioufol, G.; Rangé, G.; Teiger, E.; Delaunay, R.; Dubreuil, O.; Lhermusier, T.; Mulliez, A.; Levesque, S.; Belle, L.; Caussin, C.; Motreff, P. Mechanisms of stent thrombosis analysed by optical coherence tomography: insights from the national PESTO French registry. *Eur Heart J* **2016**, 37(15), 1208-1216.
211. Adriaenssens, T.; Joner, M.; Godschalk, T.C.; Malik, N.; Alfonso, F.; Xhepa, E.; De Cock, D.; Komukai, K.; Tada, T.; Cuesta, J.; Sirbu, V.; Feldman, L.J.; Neumann, F.J.; Goodall, A.H.; Heestermans, T.; Buyschaert, I.; Hlinomaz, O.; Belmans, A.; Desmet, W.; Ten Berg, J.M.; Gershlick, A.H.; Massberg, S.; Kastrati, A.; Guagliumi, G.; Byrne, R.A. Optical Coherence Tomography Findings in Patients With Coronary Stent Thrombosis: A Report of the PRESTIGE Consortium (Prevention of Late Stent Thrombosis by an Interdisciplinary Global European Effort). *Circulation* **2017**, 136(11), 1007-1021.
212. Vorpahl, M.; Nakano, M.; Perkins, L.E.; Otsuka, F.; Jones, R.; Acampado, E.; Lane, J.P.; Rapoza, R.; Kolodgie, F.D.; Virmani, R. Vascular healing and integration of a fully bioresorbable everolimus-eluting scaffold in a rabbit iliac arterial model. *EuroIntervention* **2014**, 10(7), 833-841.
213. Hassan, A.K.; Bergheanu, S.C.; Stijnen, T.; van der Hoeven, B.L.; Snoep, J.D.; Plevier, J.W.; Schali, M.J.; Wouter Jukema, J. Late stent malapposition risk is higher after drug-eluting stent compared with bare-metal stent implantation and associates with late stent thrombosis. *Eur Heart J* **2010**, 31(10), 1172-1180.
214. Chevalier, B.; Abizaid, A.; Carrié, D.; Frey, N.; Lutz, M.; Weber-Albers, J.; Dudek, D.; Weng, S.C.; Akodad, M.; Anderson, J.; Stone, G.W. Clinical and Angiographic Outcomes With a Novel Radiopaque Sirolimus-Eluting Bioresorbable Vascular Scaffold. *Circ Cardiovasc Interv* **2019**, 12(6), e007283.
215. Verheye, S.; Wlodarczak, A.; Montorsi, P.; Torzewski, J.; Bennett, J.; Haude, M.; Starmer, G.; Buck, T.; Wiemer, M.; Nuruddin, A.A.B.; Yan, B.P.; Lee, M.K. BIOSOLVE-IV-registry: Safety and performance of the Magmaris scaffold: 12-month outcomes of the first cohort of 1,075 patients. *Catheter Cardiovasc Interv* **2020**, 10.1002/ccd.29260.

7 Eidesstattliche Erklärung

Hiermit erkläre ich an Eides statt, dass ich die vorliegende Habilitationsschrift selbstständig und nur unter Verwendung der angegebenen Literatur und Hilfsmittel angefertigt habe.

Ein Habilitationsverfahren wurde an keiner anderen Universität eröffnet oder beantragt. Frühere Habilitationsversuche sind nicht unternommen worden.

Gießen, den 05.08.2021

Dr. med. Niklas Frederik Boeder

8 Danksagung

Ich bedanke mich bei Herrn Prof. Dr. med. Christian Hamm für die ausgezeichnete Ausbildung, Betreuung und die beständige Unterstützung und Förderung in meiner klinischen und wissenschaftlichen Aus- und Weiterbildung.

Mein besonderer Dank gilt Herrn Prof. Dr. med. Holger Nef für die persönliche Betreuung und immerwährende Motivation während dieser Arbeit, die Hilfe und Unterstützung. Allem voran möchte ich ihm auch für sein ausgewiesenes gutes Gespür für Förderung und Forderung danken, dass stets Antrieb für noch ein bisschen mehr war. Er stand mir sowohl als Mentor und Freund als auch als wichtiger Ratgeber zur Seite. Auch auf seinen Schultern stehe ich.

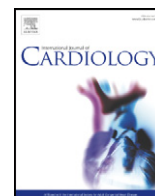
Besonderen Dank möchte ich Herrn Prof. Dr. Andreas Leunig aussprechen, der im Rahmen meiner Promotion in München mein Interesse für die wissenschaftliche Arbeit geweckt hat.

Auch meinen Kolleginnen und Kollegen aller Berufsgruppen der Klinik für Kardiologie und Angiologie möchte ich für die Unterstützung danken, die in ganz verschiedenen Aspekten meine klinisch-wissenschaftliche Weiterbildung mit unterstützt und ermöglicht haben.

Darüber hinaus danke ich meinen Eltern und meiner Familie, ohne deren Unterstützung eine zeitgleiche klinische und wissenschaftliche Weiterbildung sicherlich in dieser Form nicht möglich ist.

9 Zugrundeliegende Publikationen

Anlage 1



Impact of strut thickness on acute mechanical performance: A comparison study using optical coherence tomography between DESolve 150 and DESolve 100



Niklas F. Boeder^a, Oliver Dörr^a, Timm Bauer^a, Alessio Mattesini^b, Albrecht Elsässer^c,
Christoph Liebetrau^d, Stephan Achenbach^e, Christian W. Hamm^a, Holger M. Nef^{a,*}

^a University of Giessen, Department of Cardiology, Germany

^b Interventional Cardiology Unit, Heart and Vessels Department, Careggi Hospital, Florence, Italy

^c Klinikum Oldenburg, Department of Cardiology, Germany

^d Kerckhoff Klinik Bad Nauheim, Department of Cardiology, Germany

^e University of Erlangen, Department of Cardiology, Germany

ARTICLE INFO

Article history:

Received 17 December 2016

Received in revised form 17 April 2017

Accepted 22 May 2017

Available online 24 May 2017

Keywords:

Bioresorbable scaffold

Novolimus-eluting scaffold

Strut thickness

Optical coherence tomography

ABSTRACT

Objective: To evaluate the acute performance of a novolimus-eluting bioresorbable scaffold (BRS) with different strut thickness (DESolve system 150 and 100) using optical coherence tomography (OCT) in terms of appropriate scaffold deployment.

Background: Outcome after BRS implantation seen in registries and meta-analyses continue to show a higher rate of scaffold thrombosis than those reported with DES. Thus, second scaffold generations with lower strut thickness might have potential advantages in terms of flow disturbance. However, whether mechanical properties are comparable has to be evaluated.

Methods and results: Fifty-seven patients undergoing OCT-guided scaffold implantation were enrolled consecutively in this retrospective study. The final pullback after DESolve 150 (n = 42) and DESolve 100 (n = 15) were compared. The following indices were calculated: mean and minimum area, residual area stenosis, incomplete strut apposition, tissue prolapse, eccentricity and symmetry indexes, strut fracture, and edge dissection. Most patients suffered a multi vessel disease. Maximum pre-dilatation balloon inflation pressure was 13.5 ± 3.2 vs 14.5 ± 2.5 atm. OCT analysis showed a minimal lumen area of 6.1 ± 1.9 vs 5.2 ± 1.6 mm², p = 0.06. Mean residual area stenosis was 15.3% vs 21.3, p = 0.22. Mean eccentricity index did not differ significantly (0.8 ± 0.1 vs 0.6 ± 0.1 , p = 0.61). Prolapse area was 4.5 ± 8.8 vs 5.6 ± 9.8 mm².

Conclusion: OCT showed similar post-procedural scaffold geometry and outcome indicating that both BRS may be implanted with good acute performance. However, the trend towards a smaller MLA and a higher percentage of RAS suggest a decreased radial strength for the 100 μm BRS. The attempt to reduce strut thickness should not result in loss of radial strength.

Condensed abstract: Rates of scaffold thrombosis after bioresorbable scaffold (BRS) implantation are reported to be higher than after metallic stent (DES) implantation. Thus, second scaffold generations with lower strut thickness might have potential advantages in terms of flow disturbance. We aimed to evaluate the acute performance of a novolimus-eluting BRS with different strut thickness (DESolve system 150 and 100) using optical coherence tomography (OCT) in terms of appropriate scaffold deployment. OCT showed similar post-procedural scaffold geometry and outcome indicating that both BRS may be implanted with good acute performance. However, the data suggest a decreased radial strength for the 100 μm BRS.

© 2017 Elsevier B.V. All rights reserved.

Abbreviations: AS, Area stenosis; BRS, Bioresorbable scaffold; DES, Metallic drug-eluting stent; ISA, Incomplete strut apposition; IVUS, Intravascular ultrasound; MACE, Major adverse cardiac events; MLA, Minimal lumen area; MLD, Minimum lumen diameter; OCT, Optical coherence tomography; PCI, Percutaneous coronary intervention; QCA, Quantitative coronary angiography; RAS, Residual area stenosis; RVA, Reference vessel area; RVD, Reference vessel diameter.

* Corresponding author at: Klinikstrasse 33, 35392 Giessen, Germany.

E-mail address: holger.nef@innere.med.uni-giessen.de (H.M. Nef).

1. Introduction

The bioresorbable scaffolds (BRS) have recently emerged as a major breakthrough in interventional treatment of coronary artery disease [1]. They will be fully resorbed within two to three years and thereby potentially overcome long-term limitations of metallic drug-eluting stents (DES) like residual foreign material that may induce late thrombosis

[2]. Moreover restoration of vasomotoric function [3] as well as vascular restoration [4] has been reported.

Currently available studies have raised the concern of increased early thrombogenicity of BRS as compared to DES. The GHOST-EU registry evaluated almost 1200 patients treated with Absorb BRS [5]. Rates of scaffold thrombosis were 1.5% after 30 days, and 2.1% after 6 months respectively. Incidence was 2.1% even after 30 days in another large registry including patients with ST-elevation myocardial infarction [6]. In contrary, incidence of scaffold thrombosis in patients treated with DES is reported to be <1% after 12 months [7,8]. Mechanisms of thrombosis are multifactorial, including e.g. stent length, decreased left ventricular function, and small stent size [9,10]. However, high rates of early scaffold thrombosis in BRS patients suggest that procedural- and device-related factors may play an important role. Strut dimensions and positioning relative to the vessel wall are critical factors in modulating stent thrombogenicity [11]. Flow disturbance due to larger BRS struts as compared to DES, and the activation of coagulation may therefore significantly induce thrombosis. In addition, re-endothelialisation may be slowed due to size of scaffold struts [12].

Recently, a second generation novolimus-eluting BRS (DESolve 100, Elixir Medical Corporation, Sunnyvale, California, USA) with a strut thickness of 100 μm was approved for clinical use. The aim of this study was to evaluate the mechanical properties of this second generation device in comparison to DESolve 150 BRS using optical coherence tomography (OCT).

2. Methods

Consecutive patients undergoing percutaneous coronary intervention (PCI) with a novolimus-eluting BRS either DESolve 150 or 100 under OCT guidance with a final pullback were enrolled in this retrospective study. Patients were treated between January 2014 and October 2015.

PCI was performed in accordance with standard clinical practice using the radial approach if technically feasible, or the femoral approach, using a 6 French guiding catheter. All patients received unfractionated heparin at 70 U/kg body weight immediately prior to

the procedure. Nitroglycerine was administered to start lesion preparation. Pre-dilatation was carried out with non-compliant balloons. The pre-dilatation balloon corresponded to the vessel and BRS size in a 1:1 ratio. The use of a debulking device was left to the operator's discretion. Deployment of the BRS was accomplished using slow balloon inflation (1 atm over 10 s, 2 atm over 10 s, then 2 s per atm). Maximum pressure was maintained for 20–30 s resulting in a total implantation time of 60 s. Post-dilatation was also performed with non-compliant balloons respecting the maximum expansion limits.

Frequency domain-OCT was performed using the Ilium Optis system (St. Jude Medical, Inc., Minneapolis, MN, USA). Manual pullbacks were performed at 18 mm/s during contrast injection at a rate of 4 ml/s. OCT imaging catheters were inserted distally to the treated segments. Two sequential pullbacks were combined to image the whole lesion, if necessary. Pullbacks were typically recorded before scaffold deployment to guide the implantation procedure. Data from the final pullback were used for the analysis in this study.

OCT measurements were performed offline using the LightLab Imaging workstation (St. Jude Medical, Inc.). All images were recorded digitally, and stored within a Picture Archiving and Communication System (PACS). Longitudinal cross-sections were analysed at 1-mm intervals within the stented lesion and 5 mm proximally and distally to the scaffold. The following quantitative parameters were determined: the percentage of incomplete strut apposition (ISA) at 1-mm intervals calculated as a percentage of the total number of malapposed struts divided by the total number of struts; the ISA area; the tissue prolapse area defined as the projection of tissue into the lumen between struts [13]; residual area stenosis (RAS) calculated as $[1-MLA/RVA]$; the eccentricity index [14] computed as the ratio between the minimum and maximum diameters; the symmetry index [14] defined as the difference between maximum scaffold diameter and minimum scaffold diameter divided by the maximum scaffold diameter (see Fig. 1). An edge dissection was defined as any disruption of the vessel luminal surface at the edges of the scaffold with a visible flap (>300 μm). If isolated struts were seen unopposed within the scaffold lumen or if struts were stacked, a scaffold fracture was assumed. Struts were stated malapposed in case of distance larger than polymer thickness plus minimal axial resolution of OCT (20 μm) between of the outer strut edge and vessel wall larger.

Quantitative coronary angiography (QCA) analysis was performed with an offline QCA software (CAAS QCA, Pie Medical Imaging BV, The Netherlands). The following parameters were assessed during post-hoc analysis: reference vessel diameter (RVD) through automatic interpolation, minimum lumen diameter (MLD), percentage area stenosis (AS), and lesion length.

All patients gave written informed consent. The investigation conforms to the principles outlined in the declaration of Helsinki and was approved by the local ethics committee of the University of Giessen (AZ 203/14).

Statistical analysis was performed using IBM SPSS Statistics (SPSS Statistics 23, IBM Deutschland GmbH, Ehningen, Germany). Continuous variables with normal distribution

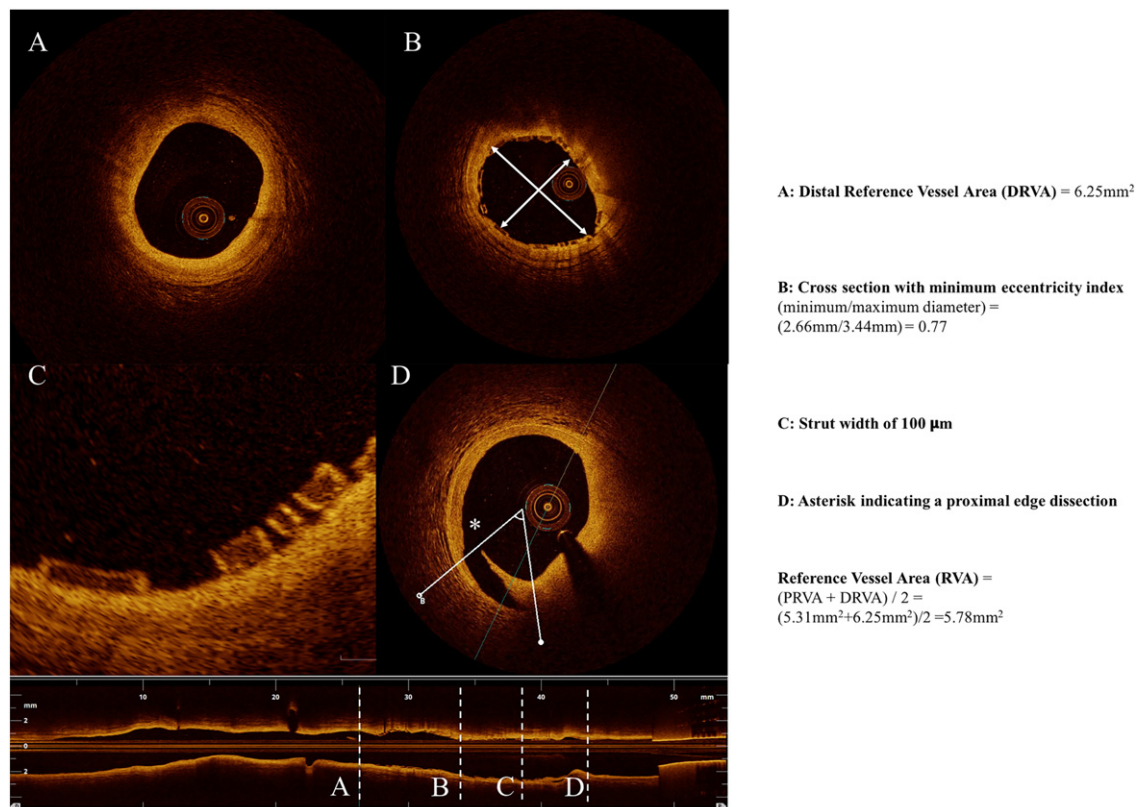


Fig. 1. Longitudinal and cross-section of OCT pullback showing calculation of minimum eccentricity index and reference vessel area.

are expressed as means and standard deviations; categorical variables are given as number and percent. Chi-square and Fisher's exact test were used for comparison of categorical variables, and Student's *t*-test or the Wilcoxon rank-sum test was applied for continuous variables. *p* values < 0.05 were considered statistically significant.

Patients were followed up via telephone after 30 days, 6 and 12 months, and hereafter yearly.

3. Results

A total of 57 patients were enrolled in this study. All patients were treated with a novolimus-eluting BRS: forty-two patients received a BRS with strut thickness of 150 μ m (group A), and fifteen patients a BRS with a thickness of 100 μ m (group B). Baseline characteristics are shown in Table 1. Patients in group A were aged 62.7 ± 9.5 years and 59.8 ± 8.5 years in group B ($p = 0.23$). Patients showed similar characteristics with respect to age, sex, and cardiovascular risk profile. The majority suffered from an arterial hypertension (90.5 vs. 80.0%, $p = 0.29$). Patients in group A were more likely diabetic in comparison to group B (19.0% vs. 6.7%, $p = 0.24$); however there was no significant difference. Patients in group A showed the tendency for less frequent prior PCI (26.2% vs. 40.0%, $p = 0.31$) and myocardial infarction (21.4% vs. 40.0%, $p = 0.61$).

Approximately half of the patients in both groups presented with stable angina as an indication for coronary angiography. The majority suffered from multi-vessel disease (group A: 73.8% vs. group B: 66.6%). Predominant lesion site was the LAD in group A and the RCA in group B (Table 2). Overall lesion sites differed not significantly between the groups ($p = 0.22$). Lesions were of de novo-type in most of the cases (88.1% vs. 86.7%, $p = 0.90$). Following the criteria by the American College of Cardiology/American Heart Association [15] lesions were classified as Type A and B1 predominantly (Table 2). Chi-square indicated no significant difference with respect to lesion type: $\chi^2(3) = 1.78$, $p = 0.61$.

Pre-dilatation prior to scaffold deployment was performed in all cases. The balloon for pre-dilatation had a maximum size of 3.0 ± 0.5 mm in group A and 2.9 ± 0.4 mm in group B ($p = 0.19$). The balloon was inflated to a maximum of 13.5 ± 3.2 atm and 14.5 ± 2.5 atm respectively ($p = 0.15$). Scaffolds were 3.2 ± 0.30 mm and 2.9 ± 0.4 mm in diameter ($p = 0.01$). Consequently, size of balloon for post-dilatation differed significantly (3.7 ± 0.7 mm vs. 3.3 ± 0.4 mm, $p = 0.01$). However, the post-dilatation/scaffold ratio did not differ significantly (1.14 ± 0.2 vs 1.15 ± 0.1 , $p = 0.80$). Maximum deployment pressure did not differ significantly between the two

Table 1
Baseline characteristics (n = 57).

	Group A: DESolve 150 (n = 42)	Group B: DESolve 100 (n = 15)	p-Value
Age (years)	62.7 \pm 9.5	59.8 \pm 8.5	0.23
Male sex (%)	61.9	60.0	0.89
Hypertension (%)	90.5	80.0	0.29
Hyperlipoproteinaemia (%)	69.0	73.3	0.76
Diabetes mellitus (%)	19.0	6.7	0.24
Current smoker (%)	54.8	80.0	0.09
Family history (%)	38.1	53.3	0.31
Prior percutaneous intervention (%)	26.2	40.0	0.31
Prior myocardial infarction (%)	21.4	40.0	0.61
Left ventricular ejection fraction (mean \pm SD, %)	55.5 \pm 10	57.2 \pm 8.3	0.6
Clinical indication			0.88
Stable angina (%)	51.1	60.0	
ST-elevation myocardial infarction (%)	21.4	6.7	
Non-ST-elevation myocardial infarction (%)	9.5	0	
Unstable angina (%)	11.9	33.3	
Number of vessels diseased			0.58
1 (%)	26.2	33.3	
2 (%)	26.2	13.3	
3 (%)	47.6	53.3	

Table 2
Angiographic, QCA lesions and procedural characteristics.

	Group A: DESolve 150 (n = 42)	Group B: DESolve 100 (n = 15)	p-Value
Target vessel			0.22
LAD (%)	45.2	20.0	
RCX (%)	21.4	33.3	
RCA (%)	33.3	46.7	
De novo lesion (%)	88.1	86.7	0.90
Total occlusion	11.9	13.3	0.90
AHA/ACC lesion classification			0.62
A (%)	31.7	20.0	
B1 (%)	36.6	40.0	
B1 (%)	19.5	33.3	
C (%)	12.2	6.7	
QCA analysis			
RVD (mm)	2.58 \pm 0.65	2.34 \pm 0.51	0.31
MLD (mm)	1.21 \pm 0.48	1.18 \pm 0.37	0.80
AS (%)	75.1	73.12	0.60
Lesion length (mm)	10.66 \pm 4.91	9.43 \pm 4.20	0.47
OCT lesion characterisation			
Calcific plaque volume (mm ³)	1.5 \pm 0.7	1.8 \pm 1.6	0.40
Calcific plaque arc (°)	41.8 \pm 8.3	51.9 \pm 38.8	0.80
Fibrous plaque volume (mm ³)	6.4 \pm 0.8	1.3 \pm 0.3	0.32
Fibrous plaque arc (°)	54.7 \pm 10.4	97.7 \pm 26.8	0.33
TCFA (%)	10	50	0.05
Max. pre-dilatation balloon diameter (mm)	3.0 \pm 0.5	2.9 \pm 0.4	0.19
Max. pre-dilatation balloon length (mm)	15.0 \pm 3.5	17.4 \pm 3.3	0.02*
Max. pre-dilatation balloon inflation (atm)	13.5 \pm 3.2	14.5 \pm 2.5	0.15
User of debulking device (%)	2.4	0	0.59
Scaffold diameter (mm)	3.2 \pm 0.3	2.9 \pm 0.4	0.01*
Scaffold length (mm)	19.8 \pm 5.8	19.6 \pm 5.8	0.94
Scaffold deployment pressure (atm)	13.1 \pm 2.7	13.8 \pm 1.7	0.44
Post-dilatation/BRS ratio	1.14 \pm 0.2	1.15 \pm 0.1	0.80
Max. post-dilatation balloon diameter (mm)	3.7 \pm 0.7	3.3 \pm 0.4	0.01*
Max. post-dilatation balloon length (mm)	15.4 \pm 3.7	14.9 \pm 4.2	0.78
Max. post-dilatation balloon inflation (atm)	16.3 \pm 3.7	17.5 \pm 2.8	0.13
Post-dilatation with NC (%)	96.0	100.0	0.42

Abbreviations: ACC, American College of Cardiology; AHA, American Heart Association; AS, area stenosis; LAD, left anterior descending; MLD, minimum lumen diameter; QCA, quantitative coronary angiography; RCA, right coronary artery; RCX, circumflex artery; RVD, reference vessel diameter; TCFA, thin cap fibroatheroma; * statistically significant, if ≤ 0.05 .

groups (13.1 ± 2.7 atm vs. 13.8 ± 1.7 atm, $p = 0.44$). Post-dilatation was performed with a non-compliant balloon in the majority of the cases. Further procedural characteristics and QCA parameters are listed in Table 2.

Optical coherence tomography findings are summarised in Table 3. A total of 1593 cross-sections and 20.0008 struts were analysed. Mean and maximum scaffold diameter were similar for both groups (mean scaffold diameter: 3.1 ± 0.4 mm vs. 2.9 ± 0.4 mm, $p = 0.09$; maximum scaffold diameter 3.5 ± 0.5 mm vs. 3.3 ± 0.4 mm, $p = 0.12$). Lumen area in group B showed a trend towards smaller mean and minimal area (mean lumen area: 7.7 ± 2.2 mm² vs. 6.7 ± 1.8 mm², $p = 0.07$; minimal lumen area: 6.1 ± 1.9 mm² vs. 5.2 ± 1.6 mm², $p = 0.06$).

The incidence of RAS > 20% was slightly higher in the group that was treated with 100 μ m BRS (45.2% vs. 52.9%, $p = 0.57$) compared with those in group A. In accordance, the mean percentage of RAS was not significantly higher for group B (15.3% vs. 21.3%, $p = 0.22$).

The symmetry index, and the mean and minimal eccentricity index were similar in the two groups (Table 3).

OCT showed five edge dissections that solely occurred in patients of group A (8.0% vs. 0%, $p = 0.28$). On the other hand, strut fractures were seen predominantly in those who were treated in group B (12.9% vs. 23.5%, $p = 0.30$). The percentage of malapposed struts was 2.5% in group A, and 1.7% in group A respectively ($p = 0.70$). Prolapse area

Table 3
Optical coherence tomography findings.

	Group A: DESolve 150 (n = 62)	Group B: DESolve 100 (n = 17)	p-Value
Mean scaffold area (mm ²)	7.8 ± 2.1	7.4 ± 2.5	0.36
Mean scaffold diameter (mm)	3.1 ± 0.4	2.9 ± 0.4	0.09
Minimum scaffold diameter (mm)	2.8 ± 0.4	2.6 ± 0.4	0.21
Maximum scaffold diameter (mm)	3.5 ± 0.5	3.3 ± 0.4	0.12
Mean lumen area (mm ²)	7.7 ± 2.2	6.7 ± 1.8	0.07
Minimal lumen area (mm ²)	6.1 ± 1.9	5.2 ± 1.6	0.06
Percentage RAS (%)	15.3	21.3	0.22
Scaffold with RAS > 20% (%)	45.2	52.9	0.57
Mean eccentricity index	0.8 ± 0.1	0.8 ± 0.4	0.53
Minimum eccentricity index	0.6 ± 0.1	0.6 ± 0.1	0.61
Symmetry index	0.4 ± 0.1	0.4 ± 0.1	0.98
ISA			
ISA area (mm ²)	1.1 ± 2.5	0.8 ± 1.3	0.93
Percentage of malapposed struts (%)	2.5	1.7	0.70
Prolapse area (mm ²)	4.5 ± 8.8	5.6 ± 9.8	0.41
Strut fracture	12.9	23.5	0.30
Edge dissection	8.0	0	0.28
Proximal edge	4.8	0	
Distal edge	3.2	0	

Abbreviations: ISA, incomplete strut apposition; RAS, residual area stenosis.

computed $4.5 \pm 8.8 \text{ mm}^2$ vs. $5.6 \pm 9.8 \text{ mm}^2$ and showed no disparity ($p = 0.41$).

Median follow-up was 356 days (IQ 132.5 days). Three patients were lost to follow-up. No adverse cardiac events occurred within the ensuing post-procedural period. Explicitly to note, no scaffold thrombosis was documented.

4. Discussion

This is the first OCT study to investigate the acute mechanical performance and mid-term outcome of everolimus-eluting BRS with a strut thickness of 150 μm and 100 μm .

The patient population selected for the study fulfilled the typical criteria for the implantation of BRS. They were relatively young ($62 \pm 9.5 \text{ y}$ vs 59.8 ± 8.5 , $p = 0.23$) and had a short history of coronary heart disease. This included a prior myocardial infarction and percutaneous coronary intervention in approximately one third of the patients. Lesion complexity as assessed with the criteria of the American College of Cardiology/American Heart Association [15] was predominantly simple and did not involve a bifurcation in any of the interventions.

In principle, the study shows that both BRS can be implanted with good acute mechanistic results. This is according to parameters derived from imaging studies that addressed the success of stent deployment [13,16]. The studies predominantly made use of intravascular ultrasound (IVUS) to assess the acute procedural and long-term clinical outcomes [17,18]. A residual area stenosis (RAS) > 20% or a final minimum cross-sectional area < 5 mm² were identified to increase the risk of stent thrombosis [19]. Patients treated with a BVS built with a strut thickness of 150 μm tended to show slightly less frequent a RAS > 20%. Mean percentage RAS was 15.3% for group A and 21.3% for group B. These results are very close to the cut off levels and reached no significance ($p = 0.22$). The expansion of the scaffolds may be further addressed by final MLA. Here, a trend towards a larger MLA in group A was observed. MLA in group B was beneath the reported lumen area and thereby indicating non-optimal deployment. These results suggest a better expansion and radial strength of the novolimus-eluting BRS with a strut thickness of 150 μm .

Concerning the geometrical parameters assessed by OCT analysis, final pullbacks depicted a mean eccentricity index of 0.8 ± 0.1 in group A and 0.8 ± 0.4 in group B ($p = 0.53$). It has been shown that an eccentricity value above 0.7 is associated with a favourable angiographic result at six-month follow-up [20]. The symmetry index

provides an additional insight into and gives supplemental information about the shape of the BRS. If the index is near zero, the scaffold is symmetric throughout the entire scaffold length [21]. Both, the eccentricity and symmetry index of both groups illustrate a good geometrical shape and results go well along with those reported in the literature [21,22].

Tissue may prolapse through the scaffold struts after the deployment of BRS. Prolapse area in group A was $4.5 \pm 8.8 \text{ mm}^2$ and $5.6 \pm 9.8 \text{ mm}^2$ in group B respectively. It did not differ significantly depending on strut thickness, however, the amount of prolapse area is directly correlated with short-term outcome, which is also reflected in a significant increase in procedural CK-MB [23]. Patients in group B may have shown larger prolapse area due to the fact that more patients presented with ACS and had more thin-cap fibroatheroma. It was shown that it is more likely to find a significant tissue prolapse in patients with thin cap fibroatheroma (OR 2.43) [22,24].

The clinical relevance of ISA is unclear [25,26]. However, it is assumed that malapposition can lead to stent-related effects and increase the rate of major adverse cardiac events [27]. Malapposed struts may disrupt the laminar flow and activate platelets due to high shear stress and ultimately promote thrombotic events due to the presence of uncovered struts and intraluminal masses [28]. Previous IVUS and OCT studies using DES were able to show a reduction of adverse events if the procedure was guided by either OCT or IVUS [29,30]. Recent data showed a percentage of malapposed struts after BRS implantation in around 2% [22]. Taking this into account, the result in the presented study did not differ significantly. However, lower rates were reported when larger scaffold diameter were used and when BRS implantation was guided by an invasive imaging modality [31].

We found a trend towards a higher incidence of strut fractures in group B. The difference between the two groups did not show significance (12.9 vs 23.5%, $p = 0.30$). Interestingly, all patients in group B showed evidence of fibroatheroma in the cross-sections near to the fractures. Patients in group A, however, did only show plaques in 20% of the cases. The small sample size of the study population clearly limits the ability to draw general conclusions, though, the higher strut fractures may be related to mechanical properties of the DESolve 100 scaffold. On the other hand, edge dissections were only seen in group A. OCT pullbacks were typically recorded before scaffold deployment to guide implantation procedure. We did not find any evidence for the occurrence of the dissection before the scaffold implantation. The edge dissections must therefore typically have occurred during BRS deployment or post-dilatation – as the inflation pressure was measured highest during this step. Interestingly, we found that 60% of the dissections were associated with the presence of a fibrous or calcific plaque. Chamiè et al. investigated the incidence and predictors of stent edge dissections [32]. They found that plaques (odds ratio 6.15[2.09,18.11]) and TCFA (odds ratio 6.16[1.42,26.69]) at the stent landing region significantly increase the risk for edge dissections. Furthermore, vessel overstretching by the stent was an independent predictor. Both factors may have played a role in the studied cohort, however, further investigations will be needed due to the small sample size.

The impact of strut width on periprocedural myocardial infarction has been studied by Kawamoto et al. [33]. They found a significant increase frequency of periprocedural myocardial infarction when comparing BRS with first-generation sirolimus-eluting stents. While both share the same strut width, they differ in strut thickness. On the long term run, however, MACE at 30 days and 1 year were not significantly different. The most probable pathophysiological mechanism for periprocedural myocardial infarction is a side branch occlusion. Given the results of this study, clinical outcome did not differ significantly between the groups. Nevertheless, further studies are needed to investigate the long-term outcome of scaffolds with reduced strut thickness in larger cohorts.

4.1. Limitations

The findings must be seen in context of significant limitations in study design, including a small sample size, lack of randomization or

blinding, no angiographic or other imaging follow-up beyond post-procedural QCA analysis, and only midterm patient follow-up of 12 months. Larger RCTs with longer follow-up duration are necessary to confirm the preliminary findings. All operators used the same protocols for lesion preparation, scaffold deployment, and post-dilation. However, whether the operator's decisions may have affected the final acute mechanical result cannot be excluded.

5. Conclusions

This is the first study to compare acute mechanical performance of two BRS with different strut thickness. Although the strut thickness of the second generation BRS device was reduced providing theoretically better blood flow characteristics. OCT showed similar post-procedural scaffold geometry and outcome indicating a satisfactory acute mechanical result and comparable mid-term outcome. However, the trend towards a smaller MLA, increased incidence of strut fractures and a higher percentage of RAS suggest a decreased radial strength for the 100 μm BRS. Further studies are required to assess the longer-term clinical outcome.

Funding

None

Conflict of interest statement

Holger Nef received speaking honoraria and a research grant (to institution) from Elixir Medical (Elixir Medical Corporation, Sunnyvale, California, USA). All other authors have no potential conflict of interest. There are no relationships with industry regarding this study.

Acknowledgment

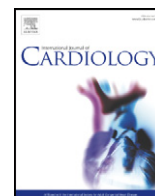
The authors thank Elizabeth Martinson, Ph.D., for editorial assistance.

References

- [1] J. Wiebe, H.M. Nef, C.W. Hamm, Current status of bioresorbable scaffolds in the treatment of coronary artery disease, *J. Am. Coll. Cardiol.* 64 (2014) 2541–2551.
- [2] T. Palmerini, G. Biondi-Zoccai, D. Della Riva, A. Mariani, P. Genereux, A. Branzi, et al., Stent thrombosis with drug-eluting stents: is the paradigm shifting? *J. Am. Coll. Cardiol.* 62 (2013) 1915–1921.
- [3] G. Roura, S. Homs, J.L. Ferreira, J. Gomez-Lara, R. Romaguera, L. Teruel, et al., Preserved endothelial vasomotor function after everolimus-eluting stent implantation, *EuroIntervention* 11 (2015) 643–649.
- [4] C. Costopoulos, T. Naganuma, A. Latib, A. Colombo, Looking into the future with bioresorbable vascular scaffolds, *Expert. Rev. Cardiovasc. Ther.* 11 (2013) 1407–1416.
- [5] D. Capodanno, T. Gori, H. Nef, A. Latib, J. Mehilli, M. Lesiak, et al., Percutaneous coronary intervention with everolimus-eluting bioresorbable vascular scaffolds in routine clinical practice: early and midterm outcomes from the European multicentre GHOST-EU registry, *EuroIntervention* 10 (2015) 1144–1153.
- [6] S. Brugaletta, T. Gori, A.F. Low, P. Tousek, E. Pinar, J. Gomez-Lara, et al., Absorb bioresorbable vascular scaffold versus everolimus-eluting metallic stent in ST-segment elevation myocardial infarction: 1-year results of a propensity score matching comparison: the BVS-EXAMINATION Study (bioresorbable vascular scaffold—a clinical evaluation of everolimus eluting coronary stents in the treatment of patients with ST-segment elevation myocardial infarction), *JACC Cardiovasc. Interv.* 8 (2015) 189–197.
- [7] T. Pilgrim, D. Heg, M. Roffi, D. Tuller, O. Muller, A. Vuilliminet, et al., Ultrathin strut biodegradable polymer sirolimus-eluting stent versus durable polymer everolimus-eluting stent for percutaneous coronary revascularisation (BIOSCIENCE): a randomised, single-blind, non-inferiority trial, *Lancet* 384 (2014) 2111–2122.
- [8] C. von Birgelen, H. Sen, M.K. Lam, P.W. Danse, G.A. Jessurun, R.W. Hautvast, et al., Third-generation zotarolimus-eluting and everolimus-eluting stents in all-comer patients requiring a percutaneous coronary intervention (DUTCH PEERS): a randomised, single-blind, multicentre, non-inferiority trial, *Lancet* 383 (2014) 413–423.
- [9] B. Brodie, Y. Pokharel, A. Garg, G. Kissling, C. Hansen, S. Milks, et al., Predictors of early, late, and very late stent thrombosis after primary percutaneous coronary intervention with bare-metal stent and drug-eluting stents for ST-segment elevation myocardial infarction, *J. Am. Coll. Cardiol. Interv.* 5 (2012) 1043–1051.
- [10] S. Lim, Y.S. Koh, P.J. Kim, H.Y. Kim, C.S. Park, J.M. Lee, et al., Incidence, implications, and predictors of stent thrombosis in acute myocardial infarction, *Am. J. Cardiol.* 117 (2016) 1562–1568.
- [11] K. Kolandaivelu, R. Swaminathan, W.J. Gibson, V.B. Kolachalama, K.L. Nguyen-Ehrenreich, V.L. Giddings, et al., Stent thrombogenicity early in high-risk interventional settings is driven by stent design and deployment and protected by polymer-drug coatings, *Circulation* 123 (2011) 1400–1409.
- [12] J. Pache, A. Kastrati, J. Mehilli, H. Schühlen, F. Dotzer, J. Hausleiter, et al., Intracoronary stenting and angiographic results: strut thickness effect on restenosis outcome (ISAR-STREO-2) trial, *J. Am. Coll. Cardiol.* 41 (2003) 1283–1288.
- [13] G.J. Tearney, E. Regar, T. Akasaka, T. Adriaenssens, P. Barlis, H.G. Bezerra, et al., Consensus standards for acquisition, measurement, and reporting of intravascular optical coherence tomography studies: a report from the International Working Group for Intravascular Optical Coherence Tomography Standardization and Validation, *J. Am. Coll. Cardiol.* 59 (2012) 1058–1072.
- [14] P. Suwannasom, Y. Sotomi, Y. Ishibashi, R. Cavalcante, F.N. Albuquerque, C. Macaya, et al., The impact of post-procedural asymmetry, expansion, and eccentricity of bioresorbable everolimus-eluting scaffold and metallic everolimus-eluting stent on clinical outcomes in the ABSORB II trial, *JACC Cardiovasc. Interv.* 9 (2016) 1231–1242.
- [15] T.J. Ryan, D.P. Faxon, R.M. Gunnar, J.W. Kennedy, S.B. King 3rd, F.D. Loop, et al., Guidelines for percutaneous transluminal coronary angioplasty. A report of the American College of Cardiology/American Heart Association task force on assessment of diagnostic and therapeutic cardiovascular procedures (subcommittee on percutaneous transluminal coronary angioplasty), *Circulation* 78 (1988) 486–502.
- [16] J. Gomez-Lara, R. Diletti, S. Brugaletta, Y. Onuma, V. Farooq, L. Thuesen, et al., Angiographic maximal luminal diameter and appropriate deployment of the everolimus-eluting bioresorbable vascular scaffold as assessed by optical coherence tomography: an ABSORB cohort B trial sub-study, *EuroIntervention* 8 (2012) 214–224.
- [17] M.A. Costa, D.J. Angiolillo, M. Tannenbaum, M. Driesman, A. Chu, J. Patterson, et al., Impact of stent deployment procedural factors on long-term effectiveness and safety of sirolimus-eluting stents (final results of the multicenter prospective STLLR trial), *Am. J. Cardiol.* 101 (2008) 1704–1711.
- [18] S. Sonoda, Y. Morino, J. Ako, M. Terashima, A.H. Hassan, H.N. Bonneau, et al., Impact of final stent dimensions on long-term results following sirolimus-eluting stent implantation: serial intravascular ultrasound analysis from the sirius trial, *J. Am. Coll. Cardiol.* 43 (2004) 1959–1963.
- [19] K. Fujii, S.G. Carlier, G.S. Mintz, Y.M. Yang, I. Moussa, G. Weisz, et al., Stent underexpansion and residual reference segment stenosis are related to stent thrombosis after sirolimus-eluting stent implantation: an intravascular ultrasound study, *J. Am. Coll. Cardiol.* 45 (2005) 995–998.
- [20] P. de Jaegere, H. Mudra, H. Figulla, Y. Almagor, S. Doucet, I. Penn, et al., Intravascular ultrasound-guided optimized stent deployment. Immediate and 6 months clinical and angiographic results from the multicenter ultrasound stenting in coronaries study (MUSIC study), *Eur. Heart J.* 19 (1998) 1214–1223.
- [21] S. Brugaletta, J. Gomez-Lara, R. Diletti, V. Farooq, R.J. van Geuns, B. de Bruyne, et al., Comparison of in vivo eccentricity and symmetry indices between metallic stents and bioresorbable vascular scaffolds: insights from the ABSORB and SPIRIT trials, *Catheter. Cardiovasc. Interv.* 79 (2012) 219–228.
- [22] A. Mattesini, G.G. Secco, G. Dall'Ara, M. Ghione, J.C. Rama-Merchan, A. Lupi, et al., ABSORB biodegradable stents versus second-generation metal stents: a comparison study of 100 complex lesions treated under OCT guidance, *JACC Cardiovasc. Interv.* 7 (2014) 741–750.
- [23] T. Sugiyama, S. Kimura, D. Akiyama, K. Hishikari, N. Kawaguchi, T. Kamiishi, et al., Quantitative assessment of tissue prolapse on optical coherence tomography and its relation to underlying plaque morphologies and clinical outcome in patients with elective stent implantation, *Int. J. Cardiol.* 176 (2014) 182–190.
- [24] N.F. Boeder, T. Koepf, O. Dorr, T. Bauer, A. Mattesini, A. Elsassner, et al., A new novolimus-eluting bioresorbable scaffold for large coronary arteries: an OCT study of acute mechanical performance, *Int. J. Cardiol.* 220 (2016) 706–710.
- [25] R. Hoffmann, M.C. Morice, J.W. Moses, P.J. Fitzgerald, L. Mauri, G. Breithardt, et al., Impact of late incomplete stent apposition after sirolimus-eluting stent implantation on 4-year clinical events: intravascular ultrasound analysis from the multicentre, randomised, RAVEL, E-SIRIUS and SIRIUS trials, *Heart* 94 (2008) 322–328.
- [26] M.K. Hong, G.S. Mintz, C.W. Lee, D.W. Park, K.M. Park, B.K. Lee, et al., Late stent malapposition after drug-eluting stent implantation: an intravascular ultrasound analysis with long-term follow-up, *Circulation* 113 (2006) 414–419.
- [27] J.M. Ahn, S.J. Kang, S.H. Yoon, H.W. Park, S.M. Kang, J.Y. Lee, et al., Meta-analysis of outcomes after intravascular ultrasound-guided versus angiography-guided drug-eluting stent implantation in 26,503 patients enrolled in three randomized trials and 14 observational studies, *Am. J. Cardiol.* 113 (2014) 1338–1347.
- [28] J. Gomez-Lara, M. Radu, S. Brugaletta, V. Farooq, R. Diletti, Y. Onuma, et al., Serial analysis of the malapposed and uncovered struts of the new generation of everolimus-eluting bioresorbable scaffold with optical coherence tomography, *JACC Cardiovasc. Interv.* 4 (2011) 992–1001.
- [29] B. Witzenbichler, A. Maehara, G. Weisz, F.J. Neumann, M.J. Rinaldi, D.C. Metzger, et al., Relationship between intravascular ultrasound guidance and clinical outcomes after drug-eluting stents: the assessment of dual antiplatelet therapy with drug-eluting stents (ADAPT-DES) study, *Circulation* 129 (2014) 463–470.
- [30] F. Prati, E. Romagnoli, F. Burzotta, U. Limbruno, L. Gatto, A. La Manna, et al., Clinical impact of OCT findings during PCI: the CLI-OPCI II study, *JACC Cardiovasc. Imaging* 8 (2015) 1297–1305.

- [31] U.K. Allahwala, J.A. Cockburn, E. Shaw, G.A. Figtree, P.S. Hansen, R. Bhindi, Clinical utility of optical coherence tomography (OCT) in the optimisation of Absorb bioresorbable vascular scaffold deployment during percutaneous coronary intervention, *EuroIntervention* 10 (2015) 1154–1159.
- [32] D. Chamie, H.G. Bezerra, G.F. Attizzani, H. Yamamoto, T. Kanaya, G.T. Stefano, et al., Incidence, predictors, morphological characteristics, and clinical outcomes of stent edge dissections detected by optical coherence tomography, *JACC Cardiovasc. Interv.* 6 (2013) 800–813.
- [33] H. Kawamoto, V.F. Panoulas, K. Sato, T. Miyazaki, T. Naganuma, A. Sticchi, et al., Impact of strut width in periprocedural myocardial infarction: a propensity-matched comparison between bioresorbable scaffolds and the first-generation sirolimus-eluting stent, *JACC Cardiovasc. Interv.* 8 (2015) 900–909.

Anlage 2



A new novolimus-eluting bioresorbable scaffold for large coronary arteries: an OCT study of acute mechanical performance



Niklas F. Boeder^a, Tim Koepp^a, Oliver Dörr^a, Timm Bauer^a, Alessio Mattesini^b, Albrecht Elsässer^c, Helge Möllmann^d, Florian Blachutzik^e, Stephan Achenbach^e, Alexander Ghanem^f, Christian W. Hamm^a, Holger M. Nef^{a,*}

^a University of Giessen, Department of Cardiology, Germany

^b Interventional Cardiology Unit, Heart and Vessels department, Careggi Hospital, Florence, Italy

^c Klinikum Oldenburg, Department of Cardiology, Germany

^d Kerckhoff Klinik Bad Nauheim, Department of Cardiology, Germany

^e University of Erlangen, Department of Cardiology, Germany

^f Asklepios Klinik St. Georg, Department of Cardiology, Germany

ARTICLE INFO

Article history:

Received 27 April 2016

Accepted 24 June 2016

Available online 26 June 2016

Keywords:

Novolimus-eluting scaffold

Large coronaries

Optical coherence tomography

ABSTRACT

Aims: To evaluate the acute performance of a novolimus-eluting bioresorbable scaffold (BRS) with a nominal diameter of 4.0 mm (DESolve® XL) using optical coherence tomography (OCT) in terms of appropriate scaffold deployment.

Methods and results: Ten patients (55.6% male, mean age 60.0 y) undergoing OCT-guided scaffold implantation were enrolled consecutively in this retrospective study. Using data from the final pullback, the following indexes were calculated: mean and minimum area, residual area stenosis, incomplete strut apposition, tissue prolapse, eccentricity and symmetry indexes, strut fracture, and edge dissection. The clinical indication for the procedure was acute coronary syndrome in roughly half (55.5%) of the cases. All three main vessels were affected equally. The maximum post-dilatation balloon inflation pressure was 14.7 ± 4.2 atm. OCT analysis showed a lumen area of 11.4 ± 1.9 mm² and a scaffold area of 11.5 ± 2.1 mm². Mean residual area stenosis was 28.6%. No strut fractures or edge dissections were apparent. The mean eccentricity index was 0.65 ± 0.16 and the mean symmetry index 0.39 ± 0.25 .

Conclusion: The size of large vessels does not adversely influence acute mechanical performance as assessed by the eccentricity and symmetry indexes. No adverse cardiac event occurred during the hospital stay or the 30-day follow-up. It is feasible to treat large vessels with the DESolve® XL BRS.

© 2016 Elsevier Ireland Ltd. All rights reserved.

1. Introduction

New techniques for the interventional treatment of coronary artery disease are continuously being developed. The bioresorbable scaffolds (BRS) have recently emerged as a potentially major breakthrough [1]. BRS offer transient vessel support to resist acute recoil but are fully resorbed within two to three years and thereby potentially overcome long-term limitations of metallic drug-eluting stents (DES). Following

implantation, this includes the restoration of vasomotoric function [2] as well as vascular healing and positive remodelling [3].

Currently available everolimus-eluting BRS (Absorb, Abbott Vascular, Santa Clara, CA, USA) are limited to vessels with a reference vessel diameter not larger than 4.0 mm as the expansion limit of the largest commercially available Absorb BVS is restricted to 0.5 mm. Overexpansion beyond this limit can lead to strut disconnection or fracture, resulting in focal loss of mechanical support. Furthermore, there is a high risk of malapposition of BRS in large coronaries [4]. This can affect all lesions larger than 3.8 mm, especially the left main stem. Thus, due to the distensibility limitation of BRS some patients have remained ineligible for treatment with the scaffolds.

Recently, a new novolimus-eluting BRS (DESolve® XL, Elixir Medical Corporation, Sunnyvale, California, USA) was approved for clinical use in coronary arteries larger than 3.5 mm. It is a poly-lactic acid-based device with a nominal diameter of 4.0 mm and a strut thickness of 150 μm.

Abbreviations: AS, Area stenosis; BRS, Bioresorbable scaffold; DES, Metallic drug-eluting stent; ISA, Incomplete strut apposition; IVUS, Intravascular ultrasound; MACE, Major adverse cardiac events; MLA, Minimal Lumen area; MLD, Minimum lumen diameter; OCT, Optical coherence tomography; PCI, Percutaneous coronary intervention; QCA, Quantitative coronary angiography; RAS, Residual area stenosis; RVA, Reference vessel area; RVD, Reference vessel diameter.

* Corresponding author at: Klinikstrasse 33, 35392 Giessen, Germany.

E-mail address: holger.nef@me.com (H.M. Nef).

The aim of this study was to evaluate the deployment of the DESolve® XL BRS using optical coherence tomography (OCT).

2. Methods

Ten consecutive patients undergoing percutaneous coronary intervention (PCI) with a novolimus-eluting BRS under OCT guidance with a final pullback were enrolled in this retrospective study. All patients gave written informed consent. The investigation conforms to the principles outlined in the declaration of Helsinki and was approved by the ethics committee of the University of Giessen (203/14).

Patients were treated at four high-volume centres in Germany (Department of Cardiology, University of Giessen; Department of Cardiology, University of Erlangen; Department of Cardiology, Klinikum Oldenburg; Department of Cardiology, Asklepios Klinik Hamburg). Patients were treated between May and September 2015.

PCI was performed in accordance with standard clinical practice using the radial approach when technically feasible or the femoral approach. Unfractionated heparin at 70 U/kg body weight was administered immediately prior to the procedure. Lesion preparation was initiated with intracoronary application of nitroglycerine. Pre-dilatation was carried out with non-compliant balloons. The pre-dilatation balloon corresponded to the vessel and BRS size in a 1:1 ratio. Deployment of the BRS (DESolve® XL, Elixir Medical Corporation, Sunnyvale, California, USA) was accomplished using slow balloon inflation (1 atm over 10 s, 2 atm over 10 s, then 2 s per atm). The recommended pressure was not exceeded and was maintained for an additional 20–30 s. Post-dilatation was also performed with non-compliant balloons. The use a debulking device was left to the operator's discretion.

Frequency domain-OCT was performed using the Ilumen Optis system (St. Jude Medical, Inc., Minneapolis, MN, USA). Automatic pullbacks were performed at 36 mm/s during contrast injection at a rate of 3 to 5 ml/s. OCT imaging catheters were inserted distally to the treated segments and the pullback was recorded until either the guiding catheter was reached or the maximum pullback length was completed. If necessary, two sequential pullbacks were combined to image the whole lesion. Pullbacks were typically carried out before scaffold deployment to guide the implantation procedure. Data from the final pullback just before the end of the procedure were used for the analysis in this study.

OCT measurements were performed offline using the LightLab Imaging workstation (St. Jude Medical, Inc.). Longitudinal cross-sections were analysed at 1-mm intervals within the stented lesion and 5 mm proximally and distally to the scaffold (see Figs. 1 and 2). The following quantitative parameters were determined: the percentage of incomplete strut apposition (ISA) at 1-mm intervals calculated as a percentage of the total number of malapposed struts divided by the total number of struts; the ISA area; the tissue prolapse area defined as the projection of tissue into the lumen between struts [5]; residual area stenosis (RAS) calculated as $[1 - \text{MLA}/\text{RVA}]$; the eccentricity index computed as the ratio between the minimum and maximum diameters; the symmetry index defined as the difference between maximum scaffold diameter and minimum scaffold diameter divided by the maximum scaffold diameter. If no meaningful value for proximal or distal reference vessel area (RVA) was obtained, the largest luminal cross-sectional area at the distal or proximal end of the scaffold was used. An edge dissection was defined as any disruption of the vessel luminal surface at the edges of the scaffold with a visible flap ($> 300 \mu\text{m}$). A scaffold fracture was assumed if isolated struts were seen unopposed within the scaffold lumen or if struts were stacked.

Quantitative coronary angiography (QCA) analysis was performed with the help of offline QCA software (CAAS QCA, Pie Medical Imaging BV, The Netherlands). The following

parameters were assessed during post-hoc analysis: reference vessel diameter (RVD) through automatic interpolation, minimum lumen diameter (MLD), percentage area stenosis (AS), and lesion length.

Statistical analysis was performed using IBM SPSS Statistics (SPSS Statistics 23, IBM Deutschland GmbH, Ehningen, Germany). Continuous variables with normal distribution are expressed as means and standard deviations; categorical variables are given as number and percent.

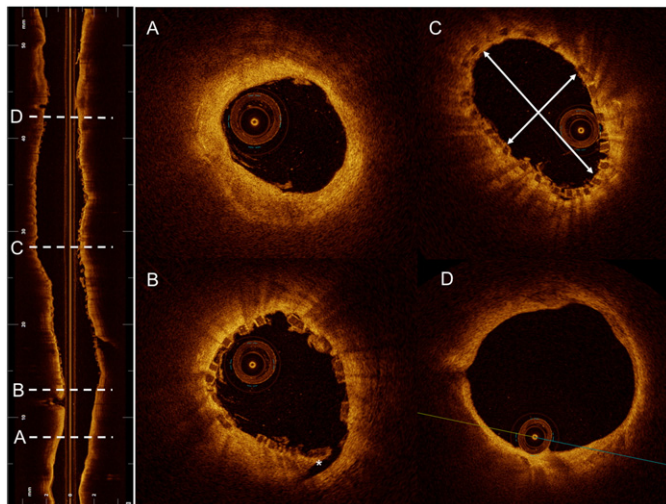
3. Results

A total of 10 patients were enrolled in this study. Baseline characteristics are shown in Table 1. Patients were aged 60.0 ± 16.1 y and 55.6% were male. They comprised a typical risk profile for coronary heart disease, including diabetes in approximately one third of the cases. None of the enrolled patients had suffered a prior myocardial infarction, but approximately half presented with acute coronary syndrome as an indication for coronary angiography. Stable angina was the indication in 44.4%. Single-vessel disease was present in 55.6%. Although severe multi-vessel disease was diagnosed in 44.4%, patients enrolled in this study were treated only with a single scaffold in a single lesion. The lesions were equally distributed between left descending, right coronary, and left circumflex arteries (Table 2). None of the lesions included a bifurcation or had ostial involvement. The majority of patients had de novo lesions. Only one patient presented with a chronic total occlusion that was older than 3 months. All lesions met the American College of Cardiology/American Heart Association classification criteria for B1 or B2 lesions [6].

QCA parameters are shown in Table 2. Pre-dilatation was performed prior to scaffold deployment in all cases. The balloon for pre-dilatation had a maximum size of 3.75 ± 0.29 mm and was inflated to a maximum of 14.7 ± 5.0 atm (Table 3). Scaffolds were 4.0 mm in diameter, 21.8 ± 5.2 mm in length, and were deployed with a maximum pressure of 13.0 ± 1.4 atm. Post-dilatation, as with pre-dilatation, was performed with non-compliant balloons in all cases. The balloons for post-dilatation had a maximum diameter of 4.8 ± 0.3 mm and the maximum inflation pressure was 14.7 ± 4.2 atm.

Optical coherence tomography findings are summarised in Table 4. A total of 192 cross-sections and 2396 struts were analysed. Maximum scaffold diameter was 4.2 ± 0.39 mm. The lumen area was calculated to be 11.4 ± 1.9 mm². The percentage of malapposed struts was 0.09 ± 0.26 and the prolapse area was 0.25 ± 0.7 mm². OCT did not reveal any strut fractures or edge dissections at distal or proximal ends.

No adverse cardiac events occurred during the hospital stay or within the ensuing 30-day post-procedural period.



A: Distal Reference Vessel Area (DRVA) = 3.37mm²

B: Distal edge dissection as indicated by asterisk

C: Cross section with minimum eccentricity index (minimum diameter/maximum diameter)= (2.29 / 3.96) = 0.57

D: Proximal reference Area (PRVA) = 11.59mm²

Reference Vessel Area = (PRVA + DRVA) / 2 = (11.59mm² + 3.37mm²)/2 = 7.48mm²

Fig. 1. Longitudinal and cross-sections of OCT pullback showing calculation of minimum eccentricity index and reference vessel area.

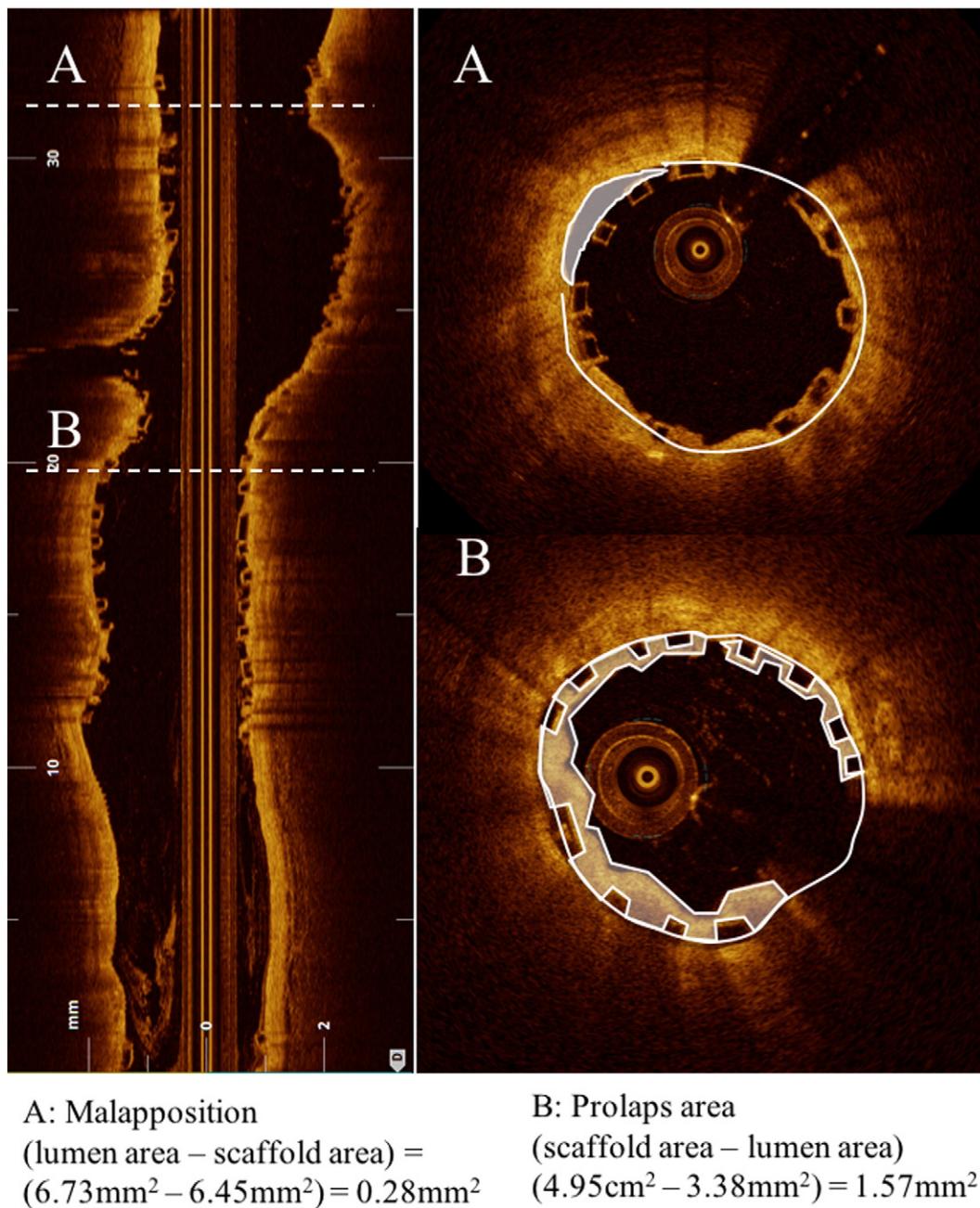


Fig. 2. Longitudinal and cross-sections of OCT pullback showing calculation of ISA and tissue prolapse area.

4. Discussion

This is the first OCT study to investigate the acute mechanical performance and short-term outcome of DESolve® XL, a novolimus-eluting BRS for large coronary arteries. The patient population selected for the study fulfilled the criteria for the implantation of BRS. They were relatively young (60 ± 16.1 y) and had a short history of coronary heart disease, with none having suffered a prior myocardial infarction and only a minority having undergone prior PCI. As the mechanical requirements for BRS implantation in large coronaries are unknown, we undertook this investigation of the acute performance of the DESolve® XL.

In general, the study shows that DESolve® XL BRS can be implanted into large coronary arteries with good acute results, according to imaging parameters that address the success of scaffold deployment [5,7].

These parameters were derived from previously published studies that mainly made use of intravascular ultrasound (IVUS) to evaluate acute procedural results and long-term outcomes [8,9]. It was shown that residual area stenosis (RAS) >20% or a final minimum cross-sectional area < 5 mm² increases the risk of stent thrombosis [10]. More than half of the patients in this study had a RAS >20%; the mean value of 28.6% is close to the calculated cut-off derived from the aforementioned studies. In particular, the MLA indicates an appropriate expansion. The expansion of BRS can be improved by aggressive plaque modification with 1:1 pre-dilatation [11]. Pre-dilatation was performed in all lesions in all of our patients; this might be due to the fact that pullbacks were typically performed after pre-dilatation had already been carried out. OCT was not routinely used for sizing the balloon. Post-dilatation, on the other hand, does not seem to improve the

Table 1
Baseline characteristics.

	DESolve XL (n = 10)
Age (years)	60.0 ± 16.1
Male sex (%)	55.6
Hypertension (%)	66.7
Hyperlipoproteinaemia (%)	55.6
Diabetes (%)	33.3
Current smoker (%)	44.4
Family history (%)	11.1
Prior percutaneous intervention (%)	11.1
Prior myocardial infarction (%)	0
Left ventricular ejection fraction (mean ± SD, %)	55.1 ± 7.8
Clinical indication	
Stable angina (%)	44.4
ST-elevation myocardial infarction (%)	33.3
Non-ST-elevation myocardial infarction (%)	22.2
Unstable angina (%)	0
Number of diseased vessels	
1 (%)	55.6
2 (%)	0
3 (%)	44.4

expansion as reported by Brown et al. [11]; however, no randomised data supporting this are available. Therefore, post-dilatation is strongly recommended whenever further optimisation is required.

In the assessment of geometrical parameters by OCT analysis, final pullbacks revealed a mean eccentricity index of 0.81 ± 0.05 . An eccentricity value of 0.70 has been associated with a favourable angiographic result at the six-month follow-up in the Multicentre Ultrasound Stenting in Coronaries Study (MUSIC study) [12]. Brugaletta et al. [13] compared the eccentricity and symmetry of everolimus-eluting BRS vs. DES and reported an eccentricity index of 0.85 ± 0.08 for the BRS group. Of note, only BRS with a diameter of 3.0 mm were implanted. Mattesini et al. [14], who studied patients treated with BRS sized up to 3.5 mm, reported an eccentricity index of 0.85 ± 0.08 . Therefore, our own results agree well with values in the literature. This holds true as well for the symmetry index (0.39 ± 0.25). The symmetry index gives additional insight into the shape of the scaffolds. If it is near zero, the scaffold is thought to be similar throughout the entire scaffold length [13].

After the deployment of BRS tissue may prolapse through the struts. In our population, the prolapse area was not clinically significant as mean and minimum lumen diameter were not affected. In fact, compared with the work of Mattesini et al. [14] the prolapse area was small. It remains unclear whether this is caused by lesion preparation

Table 2
Angiographic and QCA lesion characteristics.

	DESolve XL (n = 10)
Target vessel	
LAD (%)	33.3
RCX (%)	33.3
RCA (%)	33.3
De novo lesion (%)	88.9
Total occlusion (%)	11.1
Ostial involvement (%)	0
AHA/ACC lesion classification	
B1 (%)	88.9
B2 (%)	11.1
QCA analysis	
RVD (mm)	3.17 ± 0.6
MLD (mm)	1.31 ± 0.77
AS (%)	60.59
Lesion length (mm)	11.01 ± 4.62

Abbreviations: ACC, American College of Cardiology; AHA, American Heart Association; AS, area stenosis; LAD, left anterior descending; MLD, minimum lumen diameter; QCA, quantitative coronary angiography; RCA, right coronary artery; RCX, circumflex artery; RVD, reference vessel diameter.

Table 3
Procedural characteristics.

	DESolve XL (n = 10)
Pre-dilatation (%)	100
Max. pre-dilatation balloon diameter (mm)	3.75 ± 0.29
Max. pre-dilatation balloon length (mm)	13.0 ± 5.03
Max. pre-dilatation balloon inflation (atm)	14.7 ± 5.0
Scaffold diameter (mm)	4.0 ± 0
Scaffold length (mm)	21.8 ± 5.2
Scaffold deployment pressure (atm)	13.0 ± 1.4
Post-dilatation (%)	100
Max. post-dilatation balloon diameter (mm)	4.8 ± 0.3
Max. post-dilatation balloon length (mm)	15.8 ± 4.0
Max. post-dilatation balloon inflation (atm)	14.7 ± 4.2
Post-dilatation with non-compliant balloon (%)	100.0

or the fact that scaffold cells are expected to be smaller in the patients who have been treated with larger scaffolds such as DESolve® XL.

The clinical relevance of ISA is unclear [15,16]. It is assumed that malapposition can lead to stent-related effects and increase the rate of major adverse cardiac events (MACE) [17]. Malapposed struts may disrupt the laminar flow and activate platelets due to high shear stress and ultimately promote thrombotic events. Previous IVUS and OCT studies using DES were able to show a reduction of adverse events if the procedure was guided by either OCT or IVUS [18,19]. Gomez-Lara et al. [7] performed an OCT sub-study of the ABSORB trial Cohort B in which only BRS devices having a 3-mm diameter were deployed. The incidence of malapposed struts in vessels with a maximum diameter > 3.3 mm was higher. The percentage of malapposed struts in our cohort was almost negligible. This may indicate a negative effect of overexpansion, although within the limits of the product, upon malapposition. The clinical relevance of procedural OCT findings needs further investigation. Until then, the procedure should include an invasive imaging modality, e.g. OCT, to optimise deployment when treating patients with BRS [20].

Interventional treatment of large coronaries has been studied by Kaiser et al. [21]: in patients requiring stenting of large coronary arteries, no significant differences were found between sirolimus-eluting, everolimus-eluting, and bare-metal stents with respect to the rate of myocardial infarction or death. Hsieh et al. [22], however, reported a significant reduction of MACE in 3.0–3.75-mm vessels if DES were used. The benefit was not seen for patients who had lesions in vessels that were >3.75 mm in diameter. As BRS have shown promise as a new generation of stenting technology, it will be important to gather

Table 4
Optical coherence tomography findings.

	DESolve XL (n = 10)
Mean scaffold area (mm ²)	11.5 ± 2.1
Mean scaffold diameter (mm)	3.79 ± 0.35
Minimum scaffold diameter (mm)	3.4 ± 0.34
Maximum scaffold diameter (mm)	4.2 ± 0.39
Mean lumen area (mm ²)	11.4 ± 1.9
Minimum lumen area (mm ²)	8.7 ± 2.0
Percentage RAS (%)	28.6
Scaffold with RAS > 20% (%)	66.7
Mean eccentricity index	0.81 ± 0.05
Minimum eccentricity index	0.65 ± 0.16
Symmetry index	0.39 ± 0.25
ISA	
ISA area (mm ²)	0.1 ± 0.2
Percentage of malapposed struts (%)	0.09 ± 0.26
Prolapse area (mm ²)	0.25 ± 0.7
Strut fracture (%)	0
Edge dissection	
Proximal edge (%)	0
Distal edge (%)	0

Abbreviations: ISA, incomplete strut apposition; RAS, residual area stenosis.

data on their use in large vessels. Currently, literature describing treatment with BRS in large coronaries is rare because so far BRS use has been limited by the distensibility problem. It should be noted, however, that the newly available DESolve® XL will not only allow the treatment of large coronaries but will also potentially increase the percentage of indications for treatment of other lesions, e.g. ostial. Gori et al. [23] retrospectively investigated the outcome of patients with ostial involvement treated with BRS (BRS diameter for ostial involvement 3.19 ± 0.37 vs. 3.06 ± 0.38 mm in the non-ostial group). They found a significantly higher rate of scaffold thrombosis and a device-oriented composite endpoint. The treatment of ostial lesions was an independent predictor of this endpoint.

4.1. Study Limitations

There are several limitations inherent to this study. The protocols used for lesion preparation, scaffold deployment, and post-dilation were the same for all operators contributing to the study; however, potential discrepancies in operator decisions that may have affected the final acute mechanical result cannot be excluded. Furthermore, the sample size of the study was small.

5. Conclusions

This is the first study to investigate a novolimus-eluting BRS (DESolve® XL) for large coronaries. Data from final OCT pullbacks were analysed and showed good acute results. Implantation of DESolve® XL with the use of an invasive imaging modality demonstrated good apposition and a low incidence of strut fractures and dissections. The size of large lesions does not adversely influence acute mechanical performance as assessed by the eccentricity index. Further studies are required to assess the longer-term clinical outcome.

Funding

No funding.

Conflict of interest statement

Holger Nef received speaking honoraria and a research grant (to institution) from Elixir Medical (Elixir Medical Corporation, Sunnyvale, California, USA). All other authors have no potential conflict of interest. There are no relationships with industry regarding this study.

Acknowledgment

The authors thank Elizabeth Martinson, Ph.D., for editorial assistance.

References

- [1] J. Wiebe, H.M. Nef, C.W. Hamm, Current status of bioresorbable scaffolds in the treatment of coronary artery disease, *J. Am. Coll. Cardiol.* 64 (2014) 2541–2551.
- [2] G. Roura, S. Homs, J.L. Ferreira, J. Gomez-Lara, R. Romaguera, L. Teruel, et al., Preserved endothelial vasomotor function after everolimus-eluting stent implantation, *EuroIntervention* 11 (2015) 643–649.
- [3] C. Costopoulos, T. Naganuma, A. Latib, A. Colombo, Looking into the future with bioresorbable vascular scaffolds, *Expert. Rev. Cardiovasc. Ther.* 11 (2013) 1407–1416.
- [4] J.A. Shand, D. Sharma, C. Hanratty, A. McClelland, I.B. Menown, M.S. Spence, et al., A prospective intravascular ultrasound investigation of the necessity for and efficacy of postdilation beyond nominal diameter of 3 current generation DES platforms for the percutaneous treatment of the left main coronary artery, *Catheter. Cardiovasc. Interv.* 84 (2014) 351–358.
- [5] G.J. Tearney, E. Regar, T. Akasaka, T. Adriaenssens, P. Barlis, H.G. Bezerra, et al., Consensus standards for acquisition, measurement, and reporting of intravascular optical coherence tomography studies: a report from the International Working Group for Intravascular Optical Coherence Tomography Standardization and Validation, *J. Am. Coll. Cardiol.* 59 (2012) 1058–1072.
- [6] T.J. Ryan, D.P. Faxon, R.M. Gunnar, J.W. Kennedy, S.B. King III, F.D. Loop, et al., Guidelines for percutaneous transluminal coronary angioplasty. A report of the American College of Cardiology/American Heart Association Task Force on Assessment of Diagnostic and Therapeutic Cardiovascular Procedures (Subcommittee on Percutaneous Transluminal Coronary Angioplasty), *Circulation* 78 (1988) 486–502.
- [7] J. Gomez-Lara, R. Diletti, S. Brugaletta, Y. Onuma, V. Farooq, L. Thuesen, et al., Angiographic maximal luminal diameter and appropriate deployment of the everolimus-eluting bioresorbable vascular scaffold as assessed by optical coherence tomography: an ABSORB cohort B trial sub-study, *EuroIntervention* 8 (2012) 214–224.
- [8] M.A. Costa, D.J. Angiolillo, M. Tannenbaum, M. Driesman, A. Chu, J. Patterson, et al., Impact of stent deployment procedural factors on long-term effectiveness and safety of sirolimus-eluting stents (final results of the multicenter prospective STLLR trial), *Am. J. Cardiol.* 101 (2008) 1704–1711.
- [9] S. Sonoda, Y. Morino, J. Ako, M. Terashima, A.H. Hassan, H.N. Bonneau, et al., Impact of final stent dimensions on long-term results following sirolimus-eluting stent implantation: serial intravascular ultrasound analysis from the sirius trial, *J. Am. Coll. Cardiol.* 43 (2004) 1959–1963.
- [10] K. Fujii, S.G. Carlier, G.S. Mintz, Y.M. Yang, I. Moussa, G. Weisz, et al., Stent underexpansion and residual reference segment stenosis are related to stent thrombosis after sirolimus-eluting stent implantation: an intravascular ultrasound study, *J. Am. Coll. Cardiol.* 45 (2005) 995–998.
- [11] A.J. Brown, L.M. McCormick, D.M. Braganza, M.R. Bennett, S.P. Hoole, N.E. West, Expansion and malapposition characteristics after bioresorbable vascular scaffold implantation, *Catheter. Cardiovasc. Interv.* 84 (2014) 37–45.
- [12] P. de Jaegere, H. Mudra, H. Figulla, Y. Almagor, S. Doucet, I. Penn, et al., Intravascular ultrasound-guided optimized stent deployment. Immediate and 6 months clinical and angiographic results from the Multicenter Ultrasound Stenting in Coronaries Study (MUSIC Study), *Eur. Heart J.* 19 (1998) 1214–1223.
- [13] S. Brugaletta, J. Gomez-Lara, R. Diletti, V. Farooq, R.J. van Geuns, B. de Bruyne, et al., Comparison of in vivo eccentricity and symmetry indices between metallic stents and bioresorbable vascular scaffolds: insights from the ABSORB and SPIRIT trials, *Catheter. Cardiovasc. Interv.* 79 (2012) 219–228.
- [14] A. Mattesini, G.G. Secco, G. Dall'Ara, M. Ghione, J.C. Rama-Merchan, A. Lupi, et al., ABSORB biodegradable stents versus second-generation metal stents: a comparison study of 100 complex lesions treated under OCT guidance, *JACC Cardiovasc. Interv.* 7 (2014) 741–750.
- [15] R. Hoffmann, M.C. Morice, J.W. Moses, P.J. Fitzgerald, L. Mauri, G. Breithardt, et al., Impact of late incomplete stent apposition after sirolimus-eluting stent implantation on 4-year clinical events: intravascular ultrasound analysis from the multicentre, randomised, RAVEL, E-SIRIUS and SIRIUS trials, *Heart* 94 (2008) 322–328.
- [16] M.K. Hong, G.S. Mintz, C.W. Lee, D.W. Park, K.M. Park, B.K. Lee, et al., Late stent malapposition after drug-eluting stent implantation: an intravascular ultrasound analysis with long-term follow-up, *Circulation* 113 (2006) 414–419.
- [17] J.M. Ahn, S.J. Kang, S.H. Yoon, H.W. Park, S.M. Kang, J.Y. Lee, et al., Meta-analysis of outcomes after intravascular ultrasound-guided versus angiography-guided drug-eluting stent implantation in 26,503 patients enrolled in three randomized trials and 14 observational studies, *Am. J. Cardiol.* 113 (2014) 1338–1347.
- [18] B. Witzenbichler, A. Maehara, G. Weisz, F.J. Neumann, M.J. Rinaldi, D.C. Metzger, et al., Relationship between intravascular ultrasound guidance and clinical outcomes after drug-eluting stents: the assessment of dual antiplatelet therapy with drug-eluting stents (ADAPT-DES) study, *Circulation* 129 (2014) 463–470.
- [19] F. Prati, E. Romagnoli, F. Burzotta, U. Limbruno, L. Gatto, A. La Manna, et al., Clinical Impact of OCT Findings During PCI: The CLI-OPCI II Study, *JACC Cardiovasc. Imaging* 8 (2015) 1297–1305.
- [20] U.K. Allahwala, J.A. Cockburn, E. Shaw, G.A. Figtree, P.S. Hansen, R. Bhandi, Clinical utility of optical coherence tomography (OCT) in the optimisation of Absorb bioresorbable vascular scaffold deployment during percutaneous coronary intervention, *EuroIntervention* 10 (2015) 1154–1159.
- [21] C. Kaiser, S. Galatius, P. Erne, F. Eberli, H. Alber, H. Rickli, et al., Drug-eluting versus bare-metal stents in large coronary arteries, *N. Engl. J. Med.* 363 (2010) 2310–2319.
- [22] M.J. Hsieh, C.C. Chen, S.H. Chang, C.Y. Wang, C.H. Lee, F.C. Lin, et al., Long-term outcomes of drug-eluting stents versus bare-metal stents in large coronary arteries, *Int. J. Cardiol.* 168 (2013) 3785–3790.
- [23] T. Gori, J. Wiebe, D. Capodanno, A. Latib, M. Lesiak, S.A. Pyxaras, et al., Early and mid-term outcomes of bioresorbable vascular scaffolds for ostial coronary lesions: insights from the GHOST-EU registry, *EuroIntervention* 11 (2015).

Anlage 3



Effect of Plaque Composition, Morphology, and Burden on DESolve Novolimus-Eluting Bioresorbable Vascular Scaffold Expansion and Eccentricity – An Optical Coherence Tomography Analysis



Niklas F. Boeder^a, Oliver Dörr^a, Timm Bauer^a, Albrecht Elsässer^b, Helge Möllmann^c, Stephan Achenbach^d, Christian W. Hamm^a, Holger M. Nef^{a,*}

^a University of Giessen, Department of Cardiology, Giessen, Germany

^b Klinikum Oldenburg, Department of Cardiology, Oldenburg, Germany

^c St. Johannes Hospital Dortmund, Department of Cardiology, Dortmund, Germany

^d University of Erlangen, Department of Cardiology, Erlangen, Germany

ARTICLE INFO

Article history:

Received 2 May 2018

Received in revised form 29 July 2018

Accepted 31 July 2018

Keywords:

Novolimus-eluting scaffold

Optical coherence tomography

Plaque composition

ABSTRACT

Objective: This study of patients treated with novolimus-eluting bioresorbable scaffold (BRS) investigated the impact of plaque burden on the acute mechanical performance of the BRS and the short-term outcome.

Methods: A total of 15 patients were enrolled. The following parameters were derived from optical coherence tomography (OCT) during the final pullback: mean and minimum area, residual area stenosis, incomplete strut apposition, tissue prolapse, scaffold expansion index (SEI), scaffold eccentricity index (SEC), symmetry index, strut fracture, and edge dissection. Fibrous plaque (FP) and calcific plaque (CP) characteristics were measured at each 200 μm longitudinal cross-section. The patients were divided into two groups based on their medians of the respective plaque characteristics.

Results: OCT analysis showed a lumen area of $11.4 \pm 1.9 \text{ mm}^2$ and a scaffold area of $11.5 \pm 2.1 \text{ mm}^2$. The mean eccentricity index overall was 0.65 ± 0.16 and mean symmetry index 0.39 ± 0.25 . Statistically, scaffold expansion was not significantly influenced by a greater plaque burden as represented by greater CP area (SEI in group with CP area $<0.52 \text{ mm}^2$ 84.1% vs. SEI of 86.6% in group with CP area $\geq 0.52 \text{ mm}^2$, $p = 0.06$), thicker CP (85.7% vs. 85.1%, $p = 0.06$), greater CP arc angle (88.0% vs. 81.7%, $p = 0.08$), and CP being closer to the lumen (84.2% vs. 86.5%, $p = 0.08$). Scaffold expansion was also not significantly influenced by FP burden. The eccentricity of the implanted scaffolds was not dependent on the CP burden. On the other hand, a greater FP burden favoured a lower eccentricity index, indicating less circular expansion. Thus, greater FP area, FP thickness, and FP arc angle resulted in a more eccentric scaffold expansion.

Conclusion: In contrast to previously studied BRS, the expansion and eccentricity characteristics of the novolimus-eluting scaffold did not show the strong dependency of plaque composition, morphology, and burden. As assessed by OCT, only eccentricity was significantly affected by the FP burden. A greater FP plaque arc in our cohort and device-specific properties, e.g. self-correction, may explain the lack of a relationship between plaque, expansion, and eccentricity.

© 2018 Elsevier Inc. All rights reserved.

1. Introduction

The bioresorbable scaffolds (BRS) are considered to be the next revolution in coronary stent technology for the treatment of patients with coronary heart disease [1]. BRS are made up of a bioresorbable polymer

(poly-L-lactide) backbone coated with an anti-proliferative agent. They offer transient vessel support and are fully resorbed within 24 to 32 months [2]. Following implantation, BRS support the restoration of vasomotor function [3], vascular healing, and positive remodelling [4], thereby potentially overcoming long-term limitations of metallic drug-eluting stents (DES).

The clinical outcome of stent implantation was shown to depend on expansion parameters such as eccentricity and symmetry in the metallic stent era [5,6]. Optical coherence tomography (OCT), a light-based imaging modality with high cross-sectional resolution [7], has gained importance in the daily clinical routine and has been used to assess the expansion characteristics of the Absorb everolimus-eluting BRS

Abbreviations: AS, Area stenosis; BRS, Bioresorbable scaffold; CP, Calcific plaque; DES, Metallic drug-eluting stent; FP, Fibrous plaque; ISA, Incomplete strut apposition; MLA, Minimum lumen area; MLD, Minimum lumen diameter; OCT, Optical coherence tomography; PCI, Percutaneous coronary intervention; QCA, Quantitative coronary angiography; RAS, Residual area stenosis; RVA, Reference vessel area; RVD, Reference vessel diameter.

* Corresponding author at: Klinikstrasse 33, 35392 Giessen, Germany.

E-mail address: holger.nef@me.com (H.M. Nef).

(Absorb, Abbott Vascular, Santa Clara, CA, USA). Shaw et al. were able to demonstrate a dependence of expansion and eccentricity on plaque composition, morphology, and burden [8].

Recently, a new novolimus-eluting BRS (DESolve®, Elixir Medical Corporation, Sunnyvale, CA, USA) was approved for clinical use. Given the unique features of the DESolve BRS, including self-correction, the aim of this study was to use OCT to evaluate coronary plaque composition and its influence on the deployment of the DESolve BRS [9–11].

2. Methods

Fifteen consecutive patients undergoing percutaneous coronary intervention (PCI) with a novolimus-eluting BRS under OCT guidance with a final pullback were enrolled in this study. They were treated between April 2014 and March 2015.

The investigation was approved by the ethics committee of the University of Giessen (203/14) and conforms to the principles outlined in the declaration of Helsinki. All patients gave written informed consent.

PCI was performed in accordance with standard clinical practice. The radial approach was pursued when technically feasible. The patients were given unfractionated heparin at 70 U/kg body weight immediately prior to the procedure. Preparation of lesions was commenced with intracoronary application of nitroglycerine. Lesions were then pre-dilated with a non-compliant balloon. BRS and pre-dilatation balloon corresponded in a 1:1 ratio. The novolimus-eluting BRS device (DESolve®, Elixir Medical Corporation, Sunnyvale, CA, USA) was deployed using slow balloon inflation (1 atm over 10 s, 2 atm over 10 s, then 2 s per atm). The recommended pressure was not exceeded and was held for an additional 20–30 s. Post-dilatation following BRS placement was also performed with non-compliant balloons. It was left to the operator’s discretion whether or not to use a debulking device.

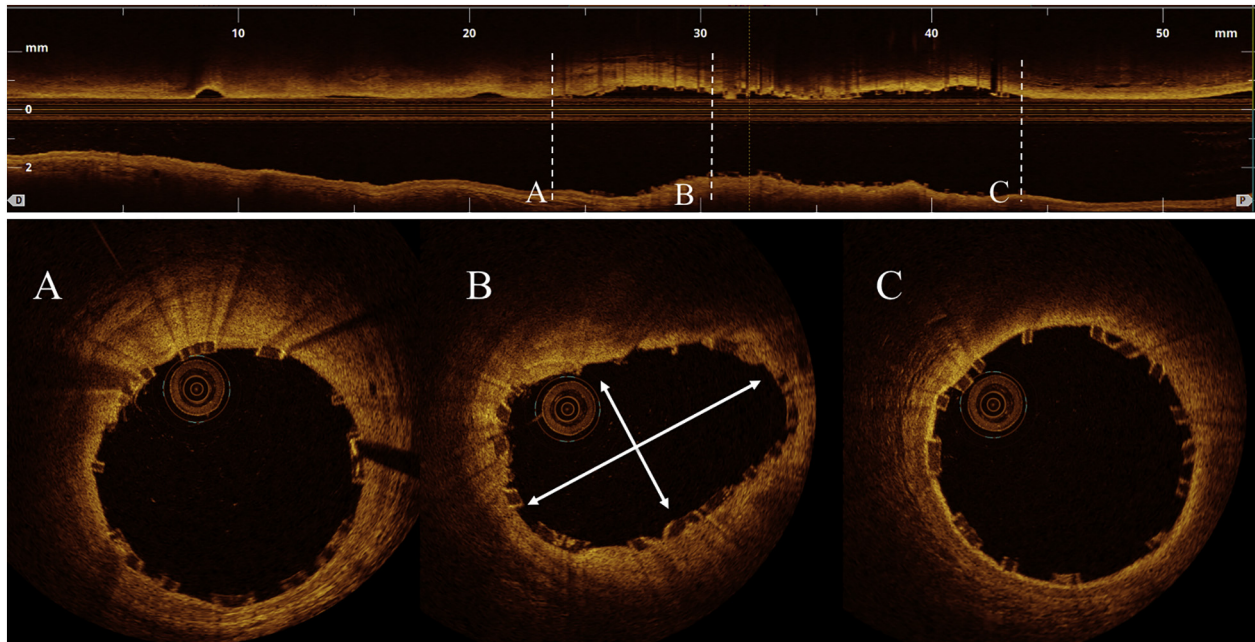
Frequency domain-OCT was performed using a C7 Dragonfly® intracoronary imaging catheter and the Ilumien Optis system (St. Jude Medical, Inc., Minneapolis, MN, USA). Automatic pullbacks were

performed at 36 mm/s during contrast injection at a rate of 3 to 5 ml/s. The pullback was recorded after placing the imaging catheters distally to the treated segments; the recording was continued until either the guiding catheter was reached or the maximum pullback length was completed. Data from the final pullback just before the end of the procedure were used for the analysis in this study.

OCT analysis was performed offline using the LightLab Imaging workstation (St. Jude Medical, Inc.). Longitudinal cross-sections were analysed at 200 µm intervals within the stented lesion and 5 mm proximally and distally to the scaffold (Fig. 1). Measurements were carried out by two independent observers. The following quantitative parameters were determined:

- the scaffold expansion index (SEI), defined as each cross-sectional area divided by the maximal scaffold area
- the scaffold eccentricity index (SEC), computed as the ratio between the minimum and maximum diameters [2,6]
- the symmetry index, defined as the difference between maximum scaffold diameter and minimum scaffold diameter divided by the maximum scaffold diameter
- the percentage of incomplete strut apposition (ISA) at cross-sections, calculated as a percentage of the total number of malapposed struts divided by the total number of struts and the ISA area
- the tissue prolapse area, defined as the projection of tissue into the lumen between struts [12]
- the residual area stenosis (RAS), calculated as $[1 - \text{MLA} / \text{RVA}]$ were MLA is the minimum lumen area and RVA is the reference vessel area

Plaque characteristics were assessed as previously defined [13]. Calcific plaque (CP) and fibrous plaque (FP) cross-sectional area was measured by tracing the plaque contour (Fig. 2). None of the lesions in the



A: Distal Reference Vessel Area (DRVA) = 8.87mm²

D: Proximal Reference Vessel Area (DRVA) = 9.76mm²

C: Cross section with minimum eccentricity index
 (minimum/maximum diameter) =
 (2.41mm/4.15mm) = 0.58

Reference Vessel Area (RVA) =
 (PRVA + DRVA) / 2 =
 (9.76mm²+8.87mm²)/2 = 9.3mm²

Fig. 1. Longitudinal and cross-sections of OCT pullback showing calculation of minimum eccentricity index and reference vessel area.

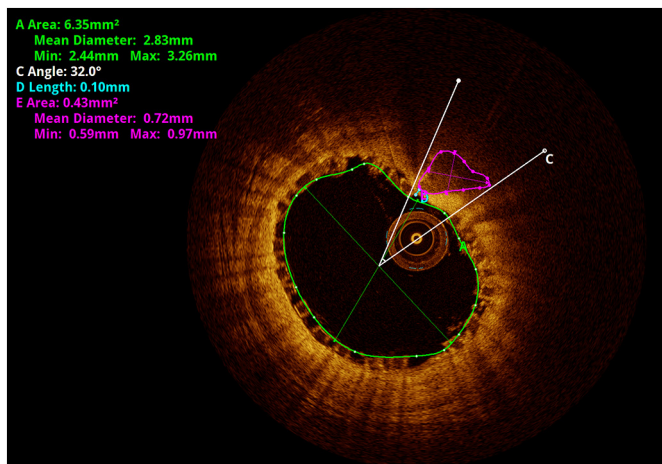


Fig. 2. Example of calcific plaque outlined in pink. CP thickness is indicated in pink. CP arc angle measurement indicated in white. CP depth indicated in aqua.

cohort were homogeneous, lipid-rich plaques, so plaques were either classified as fibrous or calcific based on their major characteristic. CP and FP thickness were measured at the thickest width of plaque. CP and FP arc angles were measured with a protractor and correlated with the angle subtended by the plaque. CP depth is the distance between the adluminal border of the plaque and the lumen border [14]. Any disruption of the vessel luminal surface at the edges of the scaffold with a visible flap ($>300\ \mu\text{m}$) was defined as edge dissection. The patients were divided into two groups based on their medians (Table 1) and analysed with respect to each plaque morphology as previously described [8].

Quantitative coronary angiography (QCA) analysis was performed using offline QCA software (CAAS QCA, Pie Medical Imaging BV, The Netherlands). The analysis was performed post hoc: reference vessel diameter (RVD) was obtained by automatic interpolation as were minimum lumen diameter (MLD), percentage area stenosis (AS), percentage diameter stenosis and lesion length.

Statistical analysis was carried out using IBM SPSS Statistics (SPSS Statistics 23, IBM Deutschland GmbH, Ehningen, Germany). Continuous variables with normal distribution are expressed as means and standard deviations; categorical variables are given as number and percent. Chi-square and Fisher's exact tests were used for comparison of categorical variables, and Student's *t*-test or the Wilcoxon rank-sum test was applied for continuous variables. *p* values <0.05 were considered statistically significant.

3. Results

A total of 15 patients were enrolled in this study. Baseline characteristics are shown in Table 2. Patients were aged 59.4 ± 8.1 years and 66.7% male. They had a risk profile that is typical for coronary heart disease, including diabetes in 54.3% of the cases. Two-thirds (66.7%) of the enrolled patients had been treated by prior percutaneous coronary

Table 1
Medians of each plaque characteristic measured.

Plaque characteristic	Median
Fibrous plaque area (mm^2)	2.21
Fibrous plaque thickness (mm)	0.52
Fibrous plaque arc angle ($^\circ$)	244.9
Calcific plaque area (mm^2)	0.55
Calcific plaque thickness (mm)	0.58
Calcific plaque arc angle ($^\circ$)	34.3
Calcific plaque depth (mm)	0.21

Table 2
Baseline characteristics.

	DESolve (n = 15)
Age (years)	59.4 ± 8.1
Male sex (%)	66.7
Hypertension (%)	100.0
Hyperlipoproteinaemia (%)	100.0
Diabetes (%)	54.3
Current smoker (%)	66.7
Family history (%)	33.3
Prior PCI (%)	66.7
Prior MI (%)	40.0
Left ventricular ejection fraction (%)	52.7 ± 15.8
Clinical indication	
Stable angina (%)	46.7
ACS (%)	53.3
Number of vessels diseased	
1 (%)	20.0
2 (%)	13.3
3 (%)	66.7

intervention (PCI); 40.0% had suffered a myocardial infarction beforehand. Clinical indications were stable angina in 46.7% and acute coronary syndrome in 53.3%. Multiple-vessel disease was present in 80.0%; however, patients enrolled in this study were treated only with a single scaffold in a single lesion. The lesions were predominantly in the left descending arteries (Table 3). None of the lesions included a bifurcation or had ostial involvement. The majority of patients had de novo lesions. QCA parameters are shown in Table 3.

Pre-dilatation was performed prior to scaffold deployment in 86.7%. The balloon for pre-dilatation had a maximum size of $2.9 \pm 0.2\ \text{mm}$ and was inflated to a maximum of $12.9 \pm 3.7\ \text{atm}$ (Table 4). Scaffolds were 3.0 mm in diameter and were deployed with a maximum pressure of $17.2 \pm 1.6\ \text{atm}$. Non-compliant balloons were used in all cases for post- and pre-dilatation. The balloons for post-dilatation had a maximum diameter of $3.1 \pm 0.2\ \text{mm}$ and the maximum inflation pressure was $18.3 \pm 5.3\ \text{atm}$.

Table 3
Angiographic and QCA lesions characteristics.

	DESolve (n = 15)
Target vessel	
LAD (%)	73.3
RCX (%)	6.7
RCA (%)	20.0
De novo lesion (%)	100.0
Total occlusion	0
QCA analysis	
RVD (mm)	2.2 ± 0.3
MLD (mm)	1.1 ± 0.4
AS (%)	70.9
Diameter stenosis (%)	46.8
Lesion length (mm)	9.7 ± 1.7

Table 4
Procedural characteristics.

	DESolve (n = 15)
Pre-dilatation (%)	86.7
Pre-dilatation with NC balloon	100.0
Max. diameter balloon pre-dilatation (mm)	2.9 ± 0.2
Max. pre-dilatation balloon length (mm)	14.3 ± 2.5
Max. pre-dilatation balloon inflation (atm)	12.9 ± 3.7
Scaffold deployment pressure (atm)	17.2 ± 1.6
Post-dilatation (%)	86.7
Post-dilatation with NC balloon	100.0
Max. post-dilatation balloon diameter (mm)	3.1 ± 0.2
Max. post-dilatation balloon length (mm)	14.2 ± 2.6
Max. post-dilatation balloon inflation (atm)	18.3 ± 5.3

Table 5
Optical coherence tomography findings.

	DESolve (n = 15)
Mean scaffold area (mm ²)	6.17 ± 0.64
Mean scaffold diameter (mm)	2.80 ± 0.17
Minimum scaffold diameter (mm)	2.52 ± 0.15
Maximum scaffold diameter (mm)	3.08 ± 0.16
Minimal lumen area (mm ²)	6.05 ± 0.80
Percentage RAS (%)	20.0 ± 4.9
Scaffold with RAS >30% (%)	13.3
Mean eccentricity index	0.83 ± 0.06
Minimum eccentricity index	0.66 ± 0.09
Symmetry index	0.37 ± 0.08
ISA	
ISA area (mm ²)	0.76 ± 2.71
Percentage of malapposed struts (%)	1.43
Prolapse area (mm ²)	2.63 ± 5.20
Strut fracture (%)	6.7
Edge dissection	
Proximal edge (%)	6.7
Distal edge (%)	0

OCT findings are summarized in Table 5. A total of 270 cross-sections and 2979 struts were analysed. The mean scaffold diameter was 2.80 ± 0.17 mm, and the lumen area was calculated to be 6.05 ± 0.80 mm². The mean RAS was 20.0%. The mean eccentricity index was computed to be 0.83 ± 0.06. The percentage of malapposed struts was 1.43 ± 0.76%, and the prolapse area was 2.63 ± 5.20 mm². OCT revealed strut fractures in 6.7%. Edge dissections were only found at the proximal end (6.7%).

Greater plaque burden, expressed by greater CP area is statistically not associated with a significant increase in scaffold expansion. SEI in group with CP area <0.52 mm² computes to be 84.1% vs. 86.6% in the group with SEI ≥0.52 mm² ($p = 0.06$). This association holds true for thicker CP (85.7% vs. 85.1%, $p = 0.06$), greater CP arc angle (88.0% vs. 81.7%, $p = 0.08$), and CP being closer to the lumen (84.2% vs. 86.5%, $p = 0.08$). Scaffold expansion was also not significantly influenced by FP burden, expressed as greater FP area. SEI in the group with FP area <1.95 mm² computed to be 88.4% vs. 87.6% in the group with FP area ≥1.95 mm² ($p = 0.07$). There was, furthermore, no statistically significance in scaffold expansion in dependence of thicker FP (85.6% vs. 89.6%, $p = 0.06$), and greater FP arc angle (90.5% vs. 84.4, $p = 0.05$).

Eccentricity showed no statistically dependency on greater plaque burden expressed by greater CP area. SEC in group with CP area <0.52 mm² computes to be 0.82 vs. 0.79 in the group with SEC ≥0.52 mm² ($p = 0.08$). This holds true for CP thickness (0.80 vs. 0.81, $p = 0.08$), the CP arc angle (0.82 vs. 0.78, $p = 0.08$), and the distance to the lumen (0.77 vs. 0.84, $p = 0.09$). On the other hand, lower eccentricity index – indicating a less circular expansion – were associated by greater FP burden (Table S1). FP area, expressing FP burden, showed a SEC of 0.86 in group with FP area <1.95 mm² and of 0.84 in the group with FP area ≥1.95 mm². This difference was statistically significant ($p = 0.03$). This effect was subsequently seen for FP thickness ($p = 0.04$) and FP arc angle ($p = 0.03$). Results are summarized in Table S1.

No adverse cardiac events (scaffold thrombosis, death, target lesion revascularization, target lesion failure) occurred during the hospital stay or within the ensuing 30-day post-procedural period.

4. Discussion and limitations

It has been shown that BRS expansion and eccentricity in patients who are treated with Absorb® BRS are significantly impacted by the coronary artery plaque composition, morphology, and burden [8]. However, it is unclear whether these observations apply to patients implanted with a novolimus-eluting BRS (DESolve® BRS). To obtain optimal BRS implantation, it is crucial to understand aspects of underlying plaque morphologies, particularly how individual lesion characteristics may play a role. Our study is the first OCT study to investigate the

impact of plaque burden on the acute mechanical performance and short-term outcome in patients treated with DESolve® BRS.

The patient population selected for the study fulfilled the criteria for the implantation of BRS: they were relatively young (59 ± 8.1 years), had a short history of coronary heart disease, and 40% had suffered a prior myocardial infarction. Approximately two-thirds had had a prior PCI. They comprised the typical cardiovascular risk profile, including the presence of diabetes (54%) and smoking (66.7%).

In our study, DESolve® BRS were implanted with good acute results, as demonstrated by imaging parameters [12,15]. These imaging parameters address the deployment of the scaffolds, and are derived from intravascular ultrasound methods that evaluate acute procedural results and long-term outcomes [16,17]. They demonstrate here that a MLA in the final OCT pullback smaller than 5 mm² or a RAS >20% increase the risk of stent thrombosis [5]. The mean residual stenosis in our population was 20%, which therefore met this criterion. Furthermore, our data show that the expansion was not significantly limited by CP area, thickness, arc angle, and distance from the lumen. On the other hand, a greater FP burden led to a lower eccentricity index, indicating less circular expansion. Thus, greater FP area, FP thickness, and FP arc angle resulted in a more eccentric scaffold expansion. This is in contrast with the results of Shaw et al. [8], who showed a dependence of expansion on the CP and FP plaque burden after Absorb® deployment. Whereas the expansion inversely correlated with CP burden, a greater FP burden resulted in a greater BRS expansion. In particular, the MLA indicates appropriate expansion. It was shown that the MLA be improved by aggressive plaque modification with 1:1 pre-dilatation [18]. Pre-dilatation was performed during 87% of the interventions in our cohort. Post-dilatation, on the other hand, does not seem to improve the expansion [18]; however, no randomised data are available supporting this observation. Currently, post-dilatation is strongly recommended whenever further optimisation is required. In our cohort, post-dilatation was performed in 87% of the cases. The preparation and post-BRS-deployment management in the aforementioned study by Shaw et al. [8] was not detailed; therefore, the diverging results could be explained by different methods of lesion preparation. This would indicate that a careful pre-dilatation can overcome the negative impact of CP plaque burden on the BRS implantation result, taking into consideration that only the median CP arc angle but not CP area, CP thickness, or CP depth is slightly smaller in our cohort compared with the patients studied by Shaw et al. [8]. A second aspect that might account for the different results may be the different BRS device used. The DESolve® has a self-expanding property that might have positively contributed to the result in our study cohort. Overall, our results indicate that scaffold expansion is reasonable, with an average SEI of 86.5%.

The assessment of geometrical parameters by OCT during final pull-back revealed a mean eccentricity index of 0.83 ± 0.06. The MUSIC study demonstrated a favourable angiographic result at six-month follow-up for an eccentricity value of 0.70 [19]. Brugaletta et al. [2], who also examined only patients treated with a 3.0 mm BRS, documented an eccentricity index of 0.85 ± 0.08. Therefore, our own results agree well with values in the literature. This also holds true for the symmetry index measured in our study (0.37 ± 0.08). The symmetry index gives additional insight into the shape of the scaffolds: if it is near zero, the scaffold is thought to be similar throughout the entire scaffold length [2]. In our cohort, CP area, CP thickness, arc angle, and less distance to the lumen did not adversely influence the eccentricity of the implanted scaffolds. However, greater fibrous plaque burden was associated with a lower eccentricity index. Greater FP area, FP thickness, and FP arc angle resulted in a more eccentric and less circular scaffold expansion. FP was typically found as circumferential clasp. The median FP arc angle in our cohort was calculated to be 250°, which was larger than that in the study conducted by Shaw et al. [6]. Median FP area and thickness, which were smaller in our cohort, still significantly influenced the BRS eccentricity. Softer, lipid-rich plaques exhibit lower dilation resistance during stenting in PCI patients [20]; thus, both the

greater circumferential extent of FP as well as a slightly different plaque composition may have influenced the deployment behaviour of the DESolve® compared to the Absorb®.

After the deployment of BRS, tissue can prolapse through the struts. In our population, the prolapse area was not clinically significant, as mean and minimum lumen diameters were not affected. The percentage of malapposed struts and the area of incomplete strut apposition were also negligible. While the clinical relevance of ISA is unclear [21,22], it is assumed that it can lead to stent-related effects and increase the rate of major adverse cardiac events [23]. Malapposed struts may disrupt laminar flow and activate platelets due to high shear stress, ultimately promoting thrombotic events. The clinical relevance of procedural OCT findings needs further investigation. Until then, BRS implantation should include an invasive imaging modality, e.g. OCT, to optimise deployment [24].

There are several limitations inherent to this study. The protocols used for lesion preparation, scaffold deployment, and post-dilation were the same for all operators contributing to the study; however, potential discrepancies in operator decisions that may have affected the final acute mechanical result cannot be excluded. Furthermore, the sample size of the study was small and OCT pullbacks prior to scaffold deployment were not available.

5. Conclusions

This is the first OCT study to investigate the impact of plaque composition, morphology, and burden on acute mechanical performance and short-term outcome in patients who were treated with DESolve® BRS. In general, DESolve® BRS were implanted with good acute results. In contrast to previously studied BRS, the expansion and eccentricity characteristics of the novolimus-eluting scaffold did not show the strong dependency of plaque composition, morphology, and burden. As assessed by OCT, only eccentricity was significantly affected by the FP burden. A greater FP plaque burden and device-specific properties such as self-correction may explain the effects on eccentricity and the lack of a correlation between CP or FP plaque burden and the scaffold expansion index.

Supplementary data to this article can be found online at <https://doi.org/10.1016/j.carrev.2018.07.030>.

Acknowledgment

The authors thank Elizabeth Martinson, Ph.D., for editorial assistance.

Funding

No funding.

Conflict of interest statement

Holger Nef received speaking honoraria and an institutional research grant from Elixir Medical (Elixir Medical Corporation, Sunnyvale, CA, USA). All other authors have no potential conflict of interest. There are no relationships with industry regarding this study.

References

- Wiebe J, Nef HM, Hamm CW. Current status of bioresorbable scaffolds in the treatment of coronary artery disease. *J Am Coll Cardiol* 2014;64:2541–51.
- Brugaletta S, Gomez-Lara J, Diletti R, Farooq V, van Geuns RJ, de Bruyne B, et al. Comparison of in vivo eccentricity and symmetry indices between metallic stents and bioresorbable vascular scaffolds: insights from the ABSORB and SPIRIT trials. *Catheter Cardiovasc Interv* 2012;79:219–28.
- Roura G, Homs S, Ferreiro JL, Gomez-Lara J, Romaguera R, Teruel L, et al. Preserved endothelial vasomotor function after everolimus-eluting stent implantation. *EuroIntervention* 2015;11:643–9.
- Costopoulos C, Naganuma T, Latib A, Colombo A. Looking into the future with bioresorbable vascular scaffolds. *Expert Rev Cardiovasc Ther* 2013;11:1407–16.
- Fujii K, Carlier SG, Mintz GS, Yang YM, Moussa I, Weisz G, et al. Stent underexpansion and residual reference segment stenosis are related to stent thrombosis after sirolimus-eluting stent implantation: an intravascular ultrasound study. *J Am Coll Cardiol* 2005;45:995–8.
- Otake H, Shite J, Ako J, Shinke T, Tanino Y, Ogasawara D, et al. Local determinants of thrombus formation following sirolimus-eluting stent implantation assessed by optical coherence tomography. *JACC Cardiovasc Interv* 2009;2:459–66.
- Ferrante G, Presbitero P, Whitbourn R, Barlis P. Current applications of optical coherence tomography for coronary intervention. *Int J Cardiol* 2013;165:7–16.
- Shaw E, Allahwala UK, Cockburn JA, Hansen TC, Mazhar J, Figtree GA, et al. The effect of coronary artery plaque composition, morphology and burden on Absorb bioresorbable vascular scaffold expansion and eccentricity – a detailed analysis with optical coherence tomography. *Int J Cardiol* 2015;184:230–6.
- Abizaid A, Costa RA, Schofer J, Ormiston J, Maeng M, Witzensbichler B, et al. Serial multimodality imaging and 2-year clinical outcomes of the novel DESolve novolimus-eluting bioresorbable coronary scaffold system for the treatment of single de novo coronary lesions. *JACC Cardiovasc Interv* 2016;9:565–74.
- Boeder NF, Koepp T, Dorr O, Bauer T, Mattesini A, Elsasser A, et al. A new novolimus-eluting bioresorbable scaffold for large coronary arteries: an OCT study of acute mechanical performance. *Int J Cardiol* 2016;220:706–10.
- Nef H, Wiebe J, Boeder N, Dorr O, Bauer T, Hauptmann KE, et al. A multicenter post-marketing evaluation of the Elixir DESolve® Novolimus-eluting bioresorbable coronary scaffold system: first results from the DESolve PMCF study. *Catheter Cardiovasc Interv* 2018.
- Tearney GJ, Regar E, Akasaka T, Adriaenssens T, Barlis P, Bezerra HG, et al. Consensus standards for acquisition, measurement, and reporting of intravascular optical coherence tomography studies: a report from the International Working Group for Intravascular Optical Coherence Tomography Standardization and Validation. *J Am Coll Cardiol* 2012;59:1058–72.
- Yabushita H, Bouma BE, Houser SL, Aretz HT, Jang IK, Schendorf KH, et al. Characterization of human atherosclerosis by optical coherence tomography. *Circulation* 2002;106:1640–5.
- Matsumoto M, Yoshikawa D, Ishii H, Hayakawa S, Tanaka M, Kumagai S, et al. Morphologic characterization and quantification of superficial calcifications of the coronary artery—in vivo assessment using optical coherence tomography. *Nagoya J Med Sci* 2012;74:253–9.
- Gomez-Lara J, Diletti R, Brugaletta S, Onuma Y, Farooq V, Thuesen L, et al. Angiographic maximal luminal diameter and appropriate deployment of the everolimus-eluting bioresorbable vascular scaffold as assessed by optical coherence tomography: an ABSORB cohort B trial sub-study. *EuroIntervention* 2012;8:214–24.
- Costa MA, Angiolillo DJ, Tannenbaum M, Driesman M, Chu A, Patterson J, et al. Impact of stent deployment procedural factors on long-term effectiveness and safety of sirolimus-eluting stents (final results of the multicenter prospective STLLR trial). *Am J Cardiol* 2008;101:1704–11.
- Sonoda S, Morino Y, Ako J, Terashima M, Hassan AH, Bonneau HN, et al. Impact of final stent dimensions on long-term results following sirolimus-eluting stent implantation: serial intravascular ultrasound analysis from the sirius trial. *J Am Coll Cardiol* 2004;43:1959–63.
- Brown AJ, McCormick LM, Braganza DM, Bennett MR, Hoole SP, West NE. Expansion and malapposition characteristics after bioresorbable vascular scaffold implantation. *Catheter Cardiovasc Interv* 2014;84:37–45.
- de Jaegere P, Mudra H, Figulla H, Almagor Y, Doucet S, Penn I, et al. Intravascular ultrasound-guided optimized stent deployment. Immediate and 6 months clinical and angiographic results from the Multicenter Ultrasound Stenting in Coronaries Study (MUSIC Study). *Eur Heart J* 1998;19:1214–23.
- Zhou Y, Chen MH, Yang K, Xiong CJ, Chen G, Yang FY, et al. Difference of dilation resistance to coronary stenting between fibrous plaques and lipid-rich plaques. *Chin Med J (Engl)* 2013;126:4149–53.
- Hoffmann R, Morice MC, Moses JW, Fitzgerald PJ, Mauri L, Breithardt G, et al. Impact of late incomplete stent apposition after sirolimus-eluting stent implantation on 4-year clinical events: intravascular ultrasound analysis from the multicenter, randomised, RAVEL, E-SIRIUS and SIRIUS trials. *Heart* 2008;94:322–8.
- Hong MK, Mintz GS, Lee CW, Park DW, Park KM, Lee BK, et al. Late stent malapposition after drug-eluting stent implantation: an intravascular ultrasound analysis with long-term follow-up. *Circulation* 2006;113:414–9.
- Ahn JM, Kang SJ, Yoon SH, Park HW, Kang SM, Lee JY, et al. Meta-analysis of outcomes after intravascular ultrasound-guided versus angiography-guided drug-eluting stent implantation in 26,503 patients enrolled in three randomized trials and 14 observational studies. *Am J Cardiol* 2014;113:1338–47.
- Allahwala UK, Cockburn JA, Shaw E, Figtree GA, Hansen PS, Bhandi R. Clinical utility of optical coherence tomography (OCT) in the optimisation of Absorb bioresorbable vascular scaffold deployment during percutaneous coronary intervention. *EuroIntervention* 2015;10:1154–9.


Table S1: SEI and SEC depending on plaque morphology and burden

	SEI (%)		SEC	
CP area < 0.52mm ²	84.1	p=0.06	0.82	p=0.08
CP area ≥ 0.52mm ²	86.6		0.79	
CP thickness < 0.58mm	85.7	p=0.06	0.80	p=0.08
CP thickness ≥ 0.58mm	85.1		0.81	
CP arc angle < 34.5°	88.9	p=0.08	0.82	p=0.08
CP arc angle ≥ 34.5°	81.7		0.78	
CP plaque depth < 0.21mm	84.2	p=0.08	0.77	p=0.09
CP plaque depth ≥ 0.21mm	86.5		0.84	
FP area < 1.95mm ²	88.4	p=0.07	0.86	p=0.03
FP area ≥ 1.95mm ²	87.6		0.84	
FP thickness < 0.5mm	85.6	p=0.06	0.86	p=0.04
FP thickness ≥ 0.5mm	89.6		0.84	
FP arc angle < 250.5°	90.5	p=0.05	0.86	p=0.03
FP arc angle ≥ 250.5°	84.4		0.85	

CP=calcific plaque; FP=fibrous plaque

Anlage 4

Post-dilatation after implantation of bioresorbable everolimus- and novolimus-eluting scaffolds: an observational optical coherence tomography study of acute mechanical effects

Florian Blachutzik¹  · Niklas Boeder² · Jens Wiebe³ · Alessio Mattesini⁴ · Oliver Dörr² · Astrid Most² · Timm Bauer² · Jens Röther¹ · Monique Tröbs¹ · Christian Schlundt¹ · Stephan Achenbach¹ · Christian W. Hamm² · Holger M. Nef²

Received: 22 July 2016 / Accepted: 12 October 2016 / Published online: 18 October 2016
© Springer-Verlag Berlin Heidelberg 2016

Abstract

Objectives The objective was to investigate the acute mechanical effects of post-dilatation on bioresorbable scaffolds (BRS) as determined by optical coherence tomography (OCT).

Background Post-dilatation with high-pressure balloons is regarded as a key component of BRS implantation for treatment of coronary artery stenoses. However, the impact of post-dilatation on BRS in vivo has not been thoroughly investigated.

Methods OCT was performed after the implantation procedure of 51 everolimus-eluting or novolimus-eluting poly(lactic acid)-based BRS with ($n = 27$) or without non-compliant balloon post-dilatation ($n = 24$). The number of malapposed struts, strut fractures, edge dissections, residual in-scaffold area stenosis, and incomplete scaffold apposition area was analyzed over the complete length of each BRS with a spacing of 1 mm.

Results OCT revealed a significantly lower incomplete scaffold apposition area if post-dilatation was performed ($0.16 \pm 0.49 \text{ mm}^2$ with post-dilatation vs. $2.65 \pm 2.78 \text{ mm}^2$

without post-dilatation, $p < 0.001$), as well as a significantly lower absolute number of malapposed struts (1 ± 2 with post-dilatation vs. 13 ± 13 without post-dilatation, $p < 0.001$). No significant differences regarding residual in-scaffold area stenosis, strut fracture, edge dissection, symmetry index, or eccentricity index were observed in patients with vs. without post-dilatation.

Conclusion Post-dilatation of BRS with non-compliant balloons significantly reduces the number of malapposed struts and incomplete scaffold apposition area without inducing higher rates of edge dissection or strut fracture.

Keywords Bioresorbable vascular scaffolds · Coronary artery disease · Optical coherence tomography · Percutaneous coronary intervention (PCI)

Introduction

The implantation of bioresorbable scaffolds (BRS) is a new concept for the treatment of coronary artery disease. Similar to metal stents, BRS initially provide mechanical scaffolding that prevents acute occlusion and early recoil after percutaneous transluminal coronary angioplasty (PTCA) and release everolimus or novolimus to prevent neointima proliferation. In contrast to metallic stents, which indefinitely impair physiological vascular biomechanics, future percutaneous coronary interventions (PCI), or grafting of the stented segment, BRS are subsequently resorbed, thus restoring pulsatility, cyclical strain, physiological shear stress, and mechanotransduction [1, 2].

Post-dilatation with an appropriately sized non-compliant (NC) balloon is considered essential for successful BRS implantation [3, 4], since underexpansion and strut malapposition might result in an increased rate of BRS

F. Blachutzik and N. Boeder contributed equally.

✉ Florian Blachutzik
florian.blachutzik@uk-erlangen.de

¹ Department of Cardiology, Friedrich-Alexander University Erlangen-Nürnberg (FAU), Erlangen, Germany

² Department of Cardiology and Angiology, University of Giessen, Giessen, Germany

³ Deutsches Herzzentrum München, Technische Universität München, Munich, Germany

⁴ Department of Heart and Vessels, Azienda Ospedaliero Universitaria Careggi, Florence, Italy

restenosis and thrombosis [5–7]. The impact of post-dilatation, however, has not been thoroughly investigated in a clinical patient cohort. Thus, the aim of this study was to analyze the acute mechanical effects of post-dilatation on BRS expansion, geometry, and apposition as determined by optical coherence tomography (OCT), which enables cross-sectional visualization of endothelial and intraluminal structures with high spatial resolution [8–11].

Materials and methods

Study design and population

We retrospectively analyzed the data of all patients undergoing implantation of everolimus-eluting Absorb BVS™ (Abbott Vascular, Santa Clara, California, USA) between March 2013 and June 2015 or of novolimus-eluting DESolve™ (Elixir Medical Corporation, Sunnyvale, California, USA) between January 2014 and June 2015 in a single center. All consecutive patients in whom OCT was performed after completion of the implantation procedure were included. The final OCT pullbacks were digitally stored and used for offline analysis. Exclusion criteria for BRS implantation were severe lesion calcification, ostial involvement, left main stem lesion, and vessel diameters for which appropriate BRS sizes are not available. OCT was not performed in the case of hemodynamic instability or renal impairment (creatinine >1.5 mg/dl). A total of 73 patients were identified to meet these criteria (Absorb 33 patients, DESolve 40 patients). Cases were excluded from this analysis if OCT quality was inadequate as assessed by two independent experienced interventional cardiologists. OCT quality was inadequate if parts of the vessel wall were invisible due to remaining blood streaks. There were no significant differences regarding baseline characteristics or procedural data between the patients excluded due to inadequate OCT quality and the patients included. The final study included 47 patients receiving 51 BRS (24 Absorb and 27 DESolve). Twenty-seven BRS were treated with post-dilatation, while in 24 BRS, no post-dilatation was performed (see Table 1).

Baseline patient characteristics, including medical history as well as clinical, angiographic, and procedural data, were collected in a standardized fashion. All patients gave written informed consent for evaluation of clinical, angiographic, procedural, and OCT data. The study was performed in accordance with the Declaration of Helsinki. The Ethics Committee of the Justus Liebig University Hospital (Giessen, Germany) approved the study protocol (reference number 203/14).

Percutaneous coronary intervention

PCI was performed via the radial or femoral approach using a 6 French guiding catheter and standard coronary guidewire (Runthrough™, Terumo Europe NV, Leuven, Belgium). Patients received intravenous heparin and intracoronary nitrates. Pre-dilatation with an NC balloon was performed in all lesions. Balloon size was selected based on visual estimation of the angiogram to achieve a 1:1 ratio of vessel and balloon diameter. Lesions were treated with either an everolimus-eluting BRS (Absorb BVS™, Abbott Vascular, Santa Clara, CA, USA) or a novolimus-eluting BRS (DESolve™, Elixir Medical Corporation, Sunnyvale, CA, USA). Absorb BRS were implanted with an initial pressure of 2 bar and increasing pressure in increments of 2 bar every 5 s until fully deployed (minimum 8 bar), and maximum pressure was maintained for 30 s. DESolve BRS were implanted starting at 1 bar for 10 s, continuing at 2 bar for 10 s, and subsequently increasing pressure in increments of 1 bar every 2 s until fully deployed, and maximum pressure was maintained for 20–30 s (minimum pressure 10 bar). Further medication, techniques, and equipment for PCI were used in accordance with the current clinical guidelines and were left to the responsible physician's discretion. If post-dilatation was performed, a non-compliant (NC) balloon (NC Trek™, Abbott Vascular, Santa Clara, CA, USA) was used at a pressure of 16 ± 9 bar (minimum pressure 10 bar; maximum pressure 26 bar). Post-dilatation was at the discretion of the operator.

Optical coherence tomography image acquisition

OCT was performed after the last step of the implantation procedure using a 2.7 French Dragonfly™ intravascular imaging catheter (St. Jude Medical, Saint Paul, MN, USA) at a mechanical pullback speed of 18 or 36 mm/s over a distance of 54 or 75 mm. Injection of 20 ml standard contrast agent (Ultravist™ 370, Bayer AG, Leverkusen, Germany) was performed at 4 ml/s with a maximum pressure of 600 psi (ACIST CVi™, ACIST Medical Systems, Eden Prairie, MN, USA). The OCT catheter was inserted distally to the treated segment and the pullback continued until either the guiding catheter was reached or the maximal pullback length (75 mm) was completed. In 25 patients (11 without and 14 with post-dilatation), pre-PCI OCT had been performed. In three patients with post-dilatation, an additional OCT pullback had been performed immediately after BRS deployment and before post-dilatation.

Table 1 Baseline characteristics

	All patients	No post-dilatation	Post-dilatation	<i>p</i> value
Number of patients	47	22	25	0.77
Number of scaffolds	51	24	27	0.78
Number of lesions	49	23	26	0.78
Age (years)	63 ± 8	63 ± 8	62 ± 7	0.66
Male gender (%)	79	78	80	0.58
BMI (kg/m ²)	29.3 ± 5.9	29.2 ± 3.5	28.1 ± 3.6	0.15
Previous MI (%)	12 (26)	6 (27)	6 (24)	0.80
Previous PCI (%)	22 (47)	13 (59)	9 (36)	0.12
Previous CABG (%)	2 (4)	1 (5)	1 (4)	0.93
LVEF (%)	56 ± 12	57 ± 12	56 ± 12	0.74
Presentation				
STEMI	8 (17)	3 (14)	5 (20)	0.58
NSTEMI	4 (9)	1 (5)	3 (12)	
Unstable AP	5 (11)	2 (10)	3 (12)	
Stable AP	21 (44)	10 (45)	11 (44)	
No complaints/atypical complaints	9 (19)	6 (27)	3 (12)	
NC pre-dilatation				
Performed (%)	100	100	100	>0.99
Pressure (bar)	15 ± 5	16 ± 5	14 ± 5	0.25
Diameter (mm)	2.9 ± 0.4	2.8 ± 0.4	3.0 ± 0.4	0.31
Length (mm)	15 ± 3	16 ± 5	16 ± 3	0.45
Scaffold				
Diameter (mm)	3.1 ± 0.3	3.1 ± 0.3	3.1 ± 0.3	0.89
Length (mm)	22 ± 6	23 ± 6	21 ± 6	0.21
Implantation pressure (bar)	13 ± 4	13 ± 3	13 ± 3	0.77
NC post-dilatation				
Diameter (mm)	3.3 ± 1.8		3.3 ± 1.8	
Pressure (bar)	16.0 ± 9.0		16.0 ± 9.0	
Number of NC balloons	2.2 ± 1.4	1.3 ± 0.4	2.8 ± 1.0	<0.001
Fluoroscopy time (min)	16 ± 9	15 ± 9	16 ± 8	0.74
Contrast volume (ml)	173 ± 82	169 ± 77	175 ± 80	0.58

Values are mean ± standard deviation or *n*

AP angina pectoris, BMI body mass index, CABG coronary artery bypass graft surgery, LVEF left ventricular ejection fraction, NC non-compliant balloon, MI myocardial infarction, PCI percutaneous coronary intervention

Optical coherence tomography image analysis

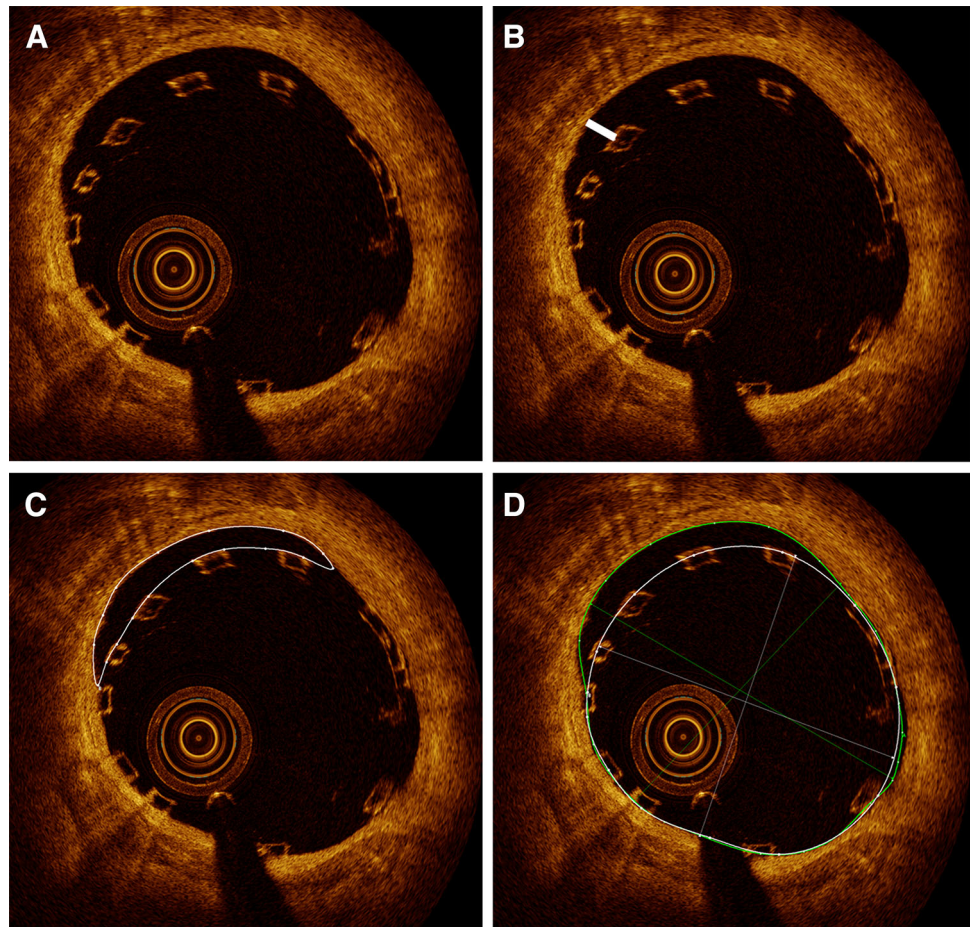
OCT image analysis was performed offline using the LightLab Imaging workstation (St. Jude Medical, Saint Paul, MN, USA) with manual calibration before each measurement. All images were digitally recorded, stored, and analyzed by two independent experienced investigators blinded to clinical characteristics and procedural data. OCT cross sections were analyzed over the complete length of implanted BRS with a spacing of 1 mm, starting 5 mm distal to the BRS, and ending 5 mm proximally. Malapposition was defined as the distance between the abluminal strut edge and the vessel wall being greater than 170 μm,

which is the sum of strut and polymer thickness (150 μm) and the minimal axial resolution of the OCT (20 μm). Proximal and distal lumen reference areas were defined as the maximum area with physiological vessel structure visible at more than 180° of circumference within 5 mm proximal and distal to the BRS. In the cases without appropriate reference on both proximal and distal ends due to a large sidebranch, only a proximal or a distal reference was used.

The following parameters were manually contoured and measured for each cross section:

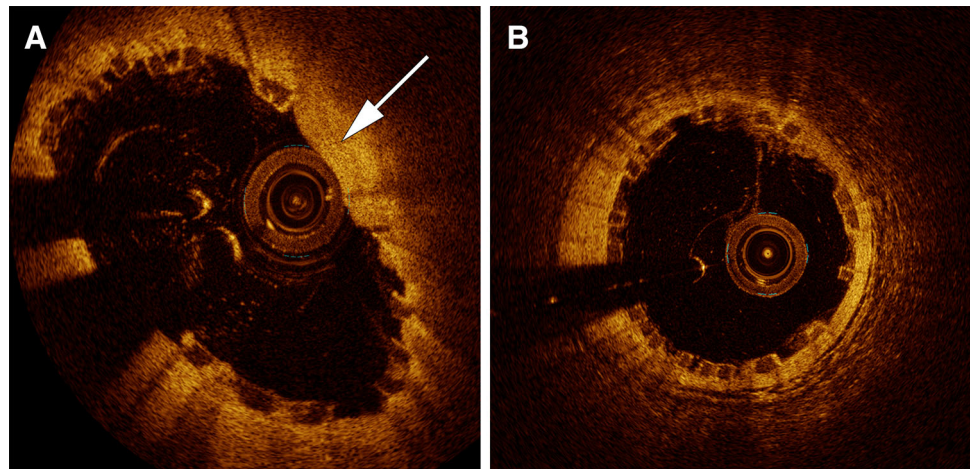
- Lumen area (mm²) (see Fig. 1d).

Fig. 1 Evaluation of OCT parameters in a cross section of an Absorb BRS implanted into the left anterior descending coronary artery. **a** Four malapposed struts and a total of 13 visible struts. **b** Distance between abluminal strut edge and vessel wall (*white line*) was measured. In this example, the maximum length of stent malapposition was 310 μm . **c** Measurement of incomplete scaffold apposition area (*white contour*). **d** Scaffold area (*white contour*) and total lumen area (*green contour*) are shown



- Scaffold area (mm^2): measured at abluminal strut edge (see Fig. 1d).
 - Maximum/minimum/mean scaffold diameter (mm).
 - Number of struts.
 - Number of malapposed struts (see Fig. 1a).
 - Maximum distance of malapposition (mm^2): maximum orthogonal distance between abluminal BRS strut and vessel wall (see Fig. 1b).
 - Incomplete scaffold apposition area (mm^2): area between abluminal edge of BRS struts and vessel wall (see Fig. 1c).
 - Tissue prolapse area (mm^2): the presence of tissue protruding between struts into the lumen as a circular arc connecting adjacent struts (see Fig. 2a and [12]).
 - Overlapping scaffolds: defined as the visibility of more than one BRS.
 - Strut fracture: struts lying isolated in the lumen or the presence of one strut on another.
 - Proximal edge dissection: flap visible within 5 mm proximal to BRS.
 - Distal edge dissection: flap visible within 5 mm distal to BRS.
 - Bifurcation.
- The following parameters were calculated (adapted from [13, 14]):
- Increment = (proximal lumen reference area – distal lumen reference area)/length in mm.
 - Reference area (mm^2) = distal lumen reference area + ($x \times$ incremental), where x is the distance between distal end of BRS and actual cross section in mm.
 - In-scaffold residual area stenosis (%) = $100 - (\text{scaffold area}/\text{reference area}) \times 100$; calculated for each cross section.
 - Incomplete strut apposition (ISA) (%) = (number of malapposed struts per cross section/total number of visible struts per cross section) $\times 100$.
 - BRS eccentricity index = (minimum scaffold diameter/maximum scaffold diameter); calculated for each cross section analyzed (see Fig. 2).
 - BRS symmetry index = (largest maximum scaffold diameter – smallest minimum scaffold diameter)/largest scaffold diameter; calculated for each cross section analyzed.
 - Mean lumen area (mm^2).
 - Minimal lumen area (mm^2).

Fig. 2 DESolve BRS with low versus high eccentricity index. **a** Eccentricity index of 0.73. **b** Eccentricity index of 0.88. A lower eccentricity index is the result of greater differences between minimum and maximum scaffold diameter. In **a**, tissue protrusion is visible (white arrow)



Statistical analysis

Continuous variables are summarized as mean \pm standard deviation; categorical variables are quoted as n (%). The Kolmogorov–Smirnov test was performed to test for parametric distribution. To test for statistical differences between two groups for comparison of continuous variables, either a t test for unpaired samples (parametric distribution) or a Mann–Whitney U test (non-parametric distribution) was performed. For categorical variables, a Chi-squared or Fischer’s exact test was carried out to test for significant differences. Statistical analysis was performed using SPSS version 21.0 (IBM SPSS Statistics, IBM Corporation, Armonk, New York, USA). A two-sided $p < 0.05$ was considered significant.

Results

Patients

A total of 51 BRS implanted in 49 lesions of 47 patients (37 male, 10 female) who were treated with either Absorb or DESolve BRS with or without post-dilatation were analyzed. Four patients were treated with two BRS, whereas 43 patients were treated with only one. Of those patients receiving more than one BRS, two received two Absorb BRS and two were treated with two DESolve BRS. In two of the patients (1 Absorb, 1 DESolve), two different lesions were treated, whereas in the other two patients (1 Absorb, 1 DESolve), lesion length required sequential overlapping implantation of BRS.

24 BRS were implanted without post-dilatation, and 27 BRS were treated with post-dilatation. There were no significant differences in baseline characteristics between the groups with and without post-dilatation performed (Table 1). Most of the patients presented with stable angina

(44 %). The target lesion was located in the left anterior descending coronary artery (LAD) in 38 % of cases, in the circumflex artery (Cx) in 19 %, and in the right coronary artery (RCA) in 43 %.

Percutaneous coronary intervention

Pre-dilatation with an NC balloon was performed in all the cases. The mean inflation pressure was 15 ± 5 bar (maximum pressure used: 22 bar), the mean balloon diameter was 2.9 ± 0.4 mm, and the mean balloon length was 15 ± 3 mm. As shown in Table 1, there were no significant differences in BRS length, diameter, or implantation pressure between the groups with or without post-dilatation (mean post-dilatation pressure: 16 ± 9 bar; maximum pressure: 20 bar; mean diameter of NC balloon: 3.3 ± 1.8 mm).

Optical coherence tomography: post-dilatation vs. no post-dilatation

A total of 1654 OCT cross sections were analyzed to obtain the data, as shown in Table 2. Incomplete scaffold apposition area was significantly smaller with post-dilatation than without post-dilatation (0.16 ± 0.49 vs. 2.65 ± 2.78 mm²; $p < 0.001$). In addition, the absolute number of malapposed struts per scaffold was significantly lower with post-dilatation (1 ± 2 vs. 13 ± 13 ; $p < 0.001$). The malapposed struts’ mean orthogonal distance to the vessel wall was significantly larger without post-dilatation (0.36 ± 0.23 mm vs. 0.09 ± 0.17 mm; $p < 0.001$). Mean, minimum, and maximum scaffold diameters as well as mean and minimal lumen areas were similar between the groups with and without post-dilatation. In addition, there were no significant differences in terms of eccentricity index or symmetry index. While mean tissue prolapse area

Table 2 OCT findings with vs. without post-dilatation

	All patients (<i>n</i> = 51)	No post-dilatation (<i>n</i> = 24)	Post-dilatation (<i>n</i> = 27)	<i>p</i> value
OCT scaffold area (mm ²)	7.47 ± 1.70	7.38 ± 1.63	7.55 ± 1.79	0.68
Residual in-scaffold area stenosis (%)	20.7 ± 15.5	25.2 ± 14.0	18.5 ± 12.4	0.14
Reference area (mm ²)	7.69 ± 1.97	8.02 ± 2.14	7.40 ± 1.79	0.35
Mean lumen area (mm ²)	7.35 ± 1.74	7.40 ± 1.78	7.30 ± 1.73	0.90
Minimal lumen area (mm ²)	5.81 ± 1.57	5.77 ± 1.41	5.84 ± 1.73	0.96
OCT ISAA (mm ²)	1.33 ± 2.30	2.65 ± 2.78	0.16 ± 0.49	<0.001
OCT tissue prolapse area (mm ²)	5.05 ± 8.49	3.44 ± 6.84	6.47 ± 9.63	0.16
Sum of malapposed struts (<i>n</i>)	6 ± 11	13 ± 13	1 ± 2	<0.001
Sum of struts (<i>n</i>)	227 ± 66	228 ± 66	226 ± 66	0.95
ISA (%)	0.04 ± 0.07	0.06 ± 0.06	0.02 ± 0.07	<0.001
Distance ^a (mm)	0.22 ± 0.24	0.36 ± 0.23	0.09 ± 0.17	<0.001
Mean stent diameter (mm)	3.05 ± 0.35	3.03 ± 0.33	3.06 ± 0.37	0.72
Minimum stent diameter (mm)	2.73 ± 0.32	2.72 ± 0.31	2.74 ± 0.32	0.79
Maximum stent diameter (mm)	3.39 ± 0.43	3.37 ± 0.39	3.41 ± 0.47	0.85
Minimum eccentricity index	0.66 ± 0.10	0.65 ± 0.09	0.67 ± 0.11	0.50
Overlapping	0.75 ± 1.70	0.88 ± 1.94	0.63 ± 1.47	0.62
Fracture	0.078 ± 0.28	0.13 ± 0.34	0.04 ± 0.19	0.25
Bifurcation	0.94 ± 1.03	0.75 ± 0.99	1.11 ± 1.05	0.19
Mean eccentricity index	0.81 ± 0.06	0.81 ± 0.06	0.79 ± 0.07	0.94
Symmetry index	0.41 ± 0.11	0.43 ± 0.11	0.39 ± 0.10	0.20
Proximal edge dissection	0	0	0	>0.99
Distal edge dissection	0	0	0	>0.99

Values are mean ± standard deviation

ISA incomplete strut apposition (ratio of number of malapposed struts per BRS to total number of struts per BRS), ISAA incomplete scaffold apposition area (area between abluminal edge of malapposed struts and vessel wall)

^a Distance: orthogonal distance between malapposed scaffold and vessel wall

was larger with post-dilatation, this difference was not significant (6.47 ± 9.63 vs. 3.44 ± 6.84 mm²; $p = 0.16$). Residual in-scaffold area stenosis was lower with post-dilatation, but also in this case, not significantly (18.5 ± 12.4 vs. 25.2 ± 14.0 %; $p = 0.14$). Post-dilatation used with BRS was not associated with a higher frequency of proximal or distal edge dissections or strut fractures.

When comparing all everolimus-eluting BRS (with and without post-dilatation) and all novolimus-eluting BRS (with and without post-dilatation), there were no significant differences regarding incomplete scaffold apposition area (1.17 ± 1.85 vs. 1.47 ± 2.66 mm²; $p = 0.63$) or the absolute number of malapposed struts per scaffold (5 ± 9 vs. 8 ± 13 ; $p = 0.33$). Nevertheless, mean tissue prolapse area (8.53 ± 10.44 vs. 1.13 ± 1.81 mm²; $p = 0.005$) was significantly larger and eccentricity was significantly higher, as displayed in a lower eccentricity index (mean eccentricity index: 0.78 ± 0.07 vs. 0.85 ± 0.04) in novolimus-eluting BRS as compared to everolimus-eluting BRS.

Discussion

Post-dilatation vs. no post-dilatation

The principal finding of this study is that post-dilatation after implantation of contemporary bioresorbable vascular scaffolds significantly reduces the incomplete scaffold apposition area and the number of malapposed struts without inducing more edge dissections or strut fractures. Previous studies have demonstrated that malapposed struts are associated with very late thrombosis of DES, most likely due to disruption of laminar flow [6, 15]. Stent thrombosis leads to myocardial infarction and has an extremely high mortality rate [16, 17]. Similar to the conventional stents, available data suggest an association of BRS underexpansion and malapposition with BRS thrombosis [5, 18]. Malapposed BRS struts do not sufficiently supply the vessel wall with novolimus or everolimus, and lumen loss due to intima proliferation is likely to occur. Furthermore, only approximately 61 % of

malapposed BRS struts are covered with neointima after 6 months [17]. On the other hand, one must keep in mind that malapposition is theoretically limited in time with BRS due to their eventual dissolution.

Clinical implications

Our data suggest that post-dilatation after implantation of Absorb or DESolve with an adequately sized NC balloon significantly improves acute deployment as evidenced by the reduced number of malapposed struts and reduced incomplete scaffold apposition area without higher rates of strut fractures or edge dissections. This may result in improved clinical outcome. Common and accepted criteria for appropriate BRS deployment were used to define the quality of the acute mechanical results [19–21]. Nevertheless, a correlation between these criteria and long-term outcome is mainly derived from previous studies comparing outcome after bare metal stents or first-generation DES using intravascular ultrasound [22–24]. Data regarding long-term outcome with BRS are very limited. De Ribamar Costa et al. reported that using post-dilatation with the Absorb device did not influence 1-year clinical outcome and concluded that post-dilatation should be performed whenever possible; however, no routine intravascular assessment was performed to evaluate the acute mechanical effects of post-dilatation and, in contrast to our study, only lesions with low-to-moderate complexity were included [25].

Whether the improvement in acute performance of BRS achieved by post-dilatation that we observed is really associated with a better clinical outcome still needs to be evaluated in controlled, randomized studies with the long-term follow-up to confirm the value of post-dilatation after BRS implantation and establish it as standard of care.

Interestingly, tissue prolapse area was significantly larger and eccentricity was significantly higher in novolimus-eluting scaffolds as compared to everolimus-eluting scaffolds. This could be due to structural differences between those two BRS, especially due to the larger scaffold cells of novolimus-eluting BRS [26]. Higher BRS eccentricity and larger tissue prolapse area have been reported to be associated with an impaired clinical outcome [27, 28].

Limitations

This is a non-randomized, retrospective, single-center study that compared acute mechanical effects of post-dilatation for two types of BRS. With 47 patients and 51 scaffolds, the sample size is relatively small. Therefore, results may have been influenced by differences in baseline characteristics, although no significant differences could be observed. A paired analysis with OCT performed

immediately after BRS deployment, and then, again, after NC balloon, post-dilatation would have been superior to our study design. Furthermore, PCI procedures were not all performed by the same operator, and therefore, we cannot exclude the possibility that individual differences in procedural approach may have influenced the results. In three patients, OCT was performed after BRS implantation and before post-dilatation. It is possible that post-implantation OCT influenced the decision to perform post-dilatation. This, however, would emphasize our results, since the effect would be to mitigate the difference between BRS with and without post-dilatation (no post-dilatation done if OCT shows a good implantation result, yet we can still demonstrate significantly more malapposition if post-dilatation is not performed).

It should also be noted that our results are not generally applicable to all PCI procedures performed with BRS implantation. The selection of cases that included the use of OCT for clinical reasons likely resulted in a cohort of more complex lesions than those typically treated with BRS. In addition, the lack of clinical outcome data is an important limitation of our study.

Conclusion

Post-dilatation of either Absorb or DESolve BRS with non-compliant balloons significantly reduces the number of malapposed struts as well as the area of incomplete scaffold apposition without inducing higher rates of edge dissection or strut fracture.

Compliance with ethical standards

Ethical standards All patients gave written informed consent for the evaluation of clinical, angiographic, procedural, and OCT data. The study was performed in accordance with the ethical standards laid down in the 1964 Declaration of Helsinki and its later amendments. The Ethics Committee of the Justus Liebig University Hospital (Giessen, Germany) approved the study protocol (reference number 203/14).

Conflict of interest Christian Hamm and Holger Nef received speaking honoraria from Abbott Vascular. Stephan Achenbach and Holger Nef have received research grants (to institution) from Abbott Vascular. Holger Nef also received a research grant (to institution) from Elixir Medical. All the other authors have no potential conflict of interest.

References


1. Iqbal J, Onuma Y, Ormiston J, Abizaid A, Waksman R, Serruys P (2014) Bioresorbable scaffolds: rationale, current status, challenges, and future. *Eur Heart J* 35:765–776
2. Simsek C, Karanasos A, Magro M, Garcia-Garcia HM, Onuma Y, Regar E, Boersma E, Serruys PW, van Geuns RJ (2016) Long-

- term invasive follow-up of the everolimus-eluting bioresorbable vascular scaffold: five-year results of multiple invasive imaging modalities. *EuroIntervention* 11:996–1003
3. Everaert B, Felix C, Koolen J, den Heijer P, Henriques J, Wykrzykowska J, van der Schaaf R, de Smet B, Hofma S, Diletti R, Van Mieghem N, Regar E, Smits P, van Geuns RJ (2015) Appropriate use of bioresorbable vascular scaffolds in percutaneous coronary interventions: a recommendation from experienced users. A position statement on the use of bioresorbable vascular scaffolds in the Netherlands. *Neth Heart J* 23:161–165
 4. Tamburino C, Latib A, van Geuns RJ, Sabate M, Mehilli J, Gori T, Achenbach S, Alvarez MP, Nef H, Lesiak M, Di Mario C, Colombo A, Naber CK, Caramanno G, Capranzano P, Brugaletta S, Geraci S, Araszkiwicz A, Mattesini A, Pyxaras SA, Rzeszutko L, Depukat R, Diletti R, Boone E, Capodanno D, Dudek D (2015) Contemporary practice and technical aspects in coronary intervention with bioresorbable scaffolds: a European perspective. *EuroIntervention* 11:45–52
 5. Cuculi F, Puricel S, Jamshidi P, Valentin J, Kallinikou Z, Toggweiler S, Weissner M, Münzel T, Cook S, Gori T (2015) Optical coherence tomography findings in bioresorbable vascular scaffolds thrombosis. *Circ Cardiovasc Interv* 8(10):e002518. doi:10.1161/CIRCINTERVENTIONS.114.002518 (Epub ahead of print)
 6. Taniwaki M, Radu MD, Zaugg S, Amabile N, Garcia-Garcia HM, Yamaji K, Jørgensen E, Kelbæk H, Pilgrim T, Caussin C, Zanchin T, Veugeois A, Abildgaard U, Jüni P, Cook S, Koskinas KC, Windecker S, Räber L (2016) Mechanisms of very late drug-eluting stent thrombosis assessed by optical coherence tomography. *Circulation*. doi:10.1161/CIRCULATIONAHA.115.019071 (Epub ahead of print)
 7. Souteyrand G, Amabile N, Mangin L, Chabin X, Meneveau N, Cayla G, Vanzetto G, Barnay P, Trouillet C, Rioufol G, Rangé G, Teiger E, Delaunay R, Dubreuil O, Lhermusier T, Mulliez A, Levesque S, Belle L, Caussin C, Motreff P; PESTO Investigators (2016) Mechanisms of stent thrombosis analysed by optical coherence tomography: insights from the national PESTO French registry. *Eur Heart J*. doi:10.1093/eurheartj/ehv711 (Epub ahead of print)
 8. Prati F, Kodama T, Romagnoli E, Gatto L, Di Vito L, Ramazzotti V, Chisari A, Marco V, Cremonesi A, Parodi G, Albertucci M, Alfonso F (2015) Suboptimal stent deployment is associated with subacute stent thrombosis: optical coherence tomography insights from a multicenter matched study. From the CLI Foundation investigators: the CLI-THRO study. *Am Heart J* 169:249–256
 9. Guagliumi G, Sirbu V, Musumeci G, Gerber R, Biondi-Zoccai G, Ikejima H, Ladich E, Lortkipanidze N, Matiashvili A, Valsecchi O, Virmani R, Stone GW (2012) Examination of the in vivo mechanisms of late drug-eluting stent thrombosis: findings from optical coherence tomography and intravascular ultrasound imaging. *J Am Coll Cardiol Interv* 5:12–20
 10. Alfonso F, Dutary J, Paulo M, Gonzalo N, Pérez-Vizcayno MJ, Jiménez-Quevedo P, Escaned J, Bañuelos C, Hernández R, Macaya C (2012) Combined use of optical coherence tomography and intravascular ultrasound imaging in patients undergoing coronary interventions for stent thrombosis. *Heart* 98:1213–1220
 11. Prati F, Regar E, Mintz GS, Arbustini E, Di Mario C, Jang IK, Akasaka T, Costa M, Guagliumi G, Grube E, Ozaki Y, Pinto F, Serruys PW (2010) Expert review document on methodology, terminology, and clinical applications of optical coherence tomography: physical principles, methodology of image acquisition, and clinical application for assessment of coronary arteries and atherosclerosis. *Eur Heart J* 31:401–415
 12. Serruys PW, Onuma Y, Ormiston JA, de Bruyne B, Regar E, Dudek D, Thuesen L, Smits PC, Chevalier B, McClean D, Koolen J, Windecker S, Whitbourn R, Meredith I, Dorange C, Veldhof S, Miquel-Hebert K, Rapoza R, García-García HM (2010) Evaluation of the second generation of a bioresorbable everolimus drug-eluting vascular scaffold for treatment of de novo coronary artery stenosis: six-month clinical and imaging outcomes. *Circulation* 122:2301–2312
 13. Mattesini A, Boeder N, Löblich K, Valente S, Foin N, Caiazza G, Ghione M, Gensini GF, Italo P, Di Mario C, Nef H (2015) TCT-514 Absorb vs DESolve: an optical coherence tomography comparison of acute mechanical performances. *J Am Coll Cardiol* 66(15_S). doi:10.1016/j.jacc.2015.08.531 (Epub ahead of print)
 14. Mattesini A, Secco GG, Dall'Ara G, Ghione M, Rama-Merchan JC, Lupi A, Viceconte N, Lindsay AC, De Silva R, Foin N, Naganuma T, Valente S, Colombo A, Di Mario C (2014) ABSORB biodegradable stents versus second-generation metal stents: a comparison study of 100 complex lesions treated under OCT guidance. *J Am Coll Cardiol Interv* 7:741–750
 15. Kimura T, Morimoto T, Kozuma K, Honda Y, Kume T, Aizawa T, Mitsudo K, Miyazaki S, Yamaguchi T, Hiyoshi E, Nishimura E, Isshiki T, RESTART Investigators (2010) Comparisons of baseline demographics, clinical presentation, and long-term outcome among patients with early, late, and very late stent thrombosis of sirolimus-eluting stents. *Circulation* 122:52–61
 16. van Werkum JW, Heestermaas AA, de Korte FI, Kelder JC, Suttorp MJ, Rensing BJ, Zwart B, Brueren BR, Koolen JJ, Dambrink JH, van't Hof AW, Verheugt FW, ten Berg JM (2009) Long-term clinical outcome after a first angiographically confirmed coronary stent thrombosis: an analysis of 431 cases. *Circulation* 119:828–834
 17. Gutiérrez-Chico JL, Gijzen F, Regar E, Wentzel J, de Bruyne B, Thuesen L, Ormiston J, McClean DR, Windecker S, Chevalier B, Dudek D, Whitbourn R, Brugaletta S, Onuma Y, Serruys PW (2012) Differences in neointimal thickness between the abluminal and the abluminal sides of malapposed and side-branch struts in a polylactide bioresorbable scaffold: evidence in vivo about the abluminal healing process. *J Am Coll Cardiol Interv* 5:428–435
 18. Karanasos A, Van Mieghem N, van Ditzhuijzen N, Felix C, Daemen J, Autar A, Onuma Y, Kurata M, Diletti R, Valgimigli M, Kauer F, van Beusekom H, de Jaegere P, Zijlstra F, van Geuns RJ, Regar E (2015) Angiographic and optical coherence tomography insights into bioresorbable scaffold thrombosis: single-center experience. *Circ Cardiovasc Interv* 8(5). doi:10.1161/CIRCINTERVENTIONS.114.002369
 19. Tearney GJ, Regar E, Akasaka T, Adriaenssens T, Barlis P, Bezerra HG, Bouma B, Bruining N, Cho JM, Chowdhary S, Costa MA, de Silva R, Dijkstra J, Di Mario C, Dudek D, Falk E, Feldman MD, Fitzgerald P, Garcia-Garcia HM, Gonzalo N, Granada JF, Guagliumi G, Holm NR, Honda Y, Ikeno F, Kawasaki M, Kochman J, Koltowski L, Kubo T, Kume T, Kyono H, Lam CC, Lamouche G, Lee DP, Leon MB, Maehara A, Manfrini O, Mintz GS, Mizuno K, Morel MA, Nadkarni S, Okura H, Otake H, Pietrasik A, Prati F, Räber L, Radu MD, Rieber J, Riga M, Rollins A, Rosenberg M, Sirbu V, Serruys PW, Shimada K, Shinke T, Shite J, Siegel E, Sonoda S, Suter M, Takarada S, Tanaka A, Terashima M, Thim T, Uemura S, Ughi GJ, van Beusekom HM, van der Steen AF, van Es GA, van Soest G, Virmani R, Waxman S, Weissman NJ, Weisz G; International Working Group for Intravascular Optical Coherence Tomography (IWG-IVOC) (2012) Consensus standards for acquisition, measurement, and reporting of intravascular optical coherence tomography studies: a report from the International Working Group for Intravascular Optical Coherence Tomography Standardization and Validation. *J Am Coll Cardiol* 59:1058–1072
 20. Uren NG, Schwarzacher SP, Metz JA, Lee DP, Honda Y, Yeung AC, Fitzgerald PJ, Yock PG, POST Registry Investigators (2002)

- Predictors and outcomes of stent thrombosis: an intravascular ultrasound registry. *Eur Heart J* 23:124–132
- 21 Gomez-Lara J, Diletti R, Brugaletta S, Onuma Y, Farooq V, Thuesen L, McClean D, Koolen J, Ormiston JA, Windecker S, Whitbourn R, Dudek D, Dorange C, Veldhof S, Rapoza R, Regar E, Garcia-Garcia HM, Serruys PW (2012) Angiographic maximal luminal diameter and appropriate deployment of the everolimus-eluting bioresorbable vascular scaffold as assessed by optical coherence tomography: an ABSORB cohort B trial sub-study. *EuroIntervention* 8:214–224
- 22 Sonoda S, Morino Y, Ako J, Terashima M, Hassan AH, Bonneau HN, Leon MB, Moses JW, Yock PG, Honda Y, Kuntz RE, Fitzgerald PJ, SIRIUS Investigators (2004) Impact of final stent dimensions on long-term results following sirolimus-eluting stent implantation: serial intravascular ultrasound analysis from the sirius trial. *J Am Coll Cardiol* 43:1959–1963
- 23 Costa MA, Angiolillo DJ, Tannenbaum M, Driesman M, Chu A, Patterson J, Kuehl W, Battaglia J, Dabbons S, Shamoon F, Flieshman B, Niederman A, Bass TA, STLLR Investigators (2008) Impact of stent deployment procedural factors on long-term effectiveness and safety of sirolimus-eluting stents (final results of the multicenter prospective STLLR trial). *Am J Cardiol* 101:1704–1711
- 24 Doi H, Maehara A, Mintz GS, Yu A, Wang H, Mandinov L, Popma JJ, Ellis SG, Grube E, Dawkins KD, Weissman NJ, Turco MA, Ormiston JA, Stone GW (2009) Impact of post-intervention minimal stent area on 9-month follow-up patency of paclitaxel-eluting stents: an integrated intravascular ultrasound analysis from the TAXUS IV, V, and VI and TAXUS ATLAS Workhorse, Long Lesion, and Direct Stent Trials. *J Am Coll Cardiol Interv* 2:1269–1275
- 25 De Ribamar Costa Jr J, Abizaid A, Bartorelli AL, Whitbourn R, van Geuns RJ, Chevalier B, Perin M, Seth A, Botelho R, Serruys PW; ABSORB EXTEND Investigators (2015) Impact of post-dilation on the acute and one-year clinical outcomes of a large cohort of patients treated solely with the Absorb bioresorbable vascular scaffold. *EuroIntervention* 11:141–148
- 26 Ormiston JA, Webber B, Ubod B, Darremont O, Webster MW (2015) An independent bench comparison of two bioresorbable drug-eluting coronary scaffolds (Absorb and DESolve) with a durable metallic drug-eluting stent (ML8/Xpedition). *EuroIntervention* 11(1):60–67
- 27 Suwannasom P, Sotomi Y, Ishibashi Y, Cavalcante R, Albuquerque FN, Macaya C, Ormiston JA, Hill J, Lang IM, Egred M, Fajadet J, Lesiak M, Tijssen JG, Wykrzykowska JJ, de Winter RJ, Chevalier B, Serruys PW, Onuma Y (2016) The impact of post-procedural asymmetry, expansion, and eccentricity of bioresorbable everolimus-eluting scaffold and metallic everolimus-eluting stent on clinical outcomes in the ABSORB II Trial. *J Am Coll Cardiol Interv* 9(12):1231–1242
- 28 Rivero F, Bastante T, Cuesta J, Benedicto A, Restrepo JA, Alfonso F (2015) Treatment of in-stent restenosis with bioresorbable vascular scaffolds: optical coherence tomography insights. *Can J Cardiol* 31(3):255–259

Anlage 5

Overlapping implantation of bioresorbable novolimus-eluting scaffolds: an observational optical coherence tomography study

Florian Blachutzik¹  · Niklas Boeder² · Jens Wiebe³ · Alessio Mattesini⁴ · Oliver Dörr² · Astrid Most² · Timm Bauer² · Monique Tröbs¹ · Jens Röther¹ · Christian Schlundt¹ · Stephan Achenbach¹ · Christian Hamm² · Holger Nef²

Received: 7 August 2016 / Accepted: 9 December 2016 / Published online: 21 December 2016
© Springer Japan 2016

Abstract Overlapping implantation of bioresorbable vascular scaffolds is frequently necessary, but its influence on vessel and scaffold structure has not been thoroughly analyzed previously. The aim of this study was to analyze the acute effects of overlapping implantation on BRS as determined by optical coherence tomography (OCT). A total of 38 patients with de novo coronary artery stenoses who underwent OCT in the context of implantation of novolimus-eluting BRS (DESolve, Elixir Medical Corporation, Sunnyvale, California, USA) were investigated. In 15 patients, overlapping implantation of two BRS was performed, while 23 patients with implantation of one single BRS served as the control group. OCT data were retrospectively analyzed regarding acute scaffold implantation results. There were no significant differences between the overlap and control group in terms of residual in-scaffold area stenosis, scaffold area, mean or minimal lumen area, eccentricity index, incomplete scaffold apposition area or malapposition. While strut fracture was slightly more frequent in BRS with overlap its incidence was low overall. In patients with overlapping BRS, overlap segments did not display smaller lumen areas than segments without overlap

(mean lumen area overlap: $8.16 \pm 2.97 \text{ mm}^2$ vs. no overlap: $7.70 \pm 2.55 \text{ mm}^2$; $p = 0.71$; minimal lumen area overlap: $6.83 \pm 2.71 \text{ mm}^2$ vs. no overlap: $6.17 \pm 2.58 \text{ mm}^2$; $p = 0.37$). Acute mechanical performance of novolimus-eluting BRS is not impaired by overlapping implantation. It can be assumed that vessel expansion compensates for the double scaffold layer in the overlap area resulting in a similar lumen area in overlap areas and in those with a single strut layer.

Keywords Percutaneous coronary intervention · Optical coherence tomography · Bioresorbable Scaffold

Introduction

While overlapping implantation of coronary stents was usually avoided for bare metal stents (BMS), given a higher frequency of target vessel revascularization and impaired clinical outcome [1], stent overlap has been used more liberally with drug eluting stents (DES). Overlapping implantation of first-generation DES remained associated with impaired angiographic and clinical outcome [2, 3], but data for second-generation DES revealed that overlapping implantation of these devices is safe without increased rates of target vessel revascularization or impaired clinical outcome [2, 4]. Bioresorbable vascular scaffolds (BRS) are a novel approach for treatment of coronary artery stenoses. They promise to overcome some limitations of DES, mainly because of their biodegradation within a period of 2–4 years. Several studies have reported non-inferiority as compared to DES [5–9], with the potential exception of very small vessels [10]. All the same, research regarding optimal use of BRS is still under progress. Notably, all randomized trials published to date have excluded the

F. Blachutzik and N. Boeder contributed equally.

✉ Florian Blachutzik
florian.blachutzik@uk-erlangen.de

¹ Friedrich-Alexander Universität Erlangen-Nürnberg (FAU), Department of Medicine 2-Cardiology, University Hospital Erlangen, Ulmenweg 18, 91054 Erlangen, Germany

² Justus Liebig Universität Giessen, University Hospital Giessen, Medical Clinic I, Giessen, Germany

³ German Heart Centre Munich, Munich, Germany

⁴ Careggi Hospital, Florence, Italy

implantation of overlapping BRS. Hence, only limited data exist regarding the performance and outcome of BRS in long lesions with overlapping device implantation. We analyzed the acute mechanical effects of overlapping BRS implantation as well as the differences between overlap areas and areas with a single BRS layer by optical coherence tomography (OCT) *in vivo*.

Materials and methods

Study design and population

Between July 2014 and August 2015, 46 patients were treated using novolimus-eluting BRS at the University Hospital of Giessen. Post-procedural OCT was pre-specified to be performed in case of a difficult implantation process due to lesion calcification, fibrosis or tortuosity in 40 patients. Two of these 40 patients displayed inadequate OCT image quality as assessed by two independent experienced interventional cardiologists. Out of the remaining 38 patients, 15 patients received two overlapping novolimus-eluting BRS and formed the study group, while 23 patients received one single novolimus-eluting BRS and constitute the control group. Overlapping BRS implantation was performed if one BRS was insufficient to cover the entire lesion length. A priori exclusion criteria for BRS implantation included severe lesion calcification, ostial involvement, lesion location in the left main coronary artery, and a reference vessel diameter exceeding 4.0 mm. OCT was not performed in case of hemodynamic instability, known contrast agent allergy or renal impairment (creatinine > 1.5 mg/dl).

Baseline characteristics of the patients including medical history, clinical, angiographic and procedural data were prospectively collected in a standardized form. Our aim was to analyze whether overlapping of novolimus-eluting BRS is associated with acute mechanical alterations in BRS structure that are different from those implanted without overlap and whether the overlap of two BRS layers results in a significantly smaller vessel lumen area compared to lesion segments without BRS overlap. The study complied with the Declaration of Helsinki. The Ethics Committee of the Justus-Liebig-University Hospital (Giessen, Germany) approved the study protocol (Reference number 203/14). Written informed consent for evaluation of clinical, procedural and OCT data was obtained from each patient before inclusion.

Percutaneous coronary intervention

Percutaneous coronary intervention (PCI) was performed via a radial or femoral approach, using 6 French guiding catheters and standard coronary guidewires (Runthrough™,

Terumo Europe NV, Leuven, Belgium). All patients received intravenous heparin and intracoronary nitrates. Pre-dilatation with an appropriately sized NC (non-compliant) balloon was performed in all lesions applying a maximal implantation pressure of 20 bar. While lesions in the control group were treated with one single novolimus-eluting BRS (DESolve™ or DESolve XL™, Elixir Medical Corporation, Sunnyvale, California, USA), lesions in the 15 patients with overlap were treated by sequential implantation of two novolimus-eluting BRS using the “marker-to-marker” method. Novolimus-eluting BRS were available with a length of 14, 18 or 28 mm and a diameter of 2.5, 3.0, 3.5 or 4.0 mm. BRS were deployed with slow balloon implantation (2 bar each 5 s keeping the delivery balloon inflated at least 30 s, if possible). Post-dilatation with an appropriately sized NC balloon (NC Trek™, Abbott Vascular, Santa Clara, California, USA) was mandatory (mean pressure: 17 ± 5 bar; mean diameter: 3.5 ± 0.6 mm). Further medication, technique and equipment for percutaneous coronary intervention were according to clinical requirements and at the discretion of the operator.

Optical coherence tomography image acquisition

After completion of the implantation procedure (including post-dilatation), OCT was performed using a 2.7 F Dragonfly™ intravascular imaging catheter (St. Jude Medical, Saint Paul, MN, USA) at a mechanical pullback speed of 18 mm/s over a distance of 54 or 36 mm/s over 75 mm. Contrast agent (20 ml, Ultravist™ 370, Bayer AG, Leverkusen, Germany) was injected through the guiding catheter at 4 ml/s with a maximum pressure of 600 psi using machine injection (ACIST CVi™, ACIST Medical Systems, Eden Prairie, MN, USA). The OCT catheter was positioned distally to the treated segment before starting the pullback. Additional OCT runs were performed in eight cases because the treated segment was not completely captured by one single pullback.

Optical coherence tomography image analysis

Offline OCT image analysis was performed using the LightLab Imaging workstation (St. Jude Medical, Saint Paul, MN, US) with manual calibration before each measurement. All images were recorded digitally, stored and analyzed by two experienced investigators blinded to clinical and procedural data. OCT cross sections were analyzed starting 5 mm distal to the BRS and ending 5 mm proximal to the BRS with a spacing of 1 mm between consecutive images. Struts were defined as malapposed if the distance between the outer strut edge and vessel wall was larger than 170 μm [equal to the sum of strut and polymer thickness (150 μm) plus the minimal axial resolution of OCT

(20 μm]). Proximal and distal lumen reference areas were defined as maximum area with a three-layered vessel wall visible at more than 180° of circumference within 5 mm proximal and distal to the BRS. In case of absence of any appropriate proximal or distal lumen reference because of ostial location or a large side branch, only one reference was used.

The following parameters were manually traced and measured for each OCT cross section:

- Lumen area (mm^2): contoured by following the area filled with contrast media (Fig. 1: green mark)
- Scaffold area (mm^2): measured at the outer strut edge of each scaffold (Fig. 1: white mark).
- Maximum/minimum/mean scaffold diameter (mm).
- Number of struts.
- Number of malapposed struts (Fig. 2).
- Maximum malapposition distance (mm): maximum orthogonal distance between outer BRS strut and vessel wall (Fig. 3).
- Incomplete scaffold apposition area (mm^2): area between outer edge of BRS struts and vessel wall (Fig. 4: white mark).
- Tissue prolapse area (mm^2): presence of tissue protruding between struts into the lumen as a circular arc connecting adjacent struts [11].
- Overlapping (Yes/No): struts of more than one BRS visible in one cross section (Fig. 1).
- Strut fracture (Yes/No): isolated struts in the vessel lumen or visible discontinuity of a strut edge (Fig. 5).
- Maximum distance inner strut edge to vessel wall for overlapping BRS.

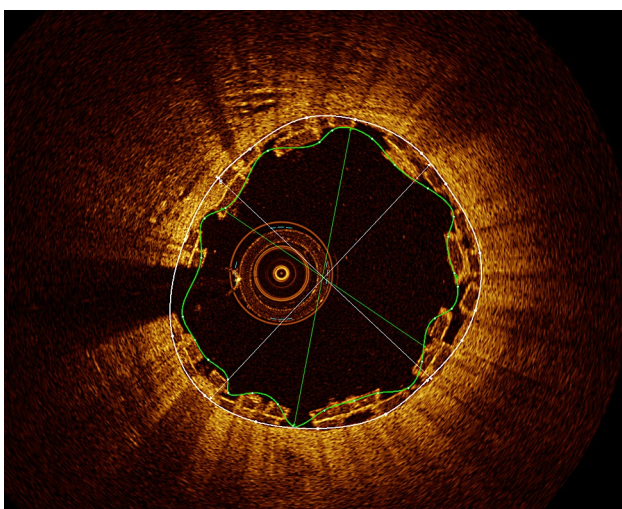


Fig. 1 Overlapping BRS OCT cross section showing two overlapping DESolve BRS. Lumen area (*green mark*) and scaffold area of the outer BRS (*white mark*) are contoured (color figure online)

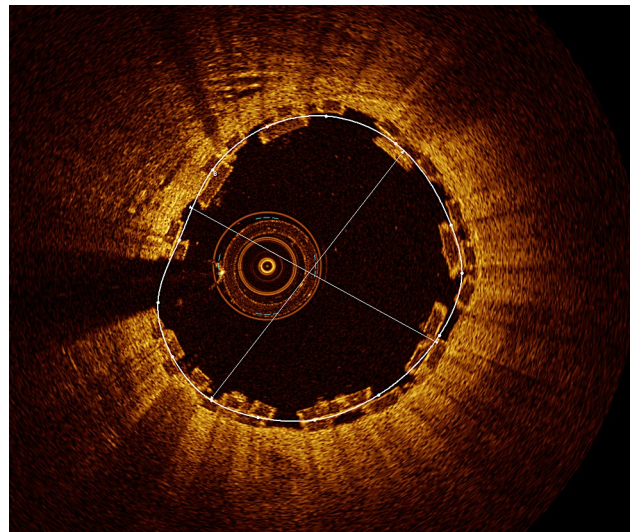


Fig. 2 BRS malapposition. OCT cross section showing six malapposed BRS struts

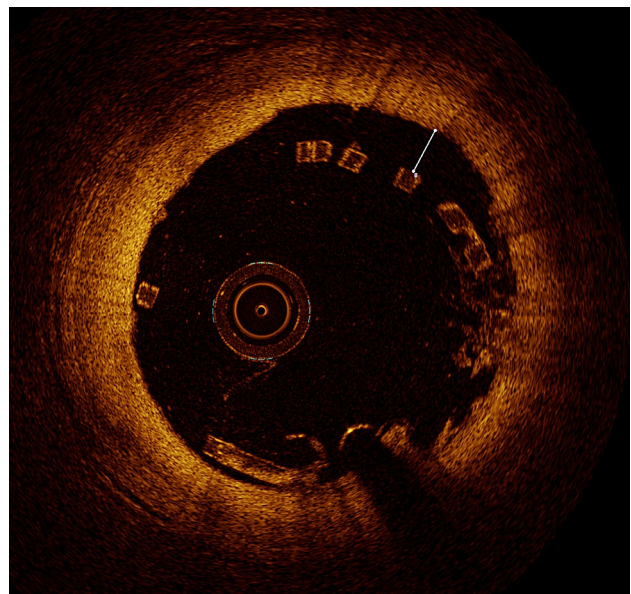


Fig. 3 Distance of malapposition. This figure shows a malapposed DESolve BRS with six malapposed struts. The malapposition distance is marked as maximum orthogonal distance between outer BRS strut and vessel wall (*white mark*)

- Proximal edge dissection (Yes/No): visible flap within 5 mm proximal of BRS.
- Distal edge dissection (Yes/No): visible flap within 5 mm distal of BRS.
- Bifurcation (Yes/No).

The following parameters were calculated (adopted from [12, 13]):

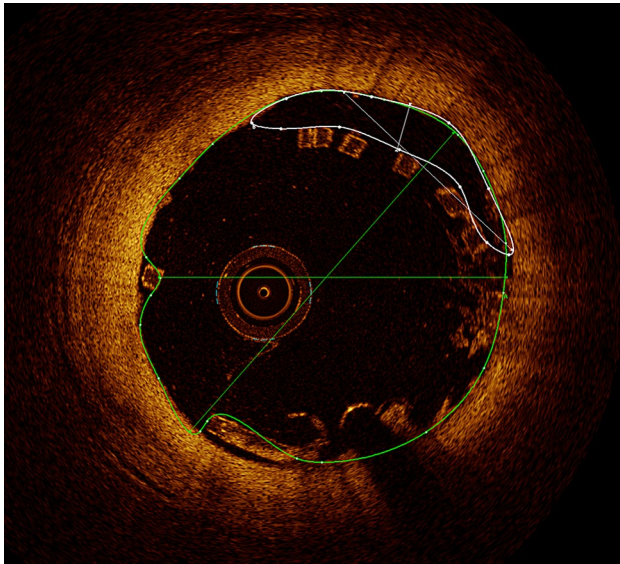


Fig. 4 Incomplete scaffold apposition area. Malapposed DESolve BRS with contoured lumen profile (green mark) and incomplete scaffold apposition area (green mark) (color figure online)

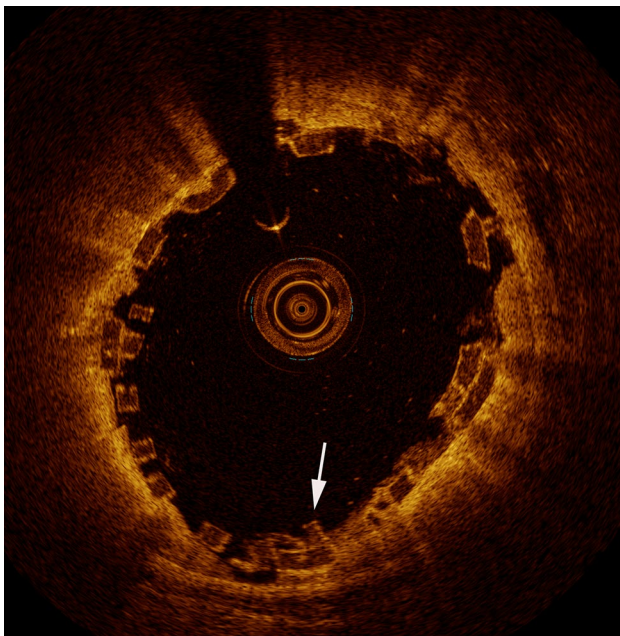


Fig. 5 Strut fracture. A strut fractures located in an overlap segment of two DESolve BRS is visible (white arrow). On the left side of the broken strut, no coating polymer is visible

- Increment = (proximal lumen reference area – distal lumen reference area)/length (mm).
- Reference area (mm²) = distal lumen reference area + (x × Increment) x = distance between distal end of BRS and actual cross section in mm.

- In-scaffold residual area stenosis (%) = 100 – (Lumen area/Reference area) × 100 calculated for each cross section.
- Incomplete strut apposition (ISA) (%) = (number of malapposed struts per cross section/total number of visible struts per cross section) × 100.
- Eccentricity index = (minimum scaffold diameter/maximum scaffold diameter); calculated for each cross section analyzed.
- Mean lumen area.
- Minimal lumen area.

Follow-up

Clinical follow-up was obtained at 1, 6 and 12 months using a standardized protocol by direct clinical examination or by phone.

Statistical analysis

Continuous variables were summarized as mean ± standard deviation; categorical variables are quoted as *n* (%). Test for binomial distribution was used to measure deviations of expected frequencies. Kolmogorov–Smirnov test was performed to test for parametric distribution. To test for statistical differences between two groups for comparison of continuous variables either *t* test for unpaired samples (parametric distribution) or Mann–Whitney *U* test (non-parametric distribution) was performed. For categorical variables, Chi-square or Fischer exact tests were carried out to test for significant differences. Statistical analysis was performed using SPSS version 21.0 (IBM SPSS Statistics, IBM Corporation, Armonk, New York, USA) and a two-sided *p* < 0.05 was considered significant.

Results

Patients and procedure

A total of 38 patients (26 male, 12 female) were included. 23 patients received one novolimus-eluting BRS for treating a single native lesion, 15 patients with 17 native lesions were treated with two overlapping novolimus-eluting BRS. In two cases, overlapping implantation was performed to cover two sequential lesions. In four cases, proximal BRS diameter was 0.5 mm larger than the diameter of the distal scaffold. Except for lesion length, which was significantly larger in the overlap group (16.8 ± 5.9 vs. 10.8 ± 5.2 mm; *p* < 0.001), no significant differences regarding baseline characteristics existed between the groups. Most patients presented with stable angina (no overlap: 52%, overlap: 60%). Pre-procedural OCT was performed in 27 patients

[control group: 15 patients (65%) vs. overlap group: 12 patients (80%); $p = 0.46$], additional intra-procedural OCT was performed in 9 patients [control group: 5 patients (22%) vs. overlap group: 4 patients (27%); $p = 0.46$]. Pre-dilatation was conducted in all cases and the length of the NC balloon applied was significantly larger in the overlap group as compared to the control group (14 ± 3 mm vs. 16 ± 3 mm; $p = 0.007$). A cutting balloon was used for lesion preparation in three cases [control group: 2 patients (9%) vs. overlap group: 1 patient (7%); $p = 0.93$]. NC balloon post-dilatation was performed in all cases, mean pressure was 17 bar. Mean BRS diameter was significantly smaller than the diameter of the NC balloon for post-dilatation (3.2 ± 0.3 vs. 3.6 ± 0.6 mm; $p < 0.001$). For detailed information regarding baseline characteristics and procedural data see Table 1.

OCT findings

Total BRS length was significantly longer in the overlap group as compared to the control group (36 ± 6 vs. 20 ± 6 mm; $p < 0.001$) and the mean overlap length determined by OCT was 3.8 ± 2.9 mm. Mean lumen area (overlap group: 7.70 ± 2.55 mm² vs. control group: 7.36 ± 2.16 mm²; $p = 0.79$) and mean residual in-scaffold area stenosis (overlap group: $10.0 \pm 6.8\%$ vs. control group: $11.5 \pm 10.1\%$; $p = 0.70$) were not different between lesions treated with and without overlapping BRS. Furthermore, there were no significant differences in terms of minimal lumen area, incomplete scaffold apposition area (ISAA), ISA, tissue prolapse area, sum of malapposed struts and stent diameters. There was a trend towards higher eccentricity in the control group compared to the overlap group (0.77 ± 0.07 vs. 0.81 ± 0.03 ; $p = 0.07$). The frequency of strut fractures (mean number of visible strut fractures per cross section along the entire scaffold length) was higher in cases of overlapping implantation, even though the difference failed to reach statistical significance (overlap group: 0.36 ± 0.49 vs. control group: 0.02 ± 0.08 ; $p = 0.09$) (for detailed results see Table 2).

OCT findings within novolimus-eluting BRS implanted with overlap

Mean and minimal lumen area was not smaller in the overlapping segment as compared to the BRS segments without overlap (mean lumen area overlap: 8.16 ± 2.97 mm² vs. no overlap: 7.70 ± 2.55 mm²; $p = 0.71$; minimal lumen area overlap: 6.83 ± 2.71 mm² vs. no overlap: 6.17 ± 2.58 mm²; $p = 0.37$). Due to the double stent layer, the maximum distance between the inner strut edge to the vessel wall was significantly higher in the overlap area compared to the BRS area with single layer (349 ± 27 vs.

182 ± 21 μm; $p < 0.001$; see Table 3) Additionally, there were no significant differences between the overlap and the adjacent scaffold area (3 mm proximal and distal to the overlap area; see Table 4).

Clinical follow-up

Median follow-up time was 9 months. One patient (3%) out of the overlap group was lost to follow-up. One rehospitalization in the overlap group was observed. The patient presented with atypical thoracic complaints. Coronary angiography revealed no progress of coronary artery disease. No events were observed in the control group.

Discussion

The main finding of this study is that overlapping implantation of novolimus-eluting BRS does not result in a reduced luminal area. Much rather the double strut layer seems to be compensated for by outward overexpansion of the vessel. Hence, we were able to confirm in atherosclerotic coronary artery lesions what Farooq et al. [14] observed after implantation of overlapping everolimus-eluting BRS in porcine coronary arteries. The “overexpansion” capabilities of the DESolve novolimus-eluting BRS [15] may be advantageous in this context. In fact, a double strut layer may increase radial force and may to some extent prevent recoil. At the same time, neither was disintegration of the BRS observed significantly more frequently, nor was vessel wall injury (dissection) observed more often in lesions treated with overlapping BRS. However, it has to be kept in mind that overlap areas in most cases will be located outside the most severely obstructed and calcified parts of a lesion by intention of the operator.

Clinical implications

Although clinical safety and efficacy of everolimus-eluting BRS have been reported to be comparable with those of second-generation DES [6, 13], a non-negligible rate of BRS thrombosis occurs and several authors have hypothesized that BRS overlap may contribute to a higher risk of scaffold thrombosis, especially because of large lumen loss due to the double layer of BRS struts [16–18]. Accordingly, trying to minimize BRS overlap length is widely recommended and standard in clinical practice [14, 19, 20].

On the one hand, data from Ishibashi et al. suggest that overlapping implantation of BRS is an independent risk factor for peri-procedural myocardial infarction [21]. On the other hand, Ortega-Paz et al. recently reported in a retrospective analysis that there were no significant differences in 1-year clinical outcome if comparing overlap

Table 1 Baseline characteristics

	BRS without overlap	BRS with overlap	<i>p</i> value
Number of patients	23	15	0.26
Number of scaffolds	23	30	0.41
Number of treated lesions	23	15	0.26
Age (years)	62 ± 9	62 ± 10	0.86
Male gender	19 (83%)	7 (47%)	0.14
BMI [†] (kg/m ²)	25.6 ± 10.8	28.0 ± 3.8	0.84
Previous MI [#] (%)	5 (22%)	6 (40%)	0.36
Previous PCI ^{††} (%)	7 (30%)	8 (53%)	0.25
Previous CABG [§] (%)	2 (9%)	1 (7)	0.93
LVEF [¶] (%)	57 ± 10	55 ± 11	0.62
Presentation			
STEMI	5 (22%)	2 (13%)	0.63
NSTEMI	3 (13%)	1 (7%)	
Unstable AP*	2 (9%)	3 (20%)	
Stable AP*	12 (52%)	9 (60%)	
No complaints/atypical complaints	1 (4%)	0 (0%)	
Vessel			
LAD [‡]	12 (52%)	3 (20%)	0.09
Cx [‡]	4 (17%)	4 (27%)	
RCA ^{‡‡}	7 (31%)	8 (53%)	
Lesion length (mm)	10.8 ± 5.2	16.8 ± 5.9	<0.001
NC** pre-dilatation			
Performed (%)	100	100	>0.99
Cutting balloon (%)	2 (9%)	1 (7%)	0.93
Pressure (bar)	14 ± 4	15 ± 4	0.59
Diameter (mm)	3.1 ± 0.4	2.9 ± 0.4	0.36
Length (mm)	14 ± 3	16 ± 3	0.007
Scaffold			
Diameter (mm)	3.2 ± 0.3	3.2 ± 0.3	0.43
Length (mm)	20 ± 6	20 ± 6	0.94
Implantation pressure (bar)	14 ± 3	13 ± 2	0.17
NC** post-dilatation			
Performed (%)	100	100	>0.99
Diameter (mm)	3.7 ± 0.6	3.4 ± 0.5	0.12
Pressure (bar)	17 ± 4	17 ± 6	0.22

Values are mean ± standard deviation or *n* (%)

* Angina pectoris

† Body mass index

‡ Circumflex artery

§ Coronary artery bypass graft surgery

‡ Left anterior descending artery

¶ Left ventricular ejection fraction

Myocardial infarction

** Non-compliant balloon

†† Percutaneous coronary intervention

‡‡ Right coronary artery

and non-overlap everolimus-eluting BRS [22]. In fact, we found no mechanical or geometric differences in novolimus-eluting BRS overlap areas that might be responsible

for a higher event rate. Especially, there were no significant differences regarding lumen area, stent diameter, residual area stenosis, eccentricity, malapposition and rate of strut

Table 2 OCT findings

	BRS without overlap (<i>n</i> = 23)	BRS with overlap (<i>n</i> = 15)	<i>p</i> value
Total BRS length (mm)	20 ± 6	36 ± 6	<0.001
Overlap length (mm)		3.8 ± 2.9	
OCT scaffold area (mm ²)	7.57 ± 2.18	7.90 ± 2.41	0.72
Residual area stenosis (%)	11.5 ± 10.1	10.0 ± 6.8	0.70
Reference area (mm ²)	7.95 ± 2.79	8.02 ± 2.49	0.88
Mean lumen area (mm ²)	7.36 ± 2.16	7.70 ± 2.55	0.79
Minimal lumen area (mm ²)	5.77 ± 1.72	6.41 ± 2.63	0.71
OCT ISAA [†] (mm ²)	0.83 ± 1.85	1.62 ± 3.25	0.72
OCT tissue prolapse area (mm ²)	7.74 ± 9.53	7.41 ± 8.68	0.95
Sum of malapposed struts (<i>n</i>)	5 ± 11	7 ± 13	0.72
Sum of struts (<i>n</i>)	246 ± 77	234 ± 85	0.72
ISA* (%)	0.03 ± 0.08	0.04 ± 0.07	0.79
Distance of malapposition [‡] (mm)	0.18 ± 0.20	0.27 ± 0.32	0.58
Mean stent diameter (mm)	3.06 ± 0.42	3.03 ± 0.37	0.70
Minimum stent diameter (mm)	2.68 ± 0.38	2.71 ± 0.31	0.29
Maximum stent diameter (mm)	3.50 ± 0.51	3.38 ± 0.44	0.88
Minimum eccentricity index	0.61 ± 0.11	0.66 ± 0.06	0.08
Overlapping	0	3.33 ± 2.23	<0.001
Fracture	0.02 ± 0.08	0.36 ± 0.49	0.09
Bifurcation	0.96 ± 10.95	0.42 ± 0.67	0.20
Mean eccentricity index	0.77 ± 0.07	0.81 ± 0.03	0.07
Proximal edge dissection	0	0	>0.99
Distal edge dissection	0	1	0.87

Values are mean ± standard deviation

* Incomplete strut apposition (ratio number of malapposed struts per BRS to total number of struts per BRS)

[†] Incomplete scaffold apposition area

[‡] Orthogonal distance between malapposed scaffold and vessel wall

Table 3 OCT findings inside BRS with overlap

	Area without overlap	Overlap area	<i>p</i> value
Minimal lumen area (mm ²)	6.17 ± 2.58	6.83 ± 2.71	0.37
Location of minimal lumen area	11 (73%)	4 (27%)	0.12
Fracture	0.28 ± 0.44	0.40 ± 0.31	0.33
Maximum distance inner strut edge to vessel wall (μm)	182 ± 21	349 ± 27	<0.001
Residual area stenosis (%)	10.56 ± 6.63	9.31 ± 5.28	0.60
Mean lumen area (mm ²)	7.70 ± 2.55	8.16 ± 2.97	0.71

Values are mean ± standard deviation or *n* (%)

Table 4 OCT findings: comparison of overlap and adjacent area (3 mm on each side)

	Adjacent area	Overlap area	<i>p</i> value
Minimal lumen area (mm ²)	6.62 ± 2.44	6.83 ± 2.71	0.54
Fracture	0.48 ± 0.38	0.40 ± 0.31	0.58
Residual area stenosis (%)	10.26 ± 5.81	9.31 ± 5.28	0.67
Mean lumen area (mm ²)	7.68 ± 3.11	8.16 ± 2.97	0.47

Values are mean ± standard deviation or *n* (%)

fractures when comparing BRS implanted with overlap to those without. Nevertheless, due to the longer distance between the vessel wall and the inner struts in overlap areas, endothelialization of these struts will hardly be sufficient leading to an increased risk for an impaired clinical outcome [14, 22]. One aspect we could not analyze in our study was the presence of turbulent flow or shear stress which may be increased in areas with particularly inhomogeneous surface patterns caused by thick BRS struts [23, 24]. Especially the double scaffold layer in overlap

segments can possibly interrupt laminar flow. This might be an explanation for the higher frequency of scaffold thrombosis if overlapping implantation of BRS is performed [21].

Our results suggest that overlapping implantation of BRS can be safely performed in terms of acute mechanical outcome. Nevertheless, reliable data regarding long-term clinical outcome after overlapping implantation of BRS are very limited so far. Hence, randomized controlled studies on long-term clinical outcome are required to analyze the effect of overlap implantation of BRS. Additionally, we have to mention that results for everolimus-eluting BRS are not completely adaptable to novolimus-eluting BRS since mechanical specifications are somewhat different. It has to be kept in mind that effects of overlap might be influenced by overlap length. However, the number of analyzed cases for this study was too low to perform a reliable sub-analysis for effect of different overlap lengths.

Limitations

This was a single-center, non-randomized retrospective observational analysis with all its limitations. Clearly there may be bias in lesion selection. However, OCT was preferentially used in complex lesions so that even more benign effects of overlapping BRS implantation should be expected in less complex lesion subsets. It has to be emphasized that BRS implantation was performed carefully, with thorough lesion preparation and mandatory post-dilatation using appropriately sized NC balloons, so that results may not be comparable when less standardized implantation protocols are used. Finally, patient numbers were small, and the lack of observed differences may be attributable to a lack of statistical power. Especially the systematic evaluation of clinical outcome would require substantially larger patient numbers.

Conclusion

Acute mechanical performance of novolimus-eluting BRS is not impaired by overlapping implantation. In particular, overlapping BRS segments do not display a smaller lumen area as compared to segments with a single layer. This would suggest that overlap implantation can be safely performed, but long-term clinical outcome remains to be investigated in future trials.

Compliance with ethical standards

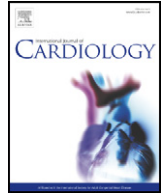
Conflict of interest Holger Nef received speaking honoraria and a research grant (to institution) from Elixir Medical. All other authors have no potential conflict of interest. There are no relationships with industry regarding this study.

References

1. Kereiakes DJ, Wang H, Popma JJ, Kuntz RE, Donohoe DJ, Schofer J, Schampaert E, Meier B, Leon MB, Moses JW (2006) Periprocedural and late consequences of overlapping Cypher sirolimus-eluting stents: pooled analysis of five clinical trials. *J Am Coll Cardiol* 48:21–31
2. O'Sullivan CJ, Stefanini GG, Räber L, Heg D, Taniwaki M, Kalesan B, Pilgrim T, Zanchin T, Moschovitis A, Büllsfeld L, Khattab AA, Meier B, Wenaweser P, Jüni P, Windecker S (2014) Impact of stent overlap on long-term clinical outcomes in patients treated with newer-generation drug-eluting stents. *Euro-Intervention* 9:1076–1084
3. Räber L, Jüni P, Löffel L, Wandel S, Cook S, Wenaweser P, Togni M, Vogel R, Seiler C, Eberli F, Lüscher T, Meier B, Windecker S (2010) Impact of stent overlap on angiographic and long-term clinical outcome in patients undergoing drug-eluting stent implantation. *J Am Coll Cardiol* 55:1178–1188
4. Farooq V, Vranckx P, Mauri L, Cutlip DE, Belardi J, Silber S, Widimsky P, Leon M, Windecker S, Meredith I, Negoita M, van Leeuwen F, Neumann FJ, Yeung AC, Garcia-Garcia HM, Serruys PW (2013) Impact of overlapping newer generation drug-eluting stents on clinical and angiographic outcomes: pooled analysis of five trials from the international Global RESOLUTE Program. *Heart* 99:626–633
5. Kimura T, Kozuma K, Tanabe K, Nakamura S, Yamane M, Muramatsu T, Saito S, Yajima J, Hagiwara N, Mitsudo K, Popma JJ, Serruys PW, Onuma Y, Ying S, Cao S, Staehr P, Cheong WF, Kusano H, Stone GW, Japan Investigators ABSORB (2015) A randomized trial evaluating everolimus-eluting Absorb bioresorbable scaffolds vs. everolimus-eluting metallic stents in patients with coronary artery disease: ABSORB Japan. *Eur Heart J* 36:3332–3342
6. Serruys PW, Chevalier B, Dudek D, Cequier A, Carrié D, Iniguez A, Dominici M, van der Schaaf RJ, Haude M, Wasungu L, Veldhof S, Peng L, Staehr P, Grundeken MJ, Ishibashi Y, Garcia-Garcia HM, Onuma Y (2015) A bioresorbable everolimus-eluting scaffold versus a metallic everolimus-eluting stent for ischaemic heart disease caused by de-novo native coronary artery lesions (ABSORB II): an interim 1-year analysis of clinical and procedural secondary outcomes from a randomised controlled trial. *Lancet* 385:43–54
7. Sabaté M, Windecker S, Iniguez A, Okkels-Jensen L, Cequier A, Brugaletta S, Hofma SH, Räber L, Christiansen EH, Suttorp M, Pilgrim T, Anne van Es G, Sotomi Y, Garcia-Garcia HM, Onuma Y, Serruys PW (2016) Everolimus-eluting bioresorbable stent vs. durable polymer everolimus-eluting metallic stent in patients with ST-segment elevation myocardial infarction: results of the randomized ABSORB ST-segment elevation myocardial infarction-TROFI II trial. *Eur Heart J* 37:229–240
8. Dörr O, Liebetrau C, Wiebe J, Hecker F, Rixe J, Möllmann H, Hamm C, Nef H (2015) Bioresorbable scaffolds for the treatment of in-stent restenosis. *Heart Vessels* 30:265–269
9. Toušek P, Kočka V, Malý M, Lisa L, Buděšínský T, Widimský P (2016) Neointimal coverage and late apposition of everolimus-eluting bioresorbable scaffolds implanted in the acute phase of myocardial infarction: OCT data from the PRAGUE-19 study. *Heart Vessels* 31:841–845
10. Ishibashi Y, Nakatani S, Sotomi Y, Suwannasom P, Grundeken MJ, Garcia-Garcia HM, Bartorelli AL, Whitbourn R, Chevalier B, Abizaid A, Ormiston JA, Rapoza RJ, Veldhof S, Onuma Y, Serruys PW (2015) Relation between bioresorbable scaffold sizing using QCA-Dmax and clinical outcomes at 1 year in 1,232 patients from 3 study cohorts (ABSORB Cohort B,

- ABSORB EXTEND, and ABSORB II). *JACC Cardiovasc Interv* 8:1715–1726
11. Serruys PW, Onuma Y, Ormiston JA, de Bruyne B, Regar E, Dudek D, Thuesen L, Smits PC, Chevalier B, McClean D, Koolen J, Windecker S, Whitbourn R, Meredith I, Dorange C, Veldhof S, Miquel-Hebert K, Rapoza R, García-García HM (2010) Evaluation of the second generation of a bioresorbable everolimus drug-eluting vascular scaffold for treatment of de novo coronary artery stenosis: six-month clinical and imaging outcomes. *Circulation* 122:2301–2312
 12. Mattesini A, Boeder N, Löblich K, Valente S, Foin N, Caiazzo G, Ghione M, Gensini GF, Italo P, Di Mario C, Nef H (2016) Absorb Vs DESolve: an optical coherence tomography comparison of acute mechanical performances. *EuroIntervention* 12:566–573
 13. Mattesini A, Secco GG, Dall’Ara G, Ghione M, Rama-Merchan JC, Lupi A, Viceconte N, Lindsay AC, De Silva R, Foin N, Naganuma T, Valente S, Colombo A, Di Mario C (2014) ABSORB biodegradable stents versus second-generation metal stents: a comparison study of 100 complex lesions treated under OCT guidance. *JACC Cardiovasc Interv* 7:741–750
 14. Farooq V, Serruys PW, Heo JH, Gogas BD, Onuma Y, Perkins LE, Diletti R, Radu MD, Räber L, Bourantas CV, Zhang Y, van Remortel E, Pawar R, Rapoza RJ, Powers JC, van Beusekom HM, García-García HM, Virmani R (2013) Intracoronary optical coherence tomography and histology of overlapping everolimus-eluting bioresorbable vascular scaffolds in a porcine coronary artery model: the potential implications for clinical practice. *JACC Cardiovasc Interv* 6:523–532
 15. Verheye S, Ormiston JA, Stewart J, Webster M, Sanidas E, Costa R, Costa JR Jr, Chamie D, Abizaid AS, Pinto I, Morrison L, Toyloy S, Bhat V, Yan J, Abizaid A (2014) A next-generation bioresorbable coronary scaffold system: from bench to first clinical evaluation: 6- and 12-month clinical and multimodality imaging results. *JACC Cardiovasc Interv* 7:89–99
 16. Everaert B, Felix C, Koolen J, den Heijer P, Henriques J, Wykrzykowska J, van der Schaaf R, de Smet B, Hofma S, Diletti R, Van Mieghem N, Regar E, Smits P, van Geuns RJ (2015) Appropriate use of bioresorbable vascular scaffolds in percutaneous coronary interventions: a recommendation from experienced users: a position statement on the use of bioresorbable vascular scaffolds in the Netherlands. *Neth Heart J* 23:161–165
 17. Tamburino C, Latib A, van Geuns RJ, Sabate M, Mehilli J, Gori T, Achenbach S, Alvarez MP, Nef H, Lesiak M, Di Mario C, Colombo A, Naber CK, Caramanno G, Capranzano P, Brugaletta S, Geraci S, Araszkiwicz A, Mattesini A, Pyxaras SA, Rzeszutko L, Depukat R, Diletti R, Boone E, Capodanno D, Dudek D (2015) Contemporary practice and technical aspects in coronary intervention with bioresorbable scaffolds: a European perspective. *EuroIntervention* 11:45–52
 18. Wiebe J, Nef HM, Hamm CW (2014) Current status of bioresorbable scaffolds in the treatment of coronary artery disease. *J Am Coll Cardiol* 64:2541–2551B
 19. Biscaglia S, Secco GG, Tumscitz C, Di Mario C, Campo G (2015) Optical coherence tomography evaluation of overlapping everolimus-eluting bioresorbable vascular scaffold implantation guided by enhanced stent visualization system. *Int J Cardiol* 182:1–3
 20. Biscaglia S, Campo G, Tebaldi M, Tumscitz C, Pavasini R, Fileti L, Secco GG, Di Mario C, Ferrari R (2016) Bioresorbable vascular scaffold overlap evaluation with optical coherence tomography after implantation with or without enhanced stent visualization system (WOLFIE study): a two-centre prospective comparison. *Int J Cardiovasc Imaging* 32:211–223
 21. Ishibashi Y, Muramatsu T, Nakatani S, Sotomi Y, Suwannasom P, Grundeken MJ, Cho YK, Garcia-Garcia HM, van Boven AJ, Piek JJ, Sabaté M, Helqvist S, Baumbach A, McClean D, de Sousa Almeida M, Wasungu L, Miquel-Hebert K, Dudek D, Chevalier B, Onuma Y, Serruys PW (2015) Incidence and potential mechanism(s) of post-procedural rise of cardiac biomarker in patients with coronary artery narrowing after implantation of an everolimus-eluting bioresorbable vascular scaffold or everolimus-eluting metallic stent. *JACC Cardiovasc Interv* 8:1053–1063
 22. Ortega-Paz L, Capodanno D, Giacchi G, Gori T, Nef H, Latib A, Caramanno G, Di Mario C, Naber C, Lesiak M, Capranzano P, Wiebe J, Mehilli J, Araszkiwicz A, Pyxaras S, Mattesini A, Geraci S, Naganuma T, Colombo A, Münzel T, Sabaté M, Tamburino C, Brugaletta S (2016) Impact of overlapping on 1-year clinical outcomes in patients undergoing everolimus-eluting bioresorbable scaffolds implantation in routine clinical practice: Insights from the European multicenter GHOST-EU registry. *Catheter Cardiovasc Interv*. doi:10.1002/ccd.26674. **[Epub ahead of print]**
 23. Bourantas CV, Papafaklis MI, Kotsia A, Farooq V, Muramatsu T, Gomez-Lara J, Zhang YJ, Iqbal J, Kalatzis FG, Naka KK, Fotiadis DI, Dorange C, Wang J, Rapoza R, Garcia-Garcia HM, Onuma Y, Michalis LK, Serruys PW (2014) Effect of the endothelial shear stress patterns on neointimal proliferation following drug-eluting bioresorbable vascular scaffold implantation: an optical coherence tomography study. *JACC Cardiovasc Interv* 7:315–324
 24. Bourantas CV, Papafaklis MI, Lakkas L, Sakellarios A, Onuma Y, Zhang YJ, Muramatsu T, Diletti R, Bizopoulos P, Kalatzis F, Naka KK, Fotiadis DI, Wang J, Garcia Garcia HM, Kimura T, Michalis LK, Serruys PW (2014) Fusion of optical coherence tomographic and angiographic data for more accurate evaluation of the endothelial shear stress patterns and neointimal distribution after bioresorbable scaffold implantation: comparison with intravascular ultrasound-derived reconstructions. *Int J Cardiovasc Imaging* 30:485–494

Anlage 6



Bioresorbable scaffold implantation in patients with indication for oral anticoagulation: A propensity matched analysis



Niklas F. Boeder^a, Victoria Johnson^a, Oliver Dörr^a, Jens Wiebe^b, Albrecht Elsässer^c, Helge Möllmann^d, Christian W. Hamm^a, Holger M. Nef^a, Timm Bauer^{a,*}

^a University of Giessen, Department of Cardiology, Giessen, Germany

^b Deutsches Herzzentrum München, Munich, Germany

^c Klinikum Oldenburg, Department of Cardiology, Oldenburg, Germany

^d St. Johannes-Hospital, Department of Internal Medicine, Dortmund, Germany

ARTICLE INFO

Article history:

Received 9 September 2016

Accepted 14 November 2016

Available online 24 November 2016

Keywords:

Bioresorbable scaffold

Oral anticoagulation

Triple therapy

Dual antiplatelet therapy

Antithrombotic therapy

ABSTRACT

Objectives: To examine ischemic and bleeding outcomes in patients on triple antithrombotic therapy (TAT) compared with dual antiplatelet therapy (DAPT) after the implantation of bioresorbable scaffolds (BRS).

Background: The optimal antithrombotic regimen in patients undergoing percutaneous coronary intervention that have an indication for oral anticoagulation is unclear, in particular among those undergoing BRS implantation.

Methods: Consecutive patients of a single-center, all-comers BRS registry were included. Patients were followed up after 30 days, 6 and 12 months, and thereafter yearly. Outcome parameters were target vessel failure (TVF), major adverse cardiac events (MACE) including target lesion revascularization (TLR), scaffold thrombosis (ST), death, myocardial infarction, and any bleeding as defined by BARC. Patients on TAT were matched to patients on DAPT. **Results:** A total of 607 patients were included. Fifty-five patients receiving TAT were matched with 165 patients treated with DAPT. Acute coronary syndrome was an indication for coronary angiography in 50.9% vs 50.4% groups ($p = 0.97$). Major adverse cardiac events occurred in 16.4% of TAT patients vs. 8.9% DAPT patients ($p = 0.12$), TLR in 5.5% vs. 1.9% ($p = 0.17$), ST in 3.6% vs. 1.9% ($p = 0.46$), and TVF in 3.6 vs. 1.9% ($p = 0.46$). Patients died in 7.3% in the TAT group vs. 5.1% in the DAPT group ($p = 0.26$). No severe bleeding was recorded in either of the groups.

Conclusion: There was no difference in bleeding or ischemic events between the patients on TAT and those on DAPT after BRS implantation. The high rate of scaffold thrombosis in all of these patients, however, is not negligible.

© 2016 Published by Elsevier Ireland Ltd.

1. Introduction

Patients undergoing percutaneous coronary intervention (PCI) with stent implantation require dual antiplatelet therapy (DAPT) consisting of aspirin and a P2Y₁₂ inhibitor [1]. This antithrombotic treatment is temporary and necessary to reduce ischemic events [2]. Approximately 5–10% of these patients are also on oral anticoagulation (OAC) for indications such as atrial fibrillation or a prosthetic valve [3].

It has been shown that DAPT after stenting reduces the incidence of stent thrombosis (ST) better than conventional anticoagulant therapy [4]. On the other hand, OAC therapy is superior to clopidogrel plus aspirin for prevention of vascular events in patients

with atrial fibrillation at high risk of stroke [5]. Therefore, patients who undergo stent implantation and have an indication for OAC are treated with triple antithrombotic therapy (TAT) [1,6]. Multiple combinations are possible. TAT, however, has a higher bleeding risk [7], and ultimately hemorrhagic complications might offset all ischemic benefits [8]. To make the issue even more complex, potent P2Y₁₂ inhibitors (prasugrel and ticagrelor) have become the standard of care in patients with acute coronary syndrome, and new oral anticoagulants are now available. Of note, the current guideline on myocardial revascularization does not recommend the combination of a potent P2Y₁₂ inhibitors as part of triple therapy [1].

The bioresorbable scaffolds (BRS) have recently emerged as a potentially major breakthrough [9]. BRS offer a transient vessel support to resist acute recoil but are fully resorbed within approximately three years, thereby potentially overcoming long-term limitations of metallic drug-eluting stents. Patients treated with BRS who have an indication for OAC have not been well examined, as chronic treatment with anticoagulants has been an exclusion criterion for most BRS studies [10,11]. Recent investigations have shown that BRS implantation is associated with an increased risk of ST [12].

Abbreviations: BRS, bioresorbable scaffold; DAPT, dual antiplatelet therapy; MACE, major adverse cardiac event; ST, stent or scaffold thrombosis; TAT, triple antithrombotic therapy; TLF, target lesion failure; TLR, target lesion revascularization; TVF, target vessel failure; TVR, target vessel revascularization.

* Corresponding author at: Klinikstr. 33, 35392 Giessen, Germany.

E-mail address: bauer-timm@gmx.de (T. Bauer).

Accordingly, we aimed to examine ischemic and bleeding outcomes in patients undergoing BRS implantation who were on TAT and compare results with those on DAPT.

2. Methods

2.1. Study design and population

All consecutive patients of a single-center, all-comers BRS registry at the Medizinische Klinik I, University of Giessen, Giessen, Germany, were included in this study. Patients were enrolled irrespective of their clinical presentation. Exclusion criteria were age < 18 years and lesions that appeared unsuitable for BRS implantation. All patients gave written informed consent. If patients were not competent to give consent, it was obtained from their legal guardians. The investigation conforms to the principles outlined in the Declaration of Helsinki and was approved by the Ethics Committee of the University of Giessen (AZ 264/12).

2.2. Percutaneous coronary intervention

PCI was performed in accordance with standard clinical practice using the radial approach, if technically feasible, or the femoral approach. Unfractionated heparin (70 U/kg body weight) was administered immediately prior to the procedure. Lesion preparation was initiated with intracoronary application of nitroglycerine. Deployment of the novolimus-eluting BRS (DESolve, Elixir Medical Corporation, Sunnyvale, California, USA) was accomplished using slow balloon inflation: 1 atm over 10 s, 2 atm over 10 s, then 2 s per atm. Deployment of everolimus-eluting BRS (Absorb BVS, Abbott Vascular, Santa Clara, CA, USA) was performed with an initial pressure of 2 atm and increasing pressure in increments of 2 atm every 5 s until fully deployed. The recommended pressure was not exceeded, and maximum pressure was maintained for 20–30 s. The use of a debulking device or intravascular imaging modalities was left to the operator's discretion.

Patients received a loading dose of aspirin 250–500 mg before PCI, unless the patients were already on chronic aspirin therapy, and thereafter 100 mg oral daily. A loading dose of clopidogrel (600 mg), prasugrel (60 mg), or ticagrelor (180 mg) was followed by a maintenance dose of clopidogrel (75 mg/day), prasugrel (10 mg/day), or ticagrelor (90 mg twice/day). The duration of DAPT and TAT was left to the operator's discretion.

2.3. Follow-up

Patients who had been successfully treated qualified for the entry in the study. They were followed up via telephone according to a standardized interview after 30 days and 6 and 12 months, and thereafter yearly. Major adverse cardiac events (MACE) included death, any myocardial infarction, emergency coronary artery bypass surgery, and ischemia-driven percutaneous or surgical target lesion revascularization (TLR). Target vessel failure (TVF) was defined as death from myocardial infarction, re-occlusion of the target vessel, and revascularization of the target vessel (TVR). Target lesion failure (TLF) comprised the combination of target vessel myocardial infarction, death from known cardiac cause, TLR, and any unexplained death within the first 30 days (probable scaffold thrombosis). The Academic Research Consortium (ARC) criteria were applied for the definition of scaffold thrombosis [13]. The standardized bleeding definitions of the Bleeding Academic Research Consortium (BARC) were used to characterize bleeding events [14].

2.4. Statistical analysis

Given the differences in baseline characteristics in eligible patients in the registry treated with either DAPT or TAT, propensity-score matching was used to identify a cohort with similar characteristics. Matching was performed with the following parameters: age (≥ 65 years or < 65 years), multi-vessel disease, left ventricular ejection fraction ($\geq 40\%$ or $< 40\%$), scaffold length (equality accepted ± 5 mm), and clinical presentation (ACS or stable angina). Patients treated with TAT were matched in a 1:3 ratio to the DAPT patients. Categorical variables are given as absolute values and percentages. Continuous variables are expressed as means and standard deviations. Chi-square and Fisher's exact test were used for comparison of categorical variables, and Student's *t*-test or the Wilcoxon rank-sum test was applied for continuous variables. *p* values < 0.05 were considered statistically significant. Kaplan–Meier methods were used to derive the event rates at follow-up and to plot time-to-event curves. Statistical difference between the survival curves was assessed by a log-rank test. Statistical analysis was performed using IBM SPSS Statistics (SPSS Statistics 23.0.0.2, IBM Deutschland GmbH, Ehningen, Germany).

3. Results

3.1. Patient characteristics

A total of 607 patients were enrolled in the BRS registry. After propensity-score matching, 55 patients treated with TAT were compared with 165 patients treated with DAPT. Patients were treated between December 2012 and July 2015. Patients in the TAT group were aged 67.7 ± 8.2 years and in the DAPT group 66.0 ± 9.1 years (Table 1). The two

Table 1
Baseline characteristics.

	TAT (n = 55)	DAPT (n = 165)	<i>p</i>
Age (years)	67.6 \pm 8.2	66.0 \pm 9.1	0.09
Male sex (%)	83.6	75.9	0.23
Body mass index (kg/m ²)	28.4 \pm 4.6	28.3 \pm 4.6	0.89
Hypertension (%)	90.9	88.6	0.64
Hyperlipoproteinemia (%)	67.3	67.1	0.98
Diabetes (%)	34.5	35.4	0.90
IDDM (%)	22.2	38.0	0.16
Current smoker (%)	21.8	31.0	0.19
Family history (%)	27.3	29.7	0.73
Chronic kidney disease (%)	23.6	12.0	0.04*
Dialysis (%)	1.8	0.6	0.43
History of POAD (%)	7.3	8.9	0.72
Prior percutaneous intervention (%)	45.5	45.2	0.97
Prior myocardial infarction (%)	20.0	27.8	0.25
Prior coronary artery bypass graft (%)	14.5	8.2	0.18
Prior stroke/transient ischemic attack (%)	5.0	7.0	0.70
History of chronic obstructive pulmonary disease (%)	14.5	10.8	0.45
Atrial fibrillation (%)	87.3	0	<0.001*
CHA ₂ DS ₂ -VASC score	3.5 \pm 1.1	3.5 \pm 1.2	0.91
HAS-BLED score	1.8 \pm 0.5	1.8 \pm 0.5	0.89
Left ventricular ejection fraction (%)	54.3 \pm 10.1	55.5 \pm 11.3	0.41
Clinical indication			
Stable angina (%)	45.6	45.6	0.98
ST-elevation myocardial infarction (%)	12.7	19.0	0.29
Non-ST-elevation myocardial infarction (%)	18.2	20.9	0.67
Unstable angina (%)	20.0	10.8	0.08
Number of diseased vessels			0.94
1 (%)	16.4	17.1	
2 (%)	43.6	41.1	
3 (%)	40.0	41.8	

Abbreviations: TAT, triple antithrombotic therapy; DAPT, dual antiplatelet therapy; IDDM, insulin dependent diabetes mellitus; POAD, peripheral occlusive arterial disease.

* Significant difference between DAPT and TAT groups.

groups did not differ significantly with respect to age, sex, and cardiovascular risk profile. Approximately one third had diabetes mellitus (34.5% vs. 35.4%, *p* = 0.90) that was not treated with insulin in most of the cases (22.2% vs. 38.0%, *p* = 0.16). Significantly more patients with chronic kidney disease were found in the TAT group (23.6% vs. 12.0%, *p* < 0.04); however, patients with TAT were on dialysis no more frequently than patients in the DAPT group (1.8% vs. 0.6%, *p* = 0.43).

3.2. Indications for anticoagulation therapy

The indication for OAC in the TAT group was in 87.3% atrial fibrillation, 3.6% apex aneurysm, 3.6% pulmonary embolism/venous thrombosis, 1.3% antiphospholipid syndrome, and 4.2% other reasons. The estimated risk of stroke as assessed by the CHA₂DS₂-VASC-score [15] was the same for the two groups (3.45 \pm 1.12 vs. 3.47 \pm 1.22, *p* = 0.91) and bleeding risk as estimated by the HAS-BLED-score was also not different (1.78 \pm 0.53 vs. 1.78 \pm 0.53, *p* = 0.89).

3.3. Coronary lesions

Approximately half of the patients presented with acute coronary syndrome as an indication for coronary angiography (50.9% in TAT group vs 50.4% in DAPT group, *p* = 0.97). Single-vessel disease was present in only 16.4% in the TAT group vs. 17.1% in the DAPT group. The predominant lesion site was the LAD in 40.0% vs. 43.7% (Table 2). Lesions were of de novo-type in the majority (89.1% vs. 91.8%, *p* = 0.55). The treated segments typically did not include bifurcations (0% vs. 3.8%, *p* = 0.14). Lesions were classified using the criteria advocated by the American College of Cardiology/American Heart Association [16] and tended to be more complex in the TAT group (Table 2).

Table 2
Angiographic and QCA lesion characteristics.

	TAT (n = 55)	DAPT (n = 165)	p
Target vessel			0.06
Left anterior descending (%)	40.0	43.7	
Right circumflex artery (%)	21.8	32.3	
Right coronary artery (%)	34.5	24.1	
Bypass graft (%)	3.6	0	
De novo lesion (%)	89.1	91.8	0.55
Total occlusion (%)	9.1	7.0	0.61
In-stent restenosis (%)	1.8	1.2	0.29
Bifurcation treatment (%)	0	3.8	0.14
Medina 1,1,0 (%)	0	25	
Medina 1,1,1 (%)	0	75	
ACC/AHA lesion classification			0.03*
A (%)	10.7	1.3	
B1 (%)	21.4	44.7	
B2 (%)	39.3	26.3	
C (%)	28.6	27.6	
QCA analysis (mean ± SD)			
Reference vessel diameter proximal (mm)	2.9 ± 0.7	2.9 ± 0.6	0.77
Reference vessel diameter distal (mm)	2.6 ± 0.8	2.6 ± 0.6	0.90
Length (mm)	18.4 ± 15.8	17.1 ± 11.3	0.64

Abbreviations: TAT, triple antithrombotic therapy; DAPT, dual antiplatelet therapy; ACC, American College of Cardiology; AHA, American Heart Association; QCA, quantitative coronary analysis.

* Significant difference between DAPT und TAT groups.

3.4. Procedural characteristics and post-procedural therapy

Pre-dilatation prior to scaffold deployment was performed in almost all cases (98.2% vs. 95.6%, $p = 0.80$). The balloon for pre-dilatation had a maximum size of 2.82 ± 0.44 mm in the TAT group and 2.79 ± 0.44 mm in DAPT group (Table 3). Implanted scaffolds were of comparable diameter (3.04 ± 0.38 mm vs. 3.07 ± 0.51 mm, $p = 0.77$) and length

Table 3
Procedural characteristics.

	TAT (n = 55)	DAPT (n = 165)	p
Pre-dilatation (%)	98.2	95.6	0.80
Frequency of pre-dilatation per patient (mean)	1.5 ± 0.7	1.5 ± 0.9	0.40
Max. pre-dilatation balloon diameter (mm, mean ± SD)	2.82 ± 0.44	2.79 ± 0.44	0.34
Max. pre-dilatation balloon length (mm, mean ± SD)	16.9 ± 4.4	16.1 ± 3.5	0.65
Max. pre-dilatation balloon pressure (atm, mean ± SD)	15.2 ± 4.0	14.5 ± 3.3	0.49
Pre-dilatation with non-compliant balloon (%)	69.1	77.2	0.13
Pre-dilatation with scoring device (%)	12.7	9.5	0.53
Number of scaffolds per patient (n, mean ± SD)	1.4 ± 0.7	1.3 ± 0.6	0.44
Scaffold length (mm, mean ± SD)	26.7 ± 15.6	28.6 ± 17.4	0.58
Scaffold diameter (mm, mean ± SD)	3.04 ± 0.38	3.07 ± 0.51	0.77
Post-dilatation (%)	67.0	66.5	0.78
Use of optical coherence tomography (%)	31.0	36.7	0.44
Use of intravascular ultrasound (%)	9.1	7.0	0.61
Post-implantation P ₂ Y ₁₂ inhibitors			
Clopidogrel (%)	61.8	42.4	0.01
Ticagrelor (%)	27.3	31.0	0.60
Prasugrel (%)	10.9	26.6	0.01
Duration of TAT			
1 month (%)	76.4		
3 months (%)	7.3		
6 months (%)	3.6		
12 months (%)	10.9		
Post-implantation oral anticoagulation			
NOAC (%)	60.0		
Phenprocoumon (%)	40.0		

Abbreviations: TAT, triple antithrombotic therapy; DAPT, dual antiplatelet therapy; NOAC, new oral anticoagulants.

(26.7 ± 15.6 mm vs. 28.6 ± 17.4 mm, $p = 0.58$) in the two groups. Further procedural details are listed in Table 3.

Post-procedural medical treatment included aspirin in all cases. It was combined with clopidogrel in 42.4%, ticagrelor in 31.0%, and prasugrel in 26.6% if no additional indication for OAC existed (Table 3). For patients on concomitant OAC therapy (TAT patients), most were treated with clopidogrel (61.8%); however, ticagrelor was prescribed in 27.3% and prasugrel in 10.9%. DAPT was combined with new oral anticoagulants in 60.0% of patients on TAT; the other 40.0% were combined with phenprocoumon. The duration of TAT varied: it was limited to 1 month in most of the cases (76.4%) and was extended to 3 months in 7.3%, 6 months in 3.6%, and 12 months in 10.9%. Hereafter, the treatment with aspirin in the TAT group was stopped. The OAC in combination with the P₂Y₁₂ inhibitor was continued until month 12 after the BRS implantation. Duration of dual antithrombotic therapy in the DAPT group was 12 months; hereafter therapy was reduced to aspirin only.

Patients were followed up for a median period of 361.5 days. All-cause mortality was 7.3% for patients in the TAT group and 3.2% in patients in the DAPT group. TLF was recorded in 8 of 220 patients (TAT 7.3% vs. DAPT 2.5%, $p = 0.11$) and occurred most frequently during the first 6 months (3 cases each for TAT and DAPT). No severe bleeding occurred. Table 4 summarizes the outcome and further results. Fig. 1 illustrates a Kaplan-Meier curve for MACE. A log-rank test indicated no significant difference between the two groups: $\chi^2(1) = 1.567$, $p = 0.21$.

4. Discussion

Optimization of antithrombotic therapy in patients undergoing stent implantation with concomitant indication for OAC represents a common clinical problem. Clinicians have to find the optimum balance between too much and too little anticoagulant and antiplatelet therapy in patients who require both forms of treatment: discontinuation of antiplatelet therapy increases the risk of ST [5], and even temporary interruption of anticoagulation increases the risk of thromboembolic events [4]. This study sought to examine ischemic and bleeding outcomes in patients implanted with BRS who were on triple therapy compared with those on dual antiplatelet therapy. The patient population selected for the study fulfilled the criteria for the implantation of BRS. They were relatively young and therefore may benefit from the temporary vessel caging of BRS. It should be noted that patients enrolled in this study reflect the high-risk features of an unselected population rather than the poorly generalizable setting of a trial. Patients possessed characteristics that would constitute exclusion criteria for a variety of BRS studies. To our knowledge this is the first study of BRS implantation in patients treated with OAC. The principle finding of this study is that BRS implantation in patients on DAPT additionally indicated for OAC is safe and has a long-term outcome comparable to that of patients on DAPT alone.

It is common practice to combine DAPT and OAC (known as triple therapy or TAT) to temporarily treat patients at high risk for

Table 4
Outcome.

	TAT (n = 55)	DAPT (n = 165)	p
Major adverse cardiac event (%)	16.4	8.9	0.12
Scaffold thrombosis according to ARC (%)	3.6	1.9	0.46
Target lesion revascularization (%)	5.5	1.9	0.17
Target lesion failure (%)	7.3	2.5	0.11
Target vessel failure (%)	3.6	1.9	0.46
All-cause mortality (%)	7.3	5.1	0.26
Bleeding (%)	22.0	25.7	0.90
BARC bleeding Type 0 (%)	75.6	74.3	
BARC bleeding Type 1 (%)	22.0	21.6	
BARC bleeding Type 2 (%)	2.4	4.1	
BARC bleeding Type ≥3 (%)	0	0	
Median follow up 361.5 days			

Abbreviations: ARC, Academic Research Consortium; BARC, Bleeding Academic Research Consortium; TAT, triple antithrombotic therapy; DAPT, dual antiplatelet therapy.

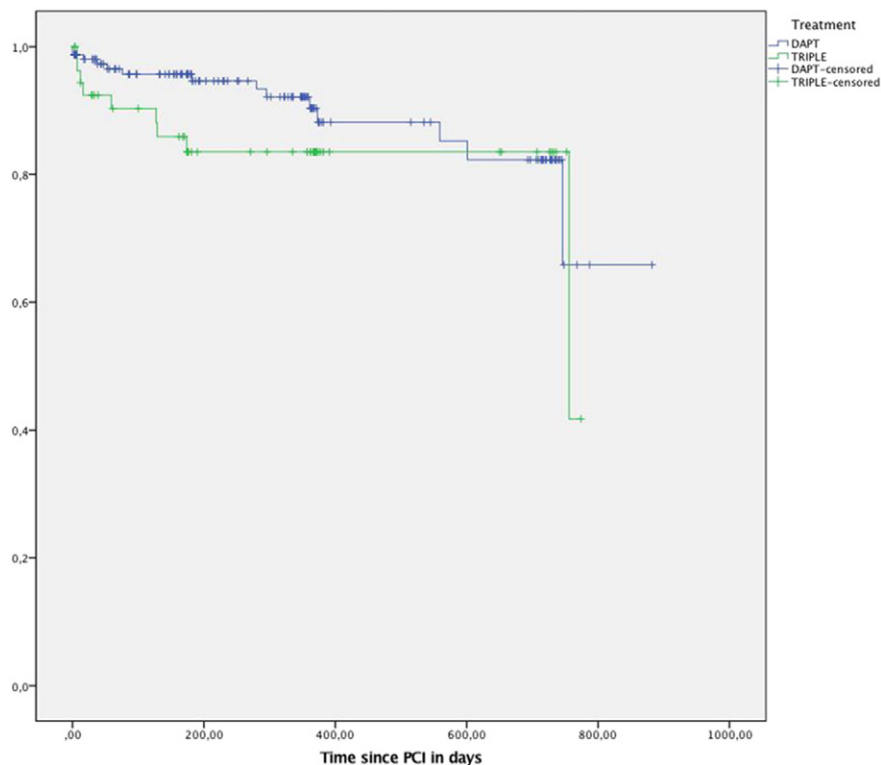


Fig. 1. Kaplan–Meier curve of MACE during follow-up.

thromboembolic and ischemic events after stent implantation. TAT potentially carries a higher risk of bleeding. Bleeding events are independently associated with a worse long-term prognosis in patients with coronary artery disease, and the mortality risk progresses with increasing severity of bleeding [8]. The patients in our cohort reported skin hematoma in most cases. Nose bleeding occurred as well but rarely led to hospitalization. Such bleeding is therefore classified as minor. We did not find a significant difference in clinically relevant and severe bleeding, as defined by BARC ≥ 3 , during follow-up between patients who received triple therapy and those who were treated with DAPT.

The latest guidelines on revascularization of the European Society of Cardiology recommend triple therapy for patients on OAC with either an adjusted-dose vitamin K antagonist or a new OAC along with aspirin and clopidogrel. The duration of TAT should be as short as possible. The ISAR-TRIPLE trial evaluated the clinical outcomes of therapy duration of 6 weeks clopidogrel versus 6 months clopidogrel after implantation of metallic drug-eluting stents [3]. The main finding was that shortening of the duration of TAT neither reduced the incidence of major bleeding nor increased the incidence of ischemic events. The majority of the patients in our cohort were on TAT for 1 month; however, therapy was extended to up to 12 months in 10.9%. TAT was conducted with clopidogrel in most cases, although ticagrelor or prasugrel were prescribed in almost one third. The stronger P2Y12 inhibitors ticagrelor and prasugrel, in combination with low-dose acetylsalicylic acid, are currently recommended as standard treatment in patients with acute coronary syndrome [1]. Sarafoff et al. compared prasugrel with clopidogrel as part of triple therapy in patients undergoing drug-eluting stent implantation [17]. Prasugrel increased TIMI major and minor bleeding fourfold, while the incidence of thrombotic events was similar. Another study compared ticagrelor as part of triple therapy with ticagrelor combined with a vitamin K antagonist in a dual therapy [18]. Major bleeding was not less with dual therapy, while ischemic events were similar. Our results indicate that major bleeding was not increased due to prasugrel or ticagrelor after BRS implantation; this, however, may be due to the low risk of bleeding in our cohort per se as assessed by the HAS-BLED score. In addition, the majority of

the patients received new OACs, which may be associated with less major bleeding than vitamin K antagonists [19]. New OACs, such as dabigatran, rivaroxaban, apixiban, and edoxaban have been shown to be alternatives to warfarin for stroke prevention in various studies [20–23]. Of note, DAPT was an exclusion criterion in most of these studies. The beneficial effect with respect to their use in TAT strategy remains unclear and is currently under investigation (PIONEER AF-PCI, REDUAL-PCI).

The fact that potent P2Y12 inhibitors were used in the present study as a component of TAT reflects that the registry was initiated when earlier versions of guideline recommendations were even more vague. Multiple antithrombotic regimens varying in duration, drug combination, and drug dosage are possible. A treatment plan must take the patient's individual risk of bleeding and thromboembolic events into account. Antithrombotic therapy must not offset ischemic benefits by causing hemorrhagic complications [24].

The GHOST-EU registry evaluated almost 1200 patients treated with Absorb BRS [25]. Rates of TLR and ST were 2.2% and 1.5% after 30 days, and 4.4% and 2.1% after 6 months, respectively. The cumulative incidence of TLF and ST was larger than anticipated, and rates of ST with Absorb BRS were comparable to those of first-generation drug-eluting stents. Patients in our cohort showed a slightly lower ST (3.6% vs 1.9%, $p = 0.46$) and TLR (5.5% vs 1.9%, $p = 0.17$) frequency. In GHOST-EU as well as in our study, ST typically occurred early after the implantation of BRS. Therefore, periprocedural aspects, including dissection, incomplete stent apposition, incomplete stent expansion or strut fractures, may have played a role. Such procedural issues can be identified and addressed by the use of intravascular imaging. Patients in this study may have benefited more from application of optical coherence tomography compared with those in GHOST-EU. Nevertheless, MACE rates (16.4% in TAT patients and 8.9% in DAPT patients) were high. The Kaplan–Meier curve shows that MACE, in accordance with ST, in our study population typically occurred early after the procedure. While TAT patients tended to experience higher event rates, we were not able to show a significant difference between the two patient groups in the long-term follow-up. Of note, the lack of significance in ischemic events may be driven by the

study design and small sample size. Other parameters, however, suggest that patients with indication for OAC are more severely ill: they had a significantly higher incidence of chronic kidney disease and their lesions, as assessed by the ACC/AHA classification, tended to be more severe. This may have finally influenced the all-cause mortality (7.3% vs. 5.1%), which was found to be higher than in other BRS studies [25,26], especially when patients had a concomitant indication for OAC. The follow-up period in these studies, however, was limited to six months and thus the further course of event rates remains speculative.

4.1. Study limitations

There are several limitations inherent to this study. The present analysis is not a randomized, controlled study but rather a single-center registry. The sample size of the study was small. This may have led to an underestimation of bleeding events. The treatment strategy was left to the discretion of the physician. This could result in selection bias that cannot be fully eliminated by using a propensity score. Furthermore, patients on dual antithrombotic therapy were not considered in this study and patients were suffering a chronic kidney disease more frequently in the TAT group.

5. Conclusions

There was no significant difference in bleeding events between the groups. The rate of adverse events, on the other side, was not different between the two groups either. The high rate of scaffold thrombosis in both groups, however, is not negligible.

Funding

No funding.

Conflict of interest statement

All authors have no potential conflict of interest. There are no relationships with industry regarding this study.

Acknowledgment

The authors thank Elizabeth Martinson, Ph.D., for editorial assistance and Mrs. Scheibelhut for assistance in statistical analysis.

References

- [1] Authors/Task Force, S. Windecker, P. Kolh, F. Alfonso, J.P. Collet, J. Cremer, et al., 2014 ESC/EACTS guidelines on myocardial revascularization: the Task Force on Myocardial Revascularization of the European Society of Cardiology (ESC) and the European Association for Cardio-Thoracic Surgery (EACTS) developed with the special contribution of the European Association of Percutaneous Cardiovascular Interventions (EAPCI), *Eur. Heart J.* 35 (2014) 2541–2619.
- [2] P. Andell, S.K. James, C.P. Cannon, D.D. Cyr, A. Himmelmann, S. Husted, et al., Ticagrelor versus clopidogrel in patients with acute coronary syndromes and chronic obstructive pulmonary disease: an analysis from the platelet inhibition and patient outcomes (PLATO) trial, *J. Am. Heart Assoc.* 4 (2015), e002490.
- [3] A. Schomig, N. Sarafoff, M. Seyfarth, Triple antithrombotic management after stent implantation: when and how? *Heart* 95 (2009) 1280–1285.
- [4] A. Schomig, F.J. Neumann, A. Kastrati, H. Schühlen, R. Blasini, M. Hadamitzky, et al., A randomized comparison of antiplatelet and anticoagulant therapy after the placement of coronary-artery stents, *N. Engl. J. Med.* 334 (1996) 1084–1089.
- [5] Investigators AWGoT, S. Connolly, J. Pogue, R. Hart, M. Pfeffer, S. Hohnloser, et al., Clopidogrel plus aspirin versus oral anticoagulation for atrial fibrillation in the atrial fibrillation clopidogrel trial with Irbesartan for prevention of vascular events (ACTIVE W): a randomised controlled trial, *Lancet* 367 (2006) 1903–1912.
- [6] H.J. Zhao, Z.T. Zheng, Z.H. Wang, S.H. Li, Y. Zhang, M. Zhong, et al., "Triple therapy" rather than "triple threat": a meta-analysis of the two antithrombotic regimens after stent implantation in patients receiving long-term oral anticoagulant treatment, *Chest* 139 (2011) 260–270.
- [7] M.L. Hansen, R. Sorensen, M.T. Clausen, M.L. Fog-Petersen, J. Raunso, N. Gadsboll, et al., Risk of bleeding with single, dual, or triple therapy with warfarin, aspirin, and clopidogrel in patients with atrial fibrillation, *Arch. Intern. Med.* 170 (2010) 1433–1441.
- [8] G. Ndrepepa, T. Schuster, M. Hadamitzky, R.A. Byrne, J. Mehilli, F.J. Neumann, et al., Validation of the Bleeding Academic Research Consortium definition of bleeding in patients with coronary artery disease undergoing percutaneous coronary intervention, *Circulation* 125 (2012) 1424–1431.
- [9] J. Wiebe, H.M. Nef, C.W. Hamm, Current status of bioresorbable scaffolds in the treatment of coronary artery disease, *J. Am. Coll. Cardiol.* 64 (2014) 2541–2551.
- [10] G.W. Stone, R. Gao, T. Kimura, D.J. Kereiakes, S.G. Ellis, Y. Onuma, et al., 1-year outcomes with the absorb bioresorbable scaffold in patients with coronary artery disease: a patient-level, pooled meta-analysis, *Lancet* 387 (2016) 1277–1289.
- [11] D.J. Kereiakes, S.G. Ellis, J.J. Popma, P.J. Fitzgerald, H. Samady, J. Jones-McMeans, et al., Evaluation of a fully bioresorbable vascular scaffold in patients with coronary artery disease: design of and rationale for the ABSORB III randomized trial, *Am. Heart J.* 170 (2015) 641–651, e3.
- [12] S. Windecker, K.C. Koskinas, G.C. Siontis, Bioresorbable scaffolds versus metallic drug-eluting stents: are we getting any closer to a paradigm shift? *J. Am. Coll. Cardiol.* 66 (2015) 2310–2314.
- [13] D.E. Cutlip, S. Windecker, R. Mehran, A. Boam, D.J. Cohen, G.A. van Es, et al., Clinical end points in coronary stent trials: a case for standardized definitions, *Circulation* 115 (2007) 2344–2351.
- [14] R. Mehran, S.V. Rao, D.L. Bhatt, C.M. Gibson, A. Caixeta, J. Eikelboom, et al., Standardized bleeding definitions for cardiovascular clinical trials: a consensus report from the Bleeding Academic Research Consortium, *Circulation* 123 (2011) 2736–2747.
- [15] A.J. Camm, G.Y. Lip, R. De Caterina, I. Savelieva, D. Atar, S.H. Hohnloser, et al., 2012 focused update of the ESC guidelines for the management of atrial fibrillation: an update of the 2010 ESC guidelines for the management of atrial fibrillation – developed with the special contribution of the European Heart Rhythm Association, *Europace* 14 (2012) 1385–1413.
- [16] T.J. Ryan, D.P. Faxon, R.M. Gunnar, J.W. Kennedy, S.B. King III, F.D. Loop, et al., Guidelines for percutaneous transluminal coronary angioplasty. A report of the American College of Cardiology/American Heart Association Task Force on Assessment of Diagnostic and Therapeutic Cardiovascular Procedures (Subcommittee on Percutaneous Transluminal Coronary Angioplasty), *Circulation* 78 (1988) 486–502.
- [17] N. Sarafoff, A. Martischinig, J. Wealer, K. Mayer, J. Mehilli, D. Sibbing, et al., Triple therapy with aspirin, prasugrel, and vitamin K antagonists in patients with drug-eluting stent implantation and an indication for oral anticoagulation, *J. Am. Coll. Cardiol.* 61 (2013) 2060–2066.
- [18] O.O. Braun, B. Bico, U. Chaudhry, H. Wagner, S. Koul, P. Tyden, et al., Concomitant use of warfarin and ticagrelor as an alternative to triple antithrombotic therapy after an acute coronary syndrome, *Thromb. Res.* 135 (2015) 26–30.
- [19] P. Sardar, S. Chatterjee, C.J. Lavie, J.S. Giri, J. Ghosh, D. Mukherjee, et al., Risk of major bleeding in different indications for new oral anticoagulants: insights from a meta-analysis of approved dosages from 50 randomized trials, *Int. J. Cardiol.* 179 (2015) 279–287.
- [20] M. Brambatti, H. Darius, J. Oldgren, A. Clemens, H.H. Noack, M. Brueckmann, et al., Comparison of dabigatran versus warfarin in diabetic patients with atrial fibrillation: results from the RE-LY trial, *Int. J. Cardiol.* 196 (2015) 127–131.
- [21] S.J. Connolly, J. Eikelboom, C. Joyner, H.C. Diener, R. Hart, S. Golitsyn, et al., Apixaban in patients with atrial fibrillation, *N. Engl. J. Med.* 364 (2011) 806–817.
- [22] C.B. Granger, J.H. Alexander, J.J. McMurray, R.D. Lopes, E.M. Hylek, M. Hanna, et al., Apixaban versus warfarin in patients with atrial fibrillation, *N. Engl. J. Med.* 365 (2011) 981–992.
- [23] M.L. O'Donoghue, C.T. Ruff, R.P. Giugliano, S.A. Murphy, L.T. Grip, M.F. Mercuri, et al., Edoxaban vs. warfarin in vitamin K antagonist experienced and naive patients with atrial fibrillation, *Eur. Heart J.* 36 (2015) 1470–1477.
- [24] F.W. Verheugt, Low-dose anticoagulation for secondary prevention in acute coronary syndrome, *Am. J. Cardiol.* 111 (2013) 618–626.
- [25] D. Capodanno, T. Gori, H. Nef, A. Latib, J. Mehilli, M. Lesiak, et al., Percutaneous coronary intervention with everolimus-eluting bioresorbable vascular scaffolds in routine clinical practice: early and midterm outcomes from the European multicentre GHOST-EU registry, *EuroIntervention* 10 (2015) 1144–1153.
- [26] J. Wiebe, O. Dorr, T. Bauer, C. Liebetrau, N. Boeder, H. Mollmann, et al., Everolimus-eluting bioresorbable scaffold implantation for the treatment of bifurcation lesions – implications from early clinical experience during daily practice, *Cardiovasc. Resusc. Med.* 17 (5) (2016) 313–317.

Anlage 7



Article

Incidental Finding of Strut Malapposition Is a Predictor of Late and Very Late Thrombosis in Coronary Bioresorbable Scaffolds

Niklas F. Boeder ^{1,2}, Melissa Weissner ², Florian Blachutzik ¹, Helen Ullrich ², Remzi Anadol ², Monique Tröbs ³, Thomas Münzel ² , Christian W. Hamm ¹, Jouke Dijkstra ⁴ , Stephan Achenbach ³, Holger M. Nef ^{1,†} and Tommaso Gori ^{2,*}

¹ Medical Clinic I, University Hospital of Giessen, Klinikstrasse 33, 35392 Giessen, Germany; niklas.boeder@innere.med.uni-giessen.de (N.F.B.); Florian.Blachutzik@innere.med.uni-giessen.de (F.B.); christian.hamm@innere.med.uni-giessen.de (C.W.H.); holger.nef@innere.med.uni-giessen.de (H.M.N.)

² Zentrum für Kardiologie, University Hospital Mainz, Langenbeckstrasse 1, 55131 Mainz, Germany and German Center for Cardiac and Vascular Research (DZHK), Standort Rhein-Main; melissaweissner@web.de (M.W.); hullrich@students.uni-mainz.de (H.U.); remzi.anadol@unimedizin-mainz.de (R.A.); tmuenzel@uni-mainz.de (T.M.)

³ Department of Cardiology, University Hospital of Erlangen, Ulmenweg 18, 91054 Erlangen, Germany; monique.troeb@uk-erlangen.de (M.T.); stephan.achenbach@uk-erlangen.de (S.A.)

⁴ Department of Radiology, Leiden University Medical Center, P.O. Box 9600 (mailstop C2-S), 2300 Leiden, The Netherlands; j.dijkstra@lumc.nl

* Correspondence: tommaso.gori@unimedizin-mainz.de; Tel.: +49-6131-17-2829; Fax: +49-6131-17-6428

† These authors contributed equally.

Received: 19 March 2019; Accepted: 25 April 2019; Published: 27 April 2019



Abstract: Malapposition is a common finding in stent and scaffold thrombosis (ScT). Evidence from studies with prospective follow-up, however, is scarce. We hypothesized that incidental observations of strut malapposition might be predictive of late ScT during subsequent follow-up. One hundred ninety-seven patients were enrolled in a multicentre registry with prospective follow-up. Optical coherence tomography (OCT), performed in an elective setting, was available in all at 353 (0–376) days after bioresorbable scaffold (BRS) implantation. Forty-four patients showed evidence of malapposition that was deemed not worthy of intervention. Malapposition was not associated with any clinical or procedural parameter except for a higher implantation pressure ($p = 0.0008$). OCT revealed that malapposition was associated with larger vessel size, less eccentricity (all $p < 0.01$), and a tendency for more uncovered struts ($p = 0.06$). Late or very late ScT was recorded in seven of these patients 293 (38–579) days after OCT. OCT-diagnosed malapposition was a predictor of late and very late scaffold thrombosis ($p < 0.001$) that was independent of the timing of diagnosis. We provide evidence that an incidental finding of malapposition—regardless of the timing of diagnosis of the malapposition—during an elective exam is a predictor of late and very late ScT. Our data provide a rationale to consider prolonged dual antiplatelet therapy if strut malapposition is observed.

Keywords: stent thrombosis; bioresorbable scaffold; optical coherence tomography

1. Introduction

Bioresorbable scaffolds (BRS) were introduced to offer transient vessel support after coronary angioplasty while avoiding long-term risks associated with permanent metallic stents [1]. However, the BRS with by far the most clinical experience, the everolimus-eluting Absorb BRS (Abbott Vascular, Santa Clara, CA, USA), showed an unexpectedly high incidence of scaffold thrombosis (ScT) both early

and late after implantation in a number of single- and multicentre observational studies [2–6] and was ultimately removed from the market. Incomplete expansion of the BRS is believed to convey the highest risk of early ScT and implantation techniques aimed to achieve full expansion of the device were shown to reduce the incidence of early ScT [7]. In contrast, studies based on quantitative coronary angiography provided evidence that undersizing (i.e., choice of a BRS smaller than the reference vessel) is strongly associated with late adverse events [8,9]. The mechanism(s) of this association remain speculative, however, it can be hypothesized that malapposition and the resulting disturbances in blood flow dynamics might play a role.

While the mechanistic rationale for the association of malapposition and late stent/scaffold thrombosis is solid [10,11], evidence to date is limited to observational studies in which malapposition was frequently found in cases of ScT [12–16]. Therefore, the aim of this study was to investigate whether incidental observation of scaffold malapposition would predict subsequent late and very late ScT.

2. Methods

2.1. Objective of the Study

The hypothesis of the study was that incidental optical coherence tomography (OCT) evidence of scaffold malapposition (observed in an elective setting and not deemed worthy of intervention at the time of OCT) might predict the occurrence of ScT during subsequent follow-up.

2.2. Patients

Consecutive patients treated at three high-volume centres in Germany (University of Mainz; University of Giessen; University of Erlangen) with Absorb BRS between April 2012 and March 2016 who satisfied the following criteria were included in this multicentre registry:

- Patients had undergone elective OCT at the end of the implantation procedure, during non-target vessel-staged procedures, or in the setting of elective invasive exams.
- In none of these patients was there evidence of ischemia in the region perfused by the vessel treated with BRS and OCTs had been performed as elective controls after implantation of these novel devices.
- An experienced interventionalist (based on current experts' recommendations [17]) reviewed the OCT and saw no clinical indication for the re-treatment of these lesions.

Patient and procedural data were entered retrospectively after inclusion in the study. Follow-up data were acquired prospectively by trained medical staff during clinical visits and telephone interviews. Referring cardiologists, general practitioners, and patients were contacted whenever necessary for further information. All data were internally audited at each centre by trained local staff and were entered retrospectively into the multicentre database in an anonymized way according to national privacy policies and laws and following the requirements of the local ethics committees. Data were audited centrally for consistency and plausibility and queries were generated when necessary.

2.3. Definitions

Frequency domain-OCT was performed using the Ilumien Optis system (St. Jude Medical, Inc., Minneapolis, MN, USA). OCT imaging catheters were inserted distally to the treated segments and the pullback was recorded until either the guiding catheter was reached or the maximum pullback length was completed. If necessary, two sequential pullbacks were acquired to image the scaffolded segment.

OCT measurements were made offline using the QCU-CMS software (Medis, Leiden, Netherlands) by trained staff using standardized operating procedures. Longitudinal cross-sections were analysed at 1 mm intervals within the stented lesion and 5 mm proximally and distally to the scaffold. Among others, the following quantitative parameters were determined: The percentage of incomplete strut

apposition (ISA) at 1 mm intervals calculated as a percentage of the total number of malapposed struts divided by the total number of struts; malapposition distance, length, and area; the eccentricity index computed as the ratio between the minimum and maximum diameters; the symmetry index defined as the difference between maximum scaffold diameter and minimum scaffold diameter divided by the maximum scaffold diameter; presence of evaginations, peri-strut low intensity areas (PSLIA), and microvessels. Evaginations were defined as any outwards protrusion in the luminal vessel contour beyond the struts' abluminal surface between well-apposed struts. Strut discontinuity/disruptions were diagnosed if there was evidence of isolated (malapposed) struts or groups of struts that did not fit the normal circular geometry of the scaffold in one or more than one cross section by more than 33% of the distance between the centre of gravity and the lumen. Further, cases where there was evidence of a clear gap (frames without any strut) were also diagnosed as strut discontinuity [18].

Definitions are described in detail in [19]. Briefly, malapposition was defined as a lack of contact of at least 1 strut with the underlying vessel wall (at least 150 μm , in the absence of a side branch) with evidence of blood flow behind the strut. It was classified as "major" malapposition if there was evidence of at least 30% of the struts in one frame. Neovessels were defined as sharply delimited, signal-poor lacunae that extended over multiple contiguous frames. Peri-strut low intensity areas (PSLIAs) were defined as homogeneous, non-signal-attenuating zones around struts that were of lower intensity than the surrounding tissue. Peri-strut intensity was measured at the mid-strut at a depth of 150 μm from the lumen and at equal distance between two contiguous struts based on intensity of the "key" component of the CMYK (cyan, magenta, yellow, and key) colour model based on raw cross-sectional images. Quantitative assessment was obtained at 5 mm proximal and distal to the BRS to measure the proximal and distal reference vessel area (RVA). RVA was calculated as the mean of the 2 largest luminal areas 5 mm proximal and distal to the BRS edge [20]. If no meaningful value for proximal or distal RVA was obtained, the largest luminal cross-sectional area at either end was used. Incomplete expansion was defined as a minimum scaffold area of at least 90% in both the proximal and distal halves of the scaffold relative to the closest reference segment.

ScT was centrally adjudicated and classified as definite, probable, and possible according to the Academic Research Consortium criteria based on the analysis of original documents [21]. Definite ScT required angiographic or autopsy confirmation with thrombus originating in the BRS or in the segment 5mm proximal or distal to the BRS. Probable ScT was considered to have occurred after intracoronary stenting in the following cases: any unexplained death within the first 30 days or any myocardial infarction—irrespective of the time after the index procedure—that is related to documented acute ischemia in the region of the implanted BRS without angiographic confirmation, in the absence of any other obvious cause. Possible ScT was considered to have occurred with any unexplained death from 30 days after intracoronary stenting until the end of trial follow-up.

2.4. Statistical Analysis

Statistical analysis was performed using IBM SPSS Statistics (SPSS Statistics 23, IBM Deutschland GmbH, Ehningen, Germany). Categorical data are presented as absolute numbers and percentages. Continuous variables are given as mean (SD) or median (IQR). The frequencies of categorical variables were compared by the Pearson chi-square test and the distribution of continuous variables was compared by the Mann–Whitney–Wilcoxon test. No imputation was performed. A Kaplan–Meier curve was used to plot time-to-event curves and the hypothesis that malapposition could be associated with incident ScT was tested using a log-rank test. Exploratory univariate and multivariable Cox regression analysis was performed to evaluate the impact of each of the above parameters on the occurrence of ScT. Potential covariates were prioritized for data analysis (a list of the covariates is presented in Supplementary Tables S4–S6). To address the impact of the timing of the OCT diagnosis on the association between malapposition and ScT, the period until diagnosis of malapposition was grouped into early (diagnosis within 48 h after implantation of BRS), mid (diagnosis from day 3 but not later than 30 days after implantation of BRS), and late (later than 30 days after the implantation of

BRS). This variable was also entered into the Cox model. The threshold for statistical significance was $p < 0.05$.

3. Results

3.1. Patient Characteristics

A total of 197 patients (219 lesions) who underwent elective OCT within 353 (0–376) days after BRS implantation were enrolled in the study (Table 1). One hundred and thirty-two patients were treated in Mainz, 36 in Giessen, and 29 in Erlangen. Follow-up was complete (100%) at a median of 1059 (1009–1110) days, during which 7 patients presented with late or very late ScT 579 [341–623] days after implantation and 293 (38–579) days after OCT. Diagnosis of ScT was supported by OCT-imaging in 5 cases and was based on angiography alone in two patients.

Table 1. Baseline characteristics of the cohort.

Baseline Characteristic	Late or Very Late Scaffold Thrombosis ScT ($n = 7$)	No ScT ($n = 190$)	p
Age (years)	58.3 ± 9.1	61.8 ± 11.9	0.37
Male Sex (%)	85.7	81.6	0.78
Hypertension (%)	100	77.9	0.16
Diabetes mellitus (%)	14.3	20.5	0.69
Current smoker (%)	43.9	36.8	0.74
Family history (%)	14.3	30.0	0.37
Hyperlipoproteinaemia (%)	43.9	47.4	0.81
Prior revascularization (%)	71.4	34.7	0.04 *
Prior bypass surgery (%)	0	3.7	0.06
Prior percutaneous intervention (%)	71.4	33.2	0.04 *
Prior stroke/TIA (%)	0	3.2	0.63
eGFR (mean ± SD, ml/min)	91.4 ± 30.8	85.4 ± 20.2	0.74
Left ventricular ejection fraction (mean ± SD, %)	54.3 ± 7.9	54 ± 8.2	0.96
Acute coronary syndrome (%)	71.4	51.4	0.30
Clinical indication			
- Stable angina (%)	28.6	37.4	0.57
- ST-elevation myocardial infarction (%)	42.9	22.1	0.29
- Non-ST-elevation myocardial infarction (%)	28.6	24.9	0.82
- Unstable angina (%)	0	13.8	0.20
Number of vessels treated	1.6 ± 0.8	1.1 ± 0.4	0.01 *
Number of scaffolds per lesion	1.0 ± 0	1.2 ± 0.5	0.25
Number of scaffolds per patient	1.7 ± 1.1	1.3 ± 0.7	0.23
Chronic total occlusion (%)	0	6.8	0.47
Lesion type AHA/ACC classification B/C2 (%)	85.7	63.5	0.22
Dual antiplatelet therapy (DAPT)			0.58
- Clopidogrel (%)	14.3	31.2	
- Prasugrel (%)	14.3	52.4	
- Ticagrelor (%)	71.4	16.4	

* = statistically significant; eGFR = estimated Glomerular filtration rate; AHA/ACC = American Heart Association/American College of Cardiology.

Patients with late or very late ScT showed similar characteristics with respect to age, sex, and cardiovascular risk profile. A history of prior revascularization was more frequent in ScT patients (71.4% vs. 34.7%; $p = 0.04$). The majority of BRS were implanted in the setting of an acute coronary syndrome (71.4% vs. 51.4%; $p = 0.30$) with no difference between the groups. While control patients tended to have a higher number of scaffolds per lesion (1.0 ± 0 vs. 1.2 ± 0.5 ; $p = 0.25$), the number

of treated vessels (1.6 ± 0.8 vs. 1.1 ± 0.4 ; $p = 0.01$) was higher in the ScT group. Parameters of lesion complexity were comparable between the groups.

Procedural characteristics divided by the incidence of ScT are shown in Table S1. The strategy used for implantation was not different between ScT patients and reference patients; pre-dilatation was performed in almost all cases (100% vs. 99.5%; $p = 0.85$) with comparable inflation pressures (13.4 ± 1.9 vs. 13.2 ± 2.3 atm; $p = 0.75$). All ScTs (except for one, occurring during clopidogrel therapy at 38 days after index) were observed after scheduled cessation of dual antiplatelet therapy (DAPT).

3.2. Optical Coherence Tomography (OCT) Characteristics

The timing of OCT from the index procedure is presented in Figure 1. OCT characteristics are shown in Table 2. Total scaffold length did not differ significantly between ScT patients and reference patients (35.4 ± 29.2 vs. 27.4 ± 16.5 mm; $p = 0.96$). At the patient level, there was no difference in scaffold nominal diameter, however, at lesion level, scaffolds that displayed an ScT during follow-up had a greater minimum (3.2 ± 0.22 vs. 3.0 ± 0.35 mm; $p = 0.01$) and maximum scaffold diameter (3.4 ± 0.24 vs. 3.1 ± 0.34 mm; $p = 0.04$). In line with this, the maximum (12.3 ± 2.5 vs. 9.1 ± 3.1 mm²; $p = 0.005$) and minimum (6.3 ± 1.0 vs. 4.8 ± 1.9 mm²; $p = 0.82$) lumen areas were significantly larger in ScT patients. The incidence of PSLIA and neovessels as well as BRS asymmetry and eccentricity were similar between ScT and reference patients (Table 2). Strut discontinuities were more frequently observed in the ScT patients (42.9% vs. 5.9%; $p < 0.001$). Furthermore, uncovered (42.9% vs. 5.9%; $p < 0.001$) and malapposed struts (85.7% vs. 20.1%; $p < 0.001$) were observed significantly more frequently in BRS that later developed ScT. Malapposition area, distance, and length were not different in patients with compared with those without ScT.

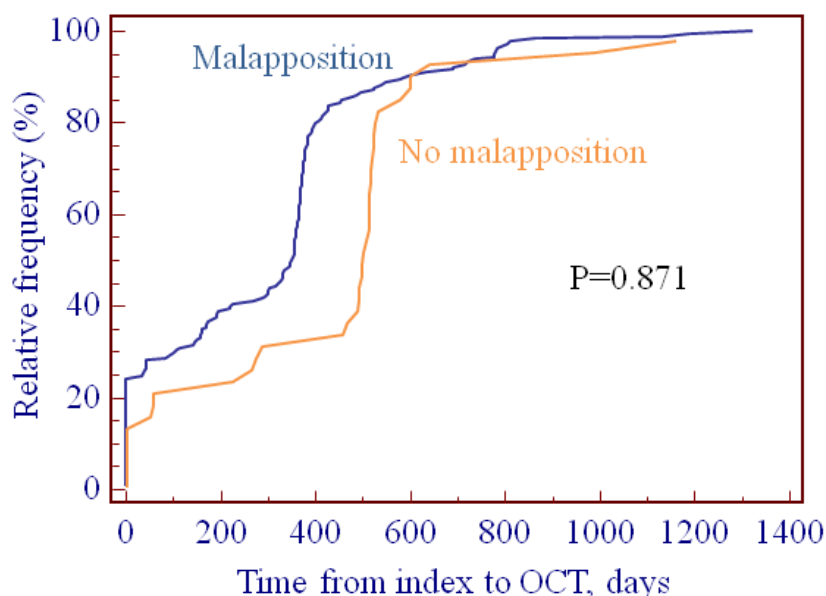


Figure 1. Timing of OCT from index procedure. There was no difference between patients with or without malapposition ($p = 0.871$).

Baseline characteristics and procedure-related parameters of patients with and without malapposition can be found in Tables S2 and S3 (supplementary materials). The presence of malapposition was not associated with any of the other OCT characteristics. Patients with malapposition, however, showed a larger lumen area (8.4 ± 2.5 vs. 11.6 ± 3.8 mm²; $p < 0.001$) and more eccentricity (0.68 ± 0.09 vs. 0.61 ± 0.12 ; $p < 0.001$) and tended to have uncovered struts more frequently ($p = 0.06$, Table S8, supplementary materials).

Table 2. Optical coherence tomography (OCT) findings.

Optical Coherence Finding	Late or Very Late ScT (n = 7)	No ScT (n = 190)	p
Number of struts	1080 ± 485	1059 ± 837	0.38
Number of frames	116.1 ± 84	120.4 ± 49	0.24
Pullback length (mm)	19.1 ± 8.1	21.1 ± 5.4	0.35
Maximum lumen area (mm ²)	12.3 ± 2.5	9.1 ± 3.1	0.005 *
Minimum lumen area (mm ²)	6.3 ± 1.0	4.8 ± 1.9	0.02 *
Average lumen area (mm ²)	8.96 ± 1.03	6.6 ± 2.20	0.003 *
Maximum lumen asymmetry	0.28 ± 0.10	0.27 ± 0.11	0.82
Maximum scaffold asymmetry	0.24 ± 0.012	0.24 ± 0.09	0.91
Maximum lumen eccentricity	0.62 ± 0.11	0.66 ± 0.10	0.29
Maximum scaffold eccentricity	0.66 ± 0.10	0.72 ± 0.08	0.07
Peri-strut low intensity area (PSLIA) (%)	20.0	5.4	0.18
Microvessels (%)	42.9	31.0	0.51
Fractures (%)	57.1	33.5	0.20
Uncovered scaffold struts (%)	42.9	5.8	<0.001 *
Malapposition (>30% in one frame, without side) (%)	71.4	15.3	<0.001 *
Any malapposition per patient (%)	85.7	20.1	<0.001 *
Malapposition length (mm)	2.33 ± 1.5	2.76 ± 1.8	0.67
Malapposition maximum area (mm ²)	1.56 ± 0.69	2.3 ± 1.9	0.64
Number of malapposed segments	1.83 ± 1.17	1.7 ± 0.99	0.88
Malapposition distance (mm)	0.52 ± 0.25	0.89 ± 0.77	0.22
Evagination (%)	57.1	27.5	0.08

* = statistically significant.

3.3. Analysis of the OCT Predictors of Scaffold Thrombosis

Figure 2 illustrates the relationship between OCT evidence of malapposition and subsequent ScT. The log rank test p was <0.001.

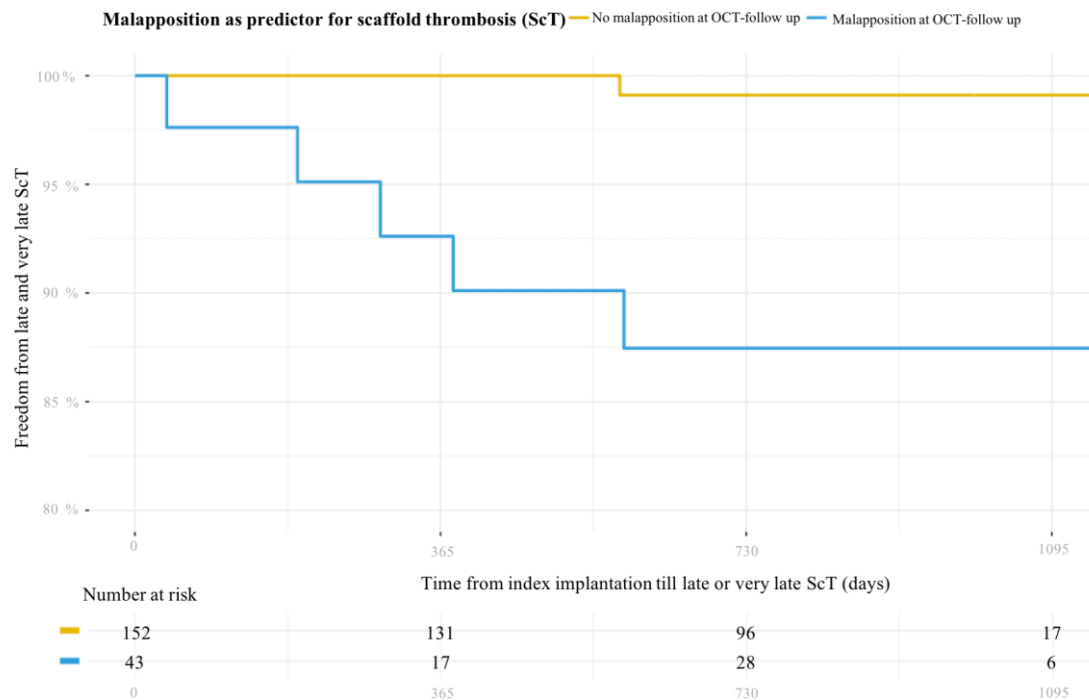


Figure 2. Kaplan–Meier curve illustrating the association between incidental finding of malapposition during elective follow-up OCT and incidence of late and very late ScT.

Multivariable Cox regression identified both malapposition diagnosed early (within 48 hours) after the index procedure (HR = 24.1, 95% CI = 1.5–387.6, $p = 0.03$) and later than day 30 (HR = 20.9, 95% CI = 2.5–179.7, $p < 0.001$) as independent predictors of ScT. Further exploratory univariate and multivariable Cox regression analysis (Tables S4–S7, supplementary materials) showed that the presence of malapposition ($p = 0.049$, hazard ratio (HR) 10.56 (1.0–110.68)) was the only independent predictor of ScT. The presence of uncovered struts and the number of vessels treated showed a threshold association ($p = 0.05$).

3.4. OCT Evidence at the Time of ScT

OCT observations at the time of ScT were collected in a separate retrospective registry. These data are presented in Appendix A.

4. Discussion

The principal findings of this study are: (1) Malapposition was identified as predictor of late and very late ScT in patients treated with BRS; this association was demonstrated for both “major” malapposition (defined as evidence of at least 30% of the struts in one frame) and for any degree of malapposition. This association was valid when malapposition was diagnosed either at implantation or >30 days thereafter. (2) The presence of uncovered struts showed a threshold association with the incidence of ScT during follow-up in multivariate analysis. (3) In an analysis of thrombi detected by OCT (see supplementary materials), evidence of malapposition was more frequent in late/very late ScT than in early ScT. This evidence was associated with larger vessel and scaffold sizes.

BRS were introduced to overcome long-term limitations of metallic stents; however, evidence from a number of registries and randomized controlled studies showed BRS to be associated with increased risk of both early and late ScT [2,4,22]. Importantly, early ScT was often shown to be associated with procedural issues (including suboptimal vessel sizing and incomplete scaffold/vessel expansion) [23]. In line with this, improvement in implantation techniques proved to be associated with reduced rates of such events [24,25]. Later, evidence was reported of late and very late ScT, i.e., at a time when the benefits of the resorbable device over metallic stents were supposed to be realized [2,4,22]. Importantly, malapposition, often associated with strut discontinuity and uncovered struts, emerged as the strongest association of very late ScT in OCT case series [13,15,16]. Although the mechanisms of this form of disruption in the geometry of the scaffold remain unknown and are probably different from case to case, the persistence of early malapposed (often uncovered) struts, or the development of late malapposition/evaginations, both resulting in struts not being embedded in the vascular wall, appear to be a prerequisite for evolution of adverse scaffold geometry. Similar data are also available for metallic stents; malapposition was the leading finding in the Bern and PESTO registries of stent thrombosis and among the three leading mechanisms in the PRESTIGE registry [26,27].

Stent malapposition results in disturbances in blood flow dynamics, abluminal areas of high shear stress, and abluminal areas of low shear stress and recirculation [10,11]. These disturbances are in turn associated with impaired strut coverage by endothelial cells (“strut healing”), strongly influence the local levels of blood viscosity, and stimulate platelet activation and neointima formation [28,29] that might amplify the supposedly higher thrombogenicity of scaffolds [30].

Despite this rationale and retrospective evidence, prospective follow-up data on the role of malapposition in determining an increased risk of late thrombosis in BRS remain limited to first-generation drug-eluting stents, in which the occurrence of late acquired malapposition at any time between imaging assessment and stent thrombosis complicates any assessment. In a meta-analysis by Hassan et al, the odds ratio for the risk of stent thrombosis in patients with diagnosed late acquired malapposition was 6.51 (1.34–34.91); however, the data were heterogeneous, with three trials supporting this conclusion and the other two leaning in the other direction. These considerations have a further level of complexity with respect to BRS use, where it would be expected that the resorption of the malapposed struts would limit their thrombogenic potential. Gomez-Lara et al. [31] performed an

OCT sub-study of the ABSORB trial Cohort B, in which BRS having a 3 mm diameter were deployed. The incidence of malapposed struts in vessels with a final distal maximal lumen diameter >3.3 mm was higher than in cases in which the final lumen diameter was smaller. In addition, we previously reported that undersizing at the time of implantation and BRS implantation in vessels larger than 3.5 mm are predictors of late/very late ScT. In contrast, oversizing and small reference vessel diameters (RVDs) were predictors of early ScT [18]. The current data provide a possible mechanism related to this observation, suggesting that malapposition, even when it is diagnosed incidentally and regardless of the length of time from implantation, is a predictor of late and very late ScT and should therefore trigger mechanical/pharmacological intervention.

In our database, total scaffold length, uncovered struts, minimum lumen area, and the number of vessels treated did not affect the chances of ScT in our cohort, although the regression model should be analyzed with caution as the covariate/case ratio may have led to overmodeling [32].

5. Limitations

There are several limitations associated with this study. First, its registry nature, with retrospective collection of patients' data and prospective follow-up, has clear inherent limitations, and the evidence provided here (particularly given the small sample size and event rate) should be seen as hypothesis generating, particularly with regard to the exploratory multivariate analysis. A strictly prospective study design to investigate malapposition as a causal factor of scaffold thrombosis would be complex from an ethical perspective. OCT follow-up was not performed at fixed time points and was not repeated, so any conclusion on the nature (early versus late acquired) of malapposition was impossible. Further, the Bern registry emphasized the importance of the longitudinal extent of malapposition (>1 mm) and suggested a cut-off >300 μm for the strut-vessel wall distance [33]. These cases are usually treated in the clinical routine and were not included in the present database. The present study expands this evidence to suggest that findings of scaffold malapposition, even those that appear as "minor" and not worthy of intervention, are indeed associated with ScT. Importantly, fluid dynamic models demonstrate that, particularly for thick struts with quadratic profile, a smaller malapposition distance might actually have the largest hemodynamic effect [28,29]. ScT is a complex phenomenon in which vessel, scaffold architecture, structure, and a number of patient characteristics play a role and it is likely that larger cohorts would have allowed identification of other clinical or procedural parameters and possible causes and mechanisms. For our analysis, late and very late ScT were pooled. However, all late ScT occurred at a time at which resorption would have already started and the two groups of patients did not differ in any of the key features. The definition of strut fracture has not yet been validated and an analysis of different types of fractures goes beyond the scope of this study. We therefore limited the definition of fracture to cases where discontinuity, altered geometry (see example in the supplement data), and/or a gap within the scaffold was evident. Our data apply to "thick strut" scaffolds; no conclusion on the importance of malapposition in (thin-strut) metallic stents can be inferred. Finally, the cross-sectional nature of our observation does not allow mechanistic insight. The (non-significantly) higher incidence of ST-segment elevation myocardial infarctions (STEMIs) at index in the patients presenting with malapposition points out the importance (and complexity) of vessel sizing in this setting.

6. Conclusions

We provide the first evidence that an incidental finding of malapposition—regardless of the timing of diagnosis of the malapposition—during an elective exam is a predictor of late and very late ScT. Whether mechanical correction of this finding also reduces events is unknown and will require further studies. However, this evidence suggests that prolonging dual antiplatelet therapy in these cases would be a prudent strategy.

Supplementary Materials: The following are available online at <http://www.mdpi.com/2077-0383/8/5/580/s1>, Table S1: Procedural characteristics of the prospective follow-up observational cohort, Table S2: Baseline characteristics of patients depending on presence of malapposition, Table S3: Procedural characteristics depending on presence of malapposition, Table S4: Univariate analysis of baseline characteristics for primary endpoint (late or very late ScT), Table S5: Univariate analysis of procedural characteristics for primary endpoint (late or very late ScT), Table S6: Univariate analysis of OCT findings for primary endpoint (late or very late ScT), Table S7: Multivariable Cox regression analysis for primary endpoint (late or very late ScT), Table S8: OCT findings depending on presence of malapposition, Table S9: Baseline characteristics of patients with ScT, Table S10: Procedural characteristics in the retrospective cohort of patients with ScT, Table S11: OCT findings in the retrospective cohort (OCT at the time of ScT), Table S12: Dual antiplatelet regime in the cases in which OCT was diagnosed at the time of ScT.

Author Contributions: Conceptualization, N.B., H.N., and T.G.; methodology, T.G. and N.B.; software, M.W., F.B., H.U., R.A., and M.T.; validation, R.A., J.D., and M.W.; formal analysis, N.B., T.G.; investigation, C.H., T.M., H.N., and S.A.; data curation, N.B., M.W., and H.U.; writing—original draft preparation, T.G., H.N., and N.B.; visualization, T.G. and N.B.; supervision, T.G. and T.M.; project administration, T.M.

Acknowledgments: The authors thank Elizabeth Martinson, Ph.D., for editorial assistance.

Conflicts of Interest: T.M., T.G., and H.N. have received speaker fees and research grants from Abbott Vascular. T.G. works in DZHK. C.H. received advisory fees from Abbott Vascular and is member of Medtronic advisory board. The other authors have no conflict to declare. Abbott Vascular had no role in any phase of this research.

Appendix A

A.1. Retrospective Cohort: Malapposition at the Time of Scaffold Thrombosis (ScT)

Optical coherence tomography (OCT) recordings of consecutive patients with ScT were collected in an additional retrospective registry study (Figure A1). Observations in cases of late/very late ScT were compared with those in patients with early ScT.

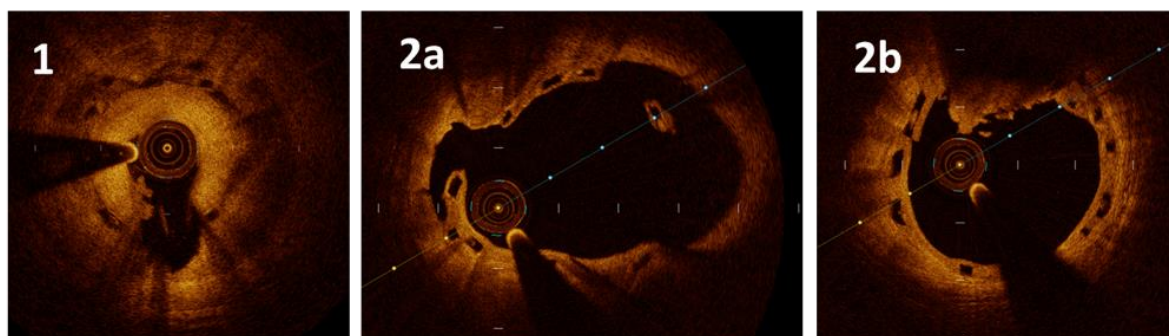


Figure A1. Representative images of cases of late/very late scaffold thrombosis (ScT) ($n = 9$). The panels are numbered according to the patient number. Case 1: ScT 563 days after index. The patient presented with ST-segment elevation myocardial infarction (STEMI). Optical coherence tomography (OCT) shows a homogeneous layer within the bioresorbable scaffold (BRS), suggestive of neointima, evidence of white thrombus (7 o'clock), and a large signal-poor, peri-strut, low intensity area (from 1 to 5 o'clock) with increased attenuation compatible with oedema/immature neointima. The architecture of the struts appears to be disrupted, but no gap was evident. Case 2: ScT 349 days after index. The patient presented with non-ST-segment elevation myocardial infarction (NSTEMI). OCT revealed malapposition (2a) immediately contiguous to white-red thrombus (2b). In this case, the strut architecture was also altered (2b; 1 o'clock) and there was evidence of incompletely covered struts (2a).

A.2. Results: OCT Evidence at the Time of ScT

All patients presenting with ScT in whom an OCT was performed at the three institutions were included in a separate retrospective registry. A total of 16 patients with OCT acquisition at the time of the ScT were identified. Five of these patients were also included in the prospective follow-up observational group (31.3%). Seven patients of the retrospective cohort were classified as acute or subacute and nine as late or very late ScT (563 (49) days after implantation). Representative images of

the thrombi are presented in Figure A1. All ScTs were classified as definite. Patients with late or very late ScT were more frequently female and more frequently had a history of prior revascularization. Further baseline and procedural characteristics were similar (Tables S9 and S10, supplementary materials).

OCT findings are listed in Table S11 (supplementary materials). The majority of frames showed evidence of thrombus (78 ± 37 vs. $55\% \pm 66\%$; $p = 0.18$). Incomplete expansion was seen predominantly in cases of early ScT (83.3% vs. 12.4% ; $p = 0.008$). Scaffold discontinuities (0% vs. 50% ; $p = 0.04$) and malapposition (16.7% vs. 87.5% ; $p = 0.008$) were features of late or very late ScT. OCT parameters expressing vessel and scaffold geometry did not differ between early and late ScT (Table S11, supplementary materials). The initial dual antiplatelet therapy (DAPT) regimen in use when implanting bioresorbable scaffold (BRS) was also not different ($p = 0.66$); however, 83% of patients developed late or very late ScT while not on DAPT ($p = 0.006$ compared to early ScT cases, Table S12, supplementary materials).

References

1. Wiebe, J.; Nef, H.M.; Hamm, C.W. Current status of bioresorbable scaffolds in the treatment of coronary artery disease. *J. Am. Coll. Cardiol.* **2014**, *64*, 2541–2551. [[CrossRef](#)]
2. Ali, Z.A.; Gao, R.; Kimura, T.; Onuma, Y.; Kereiakes, D.J.; Ellis, S.G.; Chevalier, B.; Vu, M.T.; Zhang, Z.; Simonton, C.A.; et al. Three-year outcomes with the absorb bioresorbable scaffold: individual-patient-data meta-analysis from the ABSORB randomized trials. *Circulation* **2018**, *137*, 464–479. [[CrossRef](#)]
3. Arroyo, D.; Gendre, G.; Schukraft, S.; Kallinikou, Z.; Muller, O.; Baeriswyl, G.; Stauffer, J.C.; Goy, J.J.; Togni, M.; Cook, S.; et al. Comparison of everolimus- and biolimus-eluting coronary stents with everolimus-eluting bioresorbable vascular scaffolds: Two-year clinical outcomes of the EVERBIO II trial. *Int. J. Cardiol.* **2017**, *243*, 121–125. [[CrossRef](#)] [[PubMed](#)]
4. Collet, C.; Asano, T.; Miyazaki, Y.; Tenekecioglu, E.; Katagiri, Y.; Sotomi, Y.; Cavalcante, R.; de Winter, R.J.; Kimura, T.; Gao, R.; et al. Late thrombotic events after bioresorbable scaffold implantation: a systematic review and meta-analysis of randomized clinical trials. *Eur. Heart J.* **2017**, *38*, 2559–2566. [[CrossRef](#)] [[PubMed](#)]
5. Polimeni, A.; Anadol, R.; Munzel, T.; Indolfi, C.; De Rosa, S.; Gori, T. Long-term outcome of bioresorbable vascular scaffolds for the treatment of coronary artery disease: A meta-analysis of RCTs. *BMC Cardiovasc. Disord.* **2017**, *17*, 147. [[CrossRef](#)] [[PubMed](#)]
6. Wykrzykowska, J.J.; Kraak, R.P.; Hofma, S.H.; van der Schaaf, R.J.; Arkenbout, E.K.; AJ, I.J.; Elias, J.; van Dongen, I.M.; Tijssen, R.Y.G.; Koch, K.T.; et al. Bioresorbable scaffolds versus metallic stents in routine PCI. *N. Engl. J. Med.* **2017**, *376*, 2319–2328. [[CrossRef](#)]
7. Puricel, S.; Cuculi, F.; Weissner, M.; Schermund, A.; Jamshidi, P.; Nyffenegger, T.; Binder, H.; Eggebrecht, H.; Munzel, T.; Cook, S.; et al. Bioresorbable coronary scaffold thrombosis: Multicenter comprehensive analysis of clinical presentation, mechanisms, and predictors. *J. Am. Coll. Cardiol.* **2016**, *67*, 921–931. [[CrossRef](#)] [[PubMed](#)]
8. Ellis, S.G.; Gori, T.; Serruys, P.W.; Nef, H.; Steffenino, G.; Brugaletta, S.; Munzel, T.; Feliz, C.; Schmidt, G.; Sabate, M.; et al. Clinical, angiographic, and procedural correlates of very late absorb scaffold thrombosis: Multistudy registry results. *JACC Cardiovasc. Interv.* **2018**, *11*, 638–644. [[CrossRef](#)] [[PubMed](#)]
9. Gori, T.; Weissner, M.; Gonner, S.; Wendling, F.; Ullrich, H.; Ellis, S.; Anadol, R.; Polimeni, A.; Munzel, T. Characteristics, predictors, and mechanisms of thrombosis in coronary bioresorbable scaffolds: Differences between early and late events. *JACC Cardiovasc. Interv.* **2017**, *10*, 2363–2371. [[CrossRef](#)] [[PubMed](#)]
10. Foin, N.; Gutierrez-Chico, J.L.; Nakatani, S.; Torii, R.; Bourantas, C.V.; Sen, S.; Nijjer, S.; Petraco, R.; Kousera, C.; Ghione, M.; et al. Incomplete stent apposition causes high shear flow disturbances and delay in neointimal coverage as a function of strut to wall detachment distance: Implications for the management of incomplete stent apposition. *Circ. Cardiovasc. Interv.* **2014**, *7*, 180–189. [[CrossRef](#)]
11. Foin, N.; Lu, S.; Ng, J.; Bulluck, H.; Hausenloy, D.J.; Wong, P.E.; Virmani, R.; Joner, M. Stent malapposition and the risk of stent thrombosis: Mechanistic insights from an in vitro model. *EuroIntervention* **2017**, *13*, e1096–e1098. [[CrossRef](#)]
12. Anadol, R.; Gori, T. The mechanisms of late scaffold thrombosis. *Clin. Hemorheol. Microcirc.* **2017**, *67*, 343–346. [[CrossRef](#)] [[PubMed](#)]

13. Cuculi, F.; Puricel, S.; Jamshidi, P.; Valentin, J.; Kallinikou, Z.; Toggweiler, S.; Weissner, M.; Munzel, T.; Cook, S.; Gori, T. Optical coherence tomography findings in bioresorbable vascular scaffolds thrombosis. *Circ. Cardiovasc. Interv.* **2015**, *8*, e002518. [[CrossRef](#)]
14. Kraak, R.P.; Kajita, A.H.; Garcia-Garcia, H.M.; Henriques, J.P.S.; Piek, J.J.; Arkenbout, E.K.; van der Schaaf, R.J.; Tijssen, J.G.P.; de Winter, R.J.; Wykrzykowska, J.J. Scaffold thrombosis following implantation of the ABSORB Bvs. in routine clinical practice: Insight into possible mechanisms from optical coherence tomography. *Catheter. Cardiovasc. Interv.* **2018**, *92*, E106–E114. [[CrossRef](#)]
15. Raber, L.; Brugaletta, S.; Yamaji, K.; O’Sullivan, C.J.; Otsuki, S.; Koppa, T.; Taniwaki, M.; Onuma, Y.; Freixa, X.; Eberli, F.R.; et al. Very late scaffold thrombosis: Intracoronary imaging and histopathological and spectroscopic findings. *J. Am. Coll. Cardiol.* **2015**, *66*, 1901–1914. [[CrossRef](#)] [[PubMed](#)]
16. Yamaji, K.; Ueki, Y.; Souteyrand, G.; Daemen, J.; Wiebe, J.; Nef, H.; Adriaenssens, T.; Loh, J.P.; Lattuca, B.; Wykrzykowska, J.J.; et al. Mechanisms of very late bioresorbable scaffold thrombosis: The INVEST registry. *J. Am. Coll. Cardiol.* **2017**, *70*, 2330–2344. [[CrossRef](#)] [[PubMed](#)]
17. Tamburino, C.; Latib, A.; van Geuns, R.J.; Sabate, M.; Mehilli, J.; Gori, T.; Achenbach, S.; Alvarez, M.P.; Nef, H.; Lesiak, M.; et al. Contemporary practice and technical aspects in coronary intervention with bioresorbable scaffolds: A European perspective. *EuroIntervention* **2015**, *11*, 45–52. [[CrossRef](#)] [[PubMed](#)]
18. Gori, T.; Jansen, T.; Weissner, M.; Foin, N.; Wenzel, P.; Schulz, E.; Cook, S.; Munzel, T. Coronary evaginations and peri-scaffold aneurysms following implantation of bioresorbable scaffolds: Incidence, outcome, and optical coherence tomography analysis of possible mechanisms. *Eur. Heart J.* **2016**, *37*, 2040–2049. [[CrossRef](#)] [[PubMed](#)]
19. Gori, T.; Schulz, E.; Hink, U.; Kress, M.; Weiers, N.; Weissner, M.; Jabs, A.; Wenzel, P.; Capodanno, D.; Munzel, T. Clinical, angiographic, functional, and imaging outcomes 12 months after implantation of drug-eluting bioresorbable vascular scaffolds in acute coronary syndromes. *JACC Cardiovasc. Interv.* **2015**, *8*, 770–777. [[CrossRef](#)] [[PubMed](#)]
20. Tearney, G.J.; Regar, E.; Akasaka, T.; Adriaenssens, T.; Barlis, P.; Bezerra, H.G.; Bouma, B.; Bruining, N.; Cho, J.M.; Chowdhary, S.; et al. Consensus standards for acquisition, measurement, and reporting of intravascular optical coherence tomography studies: A report from the International Working Group for Intravascular Optical Coherence Tomography Standardization and Validation. *J. Am. Coll. Cardiol.* **2012**, *59*, 1058–1072. [[CrossRef](#)] [[PubMed](#)]
21. Cutlip, D.E.; Windecker, S.; Mehran, R.; Boam, A.; Cohen, D.J.; van Es, G.A.; Steg, P.G.; Morel, M.A.; Mauri, L.; Vranckx, P.; et al. Clinical end points in coronary stent trials: A case for standardized definitions. *Circulation* **2007**, *115*, 2344–2351. [[CrossRef](#)]
22. Kereiakes, D.J.; Ellis, S.G.; Metzger, C.; Caputo, R.P.; Rizik, D.G.; Teirstein, P.S.; Litt, M.R.; Kini, A.; Kabour, A.; Marx, S.O.; et al. 3-Year clinical outcomes with everolimus-eluting bioresorbable coronary scaffolds: The ABSORB III trial. *J. Am. Coll. Cardiol.* **2017**, *70*, 2852–2862. [[CrossRef](#)]
23. Ellis, S.G.; Steffenino, G.; Kereiakes, D.J.; Stone, G.W.; van Geuns, R.J.; Abizaid, A.; Nef, H.; Cortese, B.; Testa, L.; Menichelli, M.; et al. Clinical, angiographic, and procedural correlates of acute, subacute, and late absorb scaffold thrombosis. *JACC Cardiovasc. Interv.* **2017**, *10*, 1809–1815. [[CrossRef](#)]
24. Ortega-Paz, L.; Brugaletta, S.; Sabate, M. Impact of PSP technique on clinical outcomes following bioresorbable scaffolds implantation. *J. Clin. Med.* **2018**, *7*, 27. [[CrossRef](#)] [[PubMed](#)]
25. Ortega-Paz, L.; Capodanno, D.; Gori, T.; Nef, H.; Latib, A.; Caramanno, G.; Di Mario, C.; Naber, C.; Lesiak, M.; Capranzano, P.; et al. Predilation, sizing and post-dilation scoring in patients undergoing everolimus-eluting bioresorbable scaffold implantation for prediction of cardiac adverse events: Development and internal validation of the PSP score. *EuroIntervention* **2017**, *12*, 2110–2117. [[CrossRef](#)] [[PubMed](#)]
26. Adriaenssens, T.; Joner, M.; Godschalk, T.C.; Malik, N.; Alfonso, F.; Xhepa, E.; De Cock, D.; Komukai, K.; Tada, T.; Cuesta, J.; et al. Optical coherence tomography findings in patients with coronary stent thrombosis: A report of the PRESTIGE consortium (Prevention of late stent thrombosis by an interdisciplinary global European effort). *Circulation* **2017**, *136*, 1007–1021. [[CrossRef](#)] [[PubMed](#)]
27. Souteyrand, G.; Amabile, N.; Mangin, L.; Chabin, X.; Meneveau, N.; Cayla, G.; Vanzetto, G.; Barnay, P.; Trouillet, C.; Rioufol, G.; et al. Mechanisms of stent thrombosis analysed by optical coherence tomography: Insights from the national PESTO French registry. *Eur. Heart J.* **2016**, *37*, 1208–1216. [[CrossRef](#)]
28. Chesnutt, J.K.; Han, H.C. Computational simulation of platelet interactions in the initiation of stent thrombosis due to stent malapposition. *Phys. Biol.* **2016**, *13*, 016001. [[CrossRef](#)] [[PubMed](#)]

29. Poon, E.K.W.; Thondapu, V.; Hayat, U.; Barlis, P.; Yap, C.Y.; Kuo, P.H.; Wang, Q.; Ma, J.; Zhu, S.J.; Moore, S.; et al. Elevated blood viscosity and microcirculation resulting from coronary stent malapposition. *J. Biomech. Eng.* **2018**, *140*. [[CrossRef](#)] [[PubMed](#)]
30. Vorpahl, M.; Nakano, M.; Perkins, L.E.; Otsuka, F.; Jones, R.; Acampado, E.; Lane, J.P.; Rapoza, R.; Kolodgie, F.D.; Virmani, R. Vascular healing and integration of a fully bioresorbable everolimus-eluting scaffold in a rabbit iliac arterial model. *EuroIntervention* **2014**, *10*, 833–841. [[CrossRef](#)]
31. Gomez-Lara, J.; Diletti, R.; Brugaletta, S.; Onuma, Y.; Farooq, V.; Thuesen, L.; McClean, D.; Koolen, J.; Ormiston, J.A.; Windecker, S.; et al. Angiographic maximal luminal diameter and appropriate deployment of the everolimus-eluting bioresorbable vascular scaffold as assessed by optical coherence tomography: An ABSORB cohort B trial sub-study. *EuroIntervention* **2012**, *8*, 214–224. [[CrossRef](#)] [[PubMed](#)]
32. Harrell, F.E., Jr.; Lee, K.L.; Pollock, B.G. Regression models in clinical studies: Determining relationships between predictors and response. *J. Natl. Cancer Inst.* **1988**, *80*, 1198–1202. [[CrossRef](#)] [[PubMed](#)]
33. Taniwaki, M.; Radu, M.D.; Zaugg, S.; Amabile, N.; Garcia-Garcia, H.M.; Yamaji, K.; Jorgensen, E.; Kelbaek, H.; Pilgrim, T.; Caussin, C.; et al. Mechanisms of very late drug-eluting stent thrombosis assessed by optical coherence tomography. *Circulation* **2016**, *133*, 650–660. [[CrossRef](#)] [[PubMed](#)]



© 2019 by the authors. Licensee MDPI, Basel, Switzerland. This article is an open access article distributed under the terms and conditions of the Creative Commons Attribution (CC BY) license (<http://creativecommons.org/licenses/by/4.0/>).

Incidental Finding of Strut Malapposition is a Predictor of Late and Very Late Thrombosis in Coronary Bioresorbable Scaffolds

Table S1: Procedural characteristics of the prospective follow-up observational cohort.

	Late or very late ScT (n = 7)	No ScT (n = 212)	p
Pre-dilatation (%)	100	99.5	0.85
Pre-dilatation: Balloon diameter (mm)	2.9 ± 0.19	2.8 ± 0.35	0.19
Minimum scaffold diameter per lesion (mm)	3.2 ± 0.22	3.0 ± 0.35	0.01*
Minimum scaffold diameter per patient (mm)	3.0 ± 0.45	3.0 ± 0.35	0.70
Maximum scaffold diameter per lesion (mm)	3.4 ± 0.24	3.1 ± 0.34	0.04*
Total scaffold length (mm)	35.4 ± 29.2	27.4 ± 16.5	0.96
Maximum inflation pressure scaffold deployment (atm)	13.4 ± 1.9	13.2 ± 2.3	0.75
Post-dilatation in all scaffolds (%)	42.9	39.5	0.86
Post-dilatation: Balloon diameter (mm)	3.5 ± 0.5	3.3 ± 0.4	0.48
Post-dilatation: Maximum inflation pressure (atm)	12.7 ± 1.2	12.6 ± 2.5	0.59
Overlap (%)	0	14.2	0.28

Incidental Finding of Strut Malapposition is a Predictor of Late and Very Late Thrombosis in Coronary Bioresorbable Scaffolds

Table S2: Baseline characteristics of patients depending on presence of malapposition.

	No Malapposition (n =153)	Malapposition (n = 44)	p
Age (years)	61.4 ± 11.3	62.3 ± 12.8	0.45
Male sex (%)	78.9	90.9	0.07
Hypertension (%)	78.3	79.5	0.80
Diabetes mellitus (%)	18.4	25.0	0.34
Current smoker (%)	37.5	36.4	0.89
Family history (%)	29.6	27.3	0.74
Hyperlipoproteinaemia (%)	49.3	38.6	0.12
Prior revascularization (%)	35.5	38.6	0.71
Prior percutaneous intervention (%)	34.2	36.4	0.79
Prior stroke/TIA (%)	2.6	4.5	0.51
eGFR (mean ± SD, ml/min)	84.9 ± 20.1	87.7 ± 21.7	0.42
Left ventricular ejection fraction (mean±SD, %)	54.1 ± 8.7	53.6 ± 6.0	0.27
Acute coronary syndrome (%)	50.0	58.1	0.35
Clinical indication			
Stable angina (%)	38.9	39.5	0.94
ST-elevation myocardial infarction (%)	22.2	25.6	0.65
Non-ST-elevation myocardial infarction (%)	27.1	18.6	0.26
Unstable angina (%)	11.8	16.3	0.44
Number of vessels treated	1.1 ± 0.34	1.3 ± 0.5	0.07
Number of scaffolds per lesion	1.2 ± 0.5	1.2 ± 0.4	0.93
Number of scaffolds per patient	1.3 ± 0.7	1.5 ± 0.8	0.19
Chronic total occlusion (%)	7.9	2.3	0.19
Lesion type	1.9	1.8	0.42
Dual antiplatelet therapy (DAPT)			0.58
Clopidogrel (%)	30.5	31.8	
Prasugrel (%)	51.7	56.8	
Ticagrelor (%)	17.9	11.4	

Incidental Finding of Strut Malapposition is a Predictor of Late and Very Late Thrombosis in Coronary Bioresorbable Scaffolds

Table S3: Procedural characteristics depending on presence of malapposition.

	No malapposition (n = 153)	Malapposition (n = 44)	p
Pre-dilatation (%)	99.3	100	0.58
Pre-dilatation: Balloon diameter (mm)	2.8 ± 0.36	2.8 ± 0.30	0.23
Minimum scaffold diameter per lesion (mm)	3.0 ± 0.34	3.1 ± 0.37	0.27
Minimum scaffold diameter per patient (mm)	3.0 ± 0.34	3.0 ± 0.40	0.99
Maximum scaffold diameter per lesion (mm)	3.1 ± 0.33	3.1 ± 0.37	0.30
Total scaffold length (mm)	26.8 ± 16.2	30.1 ± 19.4	0.40
Maximum inflation pressure scaffold deployment (atm)	12.9 ± 2.2	14.1 ± 2.1	0.008
Post-dilatation in all scaffolds (%)	40.1	38.6	0.85
Post-dilatation: Balloon diameter (mm)	3.3 ± 0.3	3.3 ± 0.5	0.31
Post-dilatation: Maximum inflation pressure (atm)	12.7 ± 2.7	12.3 ± 0.7	0.97
Overlap (%)	12.5	15.9	0.56

Incidental Finding of Strut Malapposition is a Predictor of Late and Very Late Thrombosis in Coronary Bioresorbable Scaffolds

Table S4: Univariate analysis of baseline characteristics for primary endpoint (late or very late ScT).

	p	Hazard ratio [95% CI]
Age (years)	0.43	0.98 [0.9–1.0]
Male sex (%)	0.72	1.5 [0.2–12.2]
Diabetes mellitus (%)	0.68	0.64 [0.1–5.3]
Current smoker (%)	0.70	1.3 [0.3–6.0]
Family history (%)	0.39	0.40 [0.04–3.3]
Hyperlipoproteinaemia (%)	0.90	0.91 [0.2–4.0]
Prior revascularization (%)	0.06	4.6 [0.9–24.5]
eGFR (mean±SD, ml/min)	0.50	1.0 [0.97–1.0]
Left ventricular ejection fraction (mean ± SD, %)	0.89	1.0 [0.91–1.1]
Acute coronary syndrome (%)	0.39	2,1 [0.4–10.7]
Clinical indication		
Stable angina (%)	0.60	0.65 [0.16–3.3]
ST-elevation myocardial infarction (%)	0.21	2.6 [0.6–11.6]
Non-ST-elevation myocardial infarction (%)	0.8	1.1 [0.2–6.2]
Number of vessels treated per patient	0.01*	3.6 [1.3–9.9]
Number of scaffolds per lesion	0.46	0.07 [0–73.9]
Number of scaffolds per patient	0.25	1.47 [0.77–2.8]
Lesion type	0.68	1.2 [0.6–2.3]
Dual antiplatelet therapy (DAPT)	0.56	1.3 [0.5–4.0]

Table S5: Univariate analysis of procedural characteristics for primary endpoint (late or very late ScT).

	p	Hazard ratio
Pre-dilatation: Balloon diameter (mm)	0.24	3.5 [0.43–27.9]
Minimum scaffold diameter per patient (mm)	0.68	1.6 [0.19–12.8]
Total scaffold length (mm)	0.25	1.0 [0.98–1.0]
Maximum inflation pressure scaffold deployment (atm)	0.89	1.0 [0.71–1.5]
Post-dilatation in all scaffolds (%)	0.72	1.3 [2.9]
Post-dilatation: Balloon diameter (mm)	0.38	3.6 [0.2–67]
Post-dilatation: Maximum inflation pressure (atm)	0.87	1.0 [0.5–1.9]

Incidental Finding of Strut Malapposition is a Predictor of Late and Very Late Thrombosis in Coronary Bioresorbable Scaffolds

Table S6: Univariate analyse of OCT findings for primary endpoint (late or very late ScT).

	p	Hazard ratio
Number of struts	0.88	1.0 [0.99–1.0]
Number of frames	0.95	1.0 [0.98–1.0]
Pullback length (mm)	0.33	0.9 [0.80–1.1]
Maximum lumen area (mm ²)	0.009	1.2 [1.1–1.5]
Minimum lumen area (mm ²)	0.53	1.4 [1.0–2.1]
Average lumen area (mm ²)	0.008	1.5 [1.1–1.9]
Maximum scaffold eccentricity	0.03	0 [0–0.4]
PSLIA (%)	0.21	4.0 [0.45–36.2]
Microvessels (%)	0.42	1.9 [0.42–8.3]
Fractures with gap (%)	0.003	9.7 [2.2–43.6]
Uncovered scaffold struts (%)	0.003	9.8 [2.2–44.0]
Malapposition (>30% of the struts in at least one frame, %)	0.004	11.4 [2.2–58.8]
Any malapposition (%)	0.005	21.3 [2.6–177.1]
Malapposition length (mm)	0.47	0.8 [0.5–1.4]
Malapposition max area (mm ²)	0.28	0.73 [0.4–1.3]
Number of malapposed segments	0.94	1.03 [0.5–2.2]
Malapposition distance (mm)	0.21	0.26 [0.03–2.1]
Evaginations (%)	0.16	2.9 [0.65–13.1]

Table S7: Multivariable Cox regression analysis for primary endpoint (late or very late ScT).

	p	Odds ratio (95% CI)
Total scaffold length (mm)	0.67	1.0 [0.9–1.0]
Any malapposition (per patient)	0.02	13.7 [1.5–124.9]
Uncovered struts	0.05	4.9 [1.0–23.7]
Minimum lumen area (mm ²)	0.42	1.2 [0.8–1.8]
Fractures with gap	0.99	0 [0]
Number of vessels treated	0.06	17.8 [0.9–345.9]

Incidental Finding of Strut Malapposition is a Predictor of Late and Very Late Thrombosis in Coronary Bioresorbable Scaffolds

Table S8: OCT findings depending on presence of malapposition.

	No malapposition (n = 153)	Malapposition (n = 44)	p
Number of struts	1105 ± 497	991 ± 499	0.15
Number of frames	121.8 ± 51.5	114.9 ± 48.4	0.64
Pullback length (mm)	20.9 ± 5.5	21.8 ± 5.9	0.25
Maximum lumen area (mm ²)	8.4 ± 2.5	11.6 ± 3.8	<0.001*
Minimum lumen area (mm ²)	4.6 ± 1.8	5.6 ± 2.1	0.008*
Average lumen area (mm ²)	6.3 ± 1.9	8.1 ± 2.5	<0.001*
Maximum lumen asymmetry	0.27 ± 0.11	0.30 ± 0.12	0.069
Maximum scaffold asymmetry	0.23 ± 0.09	0.26 ± 0.11	0.14
Maximum lumen eccentricity	0.73 ± 0.08	0.71 ± 0.09	0.17
Maximum scaffold eccentricity	0.68 ± 0.09	0.61 ± 0.12	<0.001*
PSLIA (%)	6.2	6.1	0.98
Microvessels (%)	31.3	31.8	0.95
Fractures (%)	33.8	36.4	0.75
Uncovered scaffold struts (%)	5.3	13.6	0.06
Evagination (%)	23.7	45.5	0.005

Incidental Finding of Strut Malapposition is a Predictor of Late and Very Late Thrombosis in Coronary Bioresorbable Scaffolds

Table S9: Baseline characteristics of patients with ScT.

	Acute or subacute ScT (n = 7)	Late or very late ScT (n = 9)	p
Age (years)	59.1 ± 9.1	61.6 ± 7.4	0.68
Male sex (%)	57.1	0	0.03*
Hypertension (%)	71.4	88.9	0.38
Diabetes mellitus (%)	14.3	33.3	0.38
Current smoker (%)	28.6	33.3	0.83
Family history (%)	42.9	33.3	0.70
Hyperlipoproteinaemia (%)	57.1	22.2	0.15
Prior revascularization (%)	0	66.7	0.006*
Prior percutaneous intervention (%)	0	66.7	0.006*
Prior bypass surgery (%)	0	0	n.a.
Prior stroke/TIA (%)	0	0	n.a.
eGFR (mean±SD, ml/min)	63.1 ± 22.2	87.2 ± 24.9	0.09
Left ventricular ejection fraction (mean±SD, %)	47.5 ± 13.7	47.7 ± 11.8	0.95
Acute coronary syndrome (%)	85.7	77.8	0.69
Clinical indication			
Stable angina (%)	14.3	22.2	0.68
ST-elevation myocardial infarction (%)	28.6	33.3	0.84
Non-ST-elevation myocardial infarction (%)	28.6	44.4	0.52
Unstable angina (%)	28.6	0	0.09
Number of vessels treated per patient	1.0 ± 0	1.4 ± 0.7	0.30
Number of scaffolds per lesion	1.1 ± 0.38	1.6 ± 1.3	0.76
Number of scaffolds per patient	1.1 ± 0.4	2.1 ± 1.5	0.14
Chronic total occlusion (%)	0	11.1	0.36
Lesion type B2/C, %	57.1	77.8	0.37
Dual antiplatelet therapy (DAPT)			0.66
Clopidogrel (%)	28.6	11.1	
Prasugrel (%)	57.1	66.7	
Ticagrelor (%)	14.3	22.2	

Incidental Finding of Strut Malapposition is a Predictor of Late and Very Late Thrombosis in Coronary Bioresorbable Scaffolds

Table S10: Procedural characteristics in the retrospective cohort of patients with ScT.

	Acute or subacute ScT (n = 7)	Late or very late ScT (n = 9)	p
Pre-dilatation (%)	85.7	100	0.24
Pre-dilatation: Balloon diameter (mm)	2.8 ± 0.3	2.9 ± 0.2	0.29
Minimum scaffold diameter per lesion (mm)	3.0 ± 0.3	3.1 ± 0.5	0.54
Minimum scaffold diameter per patient (mm)	3.0 ± 0.3	2.9 ± 0.5	0.46
Total scaffold length (mm)	21.3 ± 5.7	46.0 ± 38.8	0.41
Maximum inflation pressure scaffold deployment (atm)	14.6 ± 1.5	13.8 ± 1.2	0.29
Post-dilatation in all scaffolds (%)	57.1	55.6	0.95
Post-dilatation: Maximum inflation pressure (atm)	15.1 ± 1.9	14.3 ± 1.2	0.35
Overlap (%)	0	22.2	0.18

Incidental Finding of Strut Malapposition is a Predictor of Late and Very Late Thrombosis in Coronary Bioresorbable Scaffolds

Table S11: OCT findings in the retrospective cohort (OCT at the time of ScT).

	Acute or subacute ScT (n = 7)	Late or very late ScT (n = 9)	p
Number of struts	116.2 ± 43.0	147.5 ± 103.1	0.66
Frames with thrombus, n	78.0 ± 36.6	55.0 ± 66.0	0.18
Malapposed struts, n	10.0 ± 24.5	9.6 ± 9.0	0.18
Malapposed frames, n	11.3 ± 27.7	20.1 ± 17.9	0.18
Uncovered struts, n	186.8 ± 415.5	0.13 ± 0.35	0.006*
PSLIA (% of patients)	16.7	50	0.20
Evagination (% of patients)	0	25.0	0.19
Malapposition (% of patients)	16.7	87.5	0.008*
Incomplete stent apposition area (mm ²)	1.5 ± 2.1	3.5 ± 1.9	0.67
ISA at maximum lumen (mm ²)	15.5 ± 0	10.9 ± 4.9	0.67
Fractures (% of patients)	16.7	75.0	0.03*
Minimum lumen area (mm ²)	2.6 ± 2.1	4.4 ± 3.6	0.35
Maximum lumen area (mm ²)	6.2 ± 3.3	9.5 ± 4.4	0.14
Maximum scaffold area (mm ²)	6.7 ± 2.7	11.1 ± 3.4	0.06
Minimum scaffold area (mm ²)	4.5 ± 2.8	5.8 ± 2.9	0.35
Incomplete expansion (% of patients)	83.3	11.1	0.008*
Length (mm)	20.2 ± 3.7	24.0 ± 19.1	0.54
Reference lumen area (mm ²)	7.1 ± 3.4	10.2 ± 2.6	0.05
Minimum diameter (mm)	2.1 ± 0.6	2.3 ± 0.8	0.66
Maximum diameter (mm)	3.0 ± 0.8	3.7 ± 0.9	0.14
Asymmetry index	0.3 ± 0.1	0.4 ± 0.2	0.49
Minimum eccentricity index	0.7 ± 0.1	0.7 ± 0.1	1.0
Neointima (% of patients)	0	37.5	0.09
Dismantling (% of patients)	0	44.4	0.04*

Percentages are expressed as % of the patients/scaffolds (some of the analyses were not possible in all segments due to the presence of thrombus).

Incidental Finding of Strut Malapposition is a Predictor of Late and Very Late Thrombosis in Coronary Bioresorbable Scaffolds

Table S12: Dual antiplatelet regime in the cases in which OCT was diagnosed at the time of ScT.

N = 16	Acute or subacute scaffold thrombosis	Late or very late scaffold thrombosis
Clopidogrel	28.6	11.1
Prasugrel	57.1	66.7
Ticagrelor	14.3	22.2